EPITHELIAL REGULATION BY REGIONALLY DEFINED POPULATIONS OF ORAL FIBROBLASTS

Thesis submitted for the fulfilment of the requirements of the degree of Doctor of Philosophy of the University of Wales, College of Medicine.

February 2005

Matthew Locke B.D.S. MFDS RCS (Eng)

Department of Adult Dental Health,

Dental School,

Cardiff.

ProQuest LLC
789 East Eisenhower Parkway
P.O. Box 1346
Ann Arbor, MI 48106-1346

DECLARATION

This work has not previously been accepted in substance for any degree and is not being concurrently submitted in candidature for any degree.

Signed..... Candidate: Matthew Locke

Signed..... Supervisor: Professor I. C. Mackenzie

Date.....

STATEMENT 1

This thesis is the result of my own investigations, except where otherwise stated. Other sources are acknowledged by footnotes giving explicit references. A bibliography is appended.

Signed..... Candidate: Matthew Locke

Date.....

STATEMENT 2

I hereby give consent for my thesis, if accepted, to be available for photocopying and for inter-library loan, and for the title and summary to be made available to outside organisations.

Signed..... Candidate: Matthew Locke

Date.....

ACKNOWLEDGEMENTS

I would like to express my gratitude to my project supervisor, Professor Ian Mackenzie who provided constant advice and encouragement during the course of this study.

I would also like to convey my appreciation to Drs. Eleri Owen-Jones and Debbie Tudor for their help, assistance, and friendship and to Dr. Scott McKeown for his continual help and guidance on all things fibroblastic.

Thanks to Theresa Loyn and Kathy Allsop for their unending technical assistance and all the guys/girls from the "fourth floor" who provided their scientific expertise.

..... and not forgetting the departmental secretariat.

With thanks to the Wellcome trust for their sponsorship of this project.

Finally, of course, to my fiancée Geraldine (possibly even wife by the time I finish writing this) without whose support and supply of wholesome cooked meals this thesis would not have been possible!

"Tell me, does your dog bite".
"No Sir, he does not bite".
STROKES DOG – BITES HIM FEROCIOUSLY
"I thought you said your dog does not bite".
"That is not my dog".

The Pink Panther Strikes Again
Blake Edward - 1979

TABLE OF CONTENTS

Chapter 6: General discussion

INDEX OF ABBREVIATIONS

°C	Degree Celsius
µl	Microlitre
µm	Micrometre
3T3	Swiss albino mouse fibroblast line
A	Adenine
ABC	Avidin-biotin complex
ALP	Alkaline phosphatase
ATCC	American tissue culture collection
BCIP	5-Bromo-4-chloro-3-indolyl phosphatase dipotassium salt
bp	Base-pair
BrdU	Bromodeoxuridine
BSA	Bovine serum albumin
C	Cytosine
Ca^{2+}	Calcium ion
cDNA	Complementary deoxyribonucleic acid
CK	Cytokeratin
cm	Centimetre
CO_2	Carbon dioxide
CPD	Chronic periodontal disease
CSF	Colony stimulating factor
C_t	Threshold value
DAB	Diaminobenzidine tetrahydrochloride
DBA	*Dolichos biflorus agglutinin*
DD H_2O	Double distilled water
DEPC	Diethyl pyrocarbonate
DMEM	Dulbecco's modified Eagle's medium
DMSO	Dimethyl sulphoxide
DNA	Deoxyribonucleic acid
dNTPs	Deoxyribonucleotide triphosphates
DTT	Dithiothreitol
ECM	Extracellular matrix
EDTA	Ethylenediaminetetraacetic acid
EGF	Epidermal growth factor
ELISA	Enzyme-linked immunosorbent assay
FBS	Foetal bovine serum
FCS	Foetal calf serum
fg	Femtogram
FITC	Fluorescein isothiocyanate
g	Gram
G	Guanine
GAPDH	Glyceraldehyde-3-phosphate dehydrogenase
GCF	Gingival crevicular fluid
GM-CSF	Granulocyte macrophage-colony stimulating factor
GM-CSFR	Granulocyte macrophage-colony stimulating factor receptor
H_2O	Water
H_2O_2	Hydrogen peroxide
HCl	Hydrochloric acid
HGF	Hepatocyte growth factor

HGFR	Hepatocyte growth factor receptor
HRP	Horse-radish peroxidase
ICAM-1	Intercellular adhesion molecule-1
Ig	Immunoglobulin
IL-1α	Interleukin-1 alpha
IL-1αR	Interleukin-1 alpha receptor
JE	Junctional epithelium
KD	Kilo Dalton
KGF	Keratinocyte growth factor
KGF2	Keratinocyte growth factor 2
KGFR	Keratinocyte growth factor receptor
l	Litre
M	Molar
mAb	Monoclonal antibody
Mg^{2+}	Magnesium ion
Min	Minutes
mg	Milligram
ml	Millilitre
MMP	Matrix metalloproteinases
M_r	Molecular weight
mRNA	Messenger ribonucleic acid
NBT	Nitroblue tetrazolium
nm	Nanometre
NTC	No template controls
O_2	Oxygen
OGE	Oral-gingival epithelium
P1, 2, 3..	Cell line passage number
PBS	Phosphate buffered saline
PCR	Polymerase chain reaction
PDL	Periodontal ligament fibroblasts
PMN	Polymorphonuclear leukocyte
Q-PCR	Quantitative (Real-time) polymerase chain reaction
R2	Correlation coefficient
RNA	Ribonucleic acid
RNase	Ribonuclease
rpm	Revolutions per minute
RT	Reverse transcription
RT-PCR	Reverse-transcriptase polymerase chain reaction
s	Seconds
SD	Standard deviation
T	Thymine
Taq	*Thermus aquaticus*
TBE	Tris borate ethylenediaminetetraacetic acid
TBS	Tris-buffered saline
TGFα	Transforming growth factor alpha
TIMPs	Tissue inhibitor of metalloproteinases
T_m	Annealing temperature
TRITC	Tetramethyl rhodamine isothiocyanate
v/v	Volume per unit volume
w/v	Weight per unit volume

INDEX OF TABLES

INDEX OF FIGURES

INDEX OF APPENDICES

ABSTRACT

Background: Although periodontal disease is depicted as the most common disease affecting humankind little is known of the molecular events leading to its initiation and progression. The junctional and oral-gingival epithelia are functionally and histologically distinct. The junctional epithelium differs from other epithelia in its pattern of maturation and its formation of a unique epithelial attachment to the tooth. Apical migration of the junctional epithelium is a central feature of periodontal disease progression. Currently, no fully satisfactory explanation exists either for the normal stability of this epithelium at the dento-gingival attachment or for its activation to migration with the onset of periodontitis.

Aims: To test the hypothesis that the differences between the junctional and gingival epithelial phenotypes result from phenotypic differences between the fibroblast populations of sub-epithelial gingival connective tissues.

Materials and methods: Junctional and oral-gingival epithelia were successfully isolated and cultured as confirmed by immunohistochemistry using a panel of antibodies specific to the junctional phenotype. Similarly, the underlying fibroblast populations, namely the periodontal ligament and oral-gingival fibroblasts were isolated and cultured. These unique cellular phenotypes were maintained for several passages allowing amplification of cells for incorporation into organotypic co-cultures.

The mRNA derived from cell populations was subjected to TaqMan™ quantitative PCR in order to quantify expression levels of cytokines known to be involved in epithelial growth and differentiation.

Results: Within the homotypic organotypic culture system the underlying connective tissues modulated the phenotypic growth, development and differentiation of the overlying epithelium. Further, immunostaining demonstrated restoration of the *in vitro* phenotypes comparable to those of the epithelial tissues of origin. Heterotypic re-combinations showed variation in differentiation state of epithelia dependant on their underlying connective tissue. Both histologically and immunohistochemically junctional epithelium was found to revert toward the oral-gingival epithelial phenotype on culture upon oral-gingival fibroblasts. Oral-gingival keratinocytes cultured upon periodontal ligament fibroblast substrate also demonstrated a shift in phenotype toward the junctional-type, although this was less marked.

Q-PCR results for the two-fibroblast populations demonstrated striking differences in expression levels of several cytokines in particular large percentage increases in KGF and HGF expression within the oral-gingival type. Interestingly, junctional epithelial samples demonstrated statistically significant increases in IL-1α and GM-CSF receptor expression and distinct increases in several other cytokine receptor levels when compared with oral-gingival epithelium.

Conclusions: The four individual phenotypic cell populations persisted in culture. On recombination into the organotypic system, there were discernible growth variations that may be attributable to diverse cytokine/receptor levels involved in epithelial-mesenchymal interactions. It was apparent that both keratinocytes and fibroblasts have joint control of the phenotype of an epithelium. Such varying cytokine levels may represent intrinsic differences in sub-sets of the population that are at greater or lesser risk of developing periodontal disease.

CHAPTER ONE

INTRODUCTION

CHAPTER ONE
INTRODUCTION

1.1 Background

Although widely cited as being the most common disease affecting humankind little is known of the molecular events leading to the initiation and progression of periodontal disease. Epidemiological studies indicate that mild to moderate periodontitis affects the majority of the adult population; while studies suggest some 8-20% of highly susceptible individuals within the population suffer from a more severe form of the disease (Loe and Morrison, 1986).

Periodontal disease is an inflammatory condition that results in the loss of the tooth supporting structures. In health, there is a dynamic equilibrium between microflora and host defences, whereas during disease chronic periodontitis is associated with accumulation of bacterial plaque on the tooth surface and subsequent inflammation of the periodontal tissues (Page and Schroeder, 1976). Studies of periodontal disease have demonstrated a progression from gingivitis through loss of epithelial attachment to the tooth, alveolar bone destruction and ultimately to tooth loss. These processes however are not continuous, but progress in a site-specific, episodic manner with bursts of destructive activity alternating with periods of quiescence and possibly repair (Haffajee *et al.*, 1983). There is great individual variation in these patterns of destruction, which also varies over time in the same individual (Eley and Cox, 1998).

1.2 Periodontal tissues

Clinical attachment of soft tissue to the tooth is facilitated by a unique epithelium, the junctional epithelium. This epithelium is functionally and histologically distinct from its close neighbour, the gingival epithelium (Mackenzie, 1987). Apical migration of the junctional epithelium is a central feature of periodontal disease progression (Schroeder and Listgarten, 1971) but currently no satisfactory explanation exists either for the normal stability of this epithelium at the dento-gingival junction or for its activation to migration with the onset of periodontitis.

Fibroblasts are the predominant cell type in sub-epithelial connective tissues and are responsible for the major part of the production of extracellular matrix and growth factors during normal function, development, regeneration and pathologic alteration (Smith, 1997

and Lekic *et al.*, 2001). Schor and Schor (1987) suggested that specificity of fibroblast phenotype might influence not only the metabolism of connective tissues but also of adjacent epithelia.

Oral-gingival and periodontal ligament fibroblasts are the two populations of fibroblasts within the periodontium that this study will examine.

1.3 Control of the epithelial phenotype

It is now clear that the normal maintenance of tissue regeneration following damage, and the tissue responses to inflammation, are strongly influenced by various molecules that control cell growth and differentiation. Of these, a variety of epithelial mitogens have been identified as instigators and maintainers of the epithelial phenotype. Keratinocyte growth factor for example, has been shown to selectively induce keratinocyte proliferation and differentiation in tissue culture (Rubin *et al.*, 1989). Such molecules form a complex network of autocrine and paracrine acting mediators between the epithelia and their underlying connective tissues, the so-called epithelial-mesenchymal interactions (McFarlane *et al.*, 1990 and Luger and Schwartz, 1994).

Little is known about the molecular basis of apical migration of junctional epithelium observed during the transition from health to disease, but it has been postulated that the heterotypic nature of the underlying connective tissue fibroblasts could, via diffusible factors, modulate the junctional phenotype to a migratory phenotype (Mackenzie, 1987). There is now considerable interest in determining the role of these fibroblast-derived cytokines in remodelling of diseased periodontal tissues.

1.4 Aims of the thesis

The aim of this study was to investigate epithelial-mesenchymal interactions that stabilise the normal dento-gingival attachment apparatus. Such information appears essential in order to elucidate the pathological changes that are associated with activation of the junctional epithelium to a migratory phenotype.

The nature of periodontal disease poses the following questions:

1. What mechanisms result in the normal structural stability of the dento-gingival complex?
2. What occurs during advancing periodontal disease to disturb this stable state?
3. How can marginal gingivitis with connective tissue inflammation persist for extended periods of time without progression to loss of attachment?

Specifically it was intended to:

1. Confirm expression characteristics of the oral tissues of interest by *ex vivo* staining tissue sections with a panel of monoclonal antibodies to known differentiation markers.
2. To identify, isolate and culture oral-gingival and junctional epithelia together with their corresponding connective tissue fibroblasts, namely oral-gingival and periodontal ligament fibroblasts.
3. To establish whether their unique phenotypes could be maintained in culture.
4. To develop an organotypic model of gingival and junctional epithelium.
    a. Using this model, assess the ability of gingival connective tissues to support, maintain and direct the differing oral-epithelial phenotypes by series of cross-recombination experiments.
    b. To investigate a role for cytokines, in particular keratinocyte and hepatocyte growth factor in the maintenance of organotypic epithelial growth and differentiation.
5. To provide quantifiable data using polymerase chain reaction techniques, as to whether *in vitro* periodontal tissues have intrinsic differences with respect to their biochemical profile of cytokines and receptors that may be accountable for the maintenance of the stable junctional phenotype in health, and its change to a migratory phenotype in disease.
6. To attempt to formulate possible biological mechanisms for the onset and progression of chronic periodontal disease.

An increased understanding of the aetiology and pathogenesis of periodontal disease at the molecular level may help provide the rationale for improved prevention and treatments.

CHAPTER TWO

LITERATURE REVIEW

CHAPTER TWO
LITERATURE REVIEW

The literature review of this thesis will consider the structure of the periodontium, particularly that of the junctional epithelium, and the aetiology of periodontal disease. It will consider the phenotype of the gingival epithelia both *in vivo* and *in vitro* and finally the epithelial-mesenchymal interactions that are implicated in the control, growth, and differentiation of these tissues.

2.1 The periodontium

The periodontium consists of the gingiva, junctional epithelium (JE), periodontal ligament (PDL), root cementum and the alveolar bone (Figure 2.1). The teeth are supported by the alveolar processes of the maxilla and mandible and are surrounded by the periodontal tissues that provide the support essential for function.

Figure 2.1: Photomicrograph of the periodontium in health

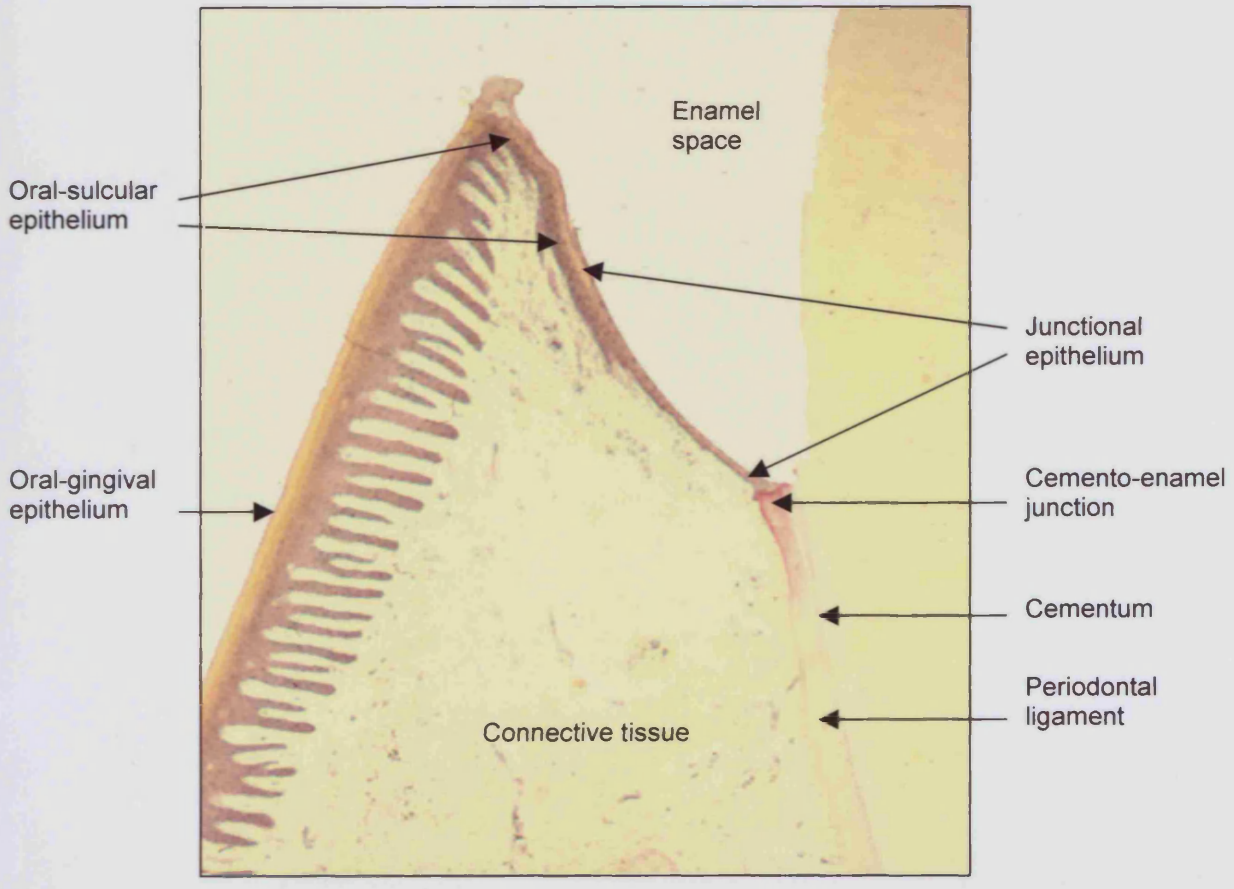

2.2 Oral epithelia

The keratinising oral epithelia, much like skin, are arranged into four distinct layers, the strata basale, spinosum, granulosum and corneum (Figure 2.2). The stratum corneum is not present within the non-keratinising oral epithelia including the oral-sulcular and junctional epithelia. The basal cell layer consists of relatively small cuboidal cells in contact with a basal lamina that connects them to the underlying connective tissue (CT). The stratum spinosum is the major epithelial layer composed of large cells with well-developed arrays of desmosomes. The stratum granulosum is generally less well defined than its counterpart in skin consisting of 1-5 layers of flattened squamous epithelial cells. The stratum corneum consists of very flat cells that have lost their nuclei and cytoplasmic organelles; they have thickened cell membranes and inter-cellular junctions that gradually disintegrate as the cells approach the surface. Nuclei and isolated organelles may be retained in the most superficial cells when keratinisation is incomplete (para-keratinisation).

Fundamentally, the oral mucosae may be classified into three different types: the gingiva and the covering of the hard palate (masticatory mucosa) the dorsum of the tongue (specialised mucosa) and the remainder of the oral mucous membranes (lining mucosa).

Figure 2.2: The strata of oral epithelium

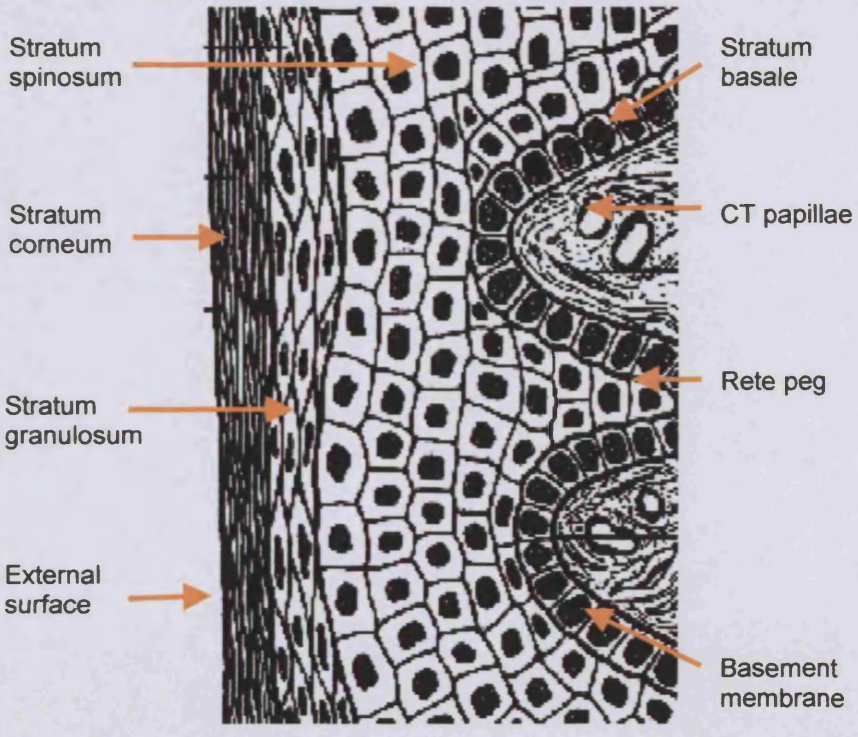

2.2.1 The gingiva

The gingivae are formed by the mucosa that covers the alveolar bone and surrounds the cervical portion of the teeth. It consist of the "attached gingivae", which run from the muco-gingival junction to the gingival margin and are bound firmly to the underlying alveolar bone, and the "free gingivae" which run from the free gingival groove to the attachment to the tooth (Figure 2.3). This attachment to the tooth results in a sulcus, a narrow space between the gingiva and the tooth. In health, it is minimal in depth maybe even absent under strict normal conditions, but it invariably exist under conditions of clinical health to between 0.2 and 3.0mm. More than 3mm clinically can be regarded as pathological in nature (Schroeder and Listgarten 1977).

Figure 2.3: Photomicrograph of the attached gingivae

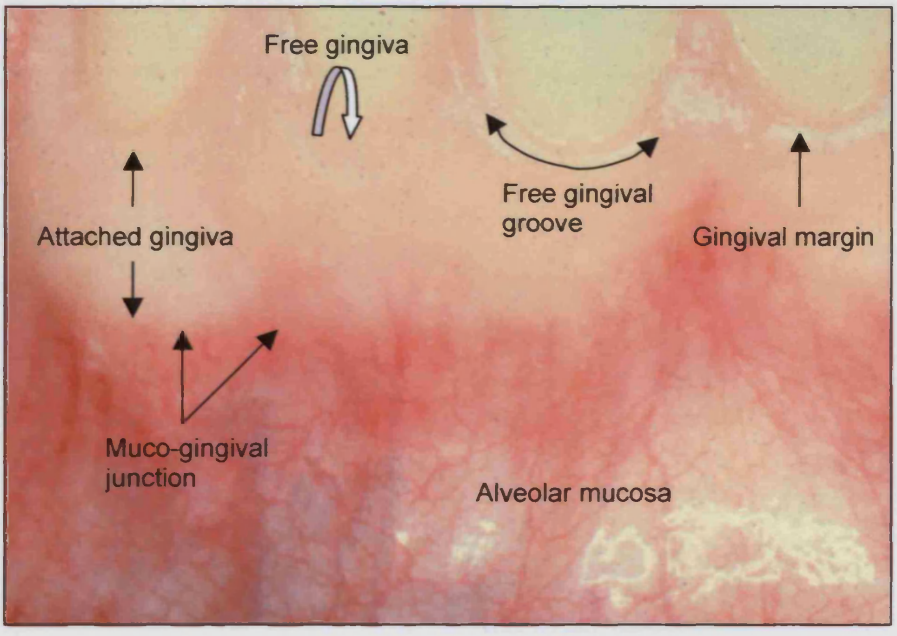

2.2.2 Oral-gingival epithelium

The oral-gingival epithelium (OGE) begins at the muco-gingival junction and is continuous at the crest of the gingiva with the oral-sulcular epithelium (facing the tooth surface but not attached to it). OGE is covered by a keratinised or parakeratinised stratified squamous epithelium.

2.2.3 Dento-gingival junction

The dento-gingival junction (attachment zone) represents a unique structure where there is an interruption in epithelial continuity at its attachment to the tooth surface. It consists of two

epithelial components: oral-sulcular (OSE) and JE, and two CT components: periodontal ligament and the gingival lamina propria.

2.2.4 Oral-sulcular epithelium

Located at the crest of the gingival margin the OSE extends downward into the gingival sulcus and is continuous with the JE. Its primary difference with OGE is that it is non-keratinised, and when compared to JE it is relatively impermeable to the passage of cells and fluid.

2.2.5 Junctional epithelium

The JE is a stratified squamous non-keratinised epithelium that attaches gingival soft tissue to the tooth surface forming a physical barrier between the external environment (oral cavity) and the internal environment of the host (periodontal CTs). However, JE is not a very effective permeability barrier as it has widened intercellular spaces (18% of the epithelium is occupied by intercellular space) that harbour elevated numbers of neutrophilic granulocytes and sulcus fluid derived from the vessels of the gingival plexus (Ten Cate, 1994, Chapter 14). Anatomically it may be located entirely on enamel, on enamel and cementum, or entirely on cementum depending on the stage of dental eruption and the degree of gingival recession. It is bounded on both sides by a basement membrane, as described by Schroeder and Listgarten (1971) with external basal lamina overlying the CT and internal basal lamina forming hemidesmosomal attachments against the non-vital tooth substrate (reviewed by Hormia and Owaribe, 2001). This results in a collar surrounding the neck of the tooth 15-30 cells wide at the floor of the gingival sulcus tapering apically to final thickness of some 3-4 cells.

Basal JE cells are attached, so an "upper" surface available for the elimination of cells is limited. The cells streaming from the high turnover of basal cells move to within two or three cell layers of the tooth surface and then join a main migratory route in a coronal direction eventually being sloughed off into the gingival sulcus (Gould *et al.*, 1983).

The JE has generated much interest due to its unique phenotype, structure and because of its involvement in the initiation of periodontal disease. The apical migration of JE attachment to the tooth is the primary indicator of destructive periodontitis. The nature of these processes leading to apical migration and formation of pocket epithelium are not fully understood.

2.3 Connective tissues of the periodontium

2.3.1 Periodontal ligament

This specialised CT consists of a band of fibrous tissue interposed between the cementum of the roots of the teeth and the inner wall of the alveolar socket. In health the PDL functions in several capacities including anchorage of the tooth in the jaw, physiological mobility during mastication and provision of proprioceptive information on tooth and jaw position (Schroeder and Listgarten, 1971 and Somerman *et al.*, 1988). Fibroblasts constitute the major cellular population, they function to synthesise collagen and the proteoglycan matrix surrounding the fibres. They also participate in the resorption of collagen fibrils and are believed to play a role in eruption due to their contractile properties (Beertsen *et al.*, 1974). With the onset of periodontal disease, pockets develop that are associated with loss of PDL and alveolar bone.

Much hope has been placed upon the ability of the PDL to help reform tissue architecture post-periodontal disease. Boyko *et al.* (1981) seeded fibroblasts from either PDL or OGF onto the surface of tooth roots that were subsequently inserted into artificial sockets. Areas of newly formed PDL attached to cementum only where PDL cells were used. So far, no one has succeeded in establishing a new and normally functioning PDL without PDL cells, indicating that these cells have specialised properties in the reformation of the dento-gingival attachment.

2.3.2 Gingival connective tissues

The CT supporting the oral mucosa (including the oral-sulcular and oral-gingiva epithelia) is termed the lamina propria. This CT supports both the overlying OSE and OGE. Much like the PDL, the principle cell component is the fibroblast, which plays a key role in tissue integrity, communication and direction of the behaviour of the overlying epithelium via a complex series of diffusible factors and matrix effects (Schor and Schor, 1987).

2.3.3 The cementum

Cementum is a hard bone-like material covering the roots of the teeth. Its function is to anchor the PDL fibre bundles to the tooth. There are two types: acellular (or primary cementum) that contains comparatively few collagen fibrils loosely packed and more or less perpendicular to the dento-cemental junction, and cellular (secondary cementum) that is deposited over the primary cementum subsequent to occlusal contact. Its matrix consists of a denser array of coarse collagen fibrils (Schroeder and Listgarten, 1971).

2.3.4 Alveolar bone

This bone is arbitrarily categorised as that bone formed in relation to the teeth. The alveolar bone proper consists of a thin lamella of cortical bone surrounding the tooth root in which are embedded fibres of the PDL. The surrounding supporting bone consists of cortical plates and cancellous bone between.

2.4 Embryological origins of the epithelial attachment

Very early in tooth development, at the cap stage, three distinct components can be recognised: the dental organ, the dental papilla and the dental follicle. The dental follicle is a well-defined layer of cells surrounding the tooth germ that is continuous with, and derived from the dental papilla at the cervical loop. It gives rise to the supporting tissues of the tooth to include cementum, alveolar bone and PDL, the fibroblasts of the PDL originating shortly after root development begins (Ten Cate, 1994, Chapter 4 and Beertsen *et al.*, 1997).

Prior to eruption a tooth is covered by a layer of ameloblasts, having completed their formative function develop hemidesmosomes, secrete a basal lamina and become firmly attached to the enamel surface (Schroeder and Listgarten, 1971). An outer layer of cells, composed of the remnants of the dental organ then separate the tooth from the overlying oral epithelium, the two together are known as the reduced enamel epithelium (REE). As the tooth erupts, these cell layers fuse and form a mass of degenerating epithelial cells that provide an epithelial-lined canal through which the tooth erupts. A component of the dento-gingival junction is now present and undergoes further tissue development after the tip of the erupting tooth emerges into the oral cavity. The oral epithelial cells migrate over the reduced enamel epithelium and a process of transformation over the course of 3-4 years then takes place whereby the REE gradually becomes the JE. Immediately following the transformation of the REE, the development of the dento-gingival junction is considered complete.

It has been demonstrated that JE formation does not require the influences of odontogenically-derived CT. OGE has the ability to re-differentiate into the JE phenotype without the intervention of PDL, or even a tooth, as verified by Mackenzie and Tonetti (1995) with the formation of an anatomically "correct" epithelial attachment to titanium dental implants.

2.5 Periodontal disease

2.5.1 Introduction

Periodontal disease is an inflammatory condition resulting in the loss of the tooth supporting structures. In health, there is a dynamic equilibrium between microflora and host defences whereas chronic periodontitis is associated with accumulation of bacterial plaque on the tooth surface, subsequent inflammation of the periodontal tissues (Figure 2.4), apical migration of the epithelial attachment, destruction of the PDL, and loss of crestal alveolar bone (Haffajee and Socransky, 1994 and Page, 2002). Together these processes can lead to formation of a pathologically deepened gingival crevice or pocket.

Figure 2.4: Photomicrograph of the junctional epithelium during disease

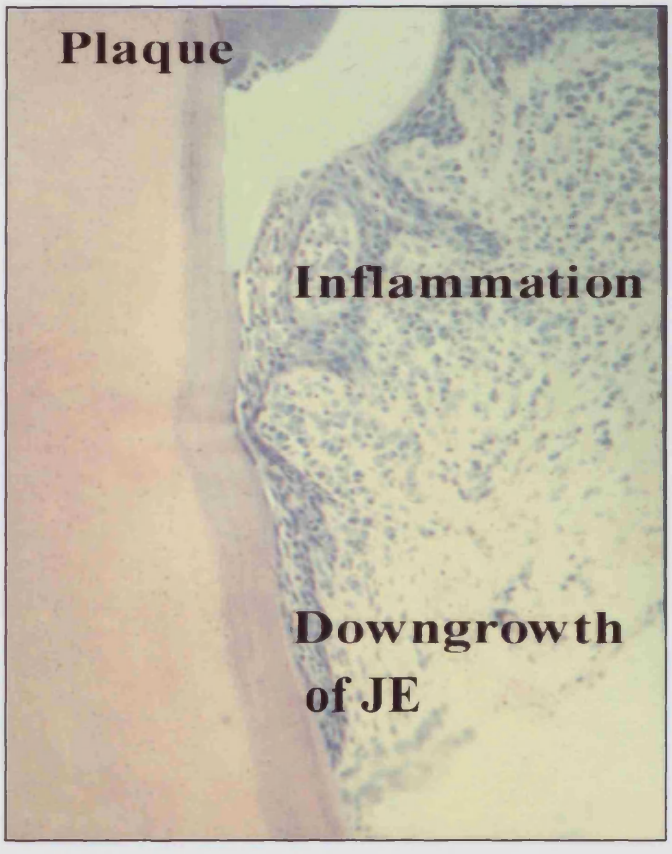

2.5.2 Gingivitis

The term gingivitis is used to describe inflammatory lesions that are confined to the marginal gingiva (Loe *et al.*, 1965). Marginal gingivitis with CT inflammation can persist for extended periods without progression to loss of attachment (Listgarten *et al.*, 1985).

2.5.1 Periodontitis

The early changes associated with the inflammatory gingival response to microbial insult were summarised by Page and Schroeder (1976) and form the basis for current understanding of the host response in human periodontitis (Haffajee and Socransky, 1994). The progression from gingivitis to periodontitis is not obligatory but the progression of gingivitis to a periodontal lesion with pocket formation is invariably associated with proliferation and apical migration of the JE (Schroeder and Listgarten, 1971). Haffajee *et al.* (1983) first proposed the theory that tissue destruction in some lesions occurs during relatively "acute bursts" of disease activity followed by "quiescent" periods. Such periods of active destruction may represent a period when the host is overwhelmed by organisms capable of evading or interfering with the gingival defence systems, or active destruction may be precipitated by an overly aggressive or inappropriate response to microbial stimulation. Whether this is a result of reaction to microbial by-products and/or changes in the host epithelial-mesenchymal signalling remain to be elucidated.

Apical epithelial migration has several important consequences:

- By creating a potential space between the gingiva and the tooth, it enhances the possibility of further plaque accumulation and a persistent inflammatory response.
- It effectively prevents reattachment by isolating the tooth surface from regenerative CT mechanisms: perpetuation of small losses of attachment thus results in the progressive nature of tissue breakdown (Mackenzie, 1987).
- Activation of JE to a migratory phenotype may be a mechanism that actively destroys CT attachment to the tooth via induction and production of proteases (Laiho and Keski-Oja, 1989).

Several possible mechanisms may explain the apical migration of JE during disease:

1) As a response to destruction of the underlying CT, there may be a tendency for the JE to migrate into the space created on the root surface (Grant *et al.*, 1979).
2) "Physiological" regulation of epithelium by its underlying CT prevents apical migration, but damage to this CT may remove its inhibitory effect on epithelial down-growth (Page and Schroeder, 1976).
3) Keratinocytes are stimulated during periodontal disease (by intrinsic host factors and/or extrinsic bacterial products) resulting in active destruction of the attachment apparatus as the JE cells migrate.

Normally, when surface continuity of an epithelium is disrupted, lateral migration of the epithelium is activated and ceases only when the free edges of epithelium meet and continuity is restored, the so-called "free edge effect" (Winter, 1972 and Clark, 1991). However, at the attachment zone epithelial migration does cease, forming an essentially "free" edge.

It has been suggested that further epithelial down-growth is prevented by the density of PDL fibres inserted into the tooth (Goldman and Cohen, 1980) but, interestingly, apical down-growth does not occur around dental implants despite lack of insertion of such a ligament (Listgarten *et al.*, 1991 and Mackenzie and Tonetti, 1995).

Recently, a number of studies have investigated the ability of keratinocytes to produce tissue-degrading mediators, in particular matrix metalloproteinases (MMPs). Studies have found evidence for production of MMP-7 (matrilysin), MMP-8 (collagenase-2) and MMP-9 (gelatinase-B) by JE (Uitto *et al.*, 2002; Kivela-Rajamaki *et al.*, 2003 and Smith *et al.*, 2004), demonstrating perhaps, an ability to degrade its underlying attachment apparatus.

However, the current literature provides no satisfactory explanation either for the normal stability of epithelium at the dento-gingival junction or for the activation of epithelial migration that occurs during the transition from gingivitis to periodontal disease.

2.5.4 Epidemiology

Epidemiological studies indicate that mild to moderate periodontitis affects the majority of the adult population; and that some 8-20% of highly susceptible individuals within the population suffer from a more severe form of the disease (Loe *et al.*, 1986). Clinical classifications of the disease are many and varied. The American Association of Periodontology last updated their classification during 1999 (as reviewed by Armitage, 1999). Briefly, periodontal diseases are categorised as:

1) Chronic - encompassing previous terms such as adult, juvenile and pre-pubertal.
2) Periodontitis as manifestations of systemic disease.
3) Necrotising periodontal diseases.
4) Periodontitis associated with endodontic lesions.
5) Developmental or acquired deformities or conditions.

2.5.5 Aetiology

Ample evidence has revealed that the initiation and progression of periodontal disease is closely associated with quantitative and qualitative changes in the subgingival dental plaque flora (Page and Schroeder, 1976; Listgarten, 1986 and Page, 2002). Examples include:

- Clinical experiments demonstrating that the withdrawal of oral hygiene in healthy mouths results in the accumulation of dental plaque paralleled by the onset of gingivitis.
- Institution of oral hygiene restores the tissues to health.
- A number of topical anti-microbials have been shown to inhibit plaque formation and prevent the onset of gingivitis.
- Animal studies have demonstrated that gnotobiotic rats are free of periodontal destruction (Heijl *et al.*, 1980). Bacteria isolated from human dental plaque introduced into the mouths of such animals can induce periodontal disease.
- Increasing evidence shows that there are differences in the bacterial flora associated with healthy gingival crevices and the various stages of disease (Lovegrove, 2004).

2.5.6 Microbiology of periodontitis

Healthy tissues are associated with a scanty flora located almost entirely supra-gingivally on the tooth surface. Gingivitis has revealed a complex accumulation 1-20 cells thick comprising mainly gram-positive bacteria including: *Streptococcus*, spirochetes and *actinomyces* species. In developing gingivitis the layers extend to 100-300 cells, *actinomyces* predominate but there is an increase in strict anaerobes and gram-negative organisms such as *porphyromonas gingivalis* and *prevotella intermedia.* In long-standing gingivitis, gram-negative bacteria may account for 35 percent of the total, the majority located subgingivally.

Periodontal bacterial pathogens persist in colonised sites by evading host defence mechanisms through the production of factors such as leukotoxins or lymphocyte-suppressing factors. Various bacterial products such as toxins (Listgarten, 1987) lipopolysaccharide (Nair *et al.*, 1983) and proteases (Uitto *et al.*, 1988) have been shown to have an array of deleterious effects on host cells. Further, mucosal keratinocytes and fibroblasts are capable of adapting under the influence of such products into highly destructive cellular phenotypes capable of expression of, or mediating activity of, host enzymes such as MMPs (Birkedal-Hanson,

1993). Ultimately they are capable of inducing the inflammatory changes clinically observed in periodontal lesions (Zambon *et al.*, 1994, Chapter 1).

2.5.7 Collagenases

Much interest has centred on the ability of periodontal pathogens to secrete collagenases capable of degrading human collagen and hence the CTs involved with attachment. Seifter and Harper (1970) found that only a small group of bacteria are capable of such a feat, in particular *Porphyromonas gingivalis* appears capable of degrading type I collagen. More recent investigations have demonstrated that the majority of the collagenase activity present in gingival fluids is host derived (Uitto *et al.*, 1990). Salonen *et al.* (1991b) found that oral-gingival derived keratinocytes grown in culture were capable of degrading an underlying collagen substratum. This only occurred in the absence of a basement membrane, which may be the signal for these cells to secrete matrix-degrading enzymes.

2.5.8 Pathogenesis of periodontal disease

Mechanisms involved in the induction and progression of the destructive chronic inflammatory lesion are unclear. Although plaque organisms have been demonstrated within periodontal tissues there is little evidence that tissue damage is the result of direct bacterial invasion. Page and Schroeder (1976) charted histologically the progression of periodontal disease following plaque accumulation thus:

Day 2-4 **The initial lesion** – This is only detectable histologically, it being localised around the base of the gingival sulcus. There occurs vasodilatation, fluid exudate, cellular exudation, enhanced transmigration of PMNs and disruption of intercellular spaces.

Day 4-7 **The early lesion** - Exacerbation of the initial lesion with disruption of intercellular spaces, failure to maintain attachment to enamel, deepening of the sulcus, subgingival plaque, lymphocytic infiltration, cytopathic changes in gingival fibroblasts, loss of collagen, hyperplasia of JE and rete ridge formation.

2-3 weeks **The established lesion** - Further disruption and hyperplasia of JE, ulceration of pocket epithelium, predominance of plasma cell infiltrate, continued destruction of gingival CT and expansion of volume of tissue involved with varying attempts at repair.

1 month + **The advanced lesion** - Characterised by the destruction of the CT attachment to the root of the tooth, loss of alveolar bone and pocket formation. As the area of inflammatory infiltrate increases, there is destruction of collagen in the supra-alveolar CT and the fibres lose their attachment to cementum. This is accompanied by the death of cementoblasts and apical migration of the JE to cover the denuded root surface to the level of the first intact attachment fibres, resulting in true pocket formation. Periods of quiescence follow.

2.5.9 The role of host immunity in periodontitis

Activation of humoral immunity leads to the differentiation of plasma cells and the production of immunoglobulins, which could be involved in tissue injury through the activation of complement and antibody mediated hypersensitivity reactions. Products of microbial plaque are also good activators of complement by the alternate pathway. Both pathways result in the generation of biologically active molecules, which can induce vascular permeability and are chemotactic for PMNs (Travis *et al.*, 2000).

Cell mediated immunity to oral bacteria is active in periodontal disease and type IV delayed hypersensitivity reactions could contribute to tissue injury. The potentially damaging effects of activation of T-cells by plaque antigens could be mediated by direct cytotoxic t-cell activity or through release of lymphocytes (Kinane, 2000).

The cells of the human oral epithelium are an active part of the host defence system rather than simply an inert barrier to bacteria and other noxious stimuli. Hillman *et al.* (1995) proposed that the gingival epithelium might participate actively in the inflammatory process and that keratinocytes secreting cytokines such as interleukin-1β (IL-1β) during inflammation may control the activity of epithelial cells and adjacent inflammatory cells of the CT. However, it remains unclear if epithelial cells contribute to tissue breakdown in periodontitis (Suchett-Kaye *et al.*, 1998).

2.5.10 Clinical treatments

As periodontal disease is characterised by a loss of CT attachment to teeth, the two goals of periodontal therapy are to halt the attachment loss and to regenerate the lost periodontal apparatus (Piche *et al.*, 1989). To date the most common treatment for chronic periodontitis is regular dental scaling and root-planning. This requires thorough removal of deposits (plaque,

calculus and stain) from the tooth and root surface and removal of cementum or surface dentine that is rough and impregnated with calculus. This decreases the bacterial load within the surrounding periodontal tissues allowing repair of the epithelial attachment. Maintenance of good oral hygiene by the patient is then essential to stop disease progression (Cobb, 1996).

These procedures however do not regenerate original tissue architecture. Several surgical techniques have been developed to aid in this including guided tissue regeneration, bone grafting and the use of enamel matrix derivatives. These techniques selectively inhibit epithelial down-growth allowing proliferation of the PDL to correctly restore the soft tissue architecture. Despite much clinical application, there remains an absence of clinical evidence that regenerative therapies increase the life span of teeth (Becker, 1999 and Clauser *et al.*, 2003).

2.6 The fibroblast phenotype

2.6.1 Introduction

Fibroblasts are the predominant cell type in sub-epithelial CTs and are responsible for the major part of the production of extracellular matrix and growth factors. They perform vital roles during normal function, development, regeneration and pathologic alterations (Smith, 1997 and Lekic *et al.*, 2001). In spite of their widespread anatomical distribution and ease with which they are grown in culture, fibroblasts remain a poorly defined cell type.

2.6.2 Fibroblasts of the periodontium

The periodontium is composed of a number of discrete CTs: cementum, alveolar bone, PDL and gingiva each with a unique architecture, composition and function. This diversity makes periodontal wound healing a more complex process than general soft tissue healing, particularly because of the interaction between hard and soft tissues as well as epithelium (Irwin *et al.*, 1994). The two populations of fibroblasts within the periodontium that this study will examine are the oral-gingival fibroblasts derived from the ectoderm and PDL fibroblasts derived from the dental follicle (mesoderm) (Ten Cate, chapter 4, 1994).

2.6.2.1 Periodontal ligament fibroblasts

Due to their unique location, PDL fibroblasts together with osteoblasts and cementoblasts have the responsibility of producing, maintaining and remodelling the PDL, cementum and bone. It has been proposed that only cells from the PDL have the potential to create new CT attachment to the root surface (Nyman *et al.*, 1982). Evidence exists that suggests a proportion of PDL fibroblasts express osteoblast-like properties that OGFs lack, (Basdra and Komposch, 1997) which would in part explain the ability of PDL fibroblasts to form mineralised nodules in culture and produce the enzyme alkaline phosphatase (ALP) (see chapter 2.6.3). Therefore, PDL fibroblasts possess the ability to form and possibly regenerate both hard and soft CT extracellular matrices.

2.6.2.2 Oral-gingival fibroblasts

In contrast, OGFs have the relatively simpler task of producing and maintaining the soft tissue lamina propria of the gingiva. They are responsible for synthesising and secreting components of the extracellular matrix and play an important part in the remodelling of CTs during periodontal inflammation (Hassell and Stanek, 1983 and McCulloch and Bordin, 1991).

2.6.3 Fibroblast heterogeneity

The apparent similarity of fibroblasts in culture belies the extensive heterogeneity now thought to exist among these cells. Although there are no clear phenotypic markers that discriminate different types of fibroblasts from each other, evidence from a number of studies indicates that fibroblasts residing within CTs including the gingiva and PDL are heterogeneous, with a number of cell subpopulations exhibiting different functional activities (Hassell and Stanek, 1983; Mackenzie *et al.*, 1993a; Irwin *et al.*, 1994 and Schor, 1995). A growing body of literature has shown that when fibroblasts from normal and diseased tissues are grown *in vitro*, there exist large variations in terms of matrix biosynthesis, enzyme activities, expression of surface proteins, response to inflammatory mediators and proliferative potentials. For example, Hassell and Stanek (1983) observed a considerable degree of stable variations in synthetic properties and proliferative rates amongst six morphologically indistinguishable cultures of human diploid fibroblasts derived from a single biopsy of a normal gingival papilla tip.

Heterogeneity has been suggested to be of fundamental importance for normal functioning as well as wound healing of CTs, in particularly for the periodontium. Studies by Schor and Schor (1987) and Mackenzie (1987) suggested that specificity of a fibroblast phenotype might influence not only the metabolism of CTs but also of adjacent epithelia. Heterogeneity in production of growth factors and in response to cytokines could be important for the regional specific differentiation pattern of adjacent epithelium (Grøn, 2001). Fibroblasts are capable of synthesizing an array of biological mediators that influence epithelial behaviour. Typical interactions involve molecules such as keratinocyte growth factor (KGF) that are targeted to receptors on epithelial cells (Boukamp *et al.*, 1990). Conversely, keratinocytes can induce specific fibroblast gene expression (Smola *et al.*, 1993). Therefore, a feedback system might result as an important part in the interaction between the two cell types (Maas-Szabowski and Shimotoyodome, 1999). There is now considerable interest in determining the role of fibroblast derived cytokines in remodelling of diseased periodontal tissues.

2.6.4 Fibroblast characterisation in culture

Morphologically, gingival and PDL cells appear to be similar, having the spindle-shaped elongated appearance characteristic of fibroblast-like cells. However, Piche *et al.* (1989) found at confluence the morphology of PDL cells to differ from those of the oral-gingival region. In addition, the two populations have been shown to differ in terms of size,

proliferative ability and in expression of extracellular macromolecules (Otsuka and Pitaru, 1988; Somerman *et al.*, 1988 and Mariotti and Cochran, 1990). PDL cells *in vitro* have been found to have osteoblast-like characteristics, which include high levels of ALP, production of predominately type I collagen and production of osteonectin (Wasi *et al.*, 1984). Typically, cells derived from attached gingivae have a fibroblastic phenotype while those derived from PDL/cementum have been reported to have either fibroblastic or osteoblastic characteristics.

2.6.4.1 Alkaline phosphatase

The term ALP is broad and describes a group of enzymes that have the capacity to remove phosphate moieties from organic substrates at an alkaline pH. In humans, at least four ALP isoenzymes are coded by separate gene loci: placental, placental-like, intestinal and tissue non-specific (the so called liver/bone/kidney type) (Harris, 1990). Nojima *et al.* (1990) found that ALP in bovine PDL cells was the tissue non-specific type which as well as bone mineralisation has been observed in vascular endothelia of small arterioles in the brain and heart. Goseki *et al.* (1995) first isolated ALP cDNA from PDL and confirmed it was identical to that of the tissue-non-specific type.

When associated with cell membranes ALP is thought to play a role in ion transport, providing phosphate ions at mineralisation sites. It has been suggested that hydrolysis of monophosphate esters by the enzyme produces a high concentration of phosphates leading to supersaturation and subsequent precipitation of calcium phosphate salts in the collagenous substrate (Beertsen and Van den Bos, 1991). In doing so, Beertsen and Everts (1990) have suggested that ALP may play a role in the deposition of calcified layers along exposed calcified surfaces. The authors found that regional variations of ALP activity in the periodontium of the rat molar were associated with regional variations in cementum thickness. Groeneveld *et al.* (1993) has shown that enzyme activity is higher adjacent to more recently deposited cellular cementum compared with acellular cementum.

Numerous studies have shown that gingival fibroblasts, like those in most other tissues contain relatively low levels of ALP activity compared to cells derived from PDL or bone (Kawase *et al.*, 1986; Somerman *et al.*, 1988 and Piche *et al.*, 1989). Further work by Gao *et al.* (1999) found that ALP activity was highest in osteoblasts, moderate in PDL and lowest in OGF cells.

Abe *et al.* (1996) conducted ultrahistochemical investigation of chronically inflamed human gingiva and found differential expression of ALP activity by OGF depending on tissue location. The majority of fibroblasts located in the inflamed gingival CT, an area with dense infiltration of inflammatory cells and scant collagen fibrils, exhibited intense membrane ALP activity, whereas the majority of fibroblasts in the adjacent non-inflamed gingival CT showed little or no membrane ALP activity. Groeneveld *et al.* (1996) found that in the CTs of the outer part of the free gingiva and that of the attached gingiva there was hardly any detectable activity except for the walls of the blood vessels. In the inner part of the gingiva, which underlies the JE, higher levels were found. This sudden transition from ALP-rich to ALP-poor fibroblasts suggests differing phenotypes localised to their own domain. This finding supports a hypothesis that the fibroblasts of the PDL and the inner part of the gingivae are involved in the processes leading to cementum formation and possible regeneration. It is feasible that those fibroblasts bordering the apical termination of the JE might also influence the phenotype of this epithelial tissue.

2.7 The epithelial phenotype

2.7.1 Introduction

During embryologic development, the phenotype of an epithelium is developmentally determined by interactions with its adjacent CT (Kollar and Baird, 1970) and such interactions persist in later life to influence epithelial maintenance and repair (Schweizer *et al.*, 1984; Hill and Mackenzie, 1984; Mackenzie, 1984 and Cunha *et al.*, 1985). These interactions have been considered as either directive (instructive) or permissive in nature (Saxen, 1977). Directive influences are distinguished by the "commitment" or permanent change that occurs in responding tissues, whereas permissive influences do not determine the phenotype but are necessary for its expression. This "developmental" phenotype can however be experimentally redirected into new phenotypic patterns by recombination with other CTs (Hill and Mackenzie, 1984; Mackenzie, 1984 and Cunha *et al.*, 1985).

The structure of human oral mucosa exhibits marked regional variations encompassing parakeratinised, orthokeratinised, keratinised, and non-keratinised epithelia. This histological variation across such a small anatomical distance makes the oral-gingival epithelia particularly important in the study of epithelial cell characteristics versus mesenchymal instruction in determining epithelial differentiation (Lindberg and Rheinwald, 1990).

2.7.2 Connective tissue influences

Breathnach (1971) found that human oral mucosa acquires its adult pattern of differentiation and keratinisation at the fifth month post-conception, approximately the same time as human skin. This goes some way in dictating that regional differences in epithelia are not brought about purely by demands placed upon them by function.

The gingival sub-epithelial CT (the lamina propria) provides instructive influences for the normal maturation of gingival stratified squamous epithelia and these influences are said to be absent from deep CT (Mackenzie and Hill, 1984; Fusenig *et al.*, 1991 and 1994 and Mackenzie *et al.*, 1993). Evidence for this was provided by Mackenzie and Hill (1981). Full thickness mouse oral mucosa was grafted to deep CT in an *in vitro* model system. The epithelium differentiated normally over its own lamina propria however, there was a small outgrowth of epithelium onto the deep CT that did not migrate to epithelialise the whole graft bed. This outgrowth was proliferative, formed a basal lamina, shared a passive non-migratory

behaviour and acquired a differentiation pattern similar to JE (See chapter 2.7.6.4). It was characterized by co-expression of the basal cell markers of a stratifying epithelium (CK4 and 5) with suprabasal expression of markers typical of a simple epithelium (CK8, 18, 19 and Lewis blood group antigens).

2.7.3 The junctional phenotype

Although very little is known about the interactions involved in the formation and maintenance of JE *in vivo,* evidence indicates that two basic processes are in operation:

1) Cell-cell interactions

The anatomical arrangement of the sulcular region is such that the gingival CT supports OGE, whereas the JE is spatially related to PDL. As discussed in chapter 2.6.3 evidence from a number of studies indicates that fibroblasts residing within CT, including the periodontium, are heterogeneous. The PDL being odontogenically derived differs in its developmental history to gingival CT and thus, possibly exerts varying levels of, or indeed different instructive and permissive influences on its overlying JE. Alternatively, if periodontal CT is a functionally "deep" CT it may lack both directive and permissive influences. Therefore, the pattern of differentiation of JE could be viewed as a regionally specific phenotype influenced by the periodontal CTs lack of signalling molecules.

The regenerative properties of the attachment zone provide further evidence of this phenomenon. When the JE is surgically removed a functionally and structurally identical tissue reforms from the residual, phenotypically different OGE (Schroeder and Listgarten, 1971). This suggests that the new epithelium, although derived from OGE, re-differentiates into JE on appositional growth against the PDL.

2) Epithelium-dental surface interactions

Biopsies of the "gingiva" reformed around oral implants stained for cytokeratins (CK) in a pattern that was phenotypically indistinguishable from those of natural teeth (Mackenzie and Tonetti, 1995). This being the case despite there being no involvement of odontogenic tissues. This provides evidence that the formation of JE, although possibly directed by underlying CT does not necessarily require its developmental odontogenic CT, the PDL. More likely an explanation is that teeth (and osseointegrated implants) create a "geometry" of apposition of epithelium to a deep CT.

Oral epithelial cells have the capacity to attach and migrate on mineralised root surfaces, deposit a basal lamina and stratify. This indicates that contact with tooth mineral and/or proteins adsorbed onto its surface affect epithelial cell attachment, migration and differentiation. This finding indicates that cell-to-tooth surface contact induces the polarised secretion of extracellular matrix proteins, which in turn may affect cell differentiation. Keratin typing and immunohistochemical (IHC) staining of the internal and external basal laminae of JE indicate that the basal cells by virtue of their tooth contact are different from those facing the CT (Salonen *et al.*, 1989).

In summary, regional variations in epithelial phenotype may thus reflect phenotypic differences between fibroblast subpopulations in the sub-epithelial CT (McKeown *et al.*, 2003).

2.7.4 Inflammatory influences

If non-permissiveness of periodontal CT is accepted as a working hypothesis, the question arises as to why apical migration of the epithelium occurs at all during periodontal disease. The epithelium adjacent to mucosal transplants fails to epithelialise the adjacent deep CT despite the absence of any physical barrier to its outgrowth (Listgarten *et al.*, 1991). Thus, loss of attachment of CT to the tooth would not in itself be sufficient to initiate epithelial down-growth.

The CT associated with the dento-gingival junction is often inflamed and it has been suggested that factors associated with inflammation can substitute for permissive factors produced by dermal cells, or can perhaps act to favour selective outgrowth of fibroblasts of the permissive phenotype. Kristofferson *et al.* (1983) proposed that it is for this reason the OSE and OGE phenotypes are markedly different (non-keratinised versus keratinised) yet both are supported by the gingival lamina propria. A direct role for inflammation in stimulating epithelial growth and differentiation is suggested by the behaviour of the rests of Malassez in periapical granulomas (Gao *et al.*, 1988). In their quiescent state within healthy PDL these rests strongly express only CK5 and 19, however, under the influence of inflammation they become activated to a proliferative state and express additional keratins characteristic of both stratifying and simple epithelia. Normally the CT is responding to signals from the epithelium itself, but similar signals are also generated by inflammation, which may alter epithelial growth and migration as discussed below.

2.7.5 Characterisation of the oral epithelial phenotypes

Although continuous with OSE and OGE, JE differs from them histologically and ultrastructurally (Schroeder and Listgarten, 1971). It has been distinguished in terms of expression of the cytokeratins (Morgan *et al.*, 1986; Shabana *et al.*, 1991 and Mackenzie *et al.*, 1991) blood group antigens (Steffensen *et al.*, 1987 and Mackenzie *et al.*, 1989) integrins (Hormia *et al.*, 1990) intracellular adhesion molecule-1 (Crawford and Hopp, 1990) type VIII collagen (Salonen *et al.*, 1991a) lectin reactivity (Bampton *et al.*, 1991) desmoplakins I+II (Carmichael *et al.*, 1991) MMP-7 (Uitto *et al.*, 2002) and MMP-9 (Smith *et al.*, 2004). Differences in expression patterns can therefore be used to demarcate the epithelia of the gingiva, particular the JE, by staining *ex vivo* sections and cells cultured *in vitro*.

2.7.6 Cytokeratins

2.7.6.1 Introduction

Cytokeratins are 7-11nm tonofilaments composed of polypeptides of a wide range of sizes (from about 40,000 to over 200,000 M_r) that vary both between different cell types and in the same cell type and between different species. They are the products of two distinct gene families (Fuchs *et al.*, 1981) composed of smaller acidic type-I filaments and the larger, more basic type-II filaments. They are assigned numbers depending upon their relative migration by charge and molecular weight on a two-dimensional polyacrylamide gel. The basic proteins numbered 1-8 and the acidic proteins numbered 9 through 20.

2.7.6.2 Keratin expression patterns

Development of monoclonal antibodies (mABs) to individual keratin polypeptides has enabled *in-situ* studies to be carried out. It has been found that keratins are expressed in size-ranked pairs containing one of each type of keratin except keratins 15 and 19 that appear to be unpaired (Sun *et al.*, 1985 and Waseem *et al.*, 1998). These are summarised in table 2.1.

Table 2.1: Epithelial type and paired keratin expression

Acidic	Basic	Markers of:
10	1	Suprabasal cells of stratifying keratinised epithelia
13	4	Suprabasal cells of stratifying non-keratinised epithelia
14	5	Basal layers of stratifying epithelia (and suprabasal in culture)
16	6	Suprabasal cells of rapidly proliferating stratifying epithelia
18	8	Simple epithelia
15		Basal cells of stratified epithelia (sporadic distribution in culture)
19		Simple and transitional epithelia

Cytokeratin expression in any epithelium is one of its most invariable characteristics, so much so that keratin mapping is now considered to be a very sensitive and specific method for following the development and differentiation of epithelial tissue (Moll and Franke, 1982; Ouhayoun and Gosselin *et al.*, 1985 and Gosselin and Magloire, 1990). There have been a number of studies of keratin expression by the different oral epithelia: alveolar mucosa (Ouhayoun and Gosselin, 1985) buccal mucosa, tongue and hard palate (Clausen *et al.*, 1986) cheek and hard palate (Morgan *et al.*, 1987) and gingiva (Shabana *et al.*, 1991; Mackenzie *et al.*, 1991 and Mackenzie and Gao, 1993).

First Ouhayoun and Gosselin (1985) and then Morgan *et al.* (1986) using a panel of mABs specific for single or small defined groups of keratin peptides, showed that the three epithelia of the human gingiva each have a distinct pattern of expression of keratin polypeptides reflecting their histologic type and differentiation state. In general, basal cells in all stratified oral epithelia express similar keratins, CK5, 14 and 15, while the suprabasal cells express a specific set of markers indicating commitment to a distinct program of differentiation. CK4 and 13 relate to non-keratinising stratified epithelia, CK1 and 10 keratinising epithelia and CK6 and 16 indicating a proliferative phenotype. These differences are summarised in table 2.2.

Table 2.2: Regional expression of cytokeratins throughout human gingivae

Phenotype	Basal keratin expression	Suprabasal keratin expression
OGE	CK5, 14 and 15 (19 at tips of rete (Morgan *et al.*, 1987))	CK1 and 10 (described as patchy) CK5 and 14 CK6 and 16
OSE	CK5, 14 and 15 (8,18,19 described by some (Bampton *et al.*, 1991))	CK4 and 13 CK6 and 16
JE	CK5, 14, 15 and 19 throughout all levels (CK8 and 18 variable and faint) (CK6 and 16 present in the developing JE (Feghali-Assaly and Sawaf, 1994))	

2.7.6.3 Oral-gingival and oral-sulcular epithelium

OGE and OSE express different sets of keratins in the suprabasal layers. The suprabasal compartment above the level of rete pegs to include the upper part of stratum spinosum and stratum granulosum of OGE expresses CK1 and 10. Expression is less pronounced in the stratum corneum. These cytokeratins characterise the orthokeratinising, terminally differentiating epidermal type. OSE expresses CK4 and 13, characteristically expressed suprabasally by non-keratinised stratified squamous epithelia. Sporadic suprabasal cells

within OGE samples also exhibited CK4/13 possibly as a response to inflammation (Morgan *et al.*, 1987). Cytokeratins 6 and 16 stain suprabasal cells predominately in keratinised regions of OGE and to include focal staining of OSE.

2.7.6.4 Junctional epithelium

Ultrastructural studies initially characterized the JE as an undifferentiated epithelium (Schroeder and Listgarten, 1971) and immunohistochemical studies showed its lack of expression of the major differentiation products that characterise other oral epithelia (Morgan *et al.*, 1986 and Steffensen *et al.*, 1987). However, it is now clear that JE is far from undifferentiated; several studies have shown that JE has a highly unusual pattern of differentiation in which markers typical of stratifying and simple epithelia are co-expressed. The JE is unique with respect to expression of CK19 and the simple cytokeratins 7, 8 and 18 (Mackenzie *et al.*, 1991). Cytokeratin 19 expression is differential across the distribution of the JE; within the coronal portion of the JE tissue, it strongly expresses CK19 in the basal cells adjacent to the CT and in the cells attached to the tooth surface, but more weakly within the interior. This differential staining would also imply that the cells are undergoing differentiation as they move away from the tooth surface or the CT (Salonen *et al.*, 1989). Interestingly, JE cells *in vivo* have not been found to express CK6 or 16, despite these being associated with tissues of rapid turnover. Feghali-Assaly *et al.* (1994 and 1997) investigated the CK profile within the developing JE of partially erupted teeth and found characteristics of a transitional epithelium, developing from a simple to stratified epithelium expressing not only CK5 and 19, but CK4, 13 and 16 also.

2.7.7 Lectins

Lectins are non-enzymatic proteins or glycoproteins of non-immune origin that bind carbohydrates and can agglutinate cells and/or precipitate glycoconjugates. They are involved in a variety of cellular processes including enzyme trafficking and immune function. Lectins have been used extensively to study skin keratinocytes, both *in-situ* and as isolated cells, and to study normal differentiation and pathological conditions (Goldstein and Hayes, 1978 and Schaumburg-Lever, 1990). Although there have been studies describing their reactivity within oral mucosa there have been few studies of their expression in gingiva. Rittman *et al.* (1982) demonstrated that the lectin binding intensity of the JE in the mouse differed from that of the OSE and OGE. Bampton *et al.* (1991) devised a panning technique to separate the JE phenotype dependant on lectin reactivity in normal human junctional, sulcular, and attached

gingival epithelia. They then confirmed the identity of the epithelia by parallel staining with cytokeratin antibodies. It was established that the reactivity of the lectin *dolichos biflorus agglutinin* with JE was specific.

2.7.8 Matrix metalloproteinase-7

Uitto *et al.* (2002) recently revealed that Matrilysin, an MMP that is expressed in exocrine and mucosal epithelia, is expressed in suprabasal cells of the JE facing the teeth and in the epithelial cell rests of Malassez. Monoclonal antibodies to MMP-7 proved successful in identifying JE cells in a tissue culture model mimicking JE (Uitto *et al.*, 2002).

2.7.9 Intercellular adhesion molecule-1

Intercellular adhesion molecule-1 (ICAM-1) is a widely distributed cell adhesion molecule involved in interactions with epithelial cells. Crawford and Hopp (1990) found ICAM-1 to be selectively expressed by JE cells in healthy gingivae at detectable levels. Moughal *et al.* (1992) confirmed this expression and found that there was a gradient, with the strongest staining at the crevicular aspect. ICAM-1 expression by keratinocytes is induced by biological mediators such as IL-1 and lipopolysaccharide (LPS); it is therefore likely that the variation in ICAM-1 expression in gingival tissues reflects that variation in the distribution of biological response modifiers to bacterial load.

2.8 Cell culture

2.8.1 Keratinocytes in culture

Mlineck and Buchner (1975) first developed a simplified method for growing gingival epithelium by explant outgrowth. However, it was Rheinwald and Green (1975), using a feeder layer of irradiated mouse fibroblasts, who first established the technique of growing human epidermal keratinocytes that allowed them to be successfully sub-cultured.

2.8.2 Junctional epithelium in culture

Salonen and Santti (1985) were the first to attempt to construct an *in vitro* JE model by simulating the JE attachment zone by growing oral epithelial cells on a membrane. It was Altman *et al.* (1988) who first successfully cultured and characterised true JE derived cells albeit from the rat.

As discussed in chapter 2.7.5 work then concentrated on finding markers that differentiate between OGE and JE and that were retained *in vitro*. Bampton *et al.* (1991) using DBA in a panning technique successfully isolated and cultured keratinocytes from human JE and compared their phenotype *in vitro* with that of cells grown from the oral-sulcular and attached OGE. All cells expressed CK4, 7, 14, 18 and 19 indicating, at least with respect to their keratin expression, that cells from the three regions of the gingiva may revert to one phenotype in culture.

Gao and Mackenzie (1992) demonstrated that during standardized *in vitro* culture conditions OGE lost expression of the differentiation markers CK1 and 10 and acquired some expression of CK19, but less so than that of JE.

Matsuyama and Izumi (1997) established a culture of human JE cells derived from gingival tissue attached to the tooth surface, and characterised these cells immunocytochemically and ultra-structurally. Again, the expression pattern of CK19 was observed not only by cells from junctional tissue but also by cells from gingival tissue. However, as with Bampton's work, DBA was specific in only reacting with cells from the junctional tissue.

Studies have been conducted into possible modulators of cytokeratin expression by keratinocytes in culture, specifically retinoic acid. This has shown minor effects on the

marker expression of JE but markedly enhanced expression of cytokeratins 8, 18, 19, vimentin and ICAM-1 in OGE. These observations indicate that the response to retinoic acid can affect the phenotypes expressed by epithelia *in vitro* and suggest that such mechanisms may be related to the different phenotypic patterns expressed by gingival epithelia *in vivo* (Gao and Mackenzie, 1996).

These results support the hypothesis that epithelial phenotype is influenced by the sub-epithelial mesenchyme, and therefore may be partly responsible for the unique phenotype of the JE (Mackenzie, 1987). It is likely that epithelial-mesenchymal interactions act to direct and maintain epithelial differentiation *in vivo* however, there are also likely to be intrinsic differences between epithelia that help maintain their phenotype. This has been demonstrated by phenotypic maintenance of epithelia under *in vitro* culture conditions despite the removal of their specific underlying mesenchymal tissues (Asselineau *et al.*, 1986 and Delcourt-Huard *et al.*, 1997).

2.8.3 Media

Complex supplemented media have been formulated to allow epithelial growth (Wu *et al.*, 1982). Generally, to a basal medium such as DMEM is added serum, hydrocortisone (promotes cell attachment and proliferation, can induce cell differentiation) EGF (mitogen for epithelial and fibroblast cells that delays terminal differentiation) and cholera toxin (mitogen for normal epithelia, promotes growth and induces differentiation). Vitamin A and retinoids have also been shown to have marked effects on cultured keratinocytes, higher levels increasing proliferation, promoting desmosome formation and increasing CK19 expression (Eckert and Green, 1984 and Kautsky *et al.*, 1995).

2.8.4 Holoclones, meroclones and paraclones

Epithelial renewal depends ultimately on a subpopulation of stem cells present within the proliferative cell population (Cotsarelis *et al.*, 1999). Within epithelial culture systems, colonies are formed from individual cells resulting in "clonal colonies". Barrandon and Green (1985 and 1987) predicted that once such clones have been derived from a single keratinocyte their growth potential can be estimated from the resulting morphology:

Holoclones - that have the greatest reproductive capacity, fewer than 5% of the colonies formed by holoclones abort and terminally differentiate. They typically consist of small, rounded cells that may be repeatedly amplified and are believed to contain the stem cell component.

Paraclones - that contain exclusively cells with a short replicative lifespan after which they uniformly abort and terminally differentiate. They appear somewhat dissociated, are generally larger and irregularly shaped and fail to passage successfully.

Meroclones - that appear as intermediate colony forms containing cells of different growth potential.

2.9 Organotypic culture

2.9.1 Introduction

Keratinocytes and fibroblasts are the most prominent cell type in epidermal and dermal tissue compartments respectively; therefore, cellular interactions during epithelial development are thought to incorporate both:

1) Direct keratinocyte-fibroblast contact and
2) Exchange of soluble mediators that function in either an autocrine or paracrine manner.

Given the complex nature of the developmental microenvironment, it has been difficult to determine the exact nature and timing of these interactions *in vivo*.

Stratifying squamous epithelia differ regionally in their suprabasal expression of differentiation markers but these characteristic patterns of *in vivo* marker expression are at least partially lost when isolated epithelial cells are grown *in vitro* (Mackenzie and Fusenig, 1983). Using the *in vitro* model systems that follow, many aspects of tissue homeostasis and control have been investigated.

2.9.2 Collagen lattice systems

Fibroblast populated collagen lattices represent a model system that addresses some of the limitations of monolayer cultures. It was Bell *et al.* (1981) who constructed the first lattice systems using grafts consisting of fibroblasts cast in collagen and seeded with epidermal cells. Later advances in this technique have allowed growth on various substrates and membranes (Nishikawa *et al.*, 1987).

2.9.3 Organotypic models or "skin equivalents"

The closest *in vitro* physiological conditions for epithelial differentiation are reproduced within organotypic culture systems in which epithelial cells are grown on fibroblast containing collagen matrices. Asselineau *et al.* (1986) and Lenoir and Bernard (1990) have demonstrated more normal *in vivo*-like patterns of stratification and cell morphology. More ordered proliferation, expression of differentiation markers and reformation of a basal lamina has been demonstrated within these systems (Smola *et al.*, 1998). Keratinocytes have been shown to express integrins, ICAM-1 and suprabasal differentiation markers typical of the epithelia of origin (Tomakidi *et al.*, 1999; Gao and Mackenzie, 1996 and Grøn and

Andersson, 1999). In such cultures, other epithelia including oral mucosa similarly express more normal phenotypic patterns (Shabana *et al.*, 1991). It has been suggested by several parties that growth of keratinocytes on CT equivalents is a valid procedure for investigating the spatial organisation of physiological processes, the role of cell-to-cell interactions, and gene expression (Garlick and Taichman, 1994 and Stark and Baur, 1999).

The latest research in skin organotypics, in particular that by Mass-Szabowski *et al.* (1999, 2000 and 2001) have begun to dissect intricate growth factor mediated processes and autocrine loops involved in epithelial growth and differentiation, in particular a role for KGF in normal epithelial growth and development (Costea *et al.*, 2003).

2.9.4 The gingival organotypic culture

Gosselin *et al.* (1989) first used gingival keratinocytes within an organotypic method consisting of human dermal fibroblasts. Odioso and Doyle (1995) used homotypic combinations of gingival fibroblasts to support gingival epithelial cells within a submerged model. Garlick *et al.* (1996) and Delcourt-huard and Corlu (1997) further refined the technique to allow epithelial maturation at the air-liquid interface. Tomakidi *et al.* (1997) using a similar raised configuration, found formation of non-keratinising stratified squamous epithelium with morphological and biochemical characteristics of non-keratinised gingiva and basement membrane formation containing type IV collagen and laminin. Latest methodologies have led to the construction of large area organotypic cultures of oral mucosa that may prove useful in intra-oral grafting procedures (Igarashi *et al.*, 2003).

2.9.5 The junctional organotypic culture

Several *in vitro* models have been developed for studying the structure and function of the JE. Salonen and Santti (1983) examined ultrastructural and immunohistochemical similarities in the attachment of human oral epithelium to the tooth *in vivo* using micro-porous filters and decalcified dentin matrix slices as culture substratum. Further, Salonen and Santti (1985) attempted to develop a JE model using gingival explants cultured on a protein-binding membrane. Epithelial cells migrated from the cut edge of epithelium and CT forming a sheet of tissue between the explant and the membrane substratum. The resultant epithelium, although not directly derived from the JE was phenotypically similar to JE cells *in vivo* by nature of its cytokeratin expression.

Pan and Firth (1995) were the first to describe an organotypic model using cultured JE cells albeit porcine derived. Papaioannou and Cassiman (1999) were the first to describe a human JE organotypic culture system using "pocket epithelium" grown on a polyester trans-well system with a keratinocyte serum-free medium. Although multi-layered epithelium was successfully cultured, immunohistochemically it confusingly resembled both junctional and "pocket" (sulcular) epithelia. An organotypic *in vitro* model that mimics the dento-epithelial junction was proposed by Oksanen and Hormia (2002) using rat enamel to provide the added physiological copy of a hard tissue surface and thus the internal basement membrane.

To date all JE based organotypic culture studies have involved the use of oral keratinocytes and a substrate (either polycarbonate membrane or dentinal tooth slice) to induce re-differentiation of the OGE into the JE phenotype.

2.10 Cytokines and their maintenance of epithelium

2.10.1 Introduction

Cytokines are small (glyco)proteins produced by cells and are capable of affecting the activities of the same (autocrine) or other cell types (paracrine). They have been implicated in the pathogenesis of many diseases (Kreuger *et al.*, 1990; Alexander and Damoulis, 1994 and Dinarello, 2002). They are ubiquitous; being produced by all cells and deliver signals over relatively short distances by binding to high affinity receptors at extremely low concentrations (Meager, 1991). A given cytokine may have different (pleiotropic) effects on different types of cells, and there are often overlapping effects (redundancy) with several different cytokines having a similar effect on the same cell type (Howells, 1995). Resting cells produce low levels of cytokines but production is upregulated when they are activated, typically by the actions of other cytokines. Cytokines thus function in networks with the actions of individual cytokines being controlled by positive and negative feedback from other cytokines (McFarlane *et al.*, 1990; Luger and Schwartz, 1994 and Hanada and Yoshimura, 2002).

Cytokine networks influence the growth and differentiation of stratified squamous epithelia. Cytokines produced by the epithelium itself influence epithelial homeostasis; for example TGFα stimulates proliferation (Derynck, 1988) and TGFβ inhibits it and enhances differentiation (Massague, 1990). The epidermis also produces cytokines that influence the immune response, for example epidermal synthesis of the interleukins (Krueger *et al.*, 1990). The complexity of these interactions makes it difficult to determine which cytokines are of particular importance to the epithelial proliferative and migratory responses seen in periodontal disease (Alexander and Damoulis, 1994) or even wound healing (Stephens and Thomas, 2002 and Thomas and Harding, 2002). However, the results of both transgenic and functional studies indicate a central role for KGF both in developmental interactions and in the normal maintenance and wound healing responses of adult epithelia (Guo *et al.*, 1993).

Many reports exist in the literature describing the spatial distribution of cytokines and their receptors in various tissue types. The skin, a close approximation of the gingivae, has been the subject of numerous *in vivo* and *in vitro* studies performed regarding certain cytokine networks (Schroeder, 1995 and Werner and Grose, 2002). However, evidence for other cytokines, in particular their presence within periodontal tissues is either conflicting or absent, summaries of which are presented below.

2.10.2 Keratinocyte growth factor

Rubin *et al.* (1989) first isolated KGF from medium conditioned by growth of a human embryonic fibroblast cell line and demonstrated its potent mitogenic activity for keratinocytes. KGF, alternatively designated FGF-7, is a member of the fibroblast growth factor family of related proteins (Finch *et al.*, 1989) that contains at least 23 related genes (Mason, 1994 and Shimada *et al.*, 2004). *In vivo,* KGF is described as a paracrine acting growth factor produced by mesenchymal cells to stimulate epithelial cell proliferation via KGF receptors expressed exclusively on epithelial cells (Rubin *et al.*, 1989; Miki *et al.*, 1992 and Werner *et al.*, 1992). There is no corresponding mitogenic activity of KGF on fibroblasts, endothelial cells or other non-epithelial targets of FGF action (Rubin, *et al.,* 1989 and Finch *et al.*, 1995a). Of particular interest are recent observations that KGF expression is upregulated early after full thickness skin injury to a much greater extent than other FGFs and remained elevated thought the first 7 days after injury, implicating KGF as a potentially important physiological mediator of wound repair (Werner, 1998).

KGF gene expression can be induced by a number of cytokines and growth factors such as IL-6, TGFα and platelet derived growth factor (PDGF). IL-1 in particular has been shown to induce raised KGF mRNA within dermal fibroblasts (Braulche *et al.,* 1994 and Chedid *et al.* 1994). The strong inductive response of fibroblasts to IL-1 appears relevant to the normal expression of KGF in the sub-epithelial stroma. The epidermis normally contains levels of IL-1 that are 100 to 1000-fold higher than most other tissues and it secretes biologically-active IL-1, predominantly as IL-1α (Cork *et al.*, 1996). By this paracrine mechanism the epithelium itself appears to induce local fibroblasts to produce the KGF required for its maintenance (Chedid *et al.*, 1994).

Many studies have reported KGF expression within both OGF and PDL fibroblasts (Dabelsteen and Wandall, 1997; Grøn *et al.*, 2001; Mackenzie and Gao, 2001 and Mckeown *et al.*, 2003). Analysis of mRNA from fibroblasts from different tissues suggests that KGF in adults is produced by a subpopulation of fibroblasts located in superficial CT adjacent to epithelium (Gao and Mackenzie, 1996); and may in this way regulate epithelial differentiation (Finch *et al.*, 1995b and Werner, 1998). This in conjunction with recent *in-situ* hybridisation studies from oral mucosa indicates that KGF is limited to fibroblasts in the lamina propria with no expression in deeper CT. This has led to the hypothesis that the

specific phenotype of JE is due to its position adjacent to the PDL, which may be regarded as a deep CT not expressing KGF (Gao and Mackenzie, 1992).

2.10.3 Keratinocyte growth factor receptor

KGF actions are dependant on its binding to a specific cell surface receptor, keratinocyte growth factor receptor (KGFR). KGFR is a membrane-spanning tyrosine kinase, which is a splice variant of the FGF receptor 2/bek gene, FGFR-2 IIIb. It has high affinity for KGF as well as for acidic-FGF but not basic-FGF (Miki *et al.*, 1992). It differs from the FGFR-2, which has high affinity for acidic and basic-FGF but no affinity for KGF (Bottaro *et al.*, 1990). The bek gene encodes both receptors with alternative splicing of exons that determine expression of immunoglobulin-like loops giving differential receptor specificity for FGF-related ligands (Cheon *et al.*, 1994). Whereas epithelial cells express transcripts containing only the exon sequence specific for KGFR, mesenchymal cells express transcripts for the exon sequence specific for FGFR-2. The KGFR and FGFR-2 sequences are structurally identical but for a stretch of 49 amino acids of the extracellular domain (Miki *et al.*, 1992).

KGFR is expressed predominately in the basal layer of most types of epithelial cells *in vivo* (Guo *et al.*, 1993) and *in vitro* (Rubin *et al.*, 1995). The receptor has been located in gingival epithelium by Das *et al.* (2001) and Ohshima *et al.* (2002a). There exists no published work relating to KGF receptor in JE tissue.

2.10.4 Keratinocyte growth factor-2

Keratinocyte growth factor-2 (KGF-2 or FGF-10) is a homologue of FGF-7. It binds with an equal affinity to the FGF-7 resident epithelial cell receptor FGFR-2 IIIb, but unlike FGF-7 also binds the IIIb splice variant of FGFR-1. Evolutionary relationships of human FGFs indicated that KGF-2 is closest to FGF-7 in both structure and biologic activity (Emoto *et al.*, 1997). Recombinant human KGF-2 shows mitogenic activity for foetal rat keratinising epidermal cells, but essentially no activity for fibroblasts. Murine KGF-2 appears to be a primary factor in the process of wound healing in conjunction with other growth factors such as TGFα and KGF (Jimenez and Rampy, 1999). There even exists a commercially available preparation, designated Repifermin (Human Genome Sciences) available for wound healing purposes.

There exist few articles on the distribution of KGF-2 within tissues, even less so within the periodontium. Using Northern blot analysis and IHC Sanale *et al.* (2002) detected expression of KGF-2 in the fibroblasts of the lamina propria.

2.10.5 Hepatocyte growth factor

HGF was isolated initially from the serum of partially hepatectomised rats, it being produced predominantly in the liver and the pancreas. Gherardi and Stoker (1990) found that HGF is structurally similar to scatter factor (SF), a molecule shown to stimulate the dissociation and scattering of epithelial cells. Later, Weidner *et al.* (1991) presented structural and functional evidence that human scatter factor and human HGF are identical proteins encoded by a single gene.

As well as being hepatotrophic HGF is a classical paracrine mediator of stromal-epithelial interactions and is expressed by mesenchymal cells in close vicinity to epithelial structures (Gherardi and Stoker, 1990). It is considered a possible mediator of epithelial-mesenchymal interaction during organogenesis and organ regeneration (Birchmeier and Gherardi, 1998). It disrupts desmosomal junctions between epithelial cells and induces a motile, fibroblast-like phenotype in individual cells. The factor therefore also influences the invasive growth of tumour cells derived from epithelial cells (Birchmeier *et al.*, 1996), and may be involved in the processes of wound-healing and early embryonic development (Sonnenberg *et al.*, 1993). In human skin, both molecular forms of IL-1 induce fibroblast synthesis of HGF. HGF is therefore a multifunctional cytokine that acts as a mitogen, motogen and a morphogen (Sonnenberg *et al.*, 1993).

Bottaro *et al.* (1991) demonstrated that the beta-subunit of the c-Met proto-oncogene product is the cell-surface receptor for HGF. c-Met is over-expressed in a significant percentage of human cancers and is amplified during the transition between primary tumours and metastasis.

Essentially, studies have shown distribution of HGF/KGF to mirror those of KGF/KGFR with expression of the cytokine demonstrated within OGF (Grøn *et al.*, 2001; Ohshima *et al.*, 2002a and McKeown *et al.*, 2003) and its receptor identified within OGE by Ohshima *et al.* (2002a).

2.10.6 Granulocyte macrophage-colony stimulating factor

Colony-stimulating factors (CSFs) are proteins necessary for the survival, proliferation and differentiation of haematopoietic progenitor cells (Metcalf, 1992). GM-CSF also plays a significant role in keratinocyte proliferation *in vitro* and speeds healing of skin wounds (Hancock *et al.*, 1988). GM-CSF is secreted together with other factors by T-cells and macrophages following cell activation by antigens or mitogens. Epithelial cells and fibroblasts respond to IL-1α by producing GM-CSF in a dose dependant fashion (Cubitt *et al.*, 1994). The synthesis of GM-CSF by various other cell types, for example endothelial cells and fibroblasts, is inducible by TNFα, TNFβ and IL-1 (Fitzgerald *et al.*, 2003). GM-CSF can be associated with the ECM of cells as a complex with heparin sulphate proteoglycans. This allows storage of the factor in a biologically inactive form. GM-CSF can be expressed also as an integral membrane protein. The membrane-bound or matrix-associated forms of the factor can interact with receptors on other nearby cells, establishing cell-to-cell contacts that may induce biological activities in juxtaposed cells (Montagnani *et al.*, 2001).

Sugiyama *et al.* (2002) identified GM-CSF within cultured gingival keratinocytes by both ELISA and PCR methods. For fibroblasts however there exist conflicting results; Nixon *et al.* (2000) did not find GM-CSF within cultured OGF, likewise the only paper relating to PDL was by Yamaji *et al.* (1995) who also did not identify GM-CSF by RT-PCR methods. Some studies have demonstrated GM-CSF induction in stimulated (wounded) epithelia (Mann *et al.*, 2001).

Under *in vitro* conditions GM-CSF receptor has been demonstrated in both CT and epithelial components of the skin (Montagnani *et al.*, 2001 and Maas-Szabowski *et al.*, 2001) but no papers relate specifically to oral tissues.

2.10.7 Transforming growth factor alpha

Transforming growth factors (TGFs) are biologically active polypeptides that reversibly confer the transformed phenotype on cultured cells. TGFα shows about 40% sequence homology with epidermal growth factor (EGF) (Derynck, 1988). The biological activities of these two growth factors are very similar and both bind to the same receptor. The transmembrane precursor of TGFα can bind to EGF receptors on near-by cells. This enables it

to establish specific cell-to-cell contacts and to elicit developmentally important responses in neighbouring cells (Derynck, 1992).

TGFα is produced by keratinocytes, macrophages, hepatocytes and platelets, and its synthesis can be stimulated by infection with viruses (Christensen and Poulsen, 1996). The physiological role of TGFα is probably the control of epidermal development during differentiation of cells as it has a known autocrine action within the skin (Mass-Szabowski *et al.*, 2001). An increased production of TGFα is commonly associated with neoplastic transformation of various cell types (Ju, 1991).

Concerning the periodontium, TGFα levels have been found to be lower in the gingival crevicular fluid of patients with chronic periodontal disease (Mogi *et al.*, 1999), which may result in delayed periodontal regeneration during the progression of the disease. TGFα has been identified within freshly isolated oral keratinocytes by Formanek *et al.* (1999) using both ELISA and PCR, and by Momose *et al.* (2002) using ELISA.

Several references state that TGFα is released by embryonic fibroblasts and plays an important role in the developing foetus (Locci *et al.*, 1993). Xu *et al.* (2000) recognised TGFα by IHC within interfacial membranes retrieved at revision total hip arthroplasty, whereas Rotaru *et al.* (2003) found TGFα localised to the basal epithelial layer and adjacent fibroblast layer in a series of oral fibromas. Li *et al.* (1997) detected TGFα in the walls of odontogenic cysts by IHC. Yamaji *et al.* (1995) however could not detect TGFα within PDL fibroblasts by means of PCR, and Tyler *et al.* (1999) did not detect TGFα in periapical granulomas again using PCR.

2.10.8 Interleukin-1 alpha

IL-1 was previously described as lymphocyte-activating factor and was thought to be produced only by monocytes, however it is now known to be synthesized by a variety of cell types including activated macrophages, keratinocytes, stimulated B-lymphocytes and fibroblasts, and is a potent mediator of inflammation and immunity (Dinarello, 2002). There are two structurally distinct forms of IL-1: IL-1α, which is the acidic form and IL-1β the neutral form. Both are 17KD proteins coded by separate genes (Dinarello, 1989). Synthesis is controlled by a complex feedback loop since IL-1 is capable also of inhibiting or promoting

its own synthesis depending on conditions and cell types. Maas-Szabowski *et al.* (1999) demonstrated that TGFα expression by skin keratinocytes upregulated KGF production by dermal fibroblasts that in-turn stimulated keratinocyte growth. Similar signalling pathways may be responsible for the normal differentiation patterns of OGE. The synthesis of IL-1 can be induced by other cytokines including TNFα, IFNα, IFNβ and by bacterial endotoxins, viruses, mitogens and antigens.

Reports providing evidence of IL-1 production by fibroblasts are however confusing, with mention of its production only by wounded skin fibroblasts and in some pathological CT disorders such as systemic sclerosis (Kawaguchi *et al.*, 1999).

Kornman *et al.* (1997) suggested that genetic polymorphisms of the IL-1 gene might be associated with severity of periodontitis. In their study, carriage of allele '2' of the IL-1A gene and allele '2' of the IL-1B gene was associated with increased severity of periodontitis in non-smokers. Further, Shirodaria *et al.* (2000) demonstrated an increase in IL-1α within gingival crevicular fluid in patients with the IL-1A genotype.

Lossdorfer *et al.* (2002) using both IHC and *in-situ* hybridisation techniques demonstrated IL-1α within OGE and PDL tissues of the rat. Miyauchi *et al.* (2001) demonstrated its expression within JE cells by IHC assay.

Two kinds of IL-1 receptor bind with different affinities. Both IL-1α and IL-1β can bind to the same receptors with equal affinity and therefore show closely similar biological activities. The type-1 receptor, isolated from T-cells, is expressed predominantly on T-cells and cells of mesenchymal origin and has been designated CD121a. The type-2 receptor has been designated CD121b and has been isolated from B-cells, granulocytes and macrophages. It is expressed predominantly on B-cells and cells of the myelomonocytic lineage.

Few reports exist with regard to IL-1α receptor distribution within the periodontium, most notable is work conducted by Chou *et al.* (2000) who found trace amounts of IL-1 receptor mRNA within gingival fibroblasts.

CHAPTER THREE

HYPOTHESES

CHAPTER THREE
HYPOTHESES

The proposed work is based on three general hypotheses:

Hypothesis 1. That differences between junctional and oral-gingival epithelia are associated with differing influences of their sub-epithelial fibroblasts.

Hypothesis 2. That periodontal and gingival fibroblasts differ in their constitutive and induced levels of expression of cytokines required for maintenance of epithelial growth, and for activation of epithelial migration.

Hypothesis 3. That junctional epithelial cells are less readily stimulated than oral-gingival epithelial cells by factors that normally activate epithelial maintenance.

CHAPTER FOUR

MATERIALS & METHODS

CHAPTER FOUR
MATERIALS AND METHODS

Unless otherwise stated reagents and chemicals used throughout this study were obtained from Sigma-Aldrich, cell culture consumables from Invitrogen™, polymerase chain reaction constituents from Promega and TaqMan™ quantitative-PCR products from Applied Biosystems.

This chapter presents methods required for: -

a) Tissue culture, fixation and immunohistochemical investigations.
b) ELISA protein level assays for three cytokines: KGF, GM-CSF and TGFα.
c) Bromodeoxuridine (BrdU) keratinocyte proliferation studies and;
d) Quantitative-polymerase chain reaction investigations.

4.1 Media

Cultured cells require a sterile environment and a supply of nutrients for growth and in addition, the culture environment should be stable in terms of pH and temperature. Various defined basal media types have been developed, modified and enriched with amino acids, vitamins, fatty acids and lipids. This study required the maintenance of human and mouse fibroblasts and human oral keratinocyte cell lines. The following media formulations were filter sterilised through 0.22μm filters (Stericup™, Millipore) and stored at 4°C. Media were warmed to 37°C prior to use.

4.1.1 Fibroblast medium

The fibroblast medium used was high glucose Dulbecco's modified Eagle's medium (DMEM) with phenol red, containing 2mM L-glutamine, antibiotic/antimycotic (Penicillin/streptomycin/amphoteracin B) and supplemented with 10 % foetal bovine serum (FBS).

4.1.2 Mouse Swiss 3T3 fibroblast medium

3T3 medium was as for fibroblast medium but with newborn calf serum (NBCS) substituting for the FBS.

4.1.3 FAD oral keratinocyte medium

FAD medium was first derived by Wu *et al.* (1982) as a supplemented medium for the culture of epithelial cells. To prepare a 500ml batch of medium firstly produce "solution A" which consists of 3 parts DMEM to 1 part Ham's F-12, dissolved in which is 9.1mg of adenine. To 450ml of solution A is added 50ml FBS, 500µl hydrocortisone, 500µl cholera toxin, 500µl epidermal growth factor (EGF), 250µl insulin and 5ml antibiotic/antimycotic.

Final concentrations of supplements were: -

- Adenine 0.089mM
- Hydrocortisone 400ng/ml
- Cholera toxin 10^{-10}M
- EGF 10ng/ml
- Insulin 5µg/ml
- Penicillin G sodium 100U/ml, streptomycin sulphate 100µl/ml, Amphoteracin B 0.25µg/ml.

4.1.5 FAD washing medium

A washing medium was devised for the initial collection and incubation of potentially infected human specimens, which had the same formulation as FAD with the addition of triple the concentration of antimycotic/antibiotic (Penicillin G sodium (300U/ml), streptomycin sulphate (300µl/ml), amphoteracin B (0.75µg/ml)), nystatin (24ml/l) and Plasmocin™ (Autogen-Bioclear, 25µg/ml) a commercial *mycoplasma* inhibitor.

4.2 Cell culture

Cells were cultured in Heraeus function line incubators set at 37°C and 5% CO_2. They were humidified with a water bath containing Sigmaclean® germicide treatment. Sterile work was undertaken in a Bioquell Microflow Class 2 safety cabinet.

4.2.1 Primary Cultures

These were derived directly from excised, normal human tissue and grown either as explant cultures or following dissociation into a single cell suspension by enzyme digestion. Epithelial cultures occasionally became over-grown by fibroblasts and as these contaminating fibroblasts proved impossible to remove, these cultures were discarded.

4.2.2 Continuous Cultures

A 3T3-Swiss albino fibroblast line (American Type Culture Collection (ATCC) Cat no. CCL-92) was serially propagated in culture indefinitely. In order to retain original growth characteristics these were sub-cultured before confluence.

4.2.3 Consent

Informed consent was obtained from patients attending the Oral Surgery department at the University of Wales, Dental School, Cardiff as approved by the local research ethics committee (see appendix I).

4.2.4 Specimens and collection

Experimental material was obtained from 18 individuals with an age range of 13 to 44 years. Patients underwent tooth extraction primarily for caries or orthodontic reasons during which samples of buccal gingiva of approximate dimensions 5mm by 4mm were collected whilst still attached to the tooth. Care was taken to obtain specimens from sites clinically unaffected by periodontal disease. Atraumatic tooth extraction was achieved using a series of elevators, avoiding the damaging introduction of extraction forceps. Samples were immediately transported to the laboratory in sterile containers containing FAD washing medium.

4.2.5 Isolation

Keratinocytes and fibroblasts were isolated from biopsies as described in detail by Gao and Mackenzie (1992). After carefully separating the tooth from the gingiva, part of each soft tissue specimen was frozen and sectioned for immunocytochemical staining. The remaining gingival sample was then micro-dissected using a dissection microscope (Nikon SM2800) to free the JE complex. The remaining portion was treated enzymatically with 0.25% trypsin overnight to separate the OGE from the underlying CTs.

Figure 4.1: Molar tooth with soft tissue attached/dissected from ACJ

4.2.5.1 Oral-gingival fibroblasts (OGF)

The CT fragment was minced thoroughly with a scalpel, gathered in a little medium, placed in a sterile 20ml universal container and centrifuged at 800rpm (50x *g*) for 5 minutes (ALC® PK120R refrigerated centrifuge). The pellet was resuspended in a collagen gel within a 6-well plate (for preparation see chapter 4.4.2). As confluence approached fibroblasts were harvested from gels by treatment with a 0.1% collagenase solution at 37°C for 15 minutes before being re-plated in T75 flasks (Iwaki, Bibby Sterilin Ltd) for amplification.

4.2.5.2 Periodontal ligament fibroblasts (PDL)

PDL tissue was obtained by scraping the mid-third portion of the tooth root and fibroblasts isolated using the method for OGF described in chapter 4.2.5.1.

4.2.5.3 Oral-gingival epithelium (OGE)

The separated epithelial sheets were minced thoroughly with a scalpel and transferred to a sterile 15ml centrifuge tube. 1ml trypsin/EDTA (0.05% (w/v) trypsin/0.53mM ethylenediaminetetraacetic acid; Gibco) was added and warmed to 37°C, gentle pipetting provided a single cell suspension that was pelleted at 1000rpm (80x *g*) for 10 minutes.

4.2.5.4 Junctional epithelium (JE)

The dissected JE tissue was minced thoroughly, 1ml trypsin/EDTA added and kept at 37°C for 15 minutes to help dissociation into a single cell suspension. 5ml of FAD was added, transferred to a 15ml tube and the cells pelleted at 1000rpm for 10 minutes. Applying the basic techniques of Rheinwald and Green (1975) OGE and JE keratinocytes were plated onto a mitomycin-C-treated 3T3 layer that had been produced one day in advance (see chapter 4.2.9). Cultures were maintained in FAD.

4.2.6 General culture morphology

Both fibroblast and epithelial cell cultures formed monolayers attached to the tissue culture flask. Epithelial cells formed small rounded colonies that conformed to the cobblestone descriptions stated in the literature (Fig 3.2a). Fibroblasts formed typical elongated spindle shapes (Fig 3.2b).

Figure 4.2a: Epithelial morphology

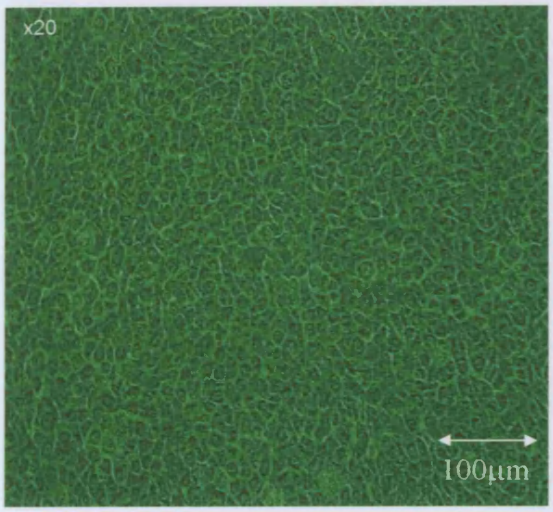

Figure 4.2b: Fibroblast morphology

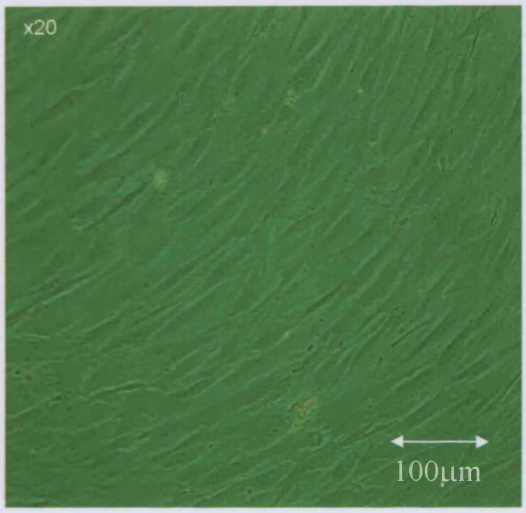

4.2.7 Cell quantification

In order to standardize cell procedures such as cryopreservation and subculture routines it was necessary to quantify numbers. This was achieved using cell-counting chambers (ISL Fast Read, Cat No. BUS100) during trypsinisation, a single drop of cell suspension is placed into a chamber, counted in triplicate and averaged. This provided an amount equivalent to "number of cells" $x10^4$/ml.

4.2.8 Amplification and sub-culture of 3T3 cells

The medium was removed, cells washed with PBS (without Ca_{2+}/Mg_{2+}), 2.5ml of Trypsin/EDTA added and the flasks incubated for 10 minutes at 37°C or until the cells became detached and rounded. The cells were removed from the flask in 5ml medium, centrifuged at 800rpm for 5 minutes and the pellet re-plated at a 1:10 dilution ratio.

Prior to use as feeder cells, 3T3 cells were growth arrested by exposure to mitomycin-C. Mitomycin-C is cytostatic and has the ability to covalently bind to DNA inhibiting its synthesis and hence cell replication. Its action is most prominent during the late G1 and early S-phases of the cell cycle; this allows just one further replication cycle to occur.

4.2.9 Mitomycin-C treatment

All procedures involving mitomycin-C required complete darkness as exposure to light readily decomposes it, inactivating its growth arresting properties (Sigma-Aldrich, product information sheet, M4287). A 2mg vial of mitomycin-C was added to 4ml of DMEM producing

a working solution of 0.5mg/ml, this was aliquotted and stored at -20°C for up to 6 months. T75 flasks were covered in foil and 0.1ml of mitomycin-C solution introduced in 5ml 3T3 medium (final mitomycin-C concentration of 0.01mg/ml). Cultures were incubated for 2.5 hours, washed 4 times in PBS, medium replaced and left overnight to undergo final replicative cycles. After 24 hours, the treated 3T3s could be trypsinised, counted and re-plated at required densities for epithelial growth ($6x10^5$/T75 flask equivalent to 8000 cells per cm^2).

4.2.10 Amplification and sub-culture of human fibroblasts

When visualised to be at 80-90% confluency fibroblasts were treated as for 3T3s and re-plated into flasks at a dilution ratio of 1:6. Cells were utilised in experiments between passage (P) 2 and P4.

4.2.11 Amplification and sub-culture of keratinocytes

Prior to confluence, primary keratinocyte colonies were passaged onto mitomycin-C treated 3T3 cells. 5ml of 0.02% EDTA solution was added to T75 culture flasks and incubated for 5 minutes or until 3T3 cells had detached and could be removed by aspiration. Then 5ml of trypsin/EDTA was added and left for 10 minutes at 37°C or until the cells became detached and rounded. Keratinocytes were centrifuged at 1000rpm for 10 minutes and passaged at a 1:4 dilution ratio.

Some flasks of epithelial and fibroblast cultures were fixed for IHC assays. Remaining flasks provided frozen cell stocks for experimental use between second and fifth passage.

4.2.12 Cryopreservation

Fibroblast, and epithelial populations were limited in the number of successful passages they could undergo, and for this reason it was essential to establish a system of master and working banks in order to maintain such lines at low passage for repeated experimentation. The basic principle of successful cryopreservation is a slow freeze and quick thaw, as a general guide cells should be cooled at a rate of –1° to –3°C per minute. Cultures should be healthy and in log-phase of growth before preservation (this was achieved by using pre-confluent cultures and by changing the culture medium 24 hours before freezing). Cells were brought into suspension in a volume of fresh medium and a cell count performed if necessary. The remaining suspension was pelleted and resuspended in freeze medium (90% FBS, 10%

Dimethyl sulphoxide (DMSO)). 1ml aliquots of cell suspension were placed into cyroprotective ampoules inside a passive freezer (Mr Frosty®, Nalgene) containing isopropyl alcohol that is in turn stored at –80°C. After 24 hours, cells were cryopreserved for indefinite periods by immersion in liquid nitrogen that maintained a temperature of -196°C.

4.2.13 Thawing of cells recovered from liquid nitrogen

The cryoprotectant DMSO is toxic above 4°C therefore; it was essential that cultures were rapidly diluted in culture medium to minimize toxic effects. This was achieved by placing ampoules in a water bath at 37°C. The outside of the ampoule was wiped with 70% alcohol and the contents pipetted drop-wise into pre-warmed growth medium.

4.2.14 Screening for *Mycoplasma* contamination

Mycoplasmas are the smallest free-living self-replicating prokaryotes. The effects of *mycoplasma* infection are more insidious than those of bacteria and fungi. They can induce several long-term effects that include: reduced growth rate, morphological changes and chromosome aberrations. An in-house technique was used to test derived samples indirectly using the DNA stain Hoechst 33258.

Sample and control cells were grown on chamber slides (Falcon; Stone, UK) for 48 hours at a density of 10^4 cells per well. They were fixed in freshly prepared fixative (1:3 glacial acetic acid: absolute methanol) for 5 minutes. This was repeated for a further 5 minutes, the slide air dried for 30 minutes and 2ml Hoechst 33258 stain (Sigma; 1μg/ml) applied for 5 minutes whilst being shielded from direct light by aluminium foil. The slides were washed four times with water, mounted in an anti-fade mountant and a coverslip placed. Cells were observed under ultra-violet light at x40 magnification.

Samples infected with *mycoplasma* were seen as fluorescing nuclei plus extra-nuclear fluorescence of *mycoplasma* DNA (small cocci or filaments). These infected cultures were discarded.

4.3 Characterisation of epithelial and fibroblast cultures

Characterisation methods involved staining fibroblast and epithelial populations with a panel of differentiation markers (Table 4.1). Cell smears; cryosections and cells grown directly on plastic substrate were used.

4.3.1 Fixation methods

Cells were prepared in several ways prior to immunological staining:

a) Cells were stained while attached to T75 flask substrate. Ice-cold methanol/acetone in equal parts was added for 10 minutes, rinsed with several changes of PBS and flasks stored at 4°C containing 10mM azide. Pieces of flask base were removed and stained in a similar manner to glass slide preparations.

b) Preparation of cell smears involved enzymatically removing the cells from their flasks, resuspending in a little FBS and smearing onto poly-l-lysine coated slides (Polysine^{TM}, Menzel-Glaser Cat. No. 041400).

4.3.2 Enzymatic unmasking and blocking of antigenic sites

Formalin fixed, paraffin embedded specimens required unmasking of antigenic sites and were deparaffinized in 100% xylene for 2 minutes, hydrated through a graded alcohol series (100% for 2 minutes x3, 70% for 2 minutes x3 and 50% for 2 minutes x3) and brought to double distilled water (DD H_2O).

Slides were then immersed in a retrieval solution: (Glycerine 90ml, 10ml of 10 mM citrate buffer (pH6.0)), micro-waved at 600 Watts on high power for 1.0 minute, on low power for 10.0 minutes and cooled to room temperature. After cooling, endogenous peroxidase activity was quenched by immersing the slides in 0.3% H_2O_2 diluted in TBS (0.05M Tris-HCl, 0.15M NaCl, pH 7.6) for 5 minutes and washed in PBS before continuing with the IHC technique.

4.3.3 Fibroblast characterisation

For the most part, the PDL and OGF cultured from explants were heterogeneous populations of cells (Hassell and Stanek, 1983; Schor and Schor, 1987 and McCulloch and Bordin, 1991).

Efforts to characterise PDL cells biochemically and so differentiate them from OGF cells have been reported (Kawase *et at.*, 1988; Somerman *et al.*, 1988 and Piche *et al.*, 1989).

4.3.3.1 Morphology and growth characteristics

Fibroblasts in monolayer culture were photographed at various time points at increasing passage numbers up to P10 using a Nikon Eclipse TS100 inverted phase microscope and a Nikon Coolpix 950 digital camera. Simple growth-rate studies were conducted; equal numbers of OGF and PDL fibroblasts ($1x10^4$) of the same passage number were plated into T75 flask and the number of days until confluence recorded.

4.3.3.2 Alkaline phosphatase detection

Fibroblasts, both grown on plastic substrate and as cell smears, were used for histochemical differentiation by examining the presence of ALP. Preparations were fixed in 4% paraformaldehyde for 10 minutes and washed 3 times in 1xTRIS buffer (see stock solution preparation - appendix II). 5-Bromo-4-chloro-3-indolyl phosphate p-toluidine salt (BCIP) substrate was made as per manufacturers instructions, applied to the sections and incubated at room temperature for up to 2 hours. The reaction was stopped by briefly washing in H_2O. Where counterstaining was required, sections were immersed in Harris's haematoxylin (Lamb, Cat No. 4975) for 2 minutes and placed under running water for 20 minutes. Slides were mounted in an aqueous mountant, Crystal/mount™ (Biomeda Corp, Cat No. MO3) viewed, photographed and digital images captured.

4.3.4 Epithelial characterisation

4.3.4.1 Morphology, growth characteristics and cell size

For later comparison, keratinocytes in monolayer culture were photographed at various time points and at increasing passage numbers up to P5.

4.3.4.2 Immunohistochemistry protocol

IHC staining was performed on cell smears, on colonies cultured on plastic substrate and on cryosections of gingival whole mounts and organotypic gels. Specimens were fixed in ice-cold acetone/methanol for 10 minutes and washed in PBS for 5 minutes and where necessary circled with a PAP pen (Dako). Specimens were treated with a blocking agent (PBS, 2% BSA and 0.2% Triton-X) for 1 hour at room temperature. This was shaken off and primary antibodies applied directly and incubated overnight in a humid chamber at 4°C. After 24

hours, specimens were washed in 3 changes of PBS over 30 minutes and the appropriate fluorescein isothiocyanate (FITC) conjugated secondary antibody applied for 2 hours at room temperature. Following a further 3 washes, all samples were incubated in Hoechst 33258 dye (1μg/ml) for 30 minutes to aid location of cellular nuclei, then mounted in an anti-fade mountant (Johnson and Nogueira-Araujo, 1981 (see appendix II)). Commercial antibodies were tested for optimal concentrations before use and supernatants used neat (see table 4.1). Controls included omission of the primary antibody, secondary antibodies alone, comparison of staining patterns between the different antibodies used and conformity of staining to known patterns of antigen distribution. Samples were viewed on an Olympus Provis AX70 fluorescent microscope and photographed using a Nikon DXM1200 digital camera. Separate images for FITC and Hoechst were obtained, and where necessary to illustrate tissue morphology, combined in Photoshop 5 (Adobe).

Table 4.1: Antibodies, suppliers, and working concentrations

Monoclonal antibody	Clone number	Concentration
Cytokeratin 1	LHK1[a]	Supernatant
Cytokeratin 4	6B10[b]	1:50
Cytokeratin 5	AF138[c]	1:500
Cytokeratin 6	HK6[a]	Supernatant
Cytokeratin 7	LP5K[a]	Supernatant
Cytokeratin 8	LE41[a]	Supernatant
Cytokeratin 10	LHP2[a]	Supernatant
Cytokeratin 13	1C7/2D7[b]	1:50
Cytokeratin 14	LL002[a]	Supernatant
Cytokeratin 15	LHK15[a]	Supernatant
Cytokeratin 16	LL025[a]	Supernatant
Cytokeratin 17	E3[b]	1:50
Cytokeratin 18	LE61[a]	Supernatant
Cytokeratin 19	LP2K[a]	Supernatant
Cytokeratin 20	K_s20.8[d]	1:10
DBA	-[e]	5μg/ml
ICAM-1	CD54[d]	1:40
MMP-7 (Matrilysin)	Ab-3[f]	1:100
Desmoplakin I+II	DP2.15[g]	10μg/ml
TGFα	Ab8610[h]	1:40

a = Gift of Prof L Leigh
b = Neomarkers
c = Berkeley Antibody
d = Dako
e = Vector labs
f = Oncogene
g = Cymbus Biotech
h = Abcam Limited

4.3.5 Assay of epithelial cell proliferation

To identify differences in cell proliferative capacity between JE and OGE, populations were subjected to S-Phase labelling by addition of 50μg/ml 5-bromo-2'-deoxyuridine (BrdU) to the medium for 2 hours prior to fixation. Populations were pulsed with BrdU separately on days 1, 2, 3, 4, 5 and 6. The cells were then fixed in 70% ethanol for 10 minutes, washed in PBS, treated with 4M hydrochloric acid (HCl) for 10 minutes and washed in PBS of pH 8.5 then pH 7.4.

4.3.5.1 Blocking of endogenous peroxidase activity and antibody application

Endogenous peroxidase was blocked using 3% hydrogen peroxide (H_2O_2) in PBS containing 0.2% Triton-X for 5 minutes before application of an anti-BrdU primary antibody (Dako) at a dilution of 1:100. After overnight incubation at 4°C, cells were washed and rabbit anti-mouse horseradish peroxidase (HRP) conjugated secondary antibody applied at a dilution of 1:200 for 2 hours (Vectastain® *elite* ABC kit, Vector Labs, Burlingame, CA).

4.3.5.2 Colour visualisation

Visualisation of binding was achieved by using a 3,3'-diaminobenzidine tetrahydrochloride (DAB) substrate kit (Vector Labs) that produced a brown colour insoluble in alcohol. The DAB substrate was applied for up to 10 minutes and the reaction terminated by washing in tap water. Haematoxylin counter-stain was provided where necessary and Crystal/mount™ applied. Fifty colonies were identified per flask per day, classified morphologically (see chapter 2.8.4 for colony classification) and labelled cells counted.

4.4 Organotypic culture

4.4.1 Preparation of collagen solution

Rat-tail collagen was extracted as previously described by Rowling *et al.* (1990). Freshly removed rat tails were washed in two changes of 70% alcohol for 15 minutes each at -20°C. Tails were washed in two changes of DD H_2O for 5 minutes at 4°C, each is then broken, the skin removed and tendons extracted. 0.8g – 0.9g of tendon and 35ml 0.1% acetic acid was then placed in 50ml centrifuge tubes on a shaker platform at 4°C for 24 hours. Tubes were then centrifuged at 10,000rpm (8000x *g*) for 2 hours at 4°C and the supernatant poured into a sterile bottle. This process was then repeated with the remaining pellet.

4.4.1.1 Dialysis of Collagen

Collagen gel solution was placed into a length of dialysis tubing in a 4-litre beaker of sterile water and stirred at 4°C for 3 days, changing water every other day. Dialysis of the gel continued until the correct consistency was obtained, bubbles should rise gently, and then the gel was placed in 50ml tubes at -80°C to freeze-dry. The lyophilised collagen was weighed into 160mg batches and irradiated at 50,000 Grey and stored at 4°C. 160mg of collagen was reconstituted using 40ml 0.1% acetic acid providing a 4mg/ml final concentration. To assess sterility, enough collagen gel to cover the bottom of a small petri dish was incubated at 37°C for 3 days and examined microscopically for evidence of bacterial or fungal growth.

4.4.1.2 Protein determination

The protein concentration of samples of the prepared rat-tail collagen was assessed using a Total Protein Kit (Sigma). A protein concentration standard curve was set up by mixing 500µl of BSA standards (0-1mg/ml in DD H_2O) with 2.2ml of Biuret reagent. This was incubated for 10 minutes at 20°C, 100µl of Folin and Ciocalteu's phenol reagent added to each tube, mixed well and incubated for a further 30 minutes. 100µl of sample was transferred to a 96-well microtitre plate. The absorbance was read at 550nm in a Dynex MRX microplate reader. To estimate the protein concentrations of samples 500µl of sample was analysed in place of the BSA standard and compared against the standard curve.

4.4.2 Organotypic culture protocol

4.4.2.1 Day 1 - Fibroblast impregnated collagen gel

Two methodologies were used to construct the collagen gels. The support for organotypic culture was either provided by:

A) Purchased 3.0μm pore size insert system contained in a deep 6-well culture plate (Falcon, Beckton Dickinson) (Figures 4.3a) or

B) A 'mesh' structure constructed from stainless steel contained in a 6-well culture plate as described by Igarashi *et al.* (2002) (Figures 4.3b).

Under ice-cold conditions, a standard ratio of constituents was used to produce a collagen gel that provided uniform setting. 8ml of collagen solution was added to a sterile 50ml centrifuge tube, 1ml of 10x DMEM and 1ml FBS added, mixed and neutralised with drop-wise addition of 1N NaOH until light pink in colour. 1ml of fibroblast medium containing the appropriate number of fibroblasts was added and the gels poured.

Sub-confluent fibroblast cultures were trypsinised, counted, pelleted and resuspended in the collagen gel mix. Method **A** required 3ml collagen containing $3x10^6$ fibroblasts to be poured into a 3μm pore cell culture insert. Method **B** required $1x10^6$ fibroblasts in 1ml collagen to be poured into each well of a 24-well plate. Once set, the fibroblast-populated gels or 'connective tissue equivalents' were maintained in an excess of fibroblast medium overnight.

4.4.2.2 Preparation of nylon mesh

Nylon meshing of 100μm pore size was used as a support device for the collagen lattices (Nitex Nylon Cat No. 3-100/35, Tetko Inc). Sterile nylon discs ≈ 2 cm in diameter were placed in a petri dish and lightly coated in collagen gel. After draining excess collagen, the petri dishes were incubated at 37°C and collagen allowed to solidify. Once set, collagen-coated discs were cross-linked by fixation in 1% glutaraldehyde for 1 hour at 4°C, before washing with four 20-minute changes of PBS and two 20-minute changes of FAD washing medium. Following the wash procedures, treated meshes were stored in FAD at 4°C until use.

4.4.2.3 Day 2 - Addition of keratinocytes to gel surface

To provide equal densities of keratinocytes used in the two methods the surface area of the gel was calculated for each: -

Method **A** - Insert: Diameter 24mm, Surface area = 452mm^2

Method **B** - 24 well plate: Diameter 18mm, Surface area = 254mm^2 (approximately half)

Keratinocytes to be used were trypsinised, counted, resuspended and plated at a concentration of 0.5x10^6/24well or 1x10^6/insert (≅ 200,000cells/cm^2) in FAD. Gels were incubated overnight to allow epithelia to become established and adherent. For gels prepared in 24-well plates the medium was aspirated, gels raised using spatulas and placed onto the nylon mesh/steel grid support system. FAD was added to all wells to just touch the underside of the mesh/porous polycarbonate membrane, the cultures being maintained at the air/liquid interface for 14 days before processing (Figure 4.3a/b).

Figure 4.3a: Method (**A**) demonstrating porous polycarbonate insert within deep-well plate

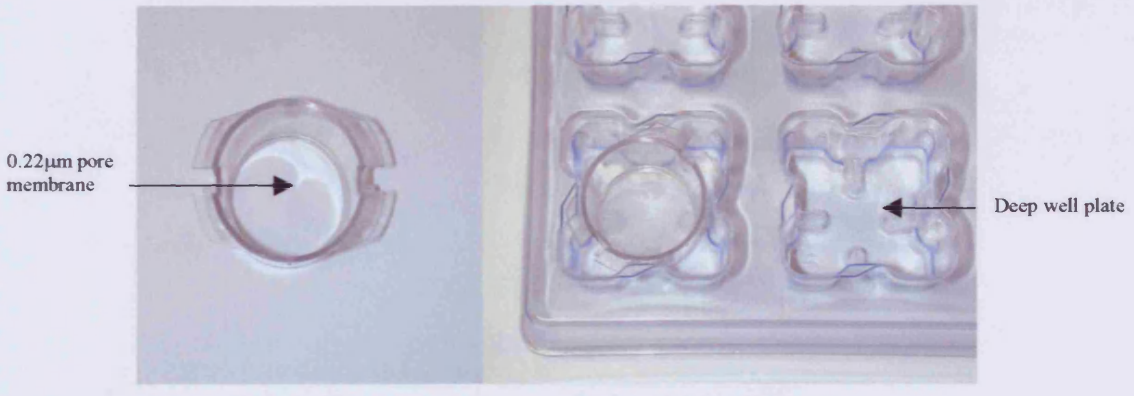

Figure 4.3b: Method (**B**) demonstrating stainless steel mesh set-up

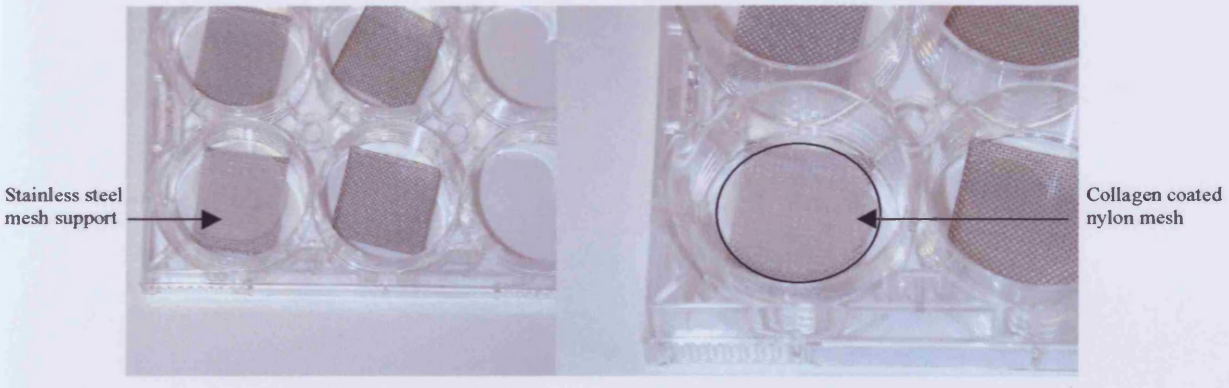

4.4.3 Processing organotypic gels

Following the culture period half the organotypic cultures were fixed in 4% paraformaldehyde at 4°C overnight and paraffin embedded. Sections were cut at a setting of 5μm and de-waxed in xylene, hydrated through graded alcohols to water and stained in Harris' haematoxylin for 15 minutes. After a five-minute wash, they were differentiated in 1% acid alcohol (1% HCl in 70% alcohol) for 5-10 seconds. Following a further wash, sections were eosin stained for 10 minutes before rinsing under warm running water. Finally, sections were dehydrated through alcohols and mounted for viewing with a light microscope.

The remaining half was orientated and mounted onto cork discs (Lamb) using embedding medium (Cryomatrix™, Thermo Shandon) and snap-frozen in isopentane chilled via liquid nitrogen (Figure 4.4). 7μm sections were cut perpendicular to the epithelial surface in a cryostat (Shandon Cryotomb) and positioned onto poly-l-lysine coated slides.

Figure 4.4: Orientating gels onto cork discs

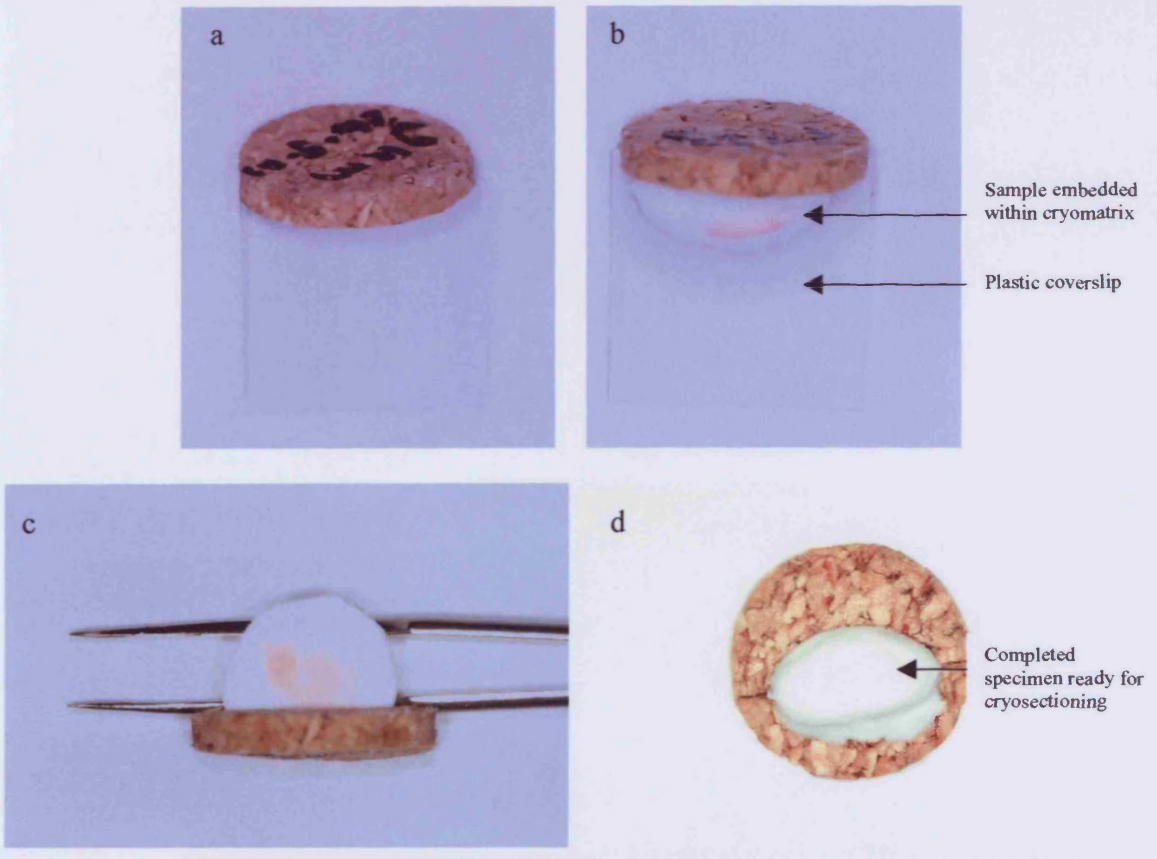

a) Plastic coverslip embedded within cork disc
b) Sample orientated and contained within embedding medium
c) Coverslip removed
d) Final sample ready for sectioning on cryostat

4.5 Polymerase chain reaction (PCR)

The PCR is an *in vitro* procedure for the amplification of DNA molecules. The technique uses two oligonucleotide primers that flank the targeted DNA and amplification occurs following repeated cycles of heat denaturation of the DNA, primer annealing and extension of annealed primers by the thermostable enzyme *taq* polymerase. TaqMan™ quantitative-PCR is an accurate method of detecting mRNA even when expressed at low levels.

4.5.1 Inventory

PCR products were supplied by Promega whilst TaqMan™ Q-PCR products, software (Primer Express® v2.0) and hardware (ABI Prism7000 sequence detection system) were supplied by Applied Biosystems. Water was rendered nuclease-free by treatment with 0.1% diethyl pyrocarbonate (DEPC), as were plastic tissue culture components.

4.5.2 RNA isolation

Total RNA was extracted from cells cultured in monolayer using the guanidinium-thiocyanate method (Chomczynski and Sacchi, 1987). Medium was changed 48 hours pre-extraction. 1ml of RNAwiz™ (Ambion; Austin, USA) was added to each T75 flask, incubated for 30 minutes and then homogenised by vigorous pipetting before being transferred to a 1.5ml microtube. 200µl of chloroform was added to the homogenate, shaken vigorously for 20 seconds and incubated for 10 minutes. This was then transferred to a heavy phase-lock gel micro-tube (Eppendorf) before centrifugation at 13,000rpm (13,000x *g*) for 25 seconds (Sorvall® Biofuge Fresco). On completion the upper aqueous phase was transferred into a clean tube, 500µl of H_2O, 1ml of isopropanol and 1µl glycogen added before incubating for a further 10 minutes. The RNA was pelleted by centrifuging at 13,000rpm for 15 minutes, washed with 1ml ice-cold 75% (v/v) ethanol, supernatant discarded and the pellet air-dried for 10 minutes. The RNA was resuspended in 20µl of H_2O before purification.

4.5.2.1 RNA purification

Contaminating DNA was removed from the RNA by treatment with DNA-Free™ Dnase I treatment (Ambion). A 0.1 volume of the 10x buffer was added together with 1µl of Dnase I (2U/µl) and incubated for 30 minutes at 37°C. A 0.1 volume of Dnase I Inactivation Reagent was added to each sample, mixed and the solution incubated at room temperature for 2 minutes. The samples were then centrifuged at 6000rpm (2800x *g*) for 1 minute to pellet the

Dnase I Inactivation Reagent. The supernatant containing the DNA-free RNA was then removed to fresh eppendorf tubes before quantification.

4.5.2.2 RNA quantification

RNA samples were quantified by diluting 2µl of RNA solution with 98µl H_2O and the absorbance read on a luminometer (GeneQuant II; Amersham Pharmacia Biotech, St Albans) at 260 and 280nm. The ratio of Abs_{260nm}/Abs_{280nm} gave the purity of the sample, 2.0 delineates pure nucleic acids, less than 1.6 indicated contamination with proteins (Sambrook *et al.*, 1989). The concentration and purity were calculated using the formula:

$$Abs_{260nm} \text{ x dilution factor (50) x RNA factor (40)} = X \text{ µg/ml}$$

4.6 Reverse-transcriptase polymerase chain reaction (RT-PCR)

4.6.1 First-strand complementary (cDNA) synthesis

First strand cDNA was synthesised by reverse-transcription, firstly 2μg of previously extracted mRNA was made up to 18μl in H_2O. To the 18μl of RNA solution was added 20 μl of reverse-transcription amplification buffer master mix (see appendix V). This was incubated at 95°C for 4 minutes then immediately quenched on ice for 2 minutes to relax any RNA secondary structures. 2.0μl of RNase inhibitor (40U/μl) and 2.5μl Moloney murine leukaemia virus reverse-transcriptase (MMLV-RT) (200U/μl) was added before incubating at 25°C for 10 minutes, 42°C for 60 minutes and 95°C for 5 minutes.

4.6.2 Primer amplification

Preliminary experiments determined the optimum PCR conditions. 2μg of previously transcribed cDNA was used as template for the PCR reaction, placed in a 200μl microtube and made up to 48μl with PCR amplification buffer master mix (see appendix V) adding the *taq* polymerase last.

The mixture was incubated as follows:

One cycle -		94°C for 2 minutes
40 cycles	(Amplification) -	94°C for 30 seconds
	(Denaturation) -	60°C for 30 seconds
	(Annealing) -	68°C for 75 seconds
Final extension step of -		68°C for 15 minutes

To monitor the efficiency of amplification and assess the quality of the cDNA glyceraldehyde-3-phosphate dehydrogenase (GAPDH) housekeeping gene was included in each reaction. Amplification of the gene verified that the target nucleic acid and reaction components were of acceptable quality.

Negative controls included the substitution of H_2O in place of the template RNA, omission of the primers and the omission of the reverse-transcription step before PCR amplification. Reactions performed with omission of either sample RNA or the primers failed to amplify product.

Primer design software was used to design both forward and reverse primers and matching TaqMan™ Probes. The primers were initially bought from Invitrogen™, tested, examined via agarose gel electrophoresis and if the appropriate weight band was visualised then the more costly TaqMan™ probes were ordered from Applied Biosystems.

4.6.3 Analysis of PCR products

Agarose gel electrophoresis and ethidium bromide staining was used to assess the presence and size of PCR products. 5µl of final PCR product was added to 10µl of loading buffer. In addition, a 100bp incremental DNA ladder and H_2O controls were added to the lanes. (For constituents of agarose gel, TBE buffer and loading dye, see appendix V). Gels were placed in an electrophoresis tank (MiniCuve 8.10 Electrophoresis Unit; Qbiogene, Livingstone) and run at a potential of 75V until the gel front was past halfway point. The bands were then visualised under a UV light documentation system (Gel Doc 2000; Bio-Rad Laboratories) and digital images captured. For the size of the PCR products see appendix VI.

4.7 Quantitative (Real-time) polymerase chain reaction

Pioneered by Higuchi *et al.* (1992) Q-PCR analysis detects specific nucleic acid amplification products as they accumulate in real-time. This real-time analysis is characterised by the point during amplification when the accumulation of product is first detected rather than the amount of product accumulated after a fixed number of cycles. The higher the starting amount of nucleic acid target the sooner a significant increase in fluorescence is observed. The cycle number at which the reporter fluorescence generated is detectable above background noise is termed the threshold. The system uses fluorescently labelled oligonucleotide probes that eliminate the need for post-PCR processing and it is capable of screening gene expression within hours, using a minimal amount of sample material, and can detect a single molecule of DNA or RNA.

4.7.1 TaqMan™ chemistries

Q-PCR using the Applied Biosystems Prism 7000 Sequence Detector is based on detection of a fluorescent signal produced proportionally during the amplification of a PCR product. Probes are designed to anneal to the target sequence between the traditional forward and reverse primers, they are labelled at the 5' end with a reporter fluorochrome, 6-carboxyfluorescein (6-FAM) and a quencher fluorochrome, 6-carboxy-tetramethyl-rhodamine (TAMRA) added at any T position or at the 3' end. The probe is designed to have a higher T_m than the primers, and during the extension phase the probe must be 100% hybridised for success of the assay. As long as both fluorochromes are on the probe, the quencher molecule stops all fluorescence by the reporter, however as *taq* polymerase extends the primer, the intrinsic 5' to 3' nuclease activity degrades the probe releasing the reporter fluorochrome. The amount of fluorescence released during the amplification cycle is proportional to the amount of product (amplicons) generated in each cycle. The intensity of the fluorescence signal increases proportionally in real-time as PCR cycles continue. At any point during the exponential phase of a reaction the amount of DNA can be calculated, then through a simple mathematical calculation the initial concentration of DNA in that reaction can also be determined (Figure 4.5).

Figure 4.5: A schematic of the Q-PCR reaction sequence

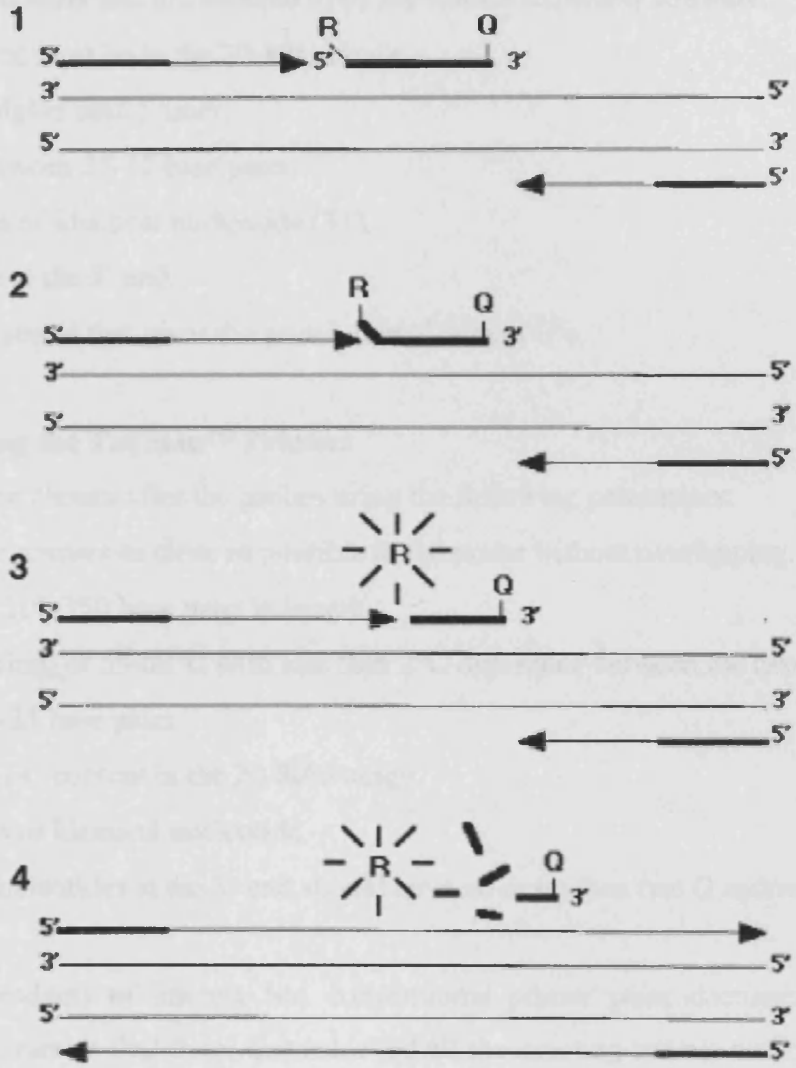

1. When the probe is intact, the proximity of the reporter dye to the quencher dye results in suppression of the reporter fluorescence primarily by Förster-type energy transfer (Lakowicz and Maliwal, 1983).
2. During PCR, if the target of interest is present, the probe specifically anneals between the forward and reverse primer sites.
3. The 5′ to 3′ nucleolytic activity of the AmpliTaq Gold DNA Polymerase cleaves the probe between the reporter and the quencher only if the probe hybridizes to the target.
4. The probe fragments are then displaced from the target and polymerization of the strand continues. The 3′ end of the probe is blocked to prevent extension of the probe during PCR. This process occurs in every cycle and does not interfere with the exponential accumulation of product.

4.7.2 Designing the TaqMan™ Probes

There are strict criteria that are adhered to by the Primer Express® software:

- G-C content must be in the 20-80% range.
- T_m 10°C higher than primer.
- Length between 25-32 base pairs.
- Avoid runs of identical nucleotide (3+).
- No G base at the 5' end.
- Select the strand that gives the probe more C's than G's.

4.7.3 Designing the TaqMan™ Primers

The primers were chosen after the probes using the following parameters:

- Design the primers as close as possible to the probe without overlapping.
- Amplicon 100-350 base pairs in length.
- T_m (annealing) of 59-60°C with less than 2°C difference between the two primers.
- Length 18-33 base pairs.
- Keep the G-C content in the 20-80% range.
- Avoid runs of identical nucleotide.
- The five nucleotides at the 3' end should have no more then two G and/or C bases.

Although all products of interest had conventional primer pairs documented within the literature, it was rare to find those that achieved all the exacting criteria outlined above. As a result, primers were designed independently using Primer Express® software. Cytokine base sequences used in the study were obtained from GenBank® at the National Centre for Biotechnology Information database at http://www.ncbi.nlm.nih.gov/Genbank.html. Primers were specifically designed to cross an exon-exon boundary ensuring that genomic DNA was not being amplified. BLAST searches confirmed the specificity of primers for the respective cytokines. TaqMan™ GAPDH housekeeping primers and probes were also constructed. To ensure successful amplification of the appropriate product, traditional PCR and gel electrophoresis was undertaken to ensure products of the correct weight were realised. On delivery, probes and primers were reconstituted in H_2O to a stock concentration of 10μM, aliquotted and stored at -20°C in darkened vials to prevent photo-bleaching.

Primer probe pairs were designed for the following cytokines (see appendix VI):

1. Keratinocyte growth factor (FGF-7/KGF).
2. Keratinocyte growth factor receptor (KGFR) (which is encoded by the fibroblast growth factor receptor type II gene - FGFR-2 IIIb).
3. Keratinocyte growth factor-2 (FGF-10/KGF-2).
4. Granulocyte macrophage-colony stimulating factor (GM-CSF).
5. Granulocyte macrophage-colony stimulating factor receptor (GM-CSFR).
6. Interleukin-1-alpha (IL-1α).
7. Interleukin-1-alpha receptor (IL-1αR).
8. Hepatocyte growth factor/Scatter factor (HGF/SF).
9. Hepatocyte growth factor receptor or c-met (HGFR).
10. Transforming growth factor alpha (TGFα).
11. Glyceraldehyde-3-phosphate dehydrogenase (GAPDH).

4.7.4 Standard curve generation

As comparisons were to be made between differing cell populations an end-point copy number or "absolute" copy number was required. This was achieved by constructing a standard curve for each PCR run from 10-fold serial dilutions of a purified DNA sample of known amount. A PCR product that included the quantified amplicon was used (prepared by "conventional" PCR from cDNA positive for the concerned target mRNA). These PCR products were purified from agarose gels.

The cDNA produced was validated in the reverse-transcription and PCR reactions to determine if it transcribed and amplified at the same efficiency as the sample RNA present in a mixture of extracted RNAs. A standard curve was generated by plotting the log10 of control template (absolute copy number or nanograms) on x-axis against the threshold (C_t) value on the y-axis. The C_t value being the cycle at which a statistically significant increase in product yield is first detected. Standard curve, linear equation and correlation coefficient (R2) are automatically computed with the ABI PRISM® software. The standard curves were found to be linear over 6 logs (10^1 to 10^6 dilutions) with R2 of 0.998. A four-cycle difference was found to approximately equal a 10-fold difference in initial target concentration.

4.7.5 GAPDH housekeeping

GAPDH primers were used as an internal reference of housekeeping gene transcription for normalisation between different cDNA samples.

4.7.6 No template controls (NTCs)

These were used to determine the limits of PCR sensitivity and test reactions for possible background that may occur during amplification. They also provided a test as to whether contamination of RNA by genomic DNA had occurred and that no genetic material had been transferred during pipetting. NTCs also assessed any generation of primer-dimer PCR artefact or amplicon contamination that should have been eliminated by the software.

4.7.7 TaqMan™ primer amplification

Q-PCR master mix was prepared (equilibrated at room temperature) using 1μg of previously transcribed cDNA as template, placed in an optically clear 96-well plate and made up to 25μl with Q-PCR amplification buffer master mix (see appendix V) adding the *taq* polymerase last. Due to the large numbers of manual pipetting sequences, (up to 96 reactions per plate) there was the possibility of introducing errors; in an effort to combat this, all reaction-wells were repeated in triplicate. This offered the opportunity of identifying and omitting erroneous data. To further confirm Q-PCR efficiency agarose gel electrophoresis was undertaken on products.

Q-PCR program:

One cycle (denaturation) -	95°C for 2 minutes
40 cycles (amplification) -	95°C for 30 seconds
One cycle (anneal) -	60°C for 1 minute
One cycle (extend) -	72°C for 1 minute

4.7.8 Data acquisition and analysis

The detection system consists of a 96-well thermal cycler connected to a laser and charge-coupled device (CCD) optics system. An optical fibre inserted through a lens is positioned over each well, and laser light is directed through the fibre to excite the fluorochrome in the PCR solution. Emissions are sent through the fibre to the CCD camera where they are analysed by the software's algorithms. Emissions are measured every 7 seconds. The sensitivity of detection allows acquisition of data when PCR amplification is still in the exponential phase. This is determined by identifying the cycle number at which the reporter

dye emission intensities rises above background noise - the threshold cycle (C_t). The C_t is determined at the most exponential phase of the reaction and is more reliable than end-point measurements of accumulated PCR products used by traditional PCR methods. The C_t is inversely proportional to the copy number of the target template; the higher the template concentration, the lower the threshold cycle measured. Measuring the C_t values and comparing with the standard curve accomplish absolute quantification of the amount of target in the unknown samples.

All statistical analyses were performed using the statistical functions of the MS Excel computer programme or SPSS® software package.

4.7.9 Normalisation

Normalisation was necessary to correct for fluorescence fluctuations due to changes in concentration or volume. It was accomplished by dividing the emission intensity of the reporter dye by the emission intensity of a passive reference to obtain a ratio defined as the normalised reporter (Rn) for a given reaction well. The passive reference is a dye automatically included in the TaqMan™ buffer and does not participate in the 5' nuclease PCR.

4.7.10 Primer/probe optimisation

Optimisation of the PCR reaction was required for each primer and probe set. The purpose of this procedure is to determine the minimum primer concentrations giving the maximum yield, and to determine the minimum probe concentrations that give the minimum C_t for each probe target. As the optimal concentration may not be the same for both this was achieved by varying the concentration of one primer relative to the other (manufacturers suggested range 100nM to 800nM). Optimal primer concentration was calculated to be 300nM. Probe concentration was suggested to range from 50nM to 200nM and found to be optimal at 150nM. The Mg^{2+} concentration was also optimised at 5.5mM.

4.8 Enzyme-linked immunosorbent assay (ELISA)

To check whether gene expression levels were similar at the protein level ELISA quantitation was undertaken. R&D Systems, Europe, supplied kits for the determination of human KGF, GM-CSF and TGFα concentrations in cell culture supernatant.

4.8.1 Principle of the assay

This assay employs the quantitative sandwich enzyme immunoassay technique. Briefly, a mAb specific for the cytokines of choice had been pre-coated into the wells of a 96-well microplate. Standards and samples were pipetted into the wells so that the immobilized antibody can bind any proteins present. After washing any unbound substances, enzyme-linked antibodies specific for the proteins were added. Following a wash to remove any unbound antibody-enzyme reagent, a substrate solution was added, colour developing in proportion to the amount of protein bound in the initial step. The colour development is stopped with an acid solution and the intensity measured spectrophotometrically.

4.8.2 Limitations of the procedure

Cytokine protein concentrations measured at any one-time point could reflect the concurrent processes of cytokine secretion, cytokine uptake by cells, and cytokine protein degradation and not correlate directly with the levels of bioactive cytokine protein. As a result of these processes, the measured level of cytokine protein may significantly underestimate the actual cytokine-producing potential of cells.

4.8.3 Sample collection

Cell culture supernatants - Particulates were removed by centrifugation and supernatant assayed immediately.

Cell lysates - In order to liberate any bound protein cells were lysed using a 5% Triton-x solution. Cells from a pre-confluent T75 flask were used ($\approx 3x10^6$ cells).

4.8.4 Reagent preparation

Cytokine standards were reconstituted in H_2O producing stock solutions of varying concentrations depending on kit (KGF 20,000pg/ml, TGFα 10,000pg/ml, GM-CSF 500pg/ml). These were allowed to sit for a minimum of 15 minutes with gentle agitation prior

to making dilutions. 900µl of calibrator diluent was pipetted into the most concentrated tube. 500µl was then pipetted into the remaining tubes producing a dilution series (Figure 4.6). The most concentrated standard served as the high standard and calibrator diluent served as the zero standard (0pg/ml).

Figure 4.6: Example TGFα standard dilution series

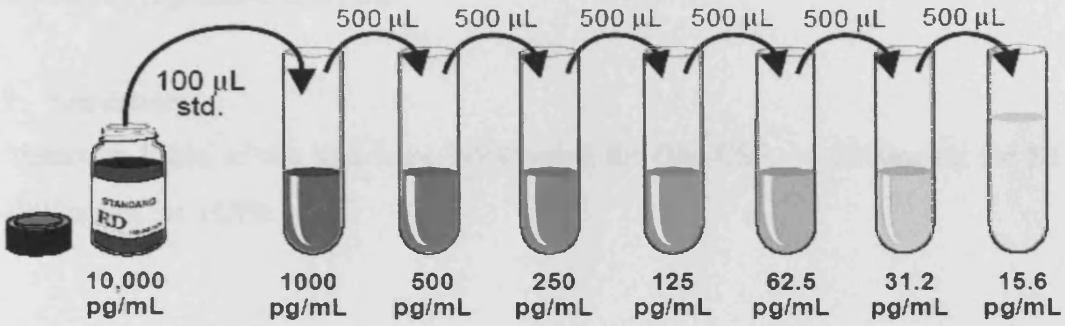

4.8.5 Assay procedure

Manufacturers instructions were followed. All samples and standards were assayed in duplicate after equilibration to room temperature. Briefly:

1. 100µl of assay diluent was added to each well.
2. 100µl of standard or sample was added per well ensuring reagent addition was uninterrupted and completed within 15 minutes. Wells were covered in foil and incubated for 2 hours at room temperature.
3. Wells were aspirated and washed with wash buffer and this process was repeated three times for four washes.
4. 200µl of cytokine conjugate was added, covered and incubated for a further 1 hour.
5. The aspiration/wash procedure of step 3 was repeated.
6. 200µl of substrate solution was added to each well and incubated for 20 minutes whilst being protected from light.
7. The reaction was halted using 50µl of stop solution.
8. The optical density (OD) of each well was determined within 30 minutes using a microplate reader set to 450nm. To ensure wavelength correction, the wavelength was set to 540nm and readings repeated. This subtraction allowed correction for optical imperfections in the plate.

4.8.6 Calculation of results

An average of the duplicate readings for each standard, control and sample was calculated and the average zero standard optical density subtracted. Using Microsoft Excel software, a standard curve was generated by plotting the mean absorbance for each standard on the x-axis versus the standard concentrations on the y-axis. The data was linearised by plotting the log concentrations versus the log of the OD and the best-fit line through the points of the graph determined by regression analysis.

4.8.7 Sensitivity

The detection limits of the kits were 3-500pg/ml for GM-CSF, 15-2000pg/ml for KGF and 2.5-1000pg/ml for TGFα.

CHAPTER FIVE

RESULTS

CHAPTER FIVE
RESULTS

This chapter presents results of an: -

a) Extensive histochemical staining analysis performed on fresh tissue cryosections, cell smears and colonies grown on a plastic substratum.
b) ELISA protein level assays for three cytokines: KGF, GM-CSF and TGFα.
c) Bromodeoxuridine (BrdU) keratinocyte proliferation studies.
d) Quantitative-polymerase chain reaction investigations.

Spreadsheets containing raw numerical data are within the appendices.

5.1 Fibroblast cultures - designation and morphology

Fibroblasts were derived from two anatomically separate regions, the superficial lamina propria, (named oral-gingival fibroblasts) and PDL connective tissues. In addition, explant culture of JE tissue samples regularly provided a third fibroblast population. These populations probably arose because of the difficulty in dissecting the JE complex from its underlying CT. It is unlikely that they originated from periodontal ligament as the JE sample is easily dissected free of the tooth surface. In addition, due to the extremely thin nature of a JE sample, the fibroblasts are unlikely to originate from directly beneath the OGE, it being some 2-3mm distant. The origin of these fibroblasts was therefore assumed to be beneath the physical attachment of JE as demonstrated in figure 5.1. The possibility of contamination during the micro-dissection procedure could not be ruled out but this population named junctional zone fibroblasts (JZF) was included in further investigations.

All three populations formed homogenous monolayer cultures that conformed to the classical spindle-shaped appearance described throughout the literature. Although Piche *et al.* (1989) documented subtle morphological changes between PDL and OGF in culture; this was not evident in our cultures, certainly not to the extent necessary to differentiate them with any authority by phase-contrast microscopy.

Cell types were assigned numbers. The same number across different cell types (epithelial or fibroblastic) indicate those cultures were derived from the same patient i.e. a matched pair.

5.1.1 Oral-gingival fibroblasts

Eight OGF lines were successfully derived namely: - OGF1, 2, 9, 11, 13, 14, 15 and 16.

5.1.2 Periodontal ligament fibroblasts

Seven PDL lines were successfully derived namely: - PDL1, 2, 9, 14, 15, 16 and 23.

5.1.3 Junctional zone fibroblasts

Four JZF lines were obtained namely: - JZF1, 9, 17 and 21.

5.2 Keratinocyte cultures - designation and morphology

In co-culture with 3T3 feeder layers proliferating JE and OGE colonies consisted of small, rounded, tightly packed cells conforming to the classical "cobblestone" appearance, which had the ability to push their surrounding 3T3 fibroblasts away as they expanded. Applying the classification proposed by Barrandon and Green (1985) (see chapter 2.8.4 for description), these most proliferative colonies initially correspond to the "holoclone" type. However, as time progressed and with repeated passage a larger number of colonies lost their "neat/rounded" appearance. They became scattered and irregular consisting of larger, flattened cells. These colonies therefore conformed to the meroclone/paraclone types. At no point during culture were morphological features evident that would enable distinction between JE and OGE populations.

5.2.1 Junctional keratinocytes

Eleven JE lines were derived namely: - JE1, 2, 4, 6, 7, 8, 9, 17, 18, 21 and 22.

5.2.2 Oral-gingival keratinocytes

Six OGE lines were derived namely: - OGE5, 6, 7, 8, 9 and 14.

Figure 5.1: Anatomical regions from which cell populations were derived

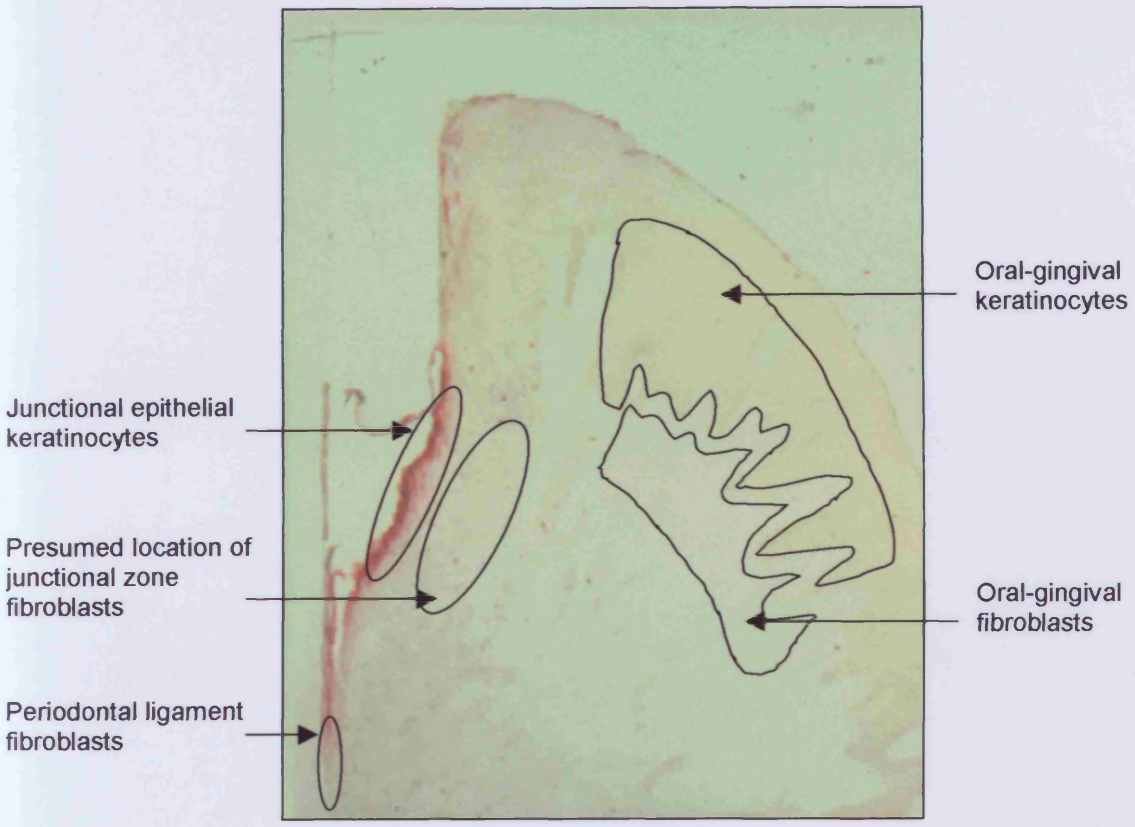

5.3 Fibroblast characterisation

5.3.1 Growth-rate studies

Sub-cultured fibroblasts divided rapidly and replating from a sub-confluent T75 flask at a 1:6 dilution ratio resulted in confluence within 5-7 days. At low passage number (below P4) OGF and PDL fibroblasts, whether matched or unmatched, took similar periods to reach confluency, there being no differences apparent to allow discrimination between populations. The graph over page shows growth rate potential of OGF, PDL and JZF fibroblast cultures using cell number as an indicator of proliferation. Mariotti and Cochran (1990) and Ogata and Niisato (1995) have performed more accurate population doubling-rate experiments and discovered that PDL fibroblasts proliferated at a slightly higher rate when compared with OGF.

With further passaging, (P5+), there was a noticeable decrease in the ability of cells to proliferate and colonise the flasks. Growth rapidly deteriorated and PDL fibroblasts were

rarely able to continue growth beyond P7 whilst OGF cells similarly faltered several passages later. Altered morphology accompanied these changes with the cells becoming larger, flattened, and blunt-ended with multiple cell-processes (Figures 5.2a-b). Other groups have reported these "high passage" features. In particular, Somerman *et al.* (1990) has referred to unpublished data demonstrating lower proliferation rates for PDL beyond P7. They attributed such characteristics to the phenomenon of senescence.

Figure 5.2: Growth curve for fibroblast cell lines

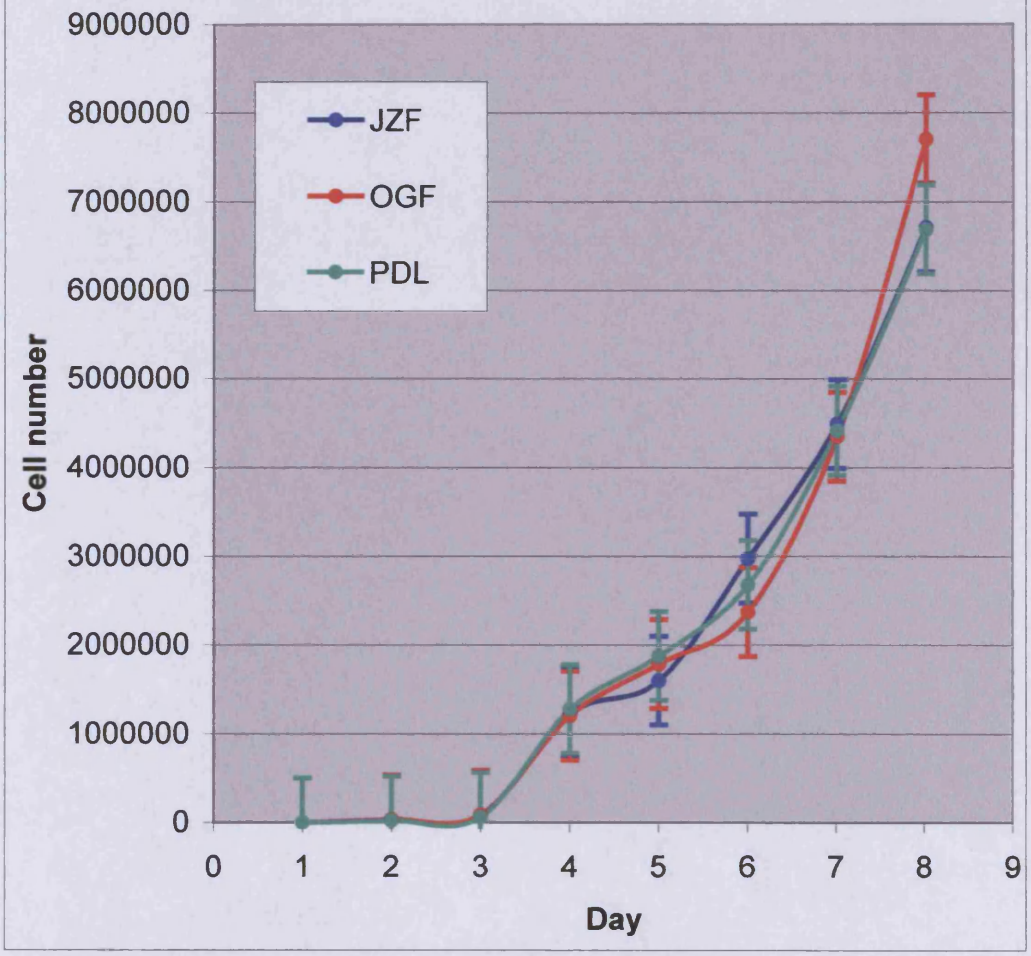

Fibroblasts were plated at 100,000 cells per T75 flask and cells counted using counting chambers on days 1 through 7. Triplicate assays of five fibroblast strains were used. Data are expressed as the mean ± the standard error mean.

Figure 5.3a: OGF1 at low passage (P1)

Typical spindle-shaped morphology of low passage oral-gingival fibroblasts as they approach sub-confluence.

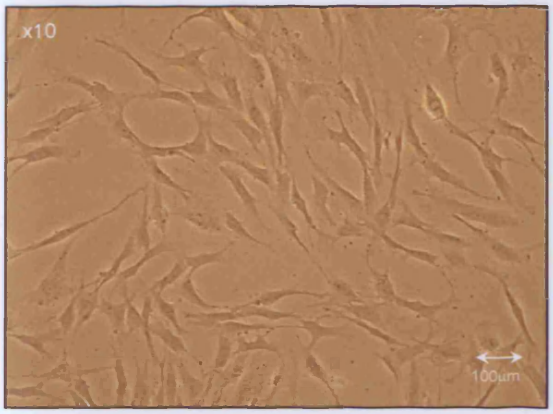

Figure 5.3b: OGF1 at high passage (P9)

Toward the end of their replicative life, the same oral-gingival fibroblasts exhibit a flattened morphology with granular cytoplasm and multiple cell processes. At this passage number, the cells did not reach confluence.

5.3.2 Histochemical staining for alkaline phosphatase

5.3.2.1 *Ex vivo* staining

Previous studies suggest that the most consistent difference observed between PDL and OGF is their differential expression of ALP. Cryosections of gingival tissue samples were stained to demonstrate the *in vivo* location of ALP positive zones. As can be seen in figure 5.3 staining was at its most intense adjacent to the tooth root and the PDL attachment zone (and possible region of derivation of JZF). This expression extended halfway through the gingival width with diminishing intensity. Toward the external surface, beneath the OGE rete pegs, was a zone apparently devoid of ALP activity. This region was interspersed with pinpoint positive cell clusters that corresponded to endothelial cells of the gingival capillary plexus.

Figure 5.4: Gingival cryosection stained for alkaline phosphatase

This figure demonstrates the reduction in intensity of ALP expression from the root surface toward the external oral-gingival surface.

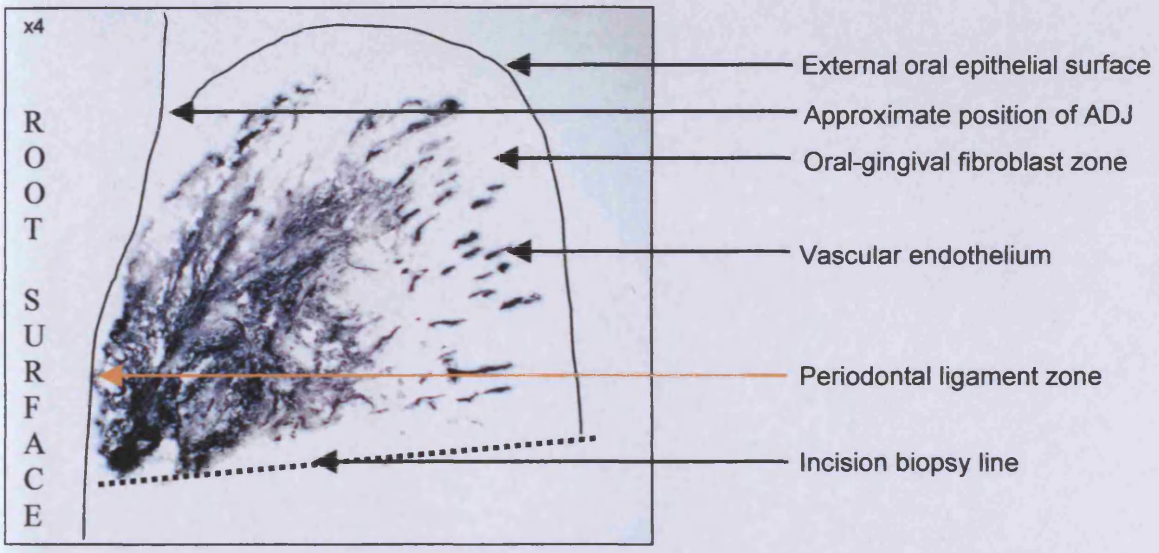

In order to investigate whether these staining characteristics were maintained throughout the isolation and culture procedures, cells growing in monolayer and smears developed from them were similarly stained.

5.3.3.2 *In vitro* staining - cultures

There were few stained cells within OGF populations whereas PDL cultures showed an abundance of positive cells (Figures 5.4a-d). Due to difficulties in visualising fibroblast boundaries in culture, cell smears were produced and stained in order to provide numerical data.

Figure 5.5a: OGF1 at sub-confluence stained for ALP

There were only occasional cells demonstrating ALP expression within the eight OGF lines tested.

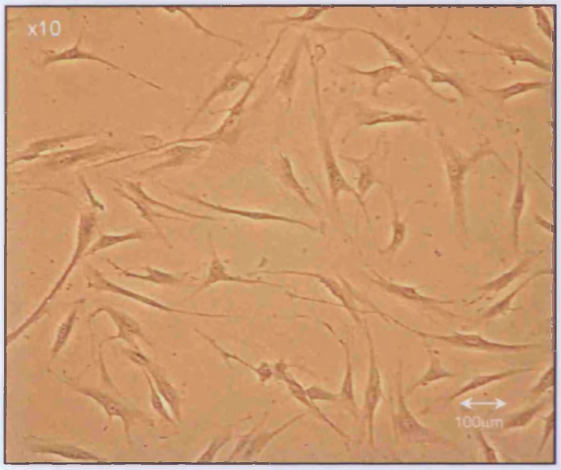

Figure 5.5b: OGF1 at confluence stained for ALP

To test whether ALP expression was not a time-dependant function, staining was repeated at confluence. Again, OGF was negative for ALP expression.

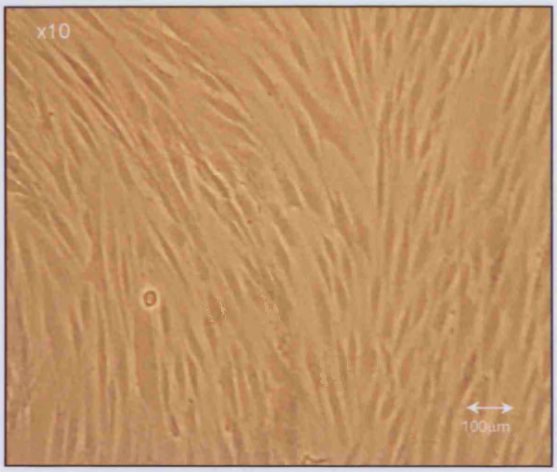

Figure 5.5c: PDL1 at sub-confluence stained for ALP

Demonstrating numerous positively stained cells.

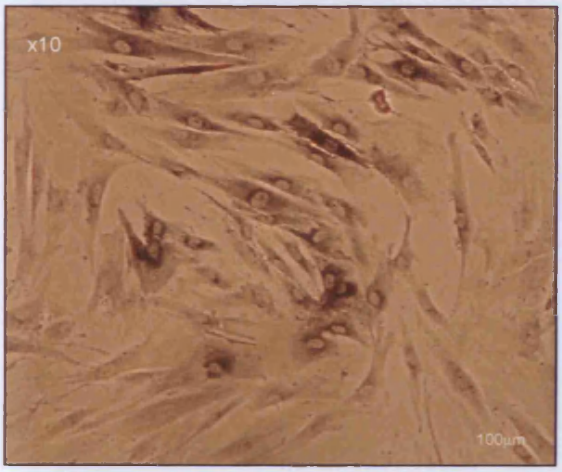

Figure 5.5d: PDL1 at confluence stained for ALP

Maintenance of ALP expression at confluence.

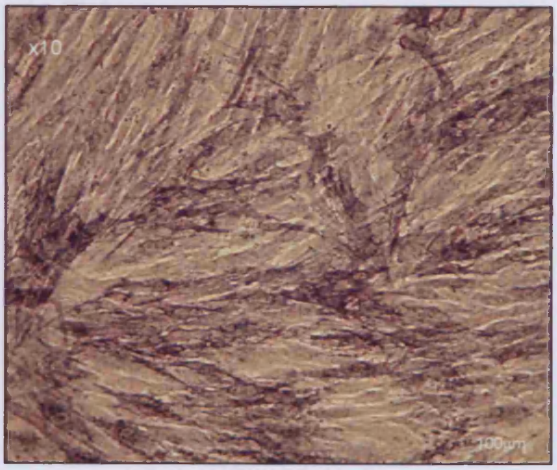

5.3.3.4 *In vitro* staining - smears

Despite photographic appearances (see figures 5.5a and b), cell smears were made with approximately equal cell densities as judged by eye under phase-contrast microscopy. PDL cell smears exhibited far higher numbers of positive cells (51-88%) compared with OGF (0-11%). Figures 5.5a and b show four paired samples.

Figure 5.6a: ALP staining PDL smears

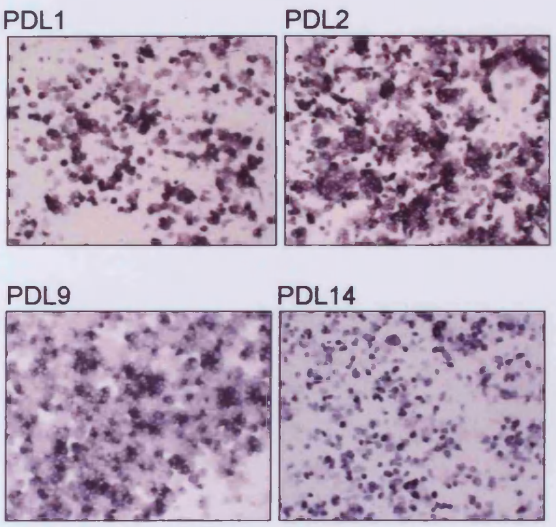

Figure 5.6b: ALP staining OGF smears

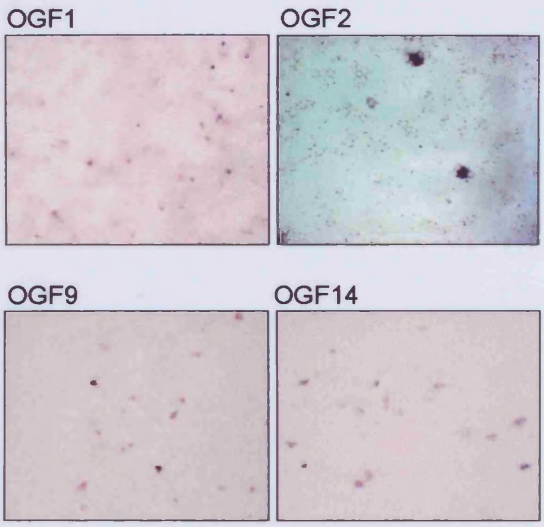

5.3.4 Effects of increasing passage number on ALP expression

In order to elucidate if the differing phenotypes, as dictated by ALP expression, were stable through increasing passage number, cultures were fixed and stained *in situ* over as many passages as possible. A palatal fibroblast line PF4, that exhibits no ALP activity, was run in tandem as a negative control. Cultures were scored as positive for ALP expression if any positive cells were present.

No OGF cultures beyond P3 exhibited ALP activity. All PDL lines expressed ALP up to P5 some as far as P7, however this expression was either lost in subsequent passages or the cells reached the end of their replicative potential. A summary of passage number versus ALP activity is shown in table 5.1.

It was likely that there would be less loss of *in vivo* phenotype during early passage; therefore, cells for subsequent experimentation were used at passage number 3 or below.

Table 5.1: Alkaline phosphatase activity with increasing passage number

+ = Positive staining
– = No positive cells
o = Cells stocks unavailable at this passage number

Blank boxes indicate inability of cell line to continue to divide and achieve this passage number.

	PASSAGE NUMBER (P)									
Cell line	1	2	3	4	5	6	7	8	9	10
OGF 1	–	–	–	–	–	–	–	–	–	
OGF 2	o	+	+	–	–	–	–	–	–	–
OGF 7	+	–	–	–	–	–	–	–		
OGF 9	o	+	–	–	–	–	–	–	–	–
OGF 11	o	+	+	–	–	–	–	–		
OGF 13	o	+	+	–	–	–	–	–	–	
OGF 14	o	+	–	–	–	–	–			
OGF 15	o	+	+	–	–	–	–			
PDL 1	o	+	+	+	+	+	+	–		
PDL 2	o	+	+	+	+	–	–			
PDL 9	+	+	+	+	+	+	+			
PDL 14	o	+	+	+	+	–				
PDL 15	o	+	+	+	+	–	–			
PDL 16	o	o	+	+	+	+	+			
JZF 1	+	+	+	+	–	–	–	–		
JZF 9	o	o	+	+	+	–	–	–	–	
JZF 17	o	o	+	+	–	–	–	–	–	
PF4	o	–	–	–	–	–	–	–	–	–

5.4 Epithelial characterisation

5.4.1 Growth-rate studies

Up to passage 3, all keratinocyte populations proliferated rapidly. On passaging at a dilution ratio of 1:10, keratinocytes reached confluence in approximately 8 days. Due to the unequal quantities in starting sample size between JE and OGE tissues, the time taken for JE to come to confluence appeared greater than that of OGE. In subsequent passages similar numbers of cells were plated into T75 flasks, however, JE colonies continued to show less growth and greater numbers of abortive, paraclone-like colonies became apparent. These results are in keeping with those of Gao and Mackenzie (1993) who found that JE showed relatively high rates of cell turnover *in vivo* but *in vitro* showed slower rates of growth than OGE. Beyond P3 JE lines showed a rapid decrease in their ability to divide and colonise the dishes. Similarly, OGE lines began to differentiate and rarely provided the rapidly proliferating holoclone-type colonies whilst paraclones became more apparent at later passages beyond P5. This increase in proportion in paraclone colonies would imply that keratinocytes were differentiating and entering into their terminal differentiation pathway. This may in part be attributable to the lack of a stem cell fraction obtained from initial explant growth, or may represent a deficiency in factors within the co-culture system required for sustainable growth.

5.4.2 BrdU labelling protocol

In order to examine the lower rate of proliferation of junctional keratinocytes, BrdU uptake was used to assess the number of dividing cells entering S-phase for a given time period. BrdU was introduced to five JE and five OGE P1 cultures on days 2, 4 and 6 post-plating. Within each flask, fifty colonies were then randomly selected and categorised as being holoclones, meroclones or paraclones. For each colony the total cell number and the number of BrdU-positive cells allowed the percentage BrdU positive cells to be calculated. This provided information about the proliferative differences between holoclones, meroclones and paraclones and differences in proliferative capacity between JE and OGE in culture. Beyond day-6, colonies were too large for manual counting and had begun to merge with each other. Raw numerical data is shown in appendix VII. Figures 5.6a-d show example staining patterns.

Figure 5.7a: BrdU staining of an OGE holoclone-type colony

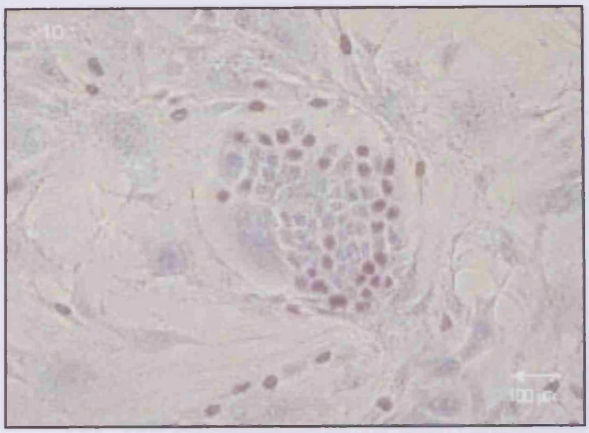

Typical example of a holoclone with small, rounded keratinocytes forming a compact colony with orderly margin. BrdU-positive cells tend to be positioned toward the periphery of the colony.

Figure 5.7b: BrdU staining of an OGE meroclone-type colony

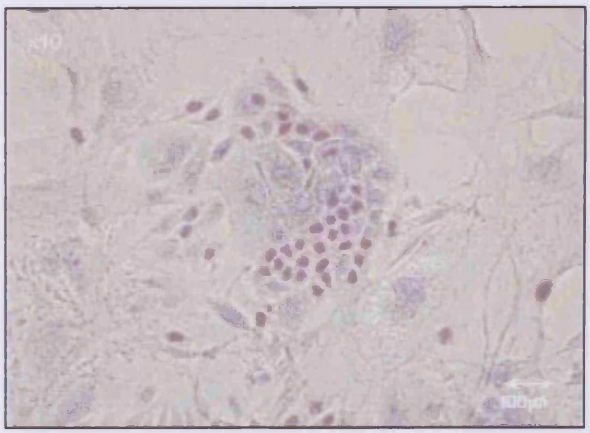

Typical example of a meroclone with some small, rounded keratinocytes and larger, flattened cells toward the periphery. Generally, the larger cells do not demonstrate BrdU incorporation, probably as they are non-replicative, terminally differentiated cells.

Figure 5.7b: BrdU staining of an OGE meroclone-type colony

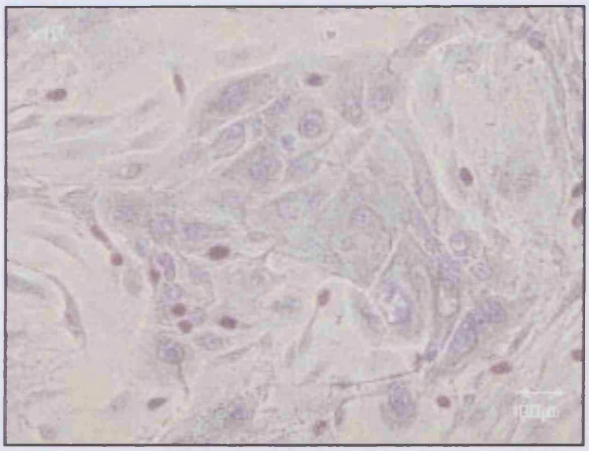

Typical example of a paraclone containing almost no small, round keratinocytes. The cells appear large, irregular and flattened. Very few cells take up the BrdU. These colonies represent the terminally differentiated fraction.

5.4.2.1 Colony cell numbers

Figures 5.7 and 5.8 demonstrate the increasing cell number within the three colony morphology classifications over a 6-day period. Holoclones show considerable growth and expansion reaching an average colony size of 96 cells for JE and 177 cells for OGE. Predictably, there were lesser increases for meroclones and paraclones.

Figure 5.8: Average junctional epithelium colony cell number

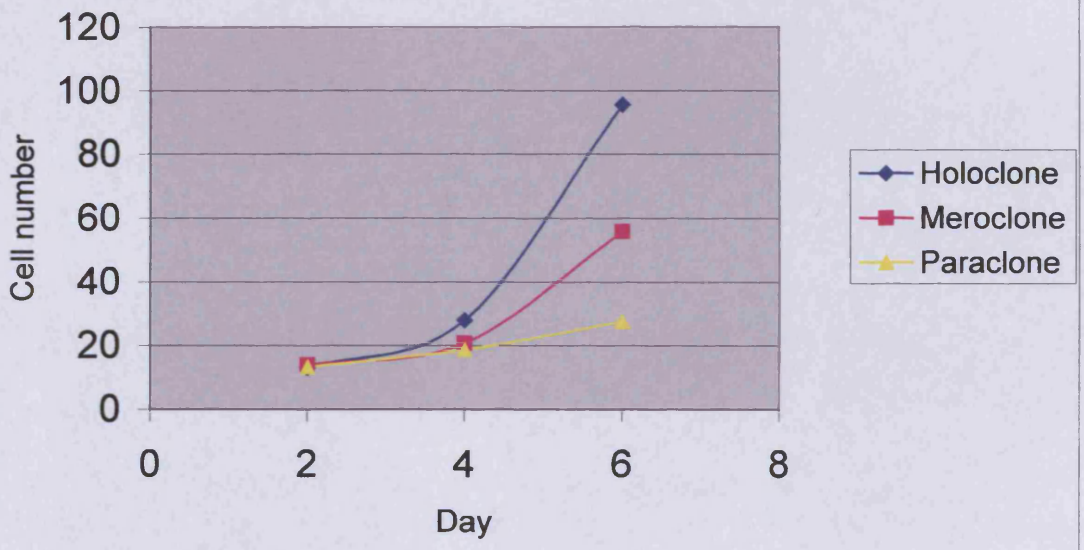

Figure 5.9: Average oral-gingival epithelium colony cell number

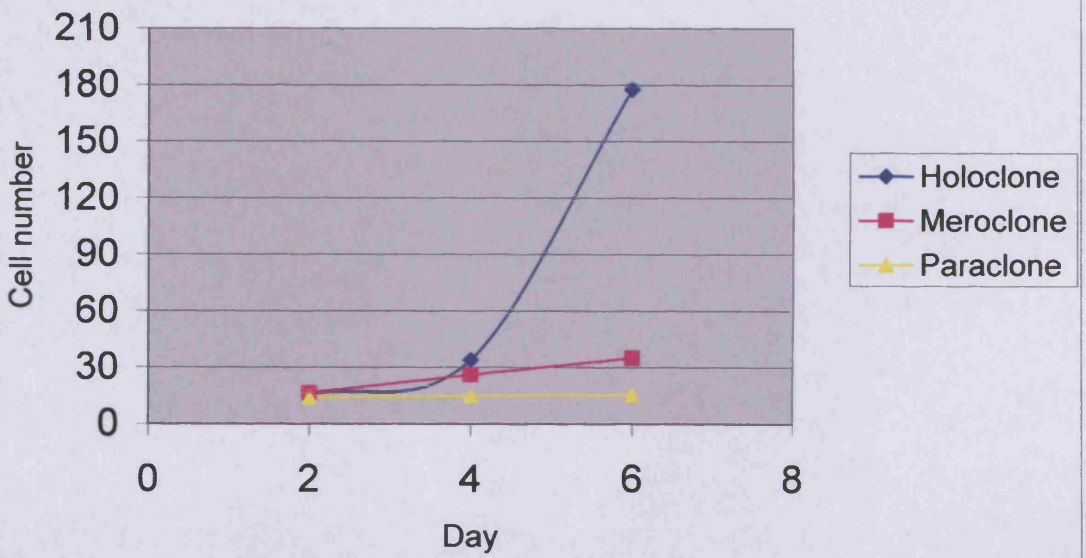

5.4.2.2 BrdU labelling of JE and OGE colonies

Figures 5.9 and 5.10 show the percentage of cells within each colony type that incorporated the BrdU substrate for junctional and oral-gingival samples respectively.

Figure 5.10: Average percentage BrdU-positive cells per colony type - junctional epithelium

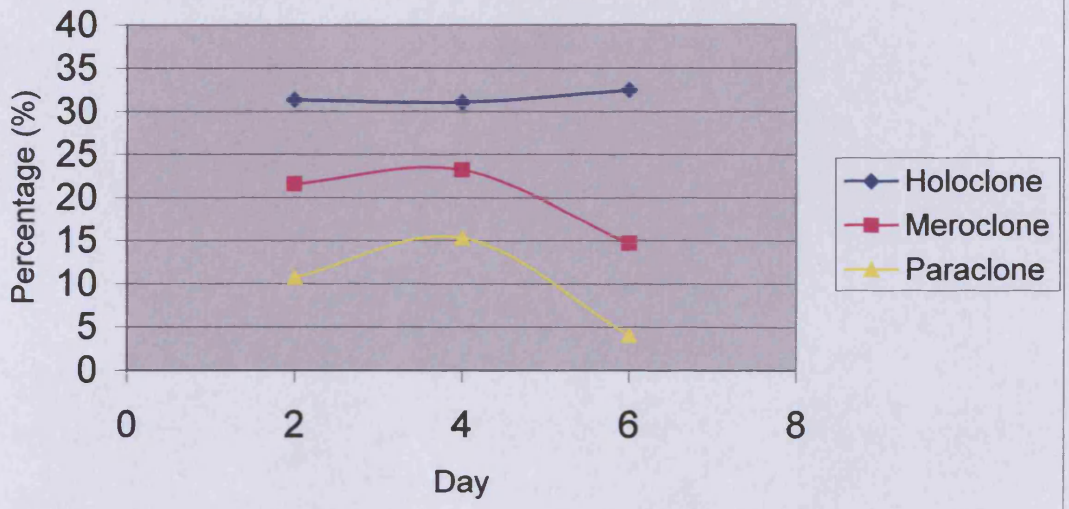

Figure 5.11: Average percentage BrdU-positive cells per colony type - oral-gingival epithelium

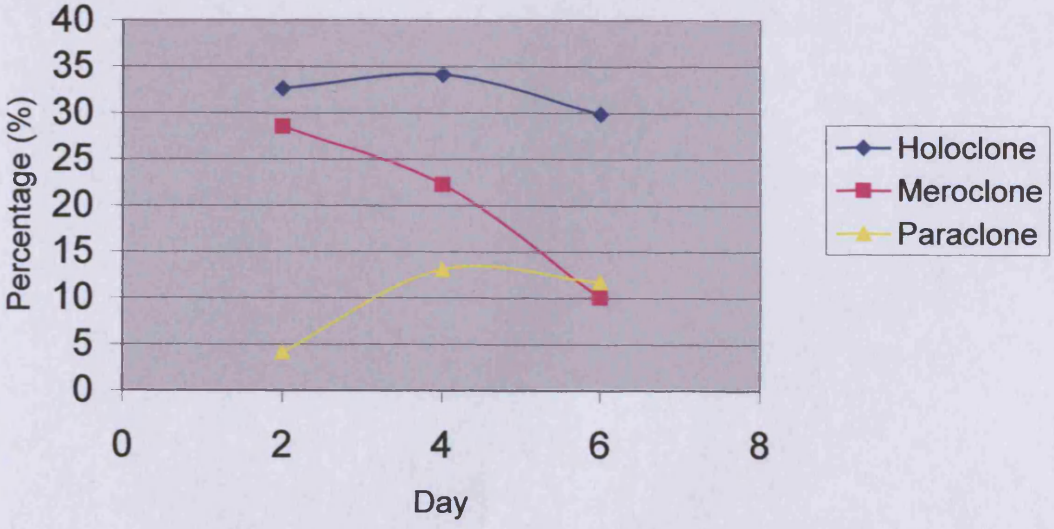

5.4.3. Summary

Holoclones demonstrated a considerable growth advantage over meroclones and paraclones. Further, OGE keratinocytes demonstrated a higher growth-rate within the holoclone fraction when compared to JE keratinocytes, producing colonies of, on average, double the number of cells. Meroclones and paraclones showed little differences between the two-keratinocyte populations.

Over each two-hour period, BrdU uptake in holoclones showed a persistently increased number of proliferating cells incorporating the thymidine analogue compared with meroclones or paraclones.

The percentage of actively dividing cells remained similar between the two-keratinocyte types with JE and OGE holoclones maintaining activity in approximately one third of cells over the 6-day period (JE – 33%, OGE – 30%).

Both meroclones and paraclones showed lower percentages of actively dividing cells and a gradual drop-off in uptake over the 6 days. Only 10-15% of meroclones and 4-11% of paraclones were incorporating the BrdU at the end of the experimental run. This would suggest that the meroclones and paraclones do indeed consist of a higher number of abortive, terminally differentiated cells that undergo little or no further proliferative activity.

5.5 Immunohistochemical staining patterns

Initial studies were undertaken to identify differences in the patterns of mAB binding throughout the periodontal epithelia *in vivo* using *ex vivo* tissue sections. Antibody panels were then applied to all 17 derived epithelial types when grown as colonies on plastic and cell smears. Organotypic cultures were constructed using five JE and five OGE samples and the same antibody panel applied to cryosections. Images were captured using 4x, 10x or 20x magnification. Occasionally for clarification, multiple images of the same section were taken, and composites produced using the Photoshop® 6.0 software (Adobe®). The nuclear dye Hoechst 33258 was used with some samples principally to aid location and highlight tissue architecture. The same UV intensity settings and image resolution were used throughout.

5.5.1 *Ex vivo* staining patterns

Cytokeratin 1 (Figure 5.12)

Antibody staining identified cytokeratin 1 throughout the suprabasal region of OGE extending into the stratum corneum. Staining intensity was lost toward the crestal/oral-sulcular interface. There were however sporadic suprabasal cells staining throughout the OSE.

Cytokeratin 10 (Figure 5.13)

Cytokeratin 10 staining was similarly distributed to that of CK1, throughout the suprabasal layers of the OGE and patchy suprabasal staining of oral-sulcular/crestal regions.

Cytokeratin 4 (Figure 5.14)

Cytokeratin 4 staining was localised to the suprabasal layers of the crestal/oral-sulcular zones with occasional patches of stain visible along the OGE.

Cytokeratin 13 (Figure 5.15)

CK13 had a similar distribution to CK4 with the entire crestal portion of the sample strongly positive. Sporadic suprabasal patches along the OGE were also visible, but to a lesser degree compared with CK4.

Cytokeratin 6 (Figure 5.16)

Suprabasal cells of the keratinised OGE showed reactivity with staining gradually fading toward the crestal zone.

Cytokeratin 16 (Figure 5.17)

Cytokeratin 16 was expected to produce a pattern similar to that of CK6, however staining was more widespread with strong positive results throughout suprabasal cells of the OGE and OSE but no staining of the JE.

Cytokeratin 8 (Figure 5.18)

Cytokeratin 8 expression was greatest throughout the layers of the JE; there was also evident patchy staining of basal cells of the rete tips at the junction between the OGE and crestal zone.

Cytokeratin 18 (Figure 5.19)

In agreement with previous studies, CK18 stain was localised to the JE zone only (Morgan *et al.*, 1986; Shabana *et al.*, 1991 and Mackenzie *et al.*, 1991).

Cytokeratin 14 (Figure 5:20)

Cytokeratin 14 was present at great intensity of fluorescence throughout all layers of all epithelia.

Cytokeratin 15 (Figure 5.21)

Cytokeratin 15 has been reported to be a potential marker of stem cell zones (Waseem *et al.*, 1998); within the gingival section, only the basal cells of the OGE and OSE regions were positive with intensity diminishing toward the JE.

Cytokeratin 17 (Figure 5.22)

There are few literature reports regarding CK17 expression within epithelia. Interestingly its distribution appeared to correlate with the basal cells of JE, however this was extremely weak.

Cytokeratin 19 (Figure 5.23)

As expected CK19 staining was identified, at high intensity, throughout the JE zone. Staining was also identified within basal cells at the rete tips of the OGE. Merkel cells adjacent to the rete tips were also positive for CK19.

Intracellular adhesion molecule-1 (Figure 5.24)

Work by Crawford and Hopp (1990) and repeated by Moughal *et al.* (1992) demonstrated distribution of ICAM-1 throughout the JE and partial expression within OSE. Disappointingly, any reactivity to the ICAM-1 mAB within the JE was at an extremely low intensity. It was unlikely that this would provide a useful differentiation tool.

Desmoplakin I+II (Figure 5.25)

Desmoplakin expression within JE tissues was first identified by Carmicheal *et al.* (1991). Later Matsuyama and Izumi (1997) identified differential staining characteristics between cultured JE and OGE populations. However, intra-cellular mAb staining showed similar intensities and patterns throughout the gingival section with no differentiating features evident.

***Dolichos biflorus agglutinin* (Figure 5.26)**

DBA was strongly located throughout the JE zone. There was evidence of weak staining of the suprabasal cells throughout the remaining section but this was regarded as background effects.

Matrix metalloproteinase-7 (Figure 5.27)

Recently identified by Uitto *et al.* (2002) as being differentially expressed by JE, MMP-7 antibody produced a pattern similar to CK19 with the internal basal compartment of JE and sporadic basal cells at the rete tips reacting positively.

Figure 5.12: Cytokeratin 1

Figure 5.13: Cytokeratin 10

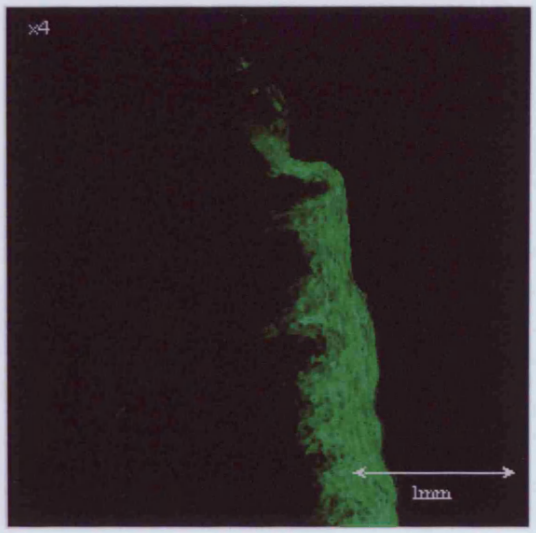

Figure 5.14: Cytokeratin 4

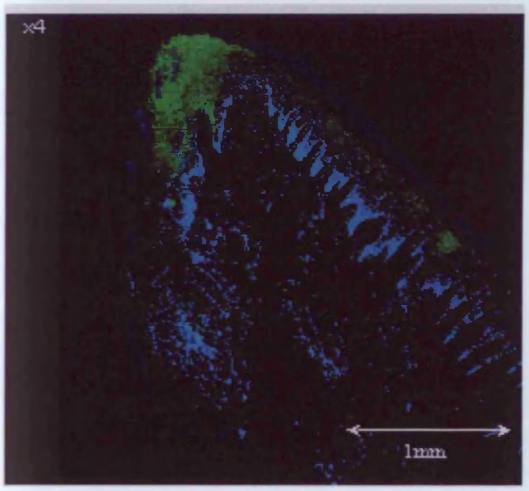

Figure 5.15: Cytokeratin 13

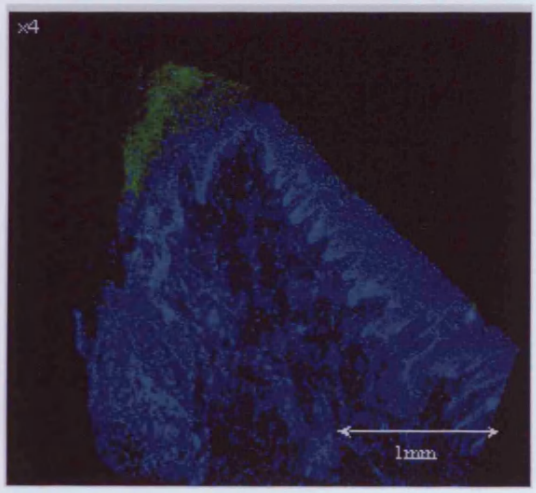

Figure 5.16: Cytokeratin 16

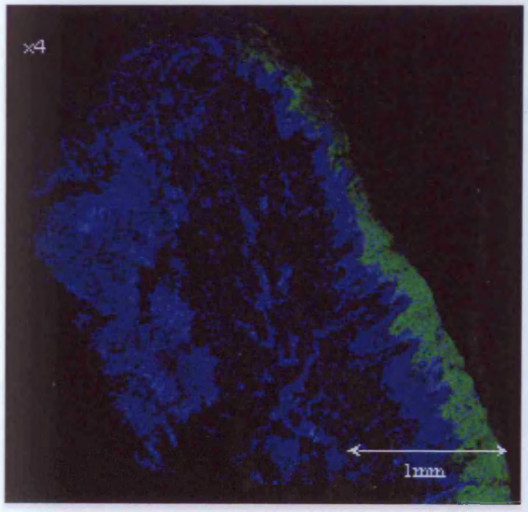

Figure 5.17: Cytokeratin 17

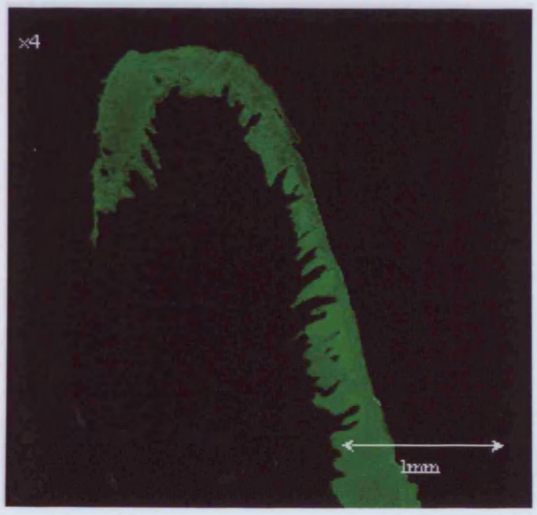

Figure 5.18: Cytokeratin 8

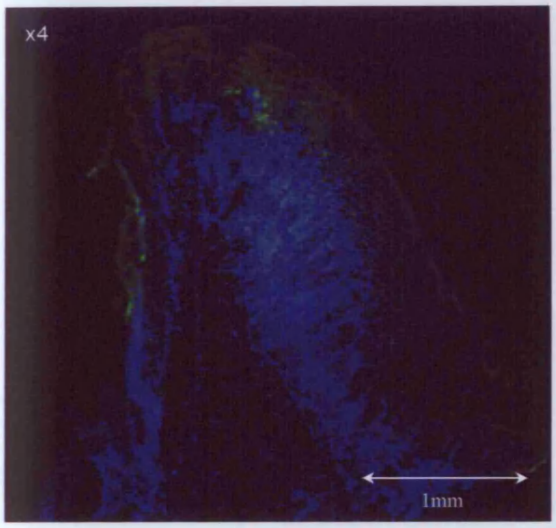

Figure 5.19: Cytokeratin 18

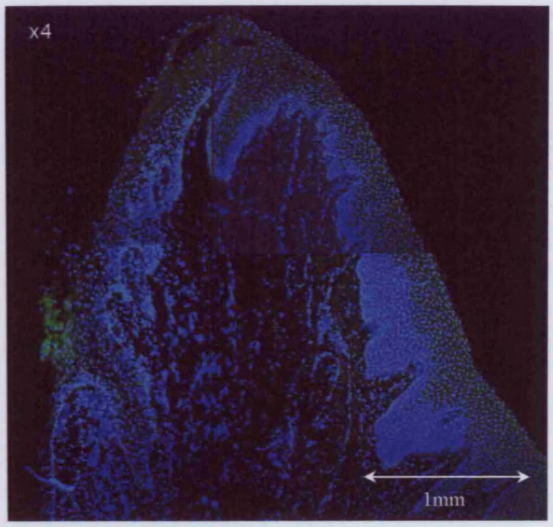

Figure 5.20: Cytokeratin 14

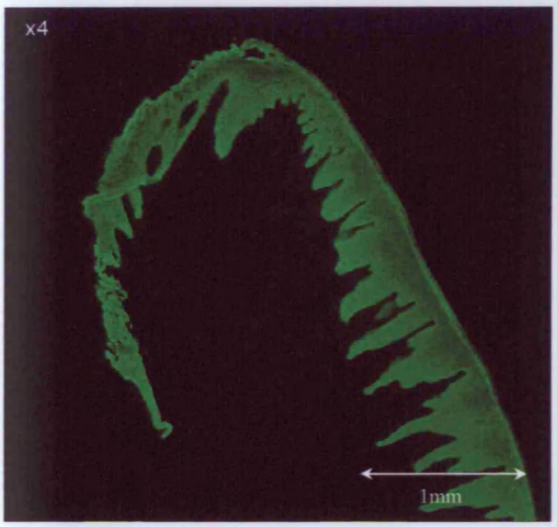

Figure 5.21: Cytokeratin 15

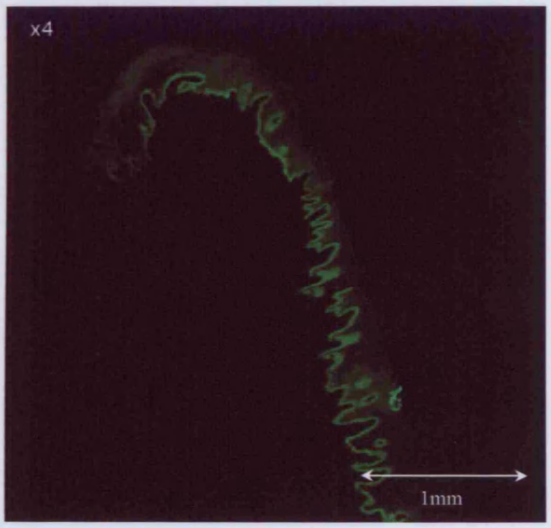

Figure 5.22: Cytokeratin 17

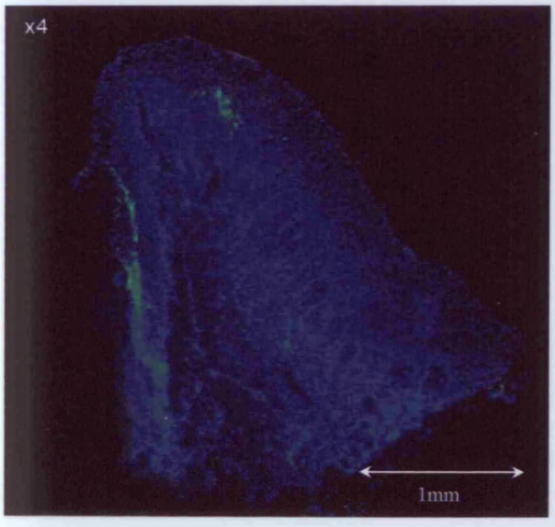

Figure 5.23: Cytokeratin 19

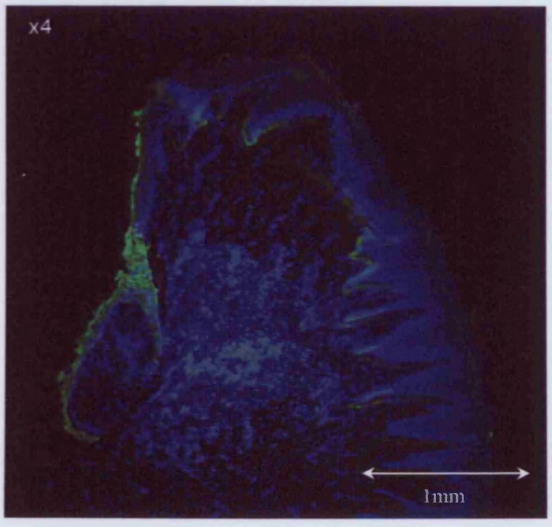

Figure 5.24: ICAM-1

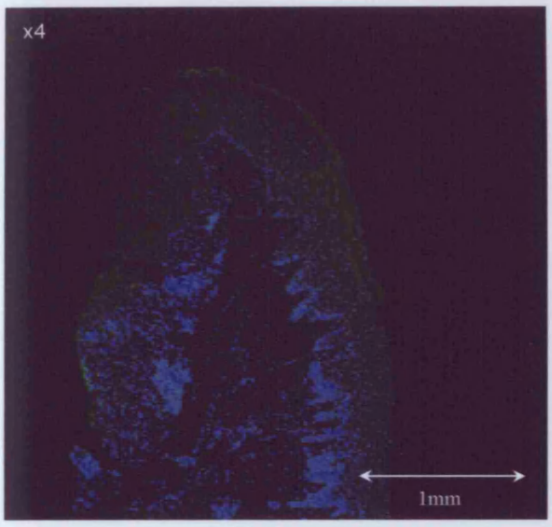

Figure 5.25: Desmoplakin I+II

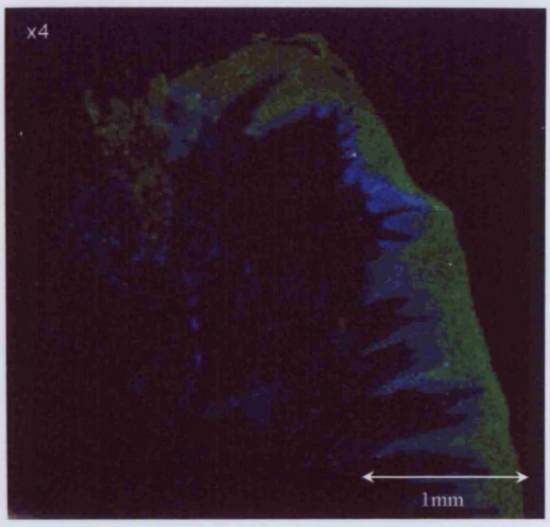

Figure 5.26: DBA

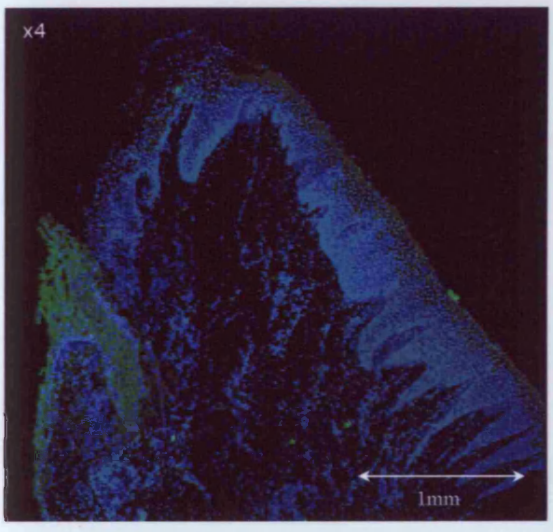

Figure 5.27: MMP-7

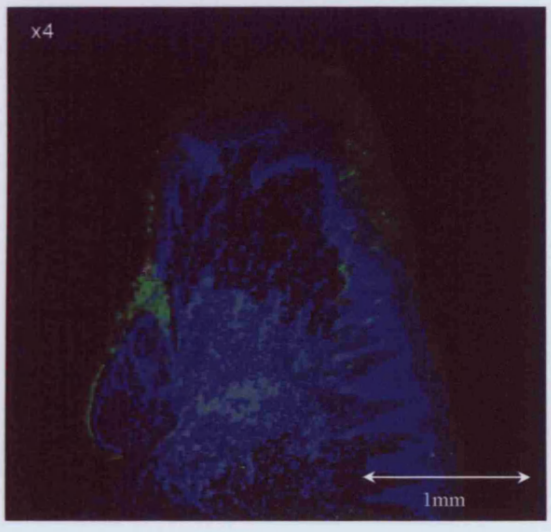

Table 5.2: Summary of mAB staining of gingival cryosections

+++ Strong positive staining
++ Positive staining
+ Weak positive staining
- Negative

mAB	Location: OGE/OSE/JE	Basal compartment	Suprabasal compartment
Cytokeratin 1	OGE	-	+++
	OSE	-	++ (Sporadic cells)
Cytokeratin 10	OGE	-	+++
	OSE	-	++ (Sporadic cells)
Cytokeratin 4	OGE	-	+ (Patches)
	OSE	-	+++
Cytokeratin 13	OGE	-	+ (Patches)
	OSE	-	++
Cytokeratin 6	OGE	-	++
	OSE	-	+ (Sporadic cells)
Cytokeratin 16	OGE	-	++
	OSE	-	++
Cytokeratin 8	OGE	+ (Rete tips)	-
	OSE	+ (Rete tips)	-
	JE	++	
Cytokeratin 18	OGE	-	-
	OSE	-	-
	JE	++	
Cytokeratin 14	OGE	+++	+++
	OSE	+++	+++
	JE	+++	
Cytokeratin 15	OGE	+	-
	OSE	+	-
	JE	+ (Very faint)	
Cytokeratin 17	JE	+	
Cytokeratin 19	Merkel cells	++	
	OGE	++ (Rete tips)	-
	OSE	++	-
	JE	+++	
ICAM-1	JE	+ (Very faint)	+ (Very faint)
Desmoplakin I+II	All strata	Intracellular +	
DBA	JE	++	
MMP-7	OGE	++ (Rete tips)	-
	OSE	++ (Rete tips)	-
	JE	+++	

In summary, the histochemical staining resulted in distributions similar to those published within the literature (Morgan *et al.*, 1986; Shabana *et al.*, 1991 and Mackenzie *et al.*, 1991). Obvious departures would include the homogenous staining patterns with desmoplakin and disappointingly low intensity binding of ICAM-1. Several mABs showed promise in their specificity for the JE phenotype including CK 8, 17, 18, 19, DBA and MMP-7.

5.5.2 *In vitro* staining patterns

To investigate the epithelial phenotype when in co-culture with 3T3s the panel of mAB staining was repeated on both epithelial colonies cultured on plastic substrate and cell smears prepared from them.

Potential differentiation markers that distinguished JE from OGE in culture (*in vitro*) as well as *in vivo* were:

- CK8 and 18 that showed marginal increases in staining intensity for JE (Figures 5.34 and 5.35).
- CK19 that demonstrated significant increase in staining intensity for JE (Figure 5.37).
- ICAM-1 that was weakly positive for JE and negative for OGE (Figure 5.38).
- DBA that showed positive JE staining but no reactivity for OGE (Figure 5.40).

Figure 5.28: Cytokeratin 1

OGE – Colony

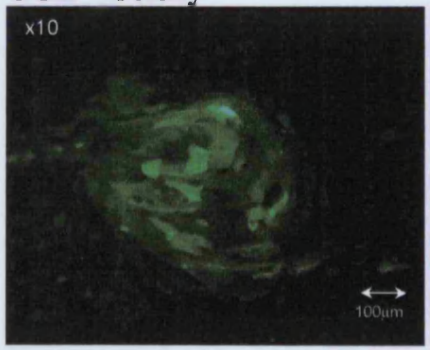

Suprabasal cells stain strongly for CK1.

OGE – Smear

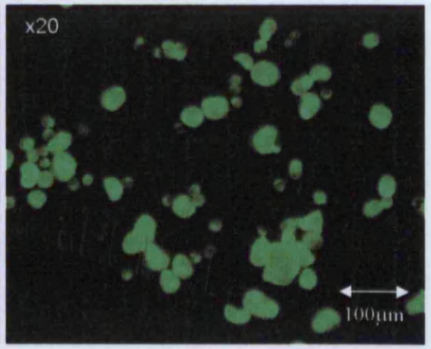

Larger, flattened cells corresponding to the stratum corneum stain positively.

JE – Colony

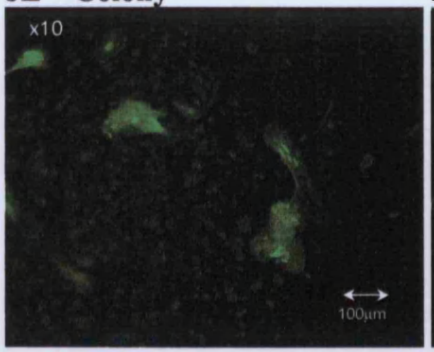

Few, large differentiated cells within JE colonies stain positively for CK1.

JE – Smear

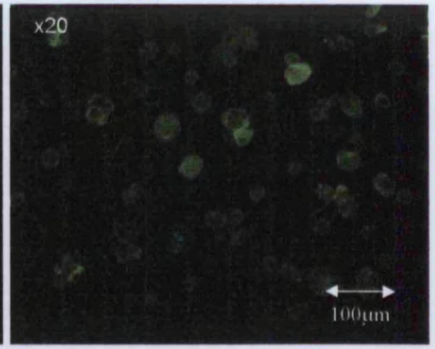

Occasional large cells within JE smears were also found to be positive.

Figure 5.29: Cytokeratin 10

OGE – Colony

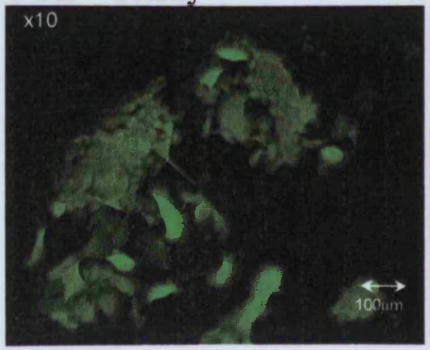

Similar staining pattern as for CK1 with larger, irregular, differentiated cells staining most intensely.

OGE – Smear

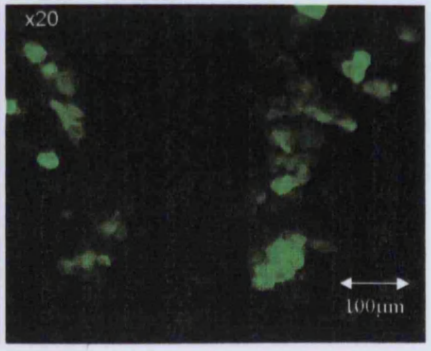

The larger, flattened cells corresponding to the stratum corneum stained positively within OGE smears.

JE – Colony

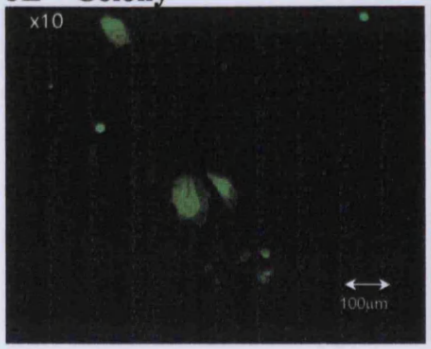

Very few cells within JE colonies stain positively for CK10.

JE – Smear

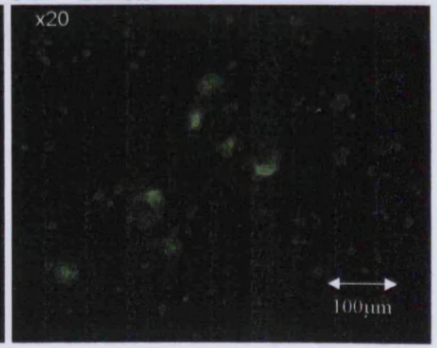

Very weak staining of a small fraction of JE cells within smears stained for CK10.

Figure 5.30: Cytokeratin 4

OGE – Colony

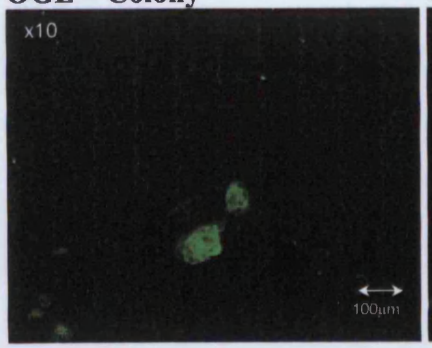

OGE – Smear

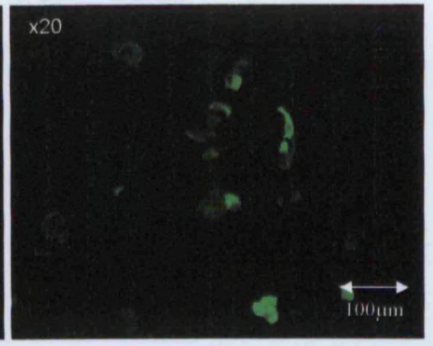

In vivo, cells at the gingival crest stained positively for CK4 whereas OGE did not. It is possible that some of these crestal cells were included into the OGE fraction during the micro-dissection procedures and are visible here sporadically in both colonies and cell smears.

JE – Colony

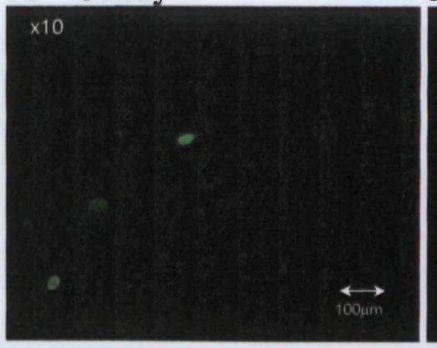

JE – Smear

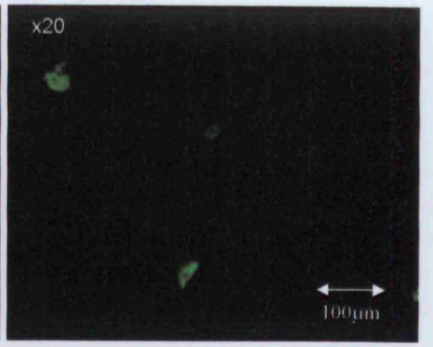

Cytokeratin 4 was not detected within JE tissue *in vivo*, and very little staining is evident throughout the colony and smear preparations.

Figure 5.31: Cytokeratin 13

OGE – Colony

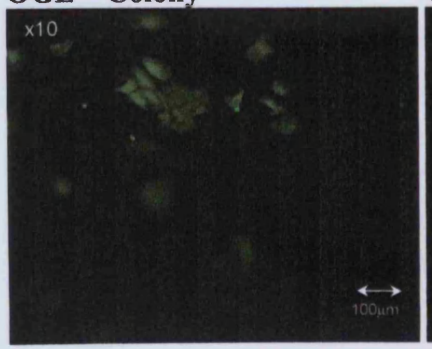

OGE – Smear

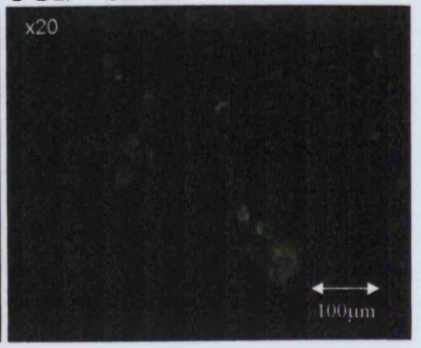

Staining *in vitro* samples for CK13 produced similar patterns to that of CK4 with very weak staining of sporadic cells within colonies and smears.

JE – Colony

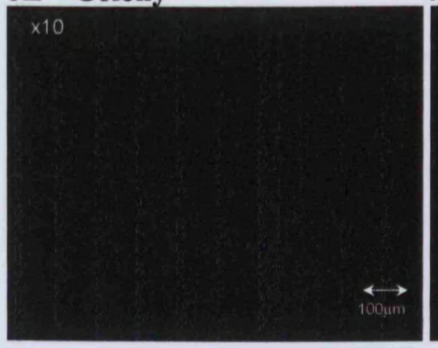

JE – Smear

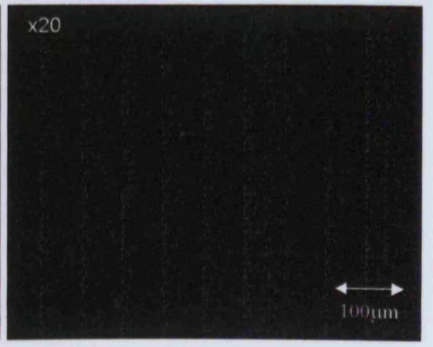

There was no CK13 staining evident within JE preparations. This mirrors the *ex vivo* IHC (Figure 5:14).

Figure 5.32: Cytokeratin 6

OGE – Colony

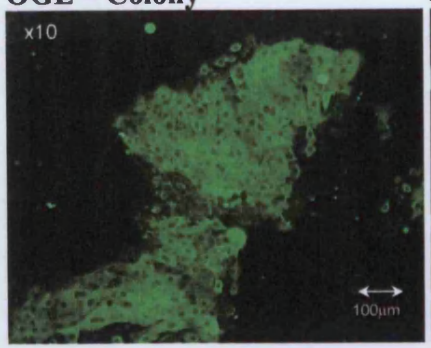

Strong positive CK6 staining of all keratinocytes within the OGE colonies.

OGE – Smear

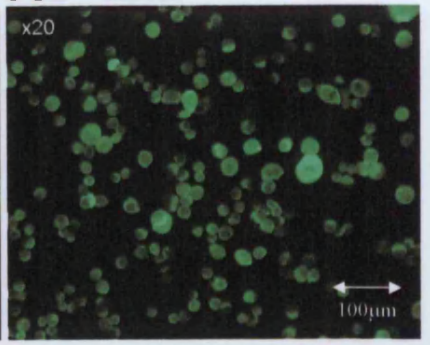

Variation in intensity of staining is apparent in smears. Larger, flattened, differentiated cells tend to stain more intensely.

JE – Colony

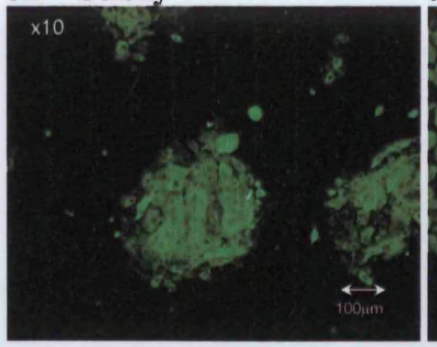

The JE zone did not stain for CK6 *in vivo* however, staining of colonies *in vitro* was present. This may represent a shift in phenotype of JE keratinocytes in culture.

JE – Smear

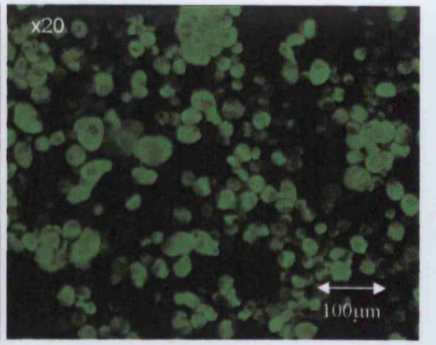

Similar staining was evident within smears although smaller cells tend to stain less intensely.

Figure 5.33: Cytokeratin 16

OGE – Colony

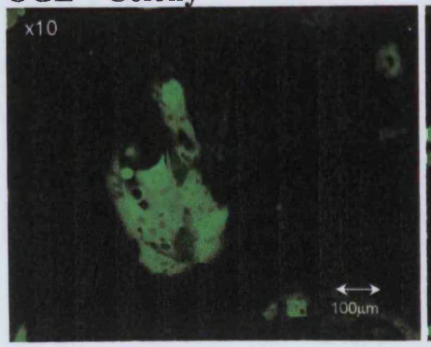

Intense positive staining for CK16 by OGE colonies.

OGE – Smear

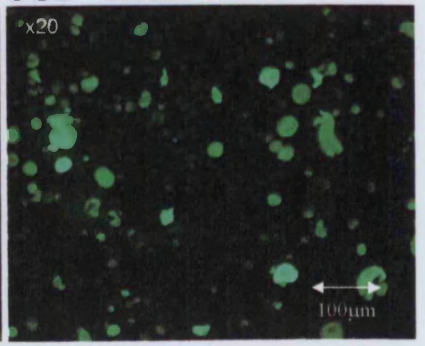

Within smears larger, differentiated cells tend to stain more intensely for CK16 in a similar manner as CK6.

JE – Colony

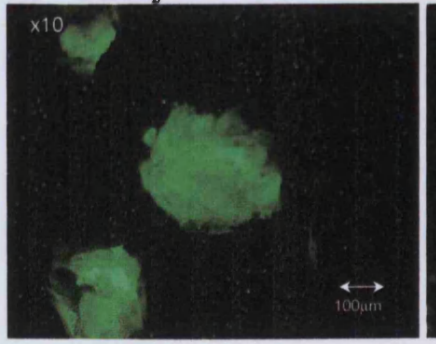

Strong, uniform colony staining of JE samples for CK16.

JE – Smear

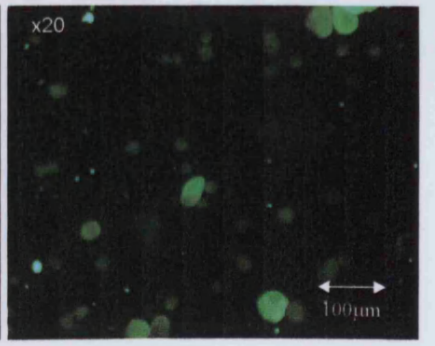

As seen with OGE smears there is variation in staining intensity with larger cells more strongly positive.

Figure 5.34: Cytokeratin 8

OGE – Colony

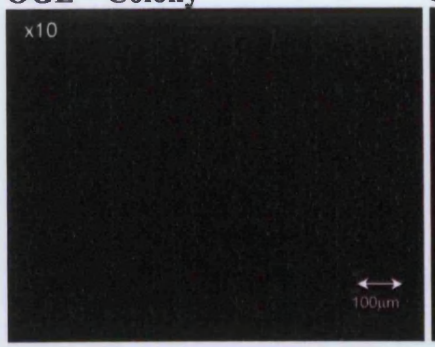

In concordance with *in vivo* expression patterns, there was no CK8 localisation within OGE preparations.

OGE – Smear

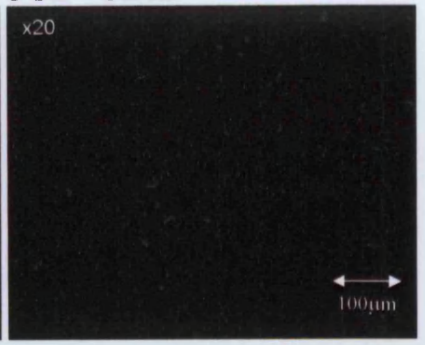

JE – Colony

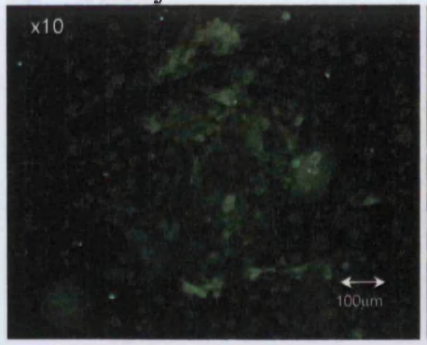

CK8 staining was evident throughout JE colonies; more intensely staining cells tend to be clustered

JE – Smear

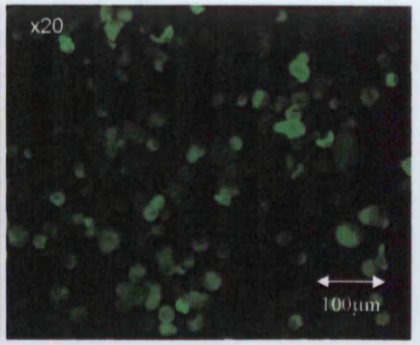

A range of fluorescence intensity was evident within JE smears. Greater intensity appeared to be associated with larger cells.

Figure 5.35: Cytokeratin 18

OGE – Colony

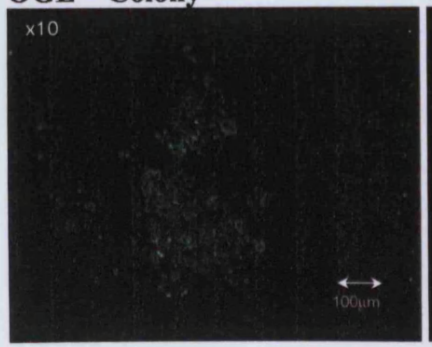

CK18 mAB provided a very weak background stain only within OGE samples.

OGE – Smear

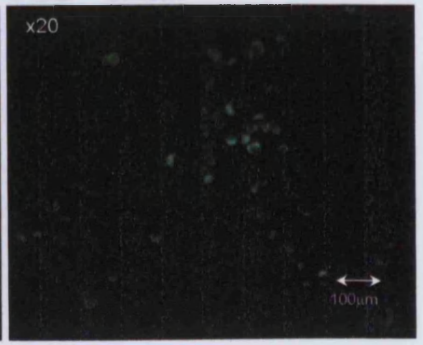

JE – Colony

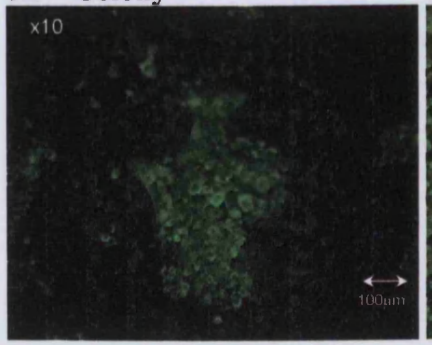

There was widespread, uniform staining for CK18 within JE colonies and cell smears. This mAB staining pattern provides evidence for phenotypic variation between OGE and JE that is maintained in culture.

JE – Smear

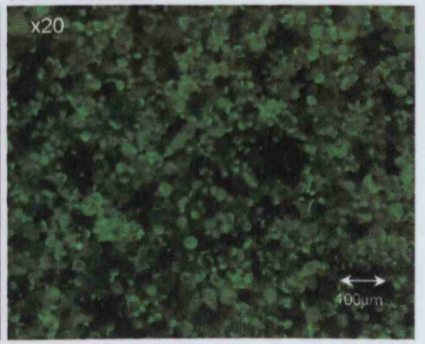

Figure 5.36: Cytokeratin 14

OGE – Colony

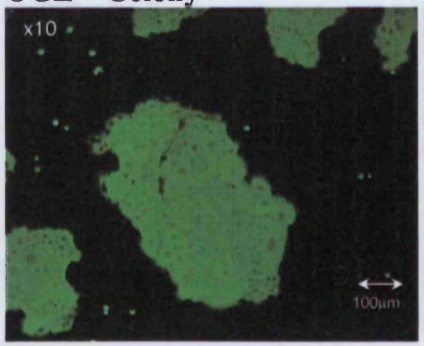

OGE – Smear

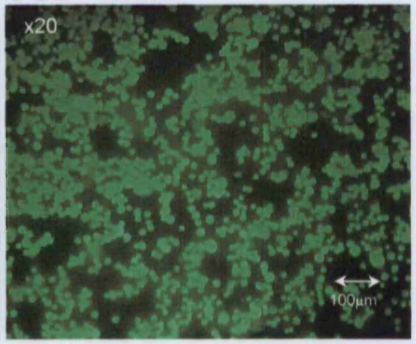

Strong positive staining for CK14 of all cells throughout OGE colonies and smears.

JE – Colony

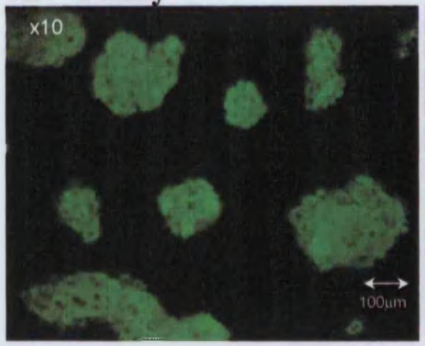

JE – Smear

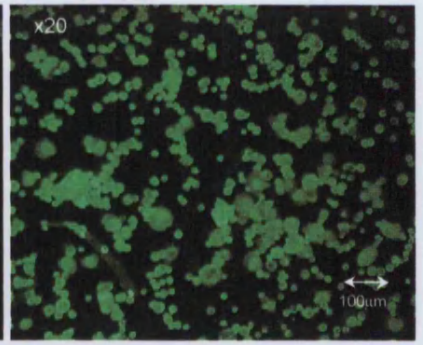

Strong positive staining throughout all cells of JE colonies and smears.

Figure 5.37: Cytokeratin 19

OGE – Colony

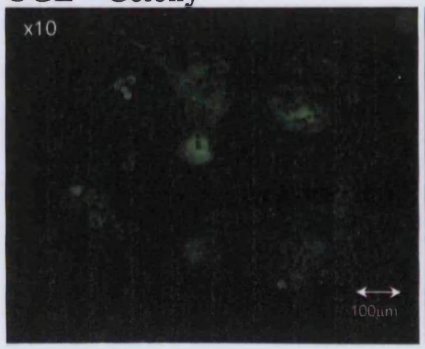

OGE – Smear

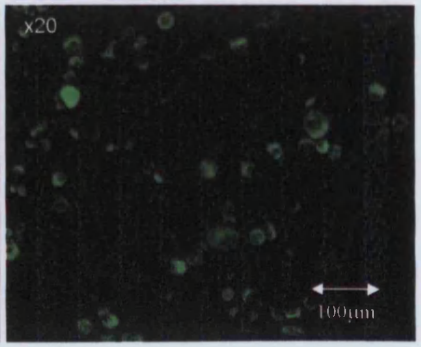

Weak CK19 staining of some cells within OGE colonies and smears. This was not seen to this extent in *ex vivo* sections. There numbered too many cells to be the sporadic basal OGE or Merkel cells seen in *ex vivo* sections. It may indicate a shifting in the phenotype from OGE toward the JE-type.

JE – Colony

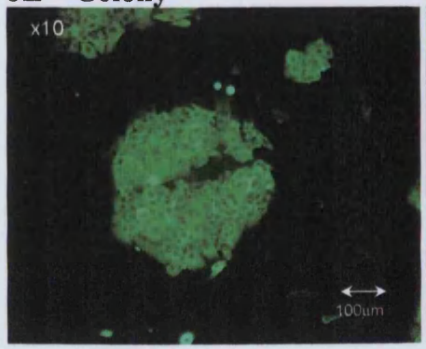

JE – Smear

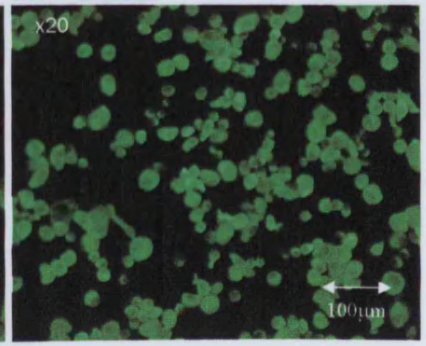

Strong positive CK19 staining of entire JE colonies and smears.

Figure 5.38: ICAM-1

OGE – Colony

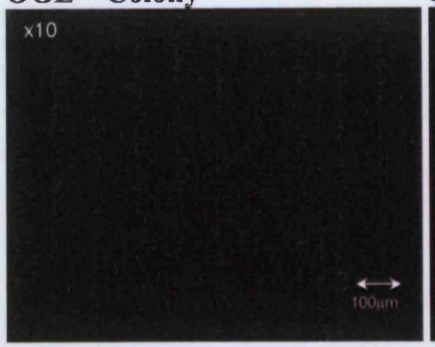

OGE – Smear

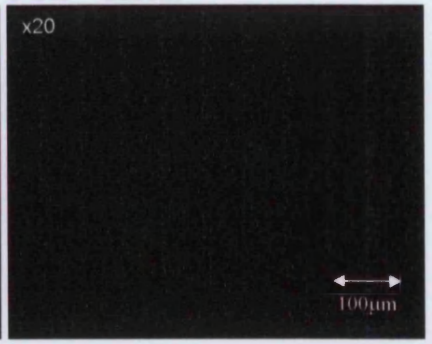

As demonstrated within *ex vivo* sections, there was no ICAM-1 staining within OGE samples.

JE – Colony

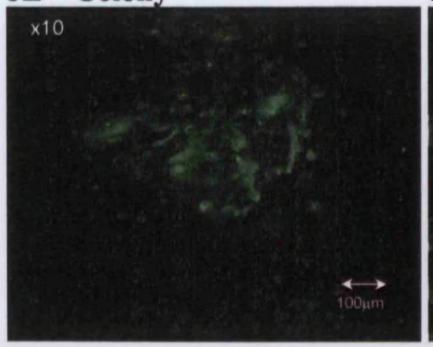

JE – Smear

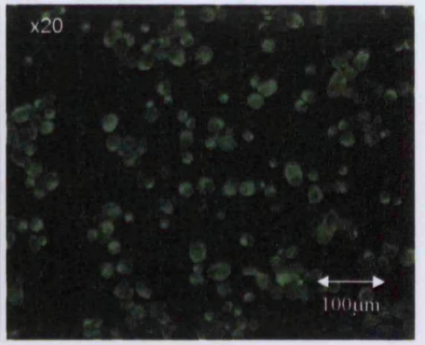

As with *ex vivo* sections there was weak ICAM-1 staining of JE colonies and smears, providing a potential differentiating marker for the JE phenotype.

Figure 5.39: Desmoplakin I+II

OGE – Colony

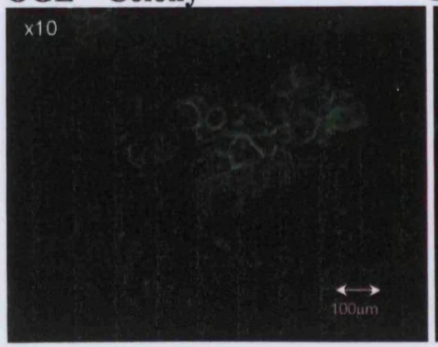

Weak intracellular staining for Desmoplakin I+II within OGE colonies.

OGE – Smear

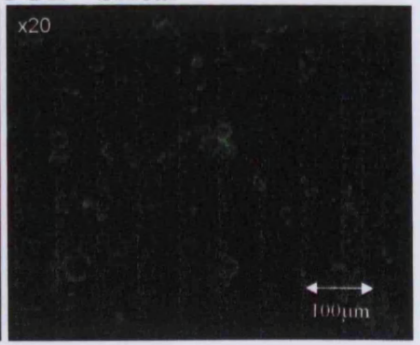

OGE smears show very weak membrane staining of some cells.

JE – Colony

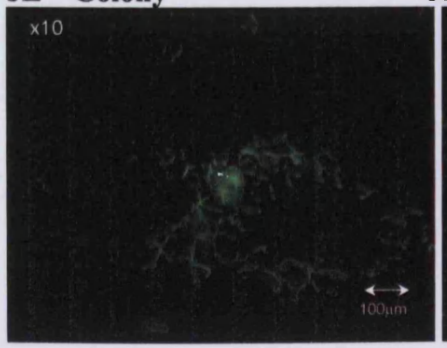

Marginally stronger intracellular Desmoplakin staining of JE colonies compared with OGE.

JE – Smear

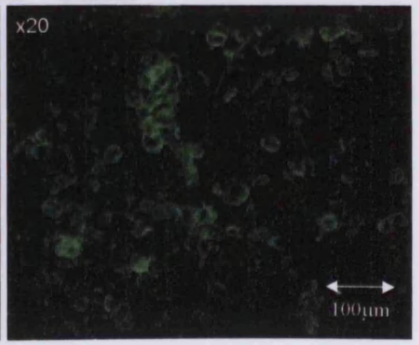

More intense cell membrane staining of JE keratinocytes compared with OGE. This difference was not evident within *ex vivo* sections.

Figure 5.40: *Dolichos biflorus agglutinin*

OGE – Colony

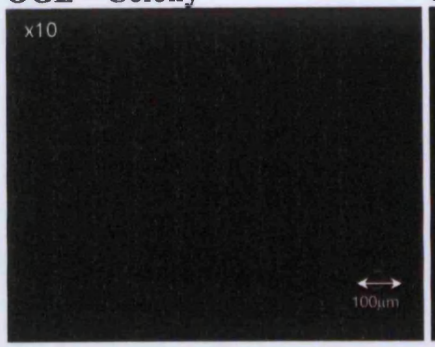

Background staining only of OGE samples stained for DBA.

OGE – Smear

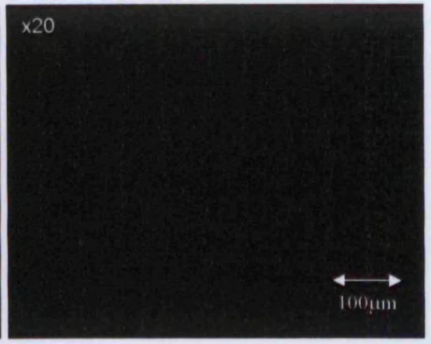

JE – Colony

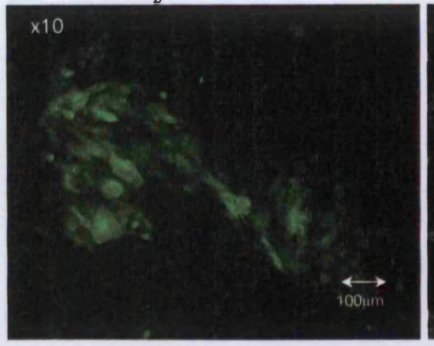

Positive DBA staining of JE colonies.

JE – Smear

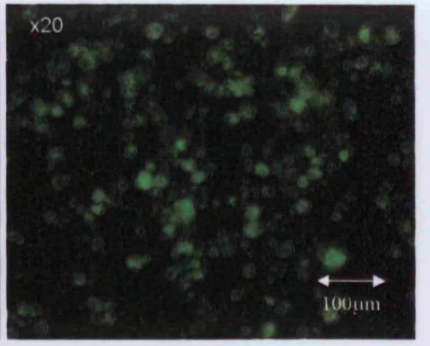

All JE keratinocytes stain for DBA within smears. DBA provides a positive differentiating marker for the JE phenotype in culture.

Figure 5.41: Matrix metalloproteinase-7

OGE – Colony

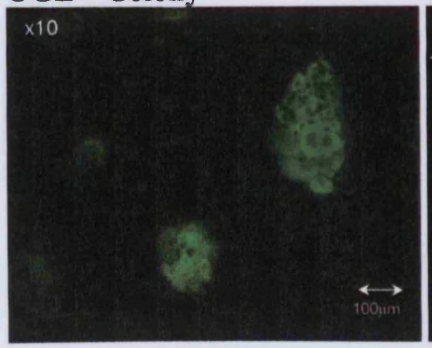

Positive MMP-7 staining in OGE colonies and larger, differentiated cells of smears. Within *ex vivo* sections MMP-7 was localised to basal cells at the rete tips and the JE zone only. This may again represent a shift in phenotype of the OGE toward the JE-type.

OGE – Smear

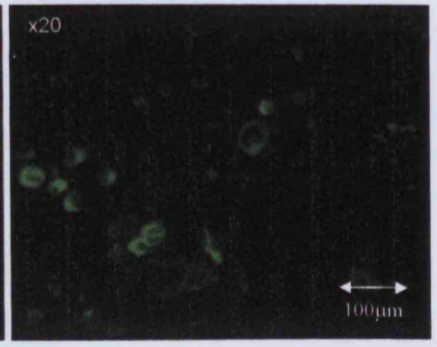

JE – Colony

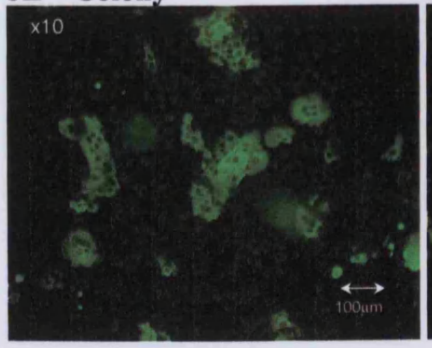

More intense MMP-7 staining of JE colonies compared with OGE, suprabasal cells appearing the most intense.

JE – Smear

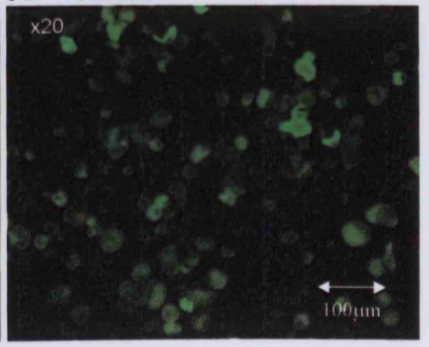

JE smears exhibit a variation in intensity of staining for MMP-7, with larger cells appearing more fluorescent.

Figure 5.42: Vimentin

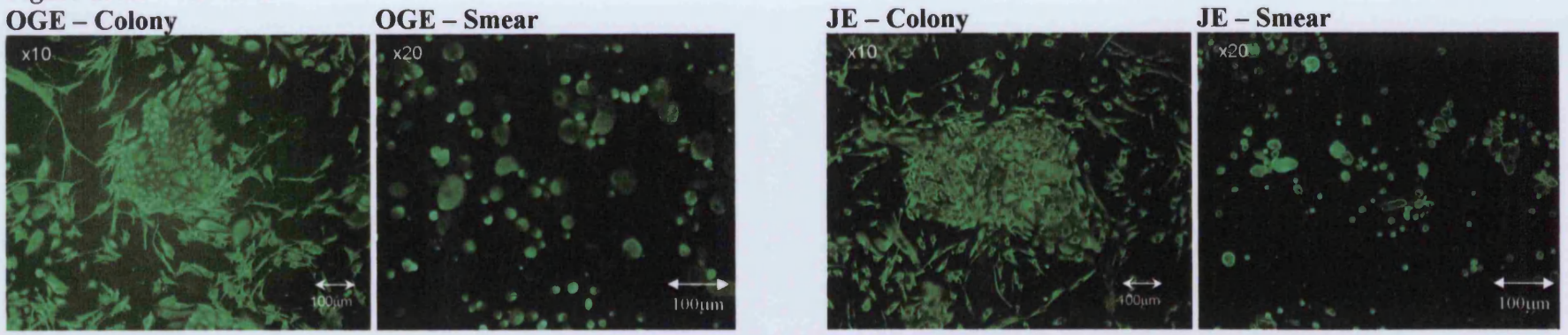

Vimentin is an intermediate filament protein (57kD) present in cells of mesenchymal origin. In normal tissues, cell types that express vimentin include endothelial cells, fibroblasts, smooth muscle cells and lymphoid cells. The images above show positive staining of both mesenchymal derived 3T3 fibroblasts and epithelial colonies. Within the cell smear the larger keratinocytes tend to show a reduced expression level, this is an *in vitro* characteristic that has been identified in several other studies (Gao and Mackenzie, 1992 and Matsuyama *et al.*, 1997).

Table 5.3: Summary of mAB staining of epithelial colonies/smears

+++ Strong positive staining
++ Positive staining
+ Weak positive staining
- Negative

mAB	Junctional epithelial colonies	Oral-gingival colonies	Differential
Cytokeratin 1	- (Sporadic differentiated cells)	++	Yes
Cytokeratin 10	- (Sporadic differentiated cells)	++	Yes
Cytokeratin 4	-	+ (Almost negligible)	No
Cytokeratin 13	-	+ (Almost negligible)	No
Cytokeratin 6	+ to +++	+ to +++	No
Cytokeratin 16	+ to +++	+ to +++	No
Cytokeratin 8	+ to ++	+ (Almost negligible)	Yes
Cytokeratin 18	++	+ (Almost negligible)	Yes
Cytokeratin 14	+++	+++	No
Cytokeratin 19	+++	- to +	Yes
ICAM-1	+	-	Yes
Desmoplakin I+II	+	+ (Almost negligible)	Yes
DBA	+ to ++	-	Yes
MMP-7	+ to +++	+ to ++	No
Vimentin	+++	+++	No

5.6 Organotypic cultures

5.6.1 Histology

Organotypic cultures were used to compare the differing abilities of periodontal ligament fibroblasts and gingival fibroblasts to support the growth of epithelium. In five series of experiments, matrices were prepared containing either periodontal ligament or gingival fibroblasts and then plated with JE or OGE. Homotypic cultures constructed with OGE supported by OGF, and JE supported by PDL simulated the *in vivo* spatial arrangement. Heterotypic combinations, OGE supported by PDL and JE supported by OGF allow fibroblasts ability to direct growth and differentiation to be assessed.

Throughout experimentation, OGE showed good patterns of growth, maturation and stratification (Figure 5.43a and c). Mucosal architecture included a layer of cuboidal cells positioned basally and many spinous cell layers demonstrating that both matrix and mesenchymal factors were effective in the reorganisation and differentiation of the epithelium. OGE supported by OGF produced a substantial, stratified layer with some features resembling the *in vivo* histology (Figures 5.43a) whilst OGE cultured with PDL showed less growth and development (Figure 5.43c). It was apparent however, that JE had a decreased growth capacity when compared with OGE. In culture with PDL, it remained flattened and atrophic; there was just a small improvement in the number of stratified layers when cultured with OGF (Figures 5.43b and d).

Figure 5.43a: Oral-gingival keratinocytes supported by oral-gingival fibroblasts

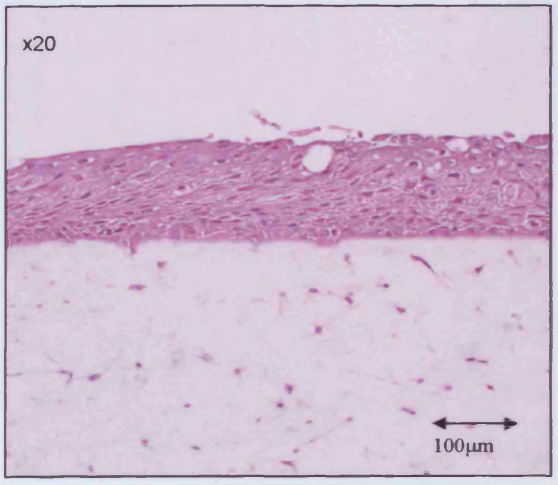

Figure 5.43b: Junctional keratinocytes Supported by periodontal ligament fibroblasts

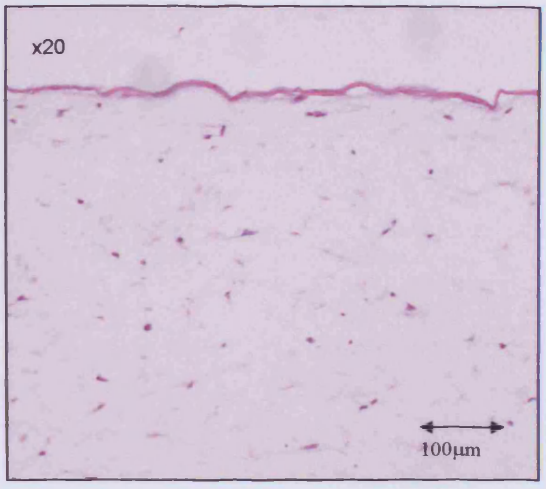

Figure 5.43c: Oral-gingival keratinocytes supported by periodontal ligament fibroblasts

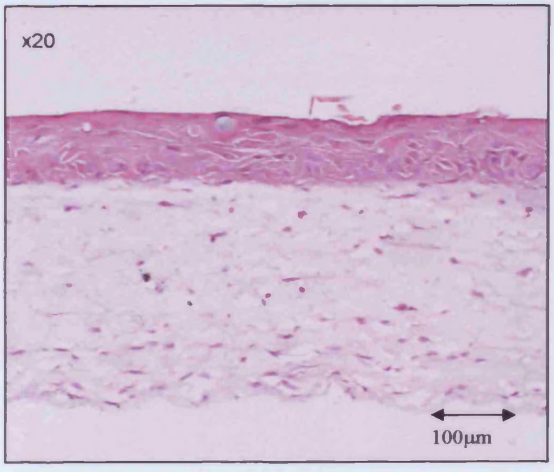

Figure 5.43b: Junctional keratinocytes Supported by oral-gingival fibroblasts

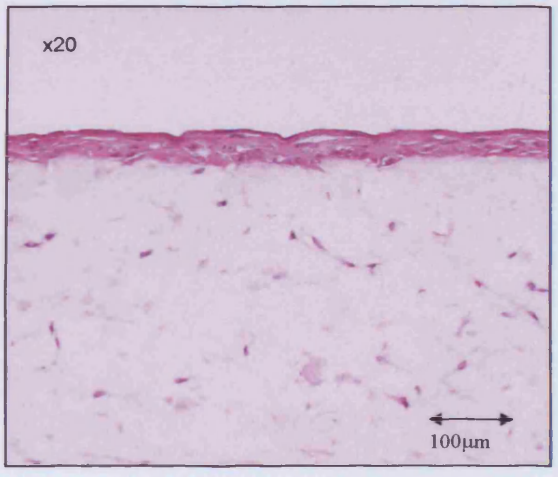

5.6.2 Immunohistochemical staining patterns

All four cultures were stained using the mAB panel in order to determine how the epithelial phenotype was retained or modulated within the organotypic system.

Figure 5.44: Cytokeratin 1

OGF/OGE

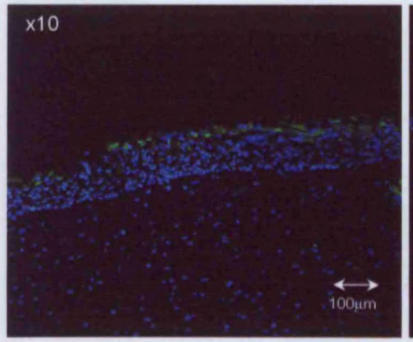

Homotypic recombination of OGF/OGE demonstrates CK1 staining of sporadic superficial cells of the stratum corneum.

OGF/JE

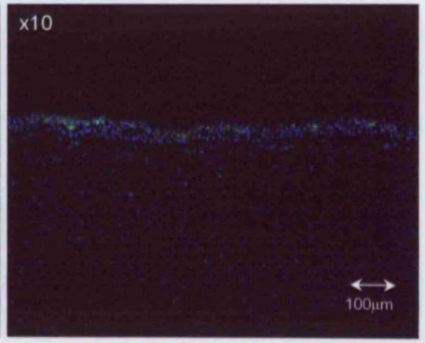

Sporadic superficially stained cells of JE cultured upon OGF staining for CK1, suggesting terminal differentiation of some JE keratinocytes.

PDL/JE

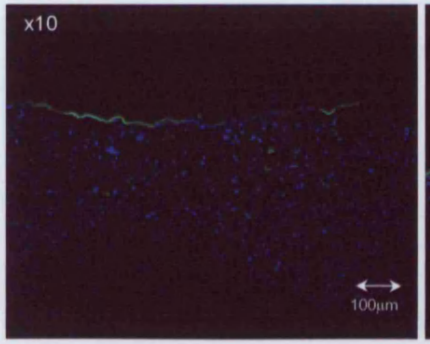

JE does not produce keratinised stratum corneum *in vivo* yet some cells have stained for CK1 in homotypic culture.

PDL/OGE

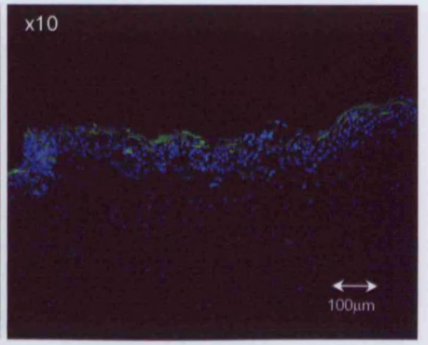

OGE demonstrating staining for CK1 within heterotypic culture.

Figure 5.45: Cytokeratin 10

OGF/OGE

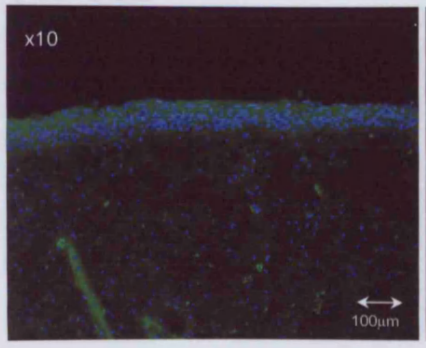

CK10 staining appears diffuse and widespread; it is not just located to the most superficial cells.

OGF/JE

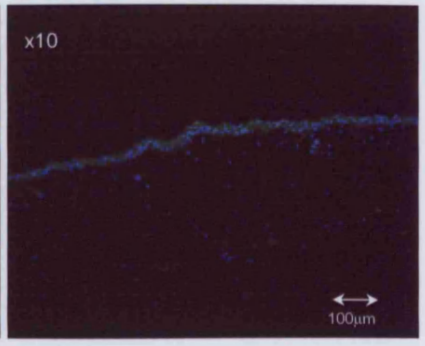

CK10 staining is barely evident within OGF/JE culture.

PDL/JE

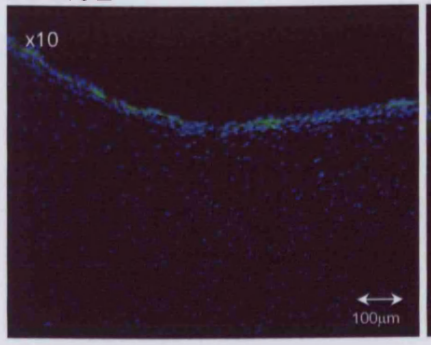

Individual JE keratinocytes unexpectedly stain positively for CK10. CK10 not normally being present within JE *in vivo*.

PDL/OGE

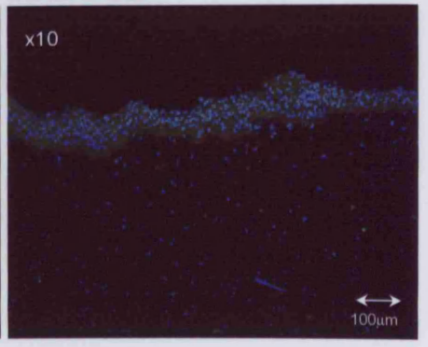

Weak staining of upper half of the epidermis for CK10 within PDL/OGE heterotypic culture.

Figure 5.46: Cytokeratin 4

OGF/OGE

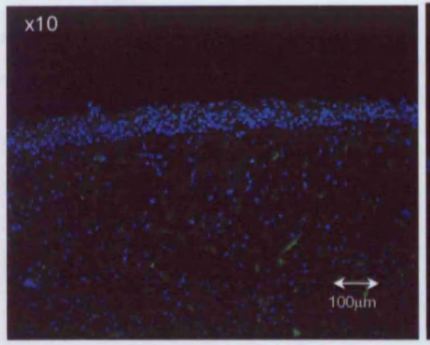

OGF/JE

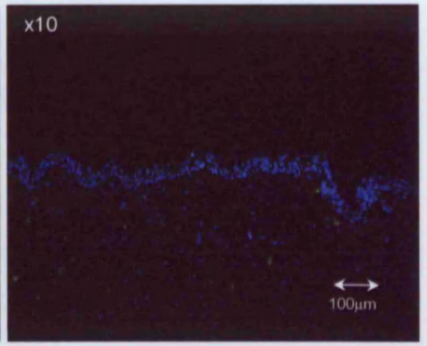

PDL/JE

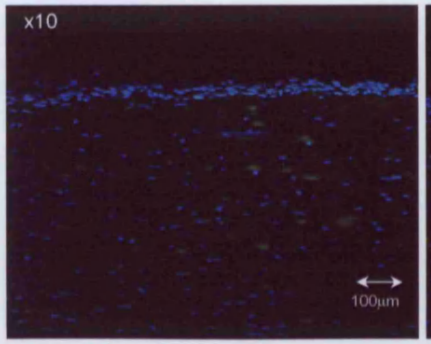

PDL/OGE

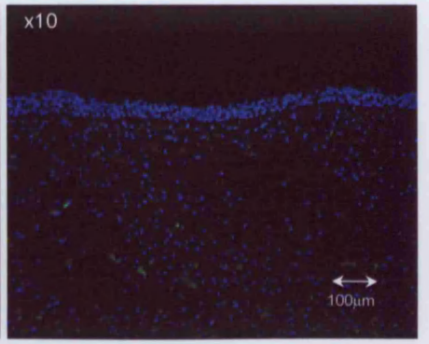

There was no staining for CK4 evident throughout all organotypic recombinations.

Figure 5.47: Cytokeratin 13

OGF/OGE

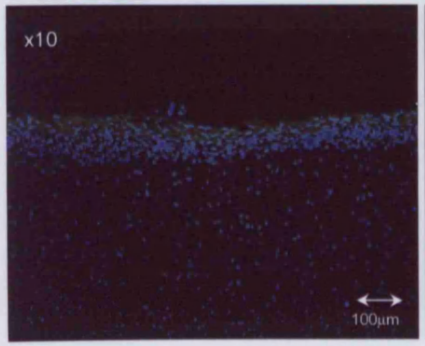

Very weak staining for CK13 throughout the superficial OGE epidermis.

OGF/JE

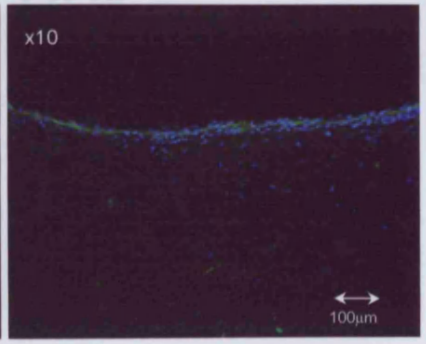

Within OGF/JE culture CK13 expression was localised to the superficial cells only.

PDL/JE

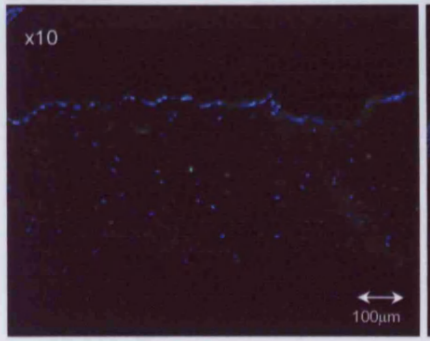

Homotypic recombination of PDL/JE was negative for CK13 stain.

PDL/OGE

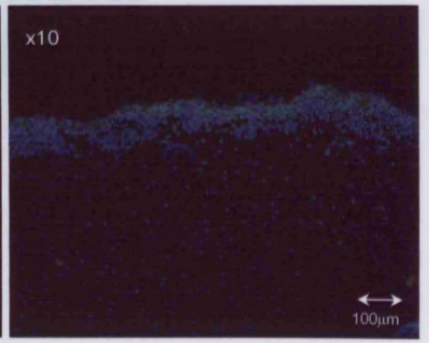

Similar staining pattern as OGF/OGE with CK13 localised to the superficial epidermis.

Figure 5.48: Cytokeratin 6

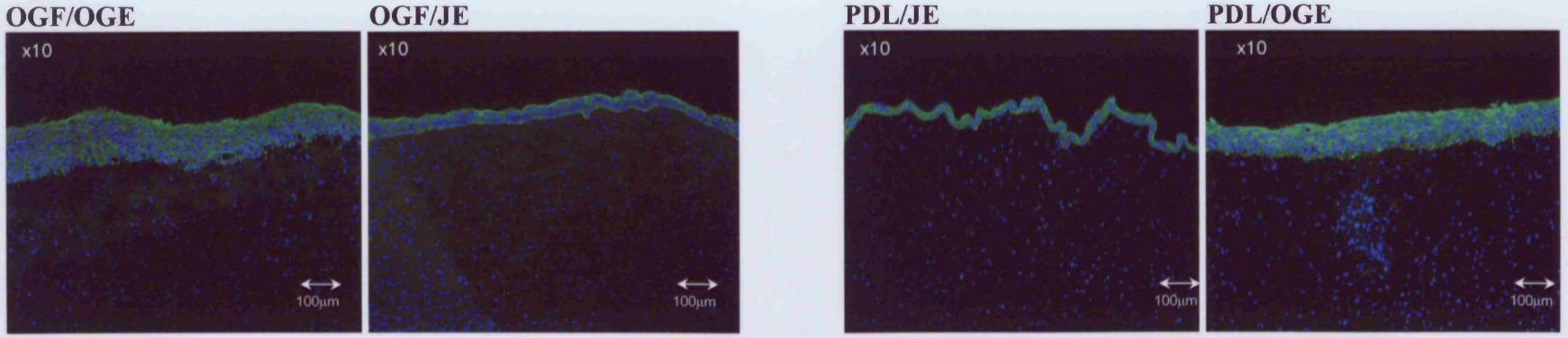

CK6 expression was present throughout the entire epithelium in all organotypic cultures

Figure 5.49: Cytokeratin 8

OGF/OGE

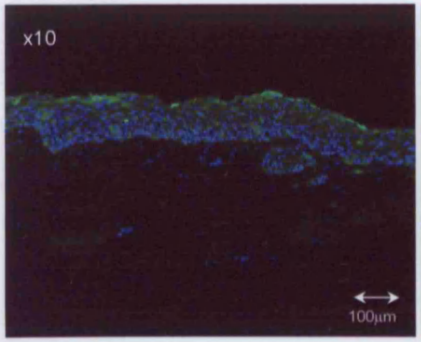

Unexpectedly, CK8 expression was found within sporadic superficial cells of the OGE within homotypic culture.

OGF/JE

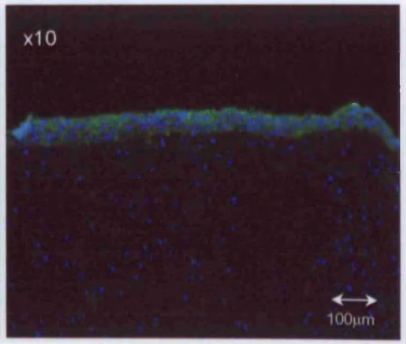

Strong positive CK8 staining of entire JE layer within heterotypic combination.

PDL/JE

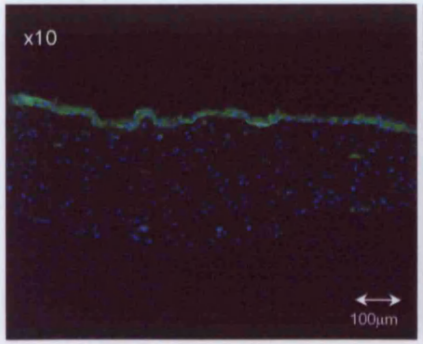

All JE cells were expressing CK8 within homotypic culture upon PDL fibroblasts.

PDL/OGE

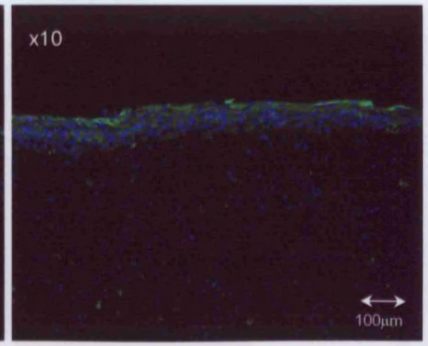

Similar appearance to OGF/OGE gel, with sporadic superficial keratinocytes expressing CK8.

Figure 5.50: Cytokeratin 18

OGF/OGE

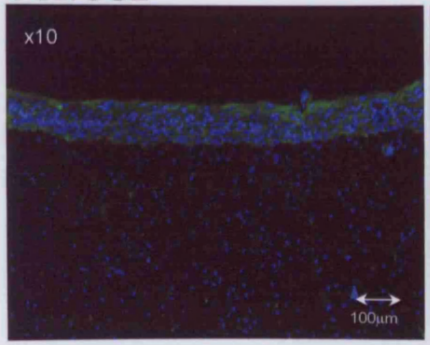

CK18 followed a similar staining pattern as CK8 above, with superficial OGE cells being positive.

OGF/JE

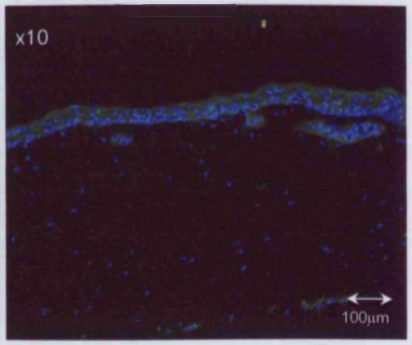

Weak, positive CK18 staining of the entire JE.

PDL/JE

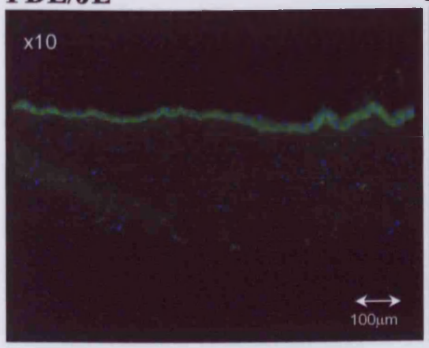

Within homotypic culture JE keratinocytes were strongly stained for CK18.

PDL/OGE

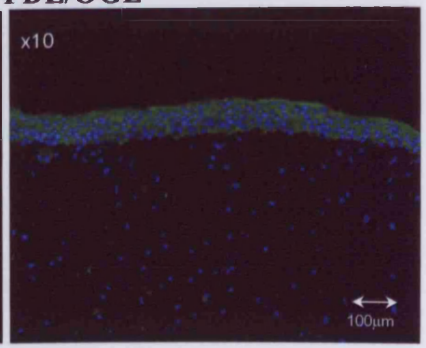

Positive CK18 staining of OGE keratinocytes cultured in conjunction with PDL fibroblasts.

Figure 5.53: *Dolichos biflorus agglutinin*

OGF/OGE

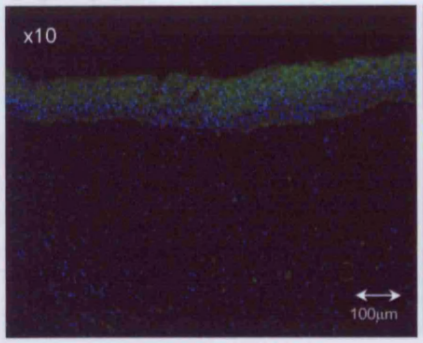

DBA was unexpectedly, weakly expressed by the superficial half of the OGE homotypic cultures.

OGF/JE

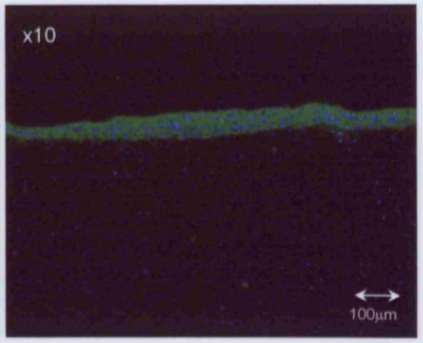

Within heterotypic culture, the entire JE layer stained for DBA.

PDL/JE

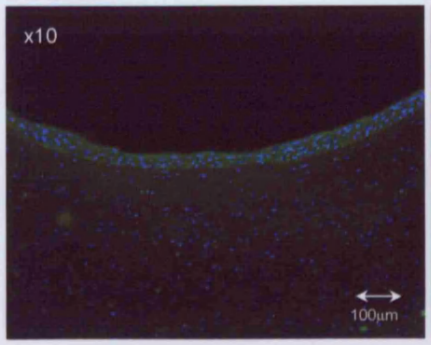

DBA staining the entire JE layer within PDL/JE homotypic culture.

PDL/OGE

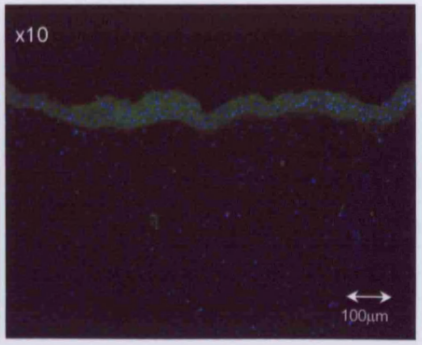

Entire OGE layer weakly staining for DBA when cultured upon PDL fibroblasts.

Table 5.4a: Antibody staining of homotypic recombined cultures

+++ Strong positive staining
++ Positive staining
+ Weak positive staining
- Negative
SB Suprabasal

Note: - PDL/JE homotypic cultures were regarded as only having a single epithelial layer not distinguished by distinct strata.

Comments highlighted in red indicate atypical staining patterns compared with those of ex vivo sections and previous literature studies.

mAB	HOMOTYPIC CULTURES				
	OGF/OGE			PDL/JE	
	Basal	SB	Comments	Single layer	Comments
Cytokeratin 1	-	+++	Conforms to *ex vivo* staining patterns	+++	Unexpected CK1 staining of JE cells, may represent differentiation induced by culture parameters
Cytokeratin 10	-	+++	As for CK1	+++	As for CK1
Cytokeratin 4	-	-	Conforms to *ex vivo* staining patterns	-	Conforms to *ex vivo* staining patterns
Cytokeratin 13	-	+	Faint SB staining for CK13 conforms with patchy SB cell staining at crestal tip of *ex vivo* sections	-	Conforms to *ex vivo* staining patterns
Cytokeratin 6	+++	+++	Conforms to *ex vivo* staining patterns	+++	CK6/16 staining was not seen in *ex vivo* sections, again may represent differentiation induced by culture parameters
Cytokeratin 8	-	+ to +++	Positive SB staining for CK8 likely represents differentiating cells found at rete tips in sections	+++	Conforms to *ex vivo* staining patterns
Cytokeratin 18	-	+ to ++	Positive SB staining for CK18 likely represents differentiating cells found at rete tips in sections	++	Conforms to *ex vivo* staining patterns
Cytokeratin 14	+++	+++	Conforms to *ex vivo* staining patterns	+++	Conforms to *ex vivo* staining patterns
Cytokeratin 19	-	++	CK19 staining of OGE within sections was localised to the rete tips	+++	Conforms to *ex vivo* staining patterns
DBA	-	+	No DBA staining was seen within OGE of *ex vivo* sections	++	Conforms to *ex vivo* staining patterns

Table 5.4b: Antibody staining of heterotypic recombined cultures

+++ Strong positive staining
++ Positive staining
+ Weak positive staining
- Negative
SB Suprabasal

mAB	HETEROTYPIC CULTURES					
	OGF/JE			PDL/OGE		
	Basal	SB	Comments	SB	Basal	Comments
keratin 1	-	+++	Within heterotypic culture JE behaves in a similar manner as OGE seen in homotypic culture – (see table 5.4a)	-	+++	OGE keratinocytes retain their *in vivo* characteristic staining patterns for CK1 when cultured upon PDL
keratin 10	-	+++	As for CK1	-	+++	As for CK1
keratin 4	-	-	Conforms to *ex vivo* staining patterns where neither OGE or JE stains positively for CK4	-	-	Conforms to *ex vivo* staining patterns where neither OGE or JE stains positively for CK4
keratin 13	-	++	JE staining positively for CK13 is more characteristic of OGE phenotype – possible redirection of differentiation by the underlying CT	-	+	This faint but positive staining would imply that OGE has retained its original phenotypic characteristics despite culturing upon heterotypic PDL CT
keratin 6	+++	+++	Conforms to *ex vivo* staining patterns as both OGE and JE stain positively for CK6/16	+++	+++	Conforms to *ex vivo* staining patterns as both OGE and JE cultures stain positively for CK6/16
keratin 8	+	++ to +++	JE keratinocytes stain positively for CK8 in a similar manner as within homotypic cultures	-	+ to +++	Too many OGE keratinocytes stain positively for CK8 to represent basal rete tip cells alone, more likely is that cells have taken on a more JE-like phenotype on culture with PDL CT
keratin 18	+	+	As for CK18	-	+ to ++	As for CK8
keratin 14	+++	+++	Conforms to *ex vivo* staining patterns	+++	+++	Conforms to *ex vivo* staining patterns
keratin 19	+++	+++	Within heterotypic culture JE has retained the positive staining pattern for CK19 seen in *ex vivo* and homotypic cultured JE	++	++	Although less intense, staining of OGE for CK19 may indicate a shift in phenotype toward the JE-type
	++	++	Within heterotypic culture JE has retained the positive staining pattern for DBA seen in *ex vivo* and homotypic cultured JE	++	++	Although less intense, staining of OGE for DBA may indicate a shift in phenotype toward the JE-type

5.7 Reverse-transcription polymerase chain reaction data

5.7.1 Primer specificities

RNA was successfully extracted for 7 PDL, 8 OGF, 4 JZF, 11 JE and 6 OGE lines. Quality and quantity was assessed spectrophotometrically and the RNA stored at -80°C until required. To confirm successful mRNA extraction each sample was incorporated within a PCR run along with housekeeping primers for the gene GAPDH. The GAPDH target DNA region was successfully amplified and a distinct product size of 176bp (Table 5.5) obtained for all isolates (Figure 5.54).

Figure 5.54: GAPDH products for 10 mRNA samples

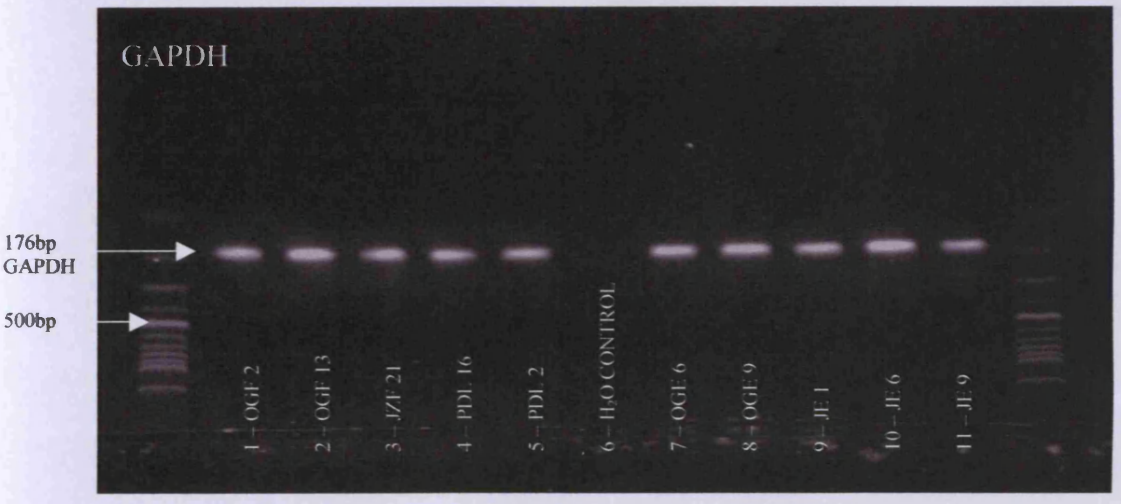

RT-PCR reactions were undertaken to ensure successful amplification of the appropriate sized product by all primer pairs. No product was detected using H_2O controls or on omission of the reverse-transcription stage. The following agarose gels demonstrate primer efficacies.

Table 5.5: PCR product sizes

PCR target	Product size
KGF	199bp
KGF2	248bp
KGFR	104bp
HGF	181bp
HGFR	203bp
GM-CSF	181bp
GM-CSFR	181bp
IL-1α	181bp
IL-1αR	181bp
TGFα	226bp
GAPDH	176bp

Figure 5.55: GelDoc image demonstrating KGF and KGFR mRNA

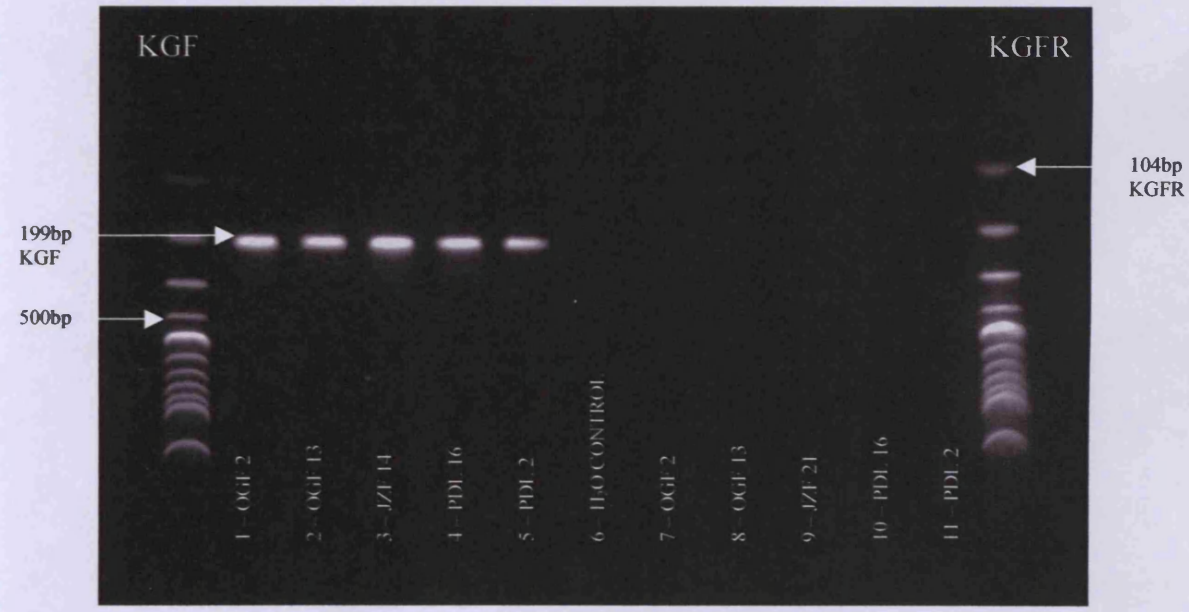

For five fibroblast RNA samples KGF was confirmed as being transcribed successfully, KGFR proved to be negative. This negative result was not attributable to failure of the primers as further amplifications within an epithelial derived RNA sample confirmed the presence of KGFR (figure 5.59).

Figure 5.56 GelDoc image demonstrating KGF2 and HGF mRNA

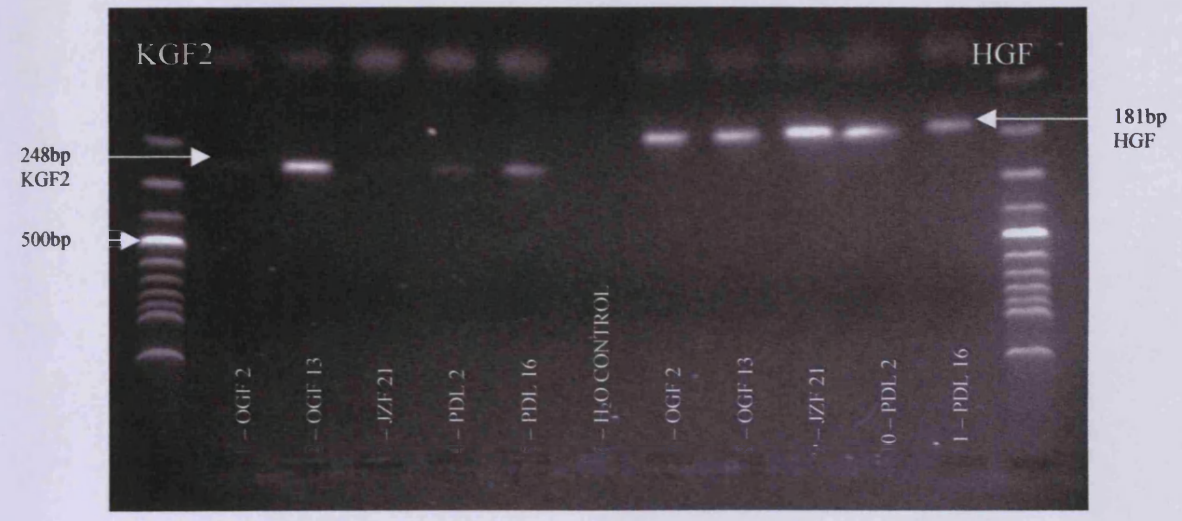

Demonstration that HGF successfully amplified within all five fibroblast populations. KGF2 primers also provided a product for all fibroblast samples, however only one sample (OGF13) was of significant intensity, other samples although evident were extremely weak. This may have been because KGF2 levels were genuinely low; later RT-PCR techniques demonstrate KGF2 presence at similar levels throughout fibroblast populations.

Figure 5.57: GelDoc image demonstrating IL-1αR and GM-CSF mRNA

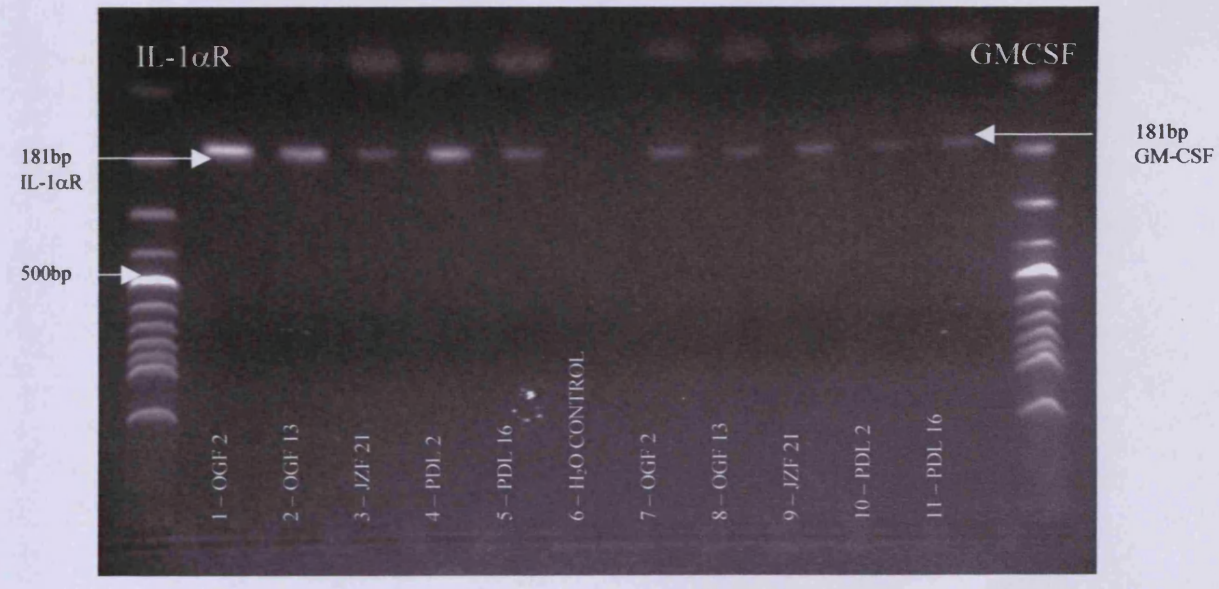

Demonstration that IL-1αR and GM-CSF primers were detecting correctly sized product within fibroblast RNA samples, GM-CSF being particularly weak. Later RT-PCR data confirmed that GM-CSF mRNA expression levels were consistently lower than those of other cytokines.

Figure 5.58: GelDoc image demonstrating HGFR mRNA

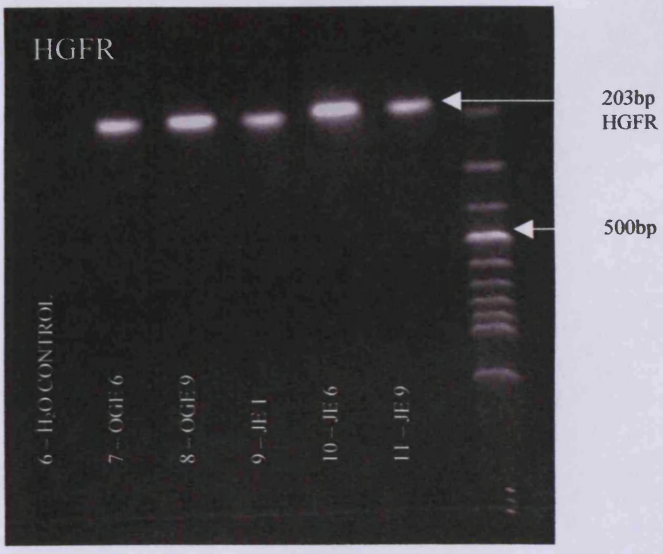

Figure 5.58 provides demonstration of HGFR amplification at 203bp within the epithelial samples. There was a lower intensity signal for JE1 and JE9 samples that was mirrored within the Q-PCR data, there being a 5-fold and 3-fold respective decrease when compared to the average HGFR mRNA values.

Figure 5.59: GelDoc image demonstrating various mRNA products

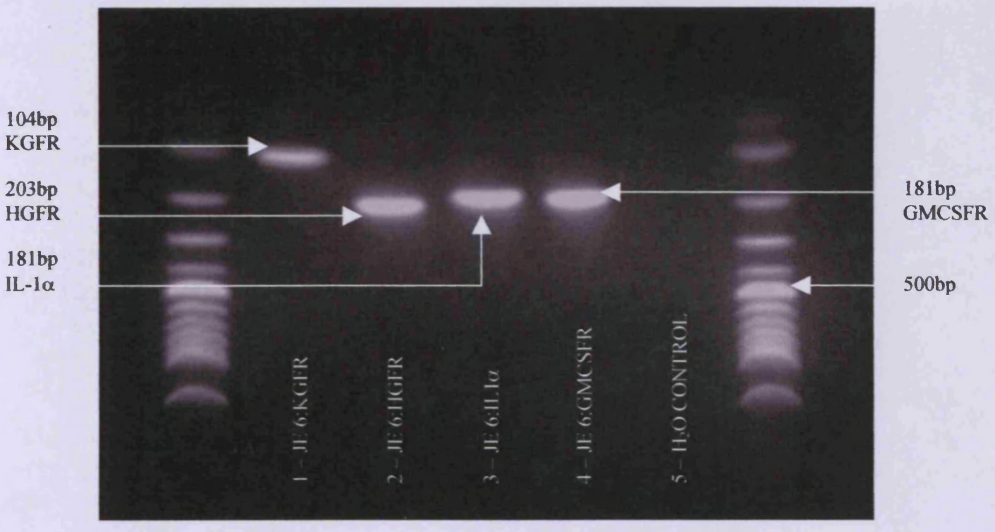

This agarose gel confirmed successful amplification of KGFR, HGFR, IL1α and GM-CSFR products from epithelial RNA samples.

Figure 5.60: GelDoc image demonstrating TGFα mRNA

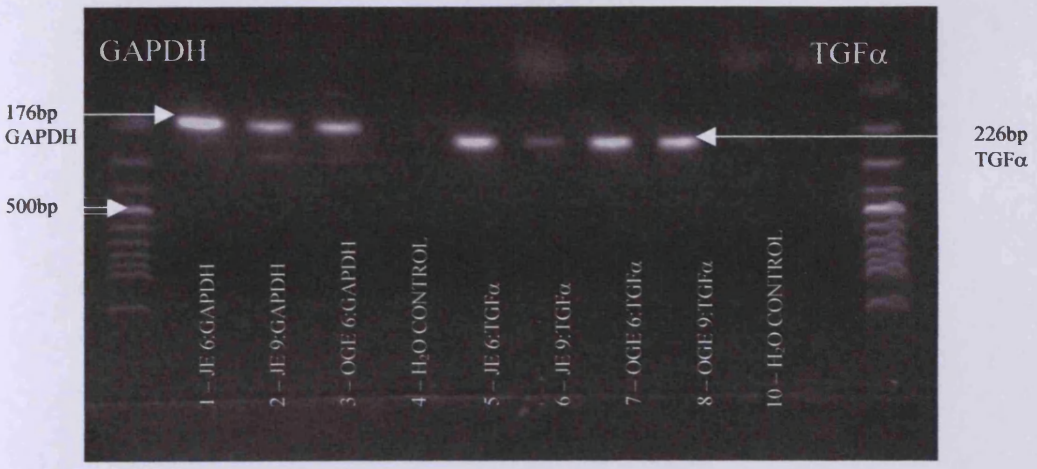

Confirmation of TGFα constructs from four epithelial lines. There was a very weak signal provided by the JE9 sample which was mirrored by the Q-PCR data, there being a 10-fold decrease in mRNA expression level compared with average for TGFα.

5.8 Quantitative-polymerase chain reaction data

Cytokine mRNA was quantified using the TaqMan™ PCR technique, an accurate method of detecting mRNA even when expressed at low levels. There was a considerable volume of data produced by the Q-PCR software. Manufacturer's literature suggested that end-point data are reproducible from as low as 1000 copy numbers, and a two-fold difference being of recognisable significance. Occasionally small copy number results were obtained toward the end of the PCR cycling – as with all PCR, this was likely to be attributable to cross-binding of primers with contaminant genomic DNA.

For the full table of results, example standard curve, and typical Q-PCR-run data see appendix VIII. Presented below are high, low and average values for each fibroblast or epithelial population. Data relating to the four JZF fibroblasts populations that underwent Q-PCR investigations are also included. Statistical differences were evaluated using the student's t-test (two samples assuming unequal variances). Due to the high variability within sample groups data was transformed to the logarithmic scale (base 2). The null hypothesis was that there was no difference between the mean of any populations (OGF/PDL, JE/OGE). A "p" value of less than 0.05 was regarded as statistically significant. Raw data plots demonstrate the mean, range of data and 95% confidence intervals.

Three mRNA samples, OGF15, PDL15 and OGE8 underwent PCR investigations but data were eliminated due to a large number of undetectable results. This was likely due to imperfect mRNA extraction procedure; evidence for this exists in the optical quantification values for the mRNA samples (See highlighted within appendix III).

Table 5.6: Summary of Q-PCR data

Shaded values represent samples for which results were of a value below the manufacturer recommended threshold. Theses are regarded as lacking expression of that product.

a = Value too low - regarded as a negative result.

b = Abnormally high value for KGF expression within epithelial population is likely due to known fibroblastic contamination of individual cultures OGE6 and JE2 pre-RNA extraction. These values have been dismissed from statistical analyses.

		Fibroblast			Keratinocyte	
Amplicon		**OGF**	**PDL**	**JZF**	**OGE**	**JE**
KGF	Low	2595	3700	4508	18 (0)[a]	0 (0)[a]
	High	39903	9787	12558	12939 (0)[b]	2822 (0)[b]
	Average	**17668**	**6555**	**7548**	**2728 (0)[b]**	**407 (0)[b]**
KGFR	Low	4 (0)[a]	0	0	4271	2784
	High	697 (0)[a]	251 (0)[a]	78 (0)[a]	18406	37174
	Average	**300 (0)[a]**	**81 (0)[a]**	**31 (0)[a]**	**10761**	**12199**
KGF2	Low	34429	15041	4209	0	0
	High	57938	58701	49685	0	0
	Average	**48729**	**34972**	**32045**	**0**	**0**
HGF	Low	10342	3740	90454	0	0
	High	229047	131511	200670	0	0
	Average	**104095**	**49685**	**140158**	**0**	**0**
HGFR	Low	55 (0)[a]	13 (0)[a]	122 (0)[a]	26242	54396
	High	1751 (0)[a]	650 (0)[a]	360 (0)[a]	270031	471758
	Average	**416 (0)[a]**	**250 (0)[a]**	**202 (0)[a]**	**109111**	**253998**
GM-CSF	Low	1095	240	3110	27 (0)[a]	8 (0)[a]
	High	33189	12014	52243	266 (0)[a]	1598 (0)[a]
	Average	**8861**	**5771**	**16286**	**139 (0)[a]**	**266 (0)[a]**
GM-CSFR	Low	0	0	0	2569	12754
	High	38 (0)[a]	0	0	7122	152528
	Average	**5 (0)[a]**	**0**	**0**	**5112**	**40906**
IL-1α	Low	0	0	0	20442	52036
	High	405 (0)[a]	539 (0)[a]	21 (0)[a]	156487	573139
	Average	**68 (0)[a]**	**103 (0)[a]**	**5 (0)[a]**	**73406**	**274476**
IL-1αR	Low	8004	1700	12365	1 (0)[a]	15 (0)[a]
	High	15891	37821	47940	24 (0)[a]	413 (0)[a]
	Average	**9768**	**10497**	**25585**	**14 (0)[a]**	**191 (0)[a]**
TGFα	Low	6472	90539	128366	15297	17040
	High	761756	665647	645141	143152	650595
	Average	**371979**	**250825**	**299261**	**79635**	**233702**
Amplicon		**OGF**	**PDL**	**JZF**	**OGE**	**JE**
		Fibroblast			**Keratinocyte**	

Table 5.7: Q-PCR data expressed as percentage change between populations

	OGF (Average)	PDL (Average)	% Change		OGE (Average)	JE (Average)	% Change
KGF	17668	6555	OGF 169% ↑				
KGFR					10761	12199	JE 13% ↑
KGF2	48729	34972	OGF 39% ↑				
HGF	104095	49685	OGF 109% ↑				
HGFR					109111	253998	JE 132% ↑
GM-CSF	8861	5771	OGF 54% ↑				
GM-CSFR					5112	40906	JE 700% ↑
IL-1α					73406	274476	JE 274% ↑
IL-1αR	9768	10497	PDL 7% ↑				
TGFα	371979	250825	OGF 48% ↑		79635	233702	JE 193% ↑

Table 5.7 displays data as percentage change of the average expression values between the four population subsets. It was apparent that with the exception of TGFα, fibroblast samples expressed cytokine molecules exclusively and keratinocyte samples solely expressed the cytokine receptor molecules. OGF was seen to express, on average, consistently more of the measured cytokines compared with PDL samples. Interestingly JE samples were seen to express greater levels of receptor molecules compared with OGE samples. Statistical analyses of these data are presented in table 5.8.

Table 5.8: Statistical analyses of Q-PCR log2 transformed data

FIBROBLASTS	log2 data					
	Number of samples (n) (OGF/PDL)	t-test log2 data unequal variances : p-value	Estimated difference in means: OGF - PDL	log2 data fold-change (=2^difference)	95% Confidence Interval	
Cytokine					Lower limit	Upper limit
KGF	7/6	0.09	1.1	2.1	-0.2	2.3
KGF2	7/6	0.10	0.6	1.5	-0.1	1.3
HGF	7/6	0.10	1.7	3.2	-0.4	3.7
GM-CSF	7/6	0.61	0.6	1.5	-2.0	3.2
IL-1αR	7/6	0.36	0.7	1.6	-1.0	2.4
TGFα	7/5	0.48	1.4	2.6	-3.0	5.7

There were noticeable fold-changes in expression levels for several cytokines, OGF being 2.1-fold greater for KGF, 1.5-fold for KGF, 3.2-fold for HGF, 1.5-fold for GM-CSF, 1.6-fold for IL-1α receptor and 2.6-fold greater for TGFα, although no differences between OGF and PDL populations were statistically significant at the 0.05 level.

EPITHELIA	log2 data					
	Number of samples (n) (OGE/JE)	t-test log2 data unequal variances : p-value	Estimated difference in means: JE - OGE	log2 data fold-change (=2^difference)	95% Confidence Interval	
Cytokine					Lower limit	Upper limit
KGFR	5/10	0.97	0.0	Nil	-1.5	1.4
HGFR	5/11	0.09	1.3	2.5	-2.8	0.2
GM-CSFR	5/11	*0.00	2.7	6.5	-3.6	-1.8
IL-1α	5/11	*0.01	2.0	4.0	-3.4	-0.5
TGFα	5/11	0.26	1.1	2.1	-3.0	0.9

* = Statistically significant ($p<0.05$)

There were also large differences between OGE and JE, with JE demonstrating a 2.5-fold higher level of HGFR, and 2.1-fold increase in TGFα when compared to OGF. Of statistical significance was the increased IL-1α levels (4.0-fold, p=0.01) and 6.5-fold greater GM-CSF levels (p=0) within JE keratinocytes compared with OGE.

Table 5.9: Raw data plot – fibroblast:KGF

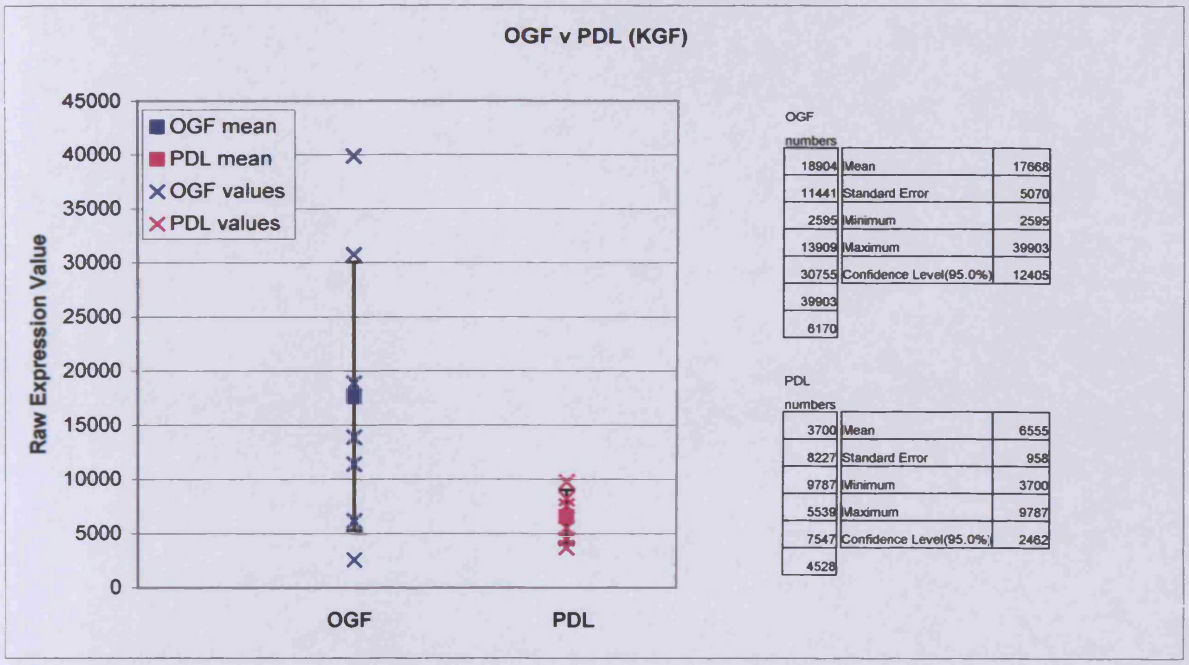

OGF numbers		
18904	Mean	17668
11441	Standard Error	5070
2595	Minimum	2595
13909	Maximum	39903
30755	Confidence Level(95.0%)	12405
39903		
6170		

PDL numbers		
3700	Mean	6555
8227	Standard Error	958
9787	Minimum	3700
5539	Maximum	9787
7547	Confidence Level(95.0%)	2462
4528		

Table 5.10: Raw data plot – fibroblast:KGF2

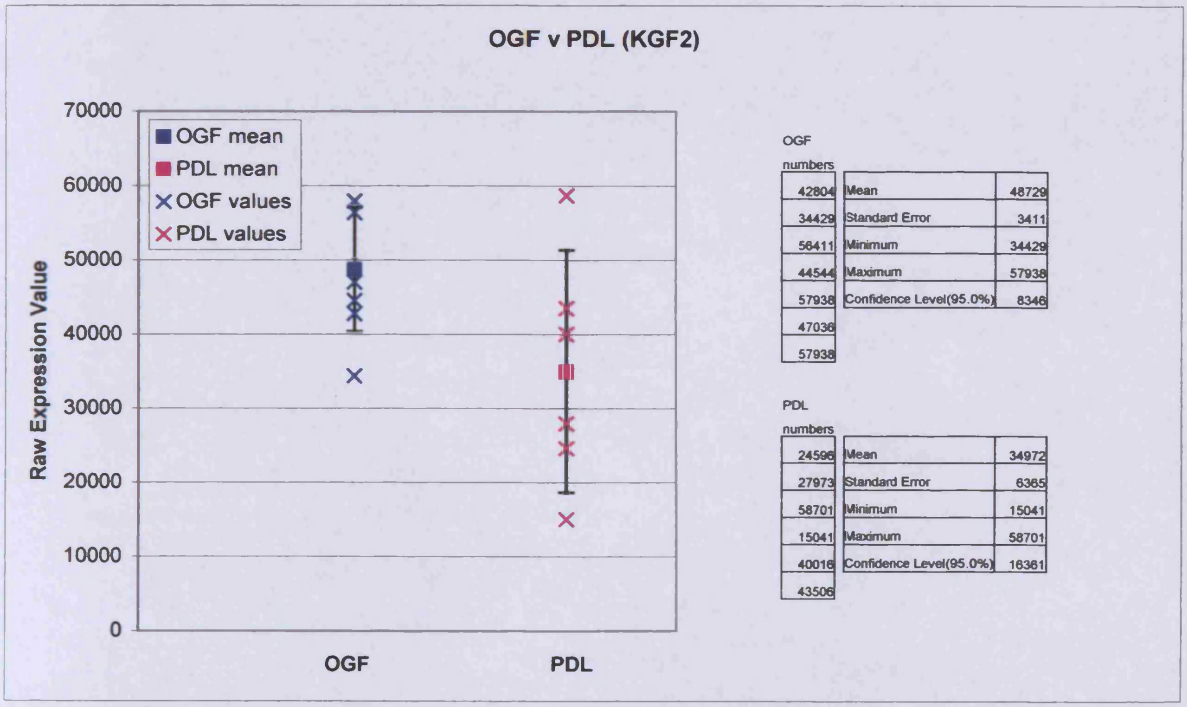

OGF numbers		
42804	Mean	48729
34429	Standard Error	3411
56411	Minimum	34429
44544	Maximum	57938
57938	Confidence Level(95.0%)	8346
47036		
57938		

PDL numbers		
24596	Mean	34972
27973	Standard Error	6385
58701	Minimum	15041
15041	Maximum	58701
40016	Confidence Level(95.0%)	16361
43506		

Table 5.11: Raw data plot – fibroblast:HGF

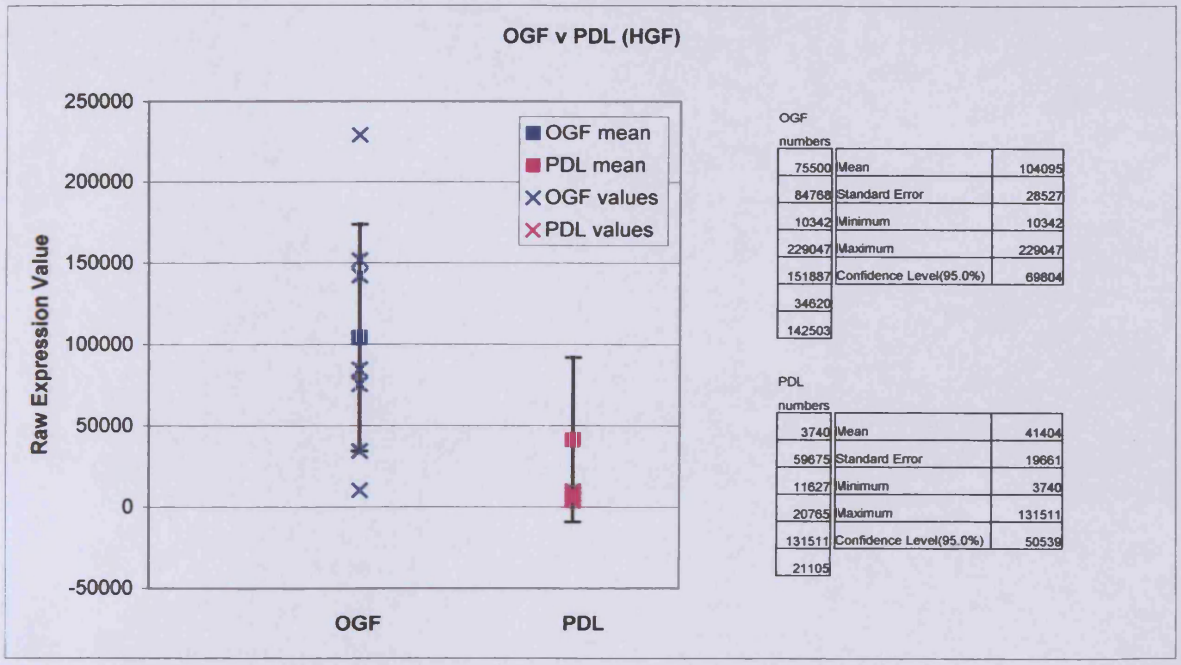

OGF

numbers		
75500	Mean	104095
84768	Standard Error	28527
10342	Minimum	10342
229047	Maximum	229047
151887	Confidence Level(95.0%)	69804
34620		
142503		

PDL

numbers		
3740	Mean	41404
59675	Standard Error	19661
11627	Minimum	3740
20765	Maximum	131511
131511	Confidence Level(95.0%)	50539
21105		

Table 5.12: Raw data plot – fibroblast:GM-CSF

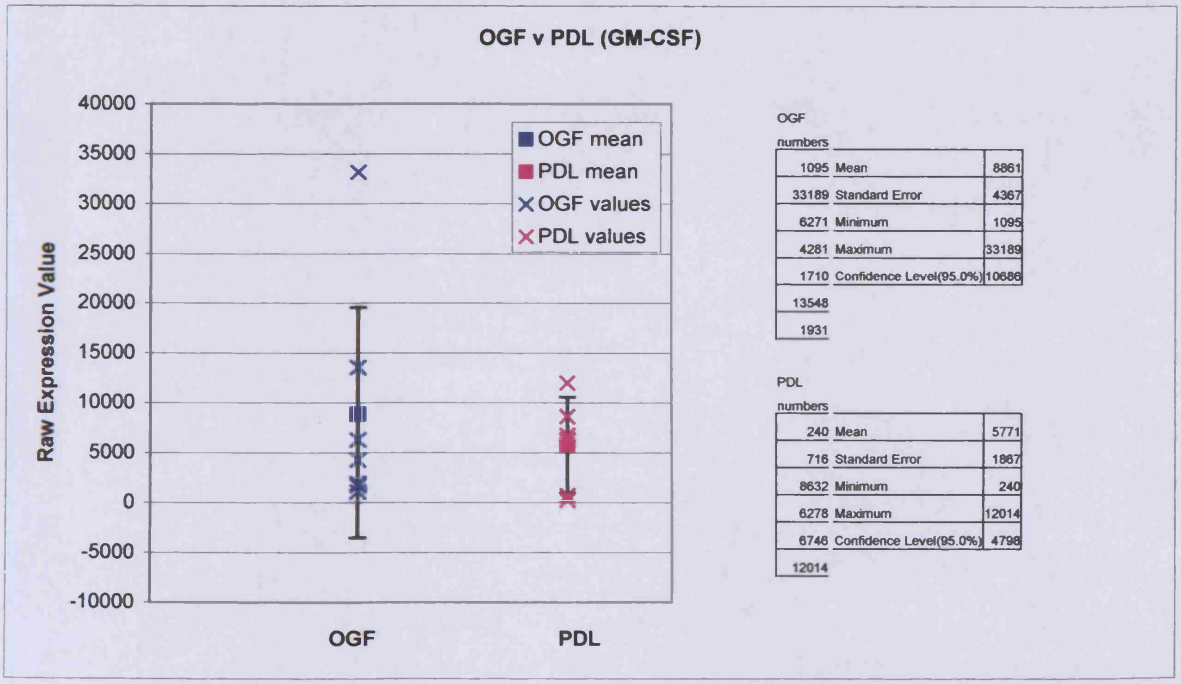

OGF

numbers		
1095	Mean	8861
33189	Standard Error	4367
6271	Minimum	1095
4281	Maximum	33189
1710	Confidence Level(95.0%)	10686
13548		
1931		

PDL

numbers		
240	Mean	5771
716	Standard Error	1867
8632	Minimum	240
6278	Maximum	12014
6746	Confidence Level(95.0%)	4798
12014		

Table 5.13: Raw data plot – fibroblast:IL-1αR

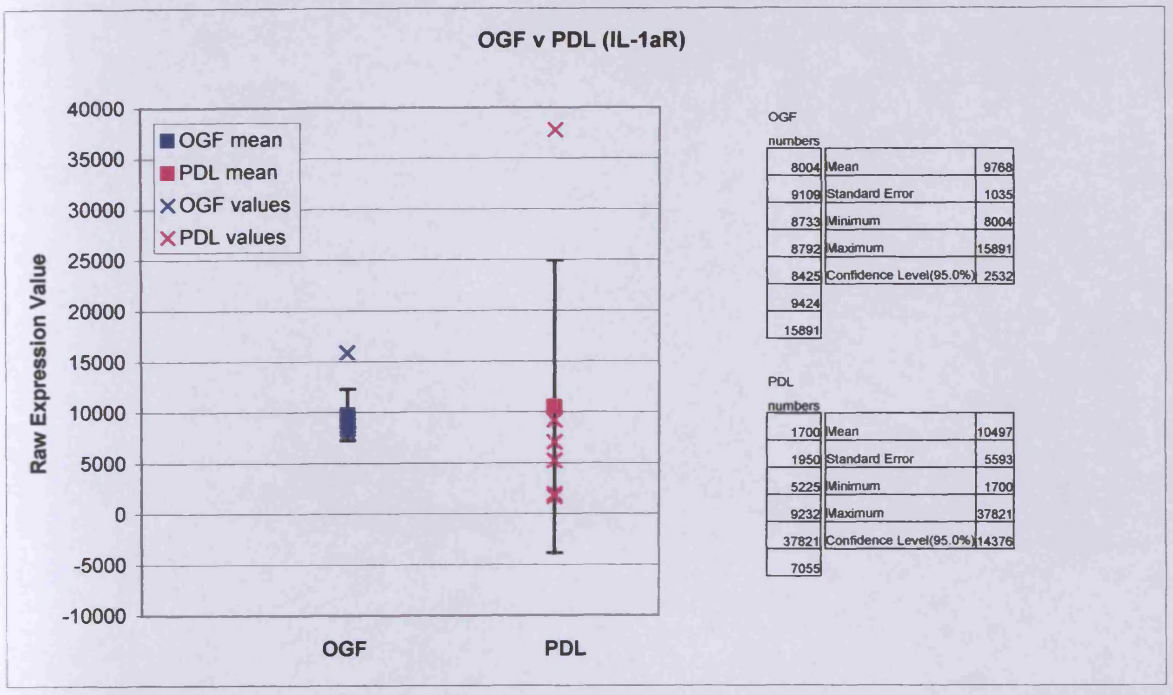

OGF numbers		
8004	Mean	9768
9109	Standard Error	1035
8733	Minimum	8004
8792	Maximum	15891
8425	Confidence Level(95.0%)	2532
9424		
15891		

PDL numbers		
1700	Mean	10497
1950	Standard Error	5593
5225	Minimum	1700
9232	Maximum	37821
37821	Confidence Level(95.0%)	14376
7055		

Table 5.14: Raw data plot – fibroblast:TGFα

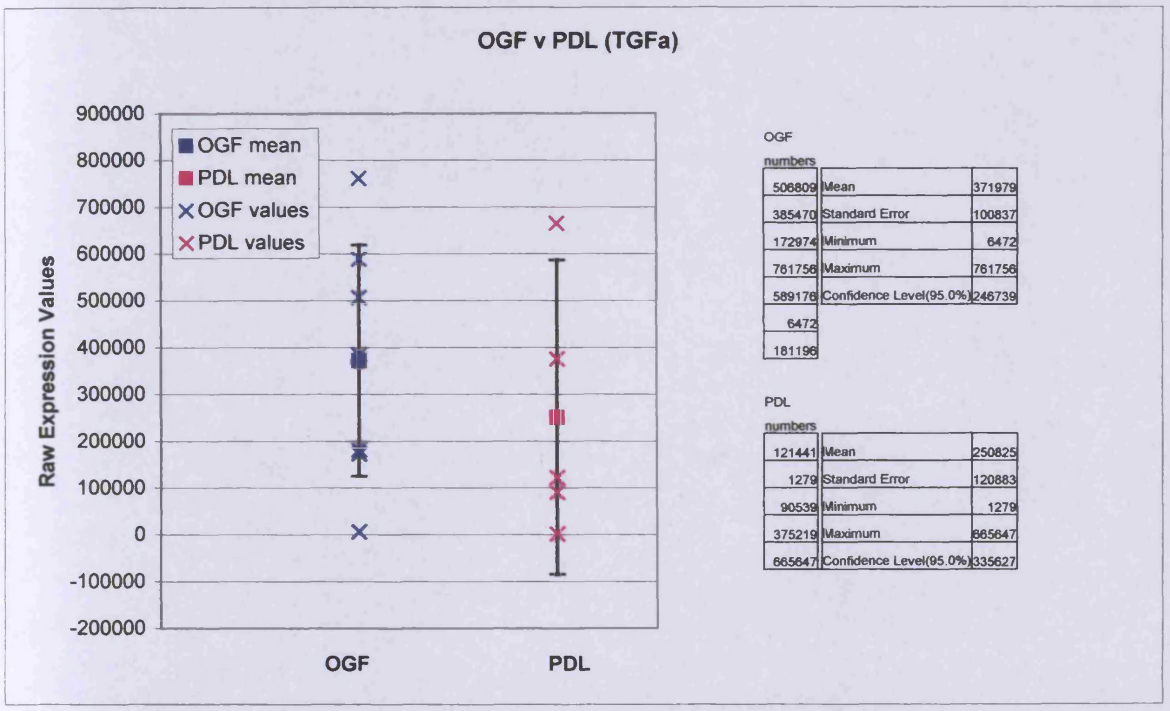

OGF numbers		
506809	Mean	371979
385470	Standard Error	100837
172974	Minimum	6472
761756	Maximum	761756
589176	Confidence Level(95.0%)	246739
6472		
181196		

PDL numbers		
121441	Mean	250825
1279	Standard Error	120883
90539	Minimum	1279
375219	Maximum	665647
665647	Confidence Level(95.0%)	335627

Table 5.15: Raw data plot – epithelia:KGFR

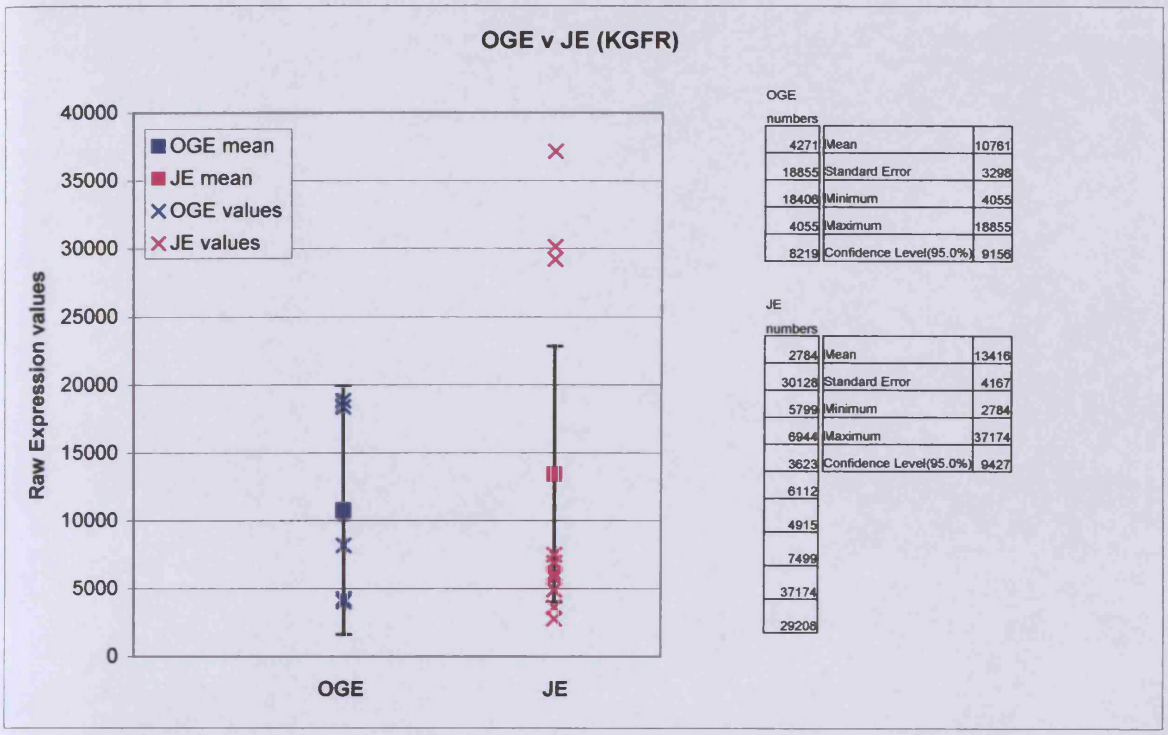

OGE

numbers		
4271	Mean	10761
18855	Standard Error	3298
18406	Minimum	4055
4055	Maximum	18855
8219	Confidence Level(95.0%)	9156

JE

numbers		
2784	Mean	13416
30128	Standard Error	4167
5799	Minimum	2784
6944	Maximum	37174
3623	Confidence Level(95.0%)	9427
6112		
4915		
7499		
37174		
29208		

Table 5.16: Raw data plot – epithelia:HGFR

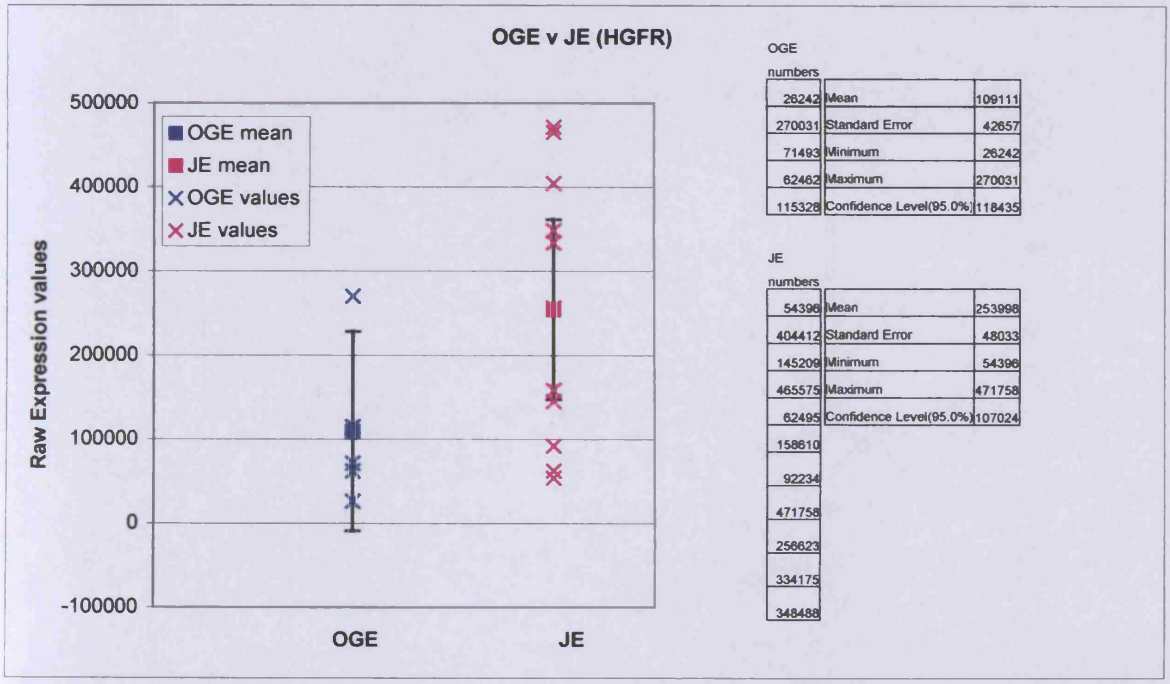

OGE

numbers		
26242	Mean	109111
270031	Standard Error	42657
71493	Minimum	26242
62462	Maximum	270031
115328	Confidence Level(95.0%)	118435

JE

numbers		
54396	Mean	253998
404412	Standard Error	48033
145209	Minimum	54396
465575	Maximum	471758
62495	Confidence Level(95.0%)	107024
158610		
92234		
471758		
256623		
334175		
348488		

Table 5.17: Raw data plot – epithelia:GM-CSFR

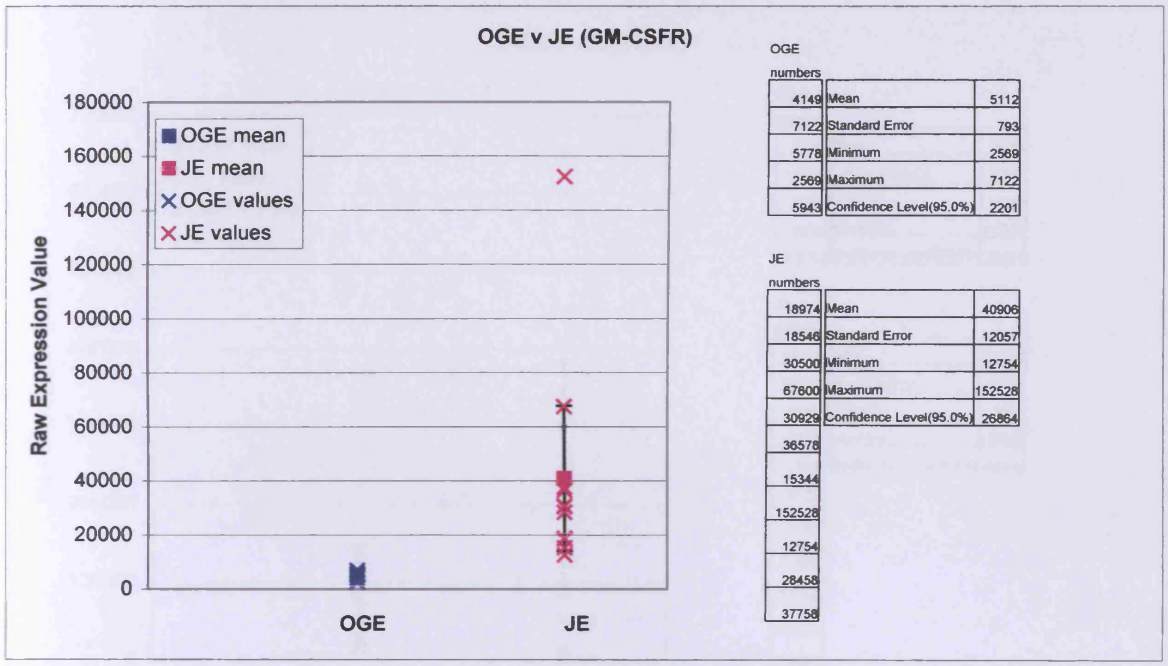

OGE numbers

4149	Mean	5112
7122	Standard Error	793
5778	Minimum	2569
2569	Maximum	7122
5943	Confidence Level(95.0%)	2201

JE numbers

18974	Mean	40906
18546	Standard Error	12057
30500	Minimum	12754
67600	Maximum	152528
30929	Confidence Level(95.0%)	26864
36578		
15344		
152528		
12754		
28458		
37758		

Table 5.18: Raw data plot – epithelia:IL-1α

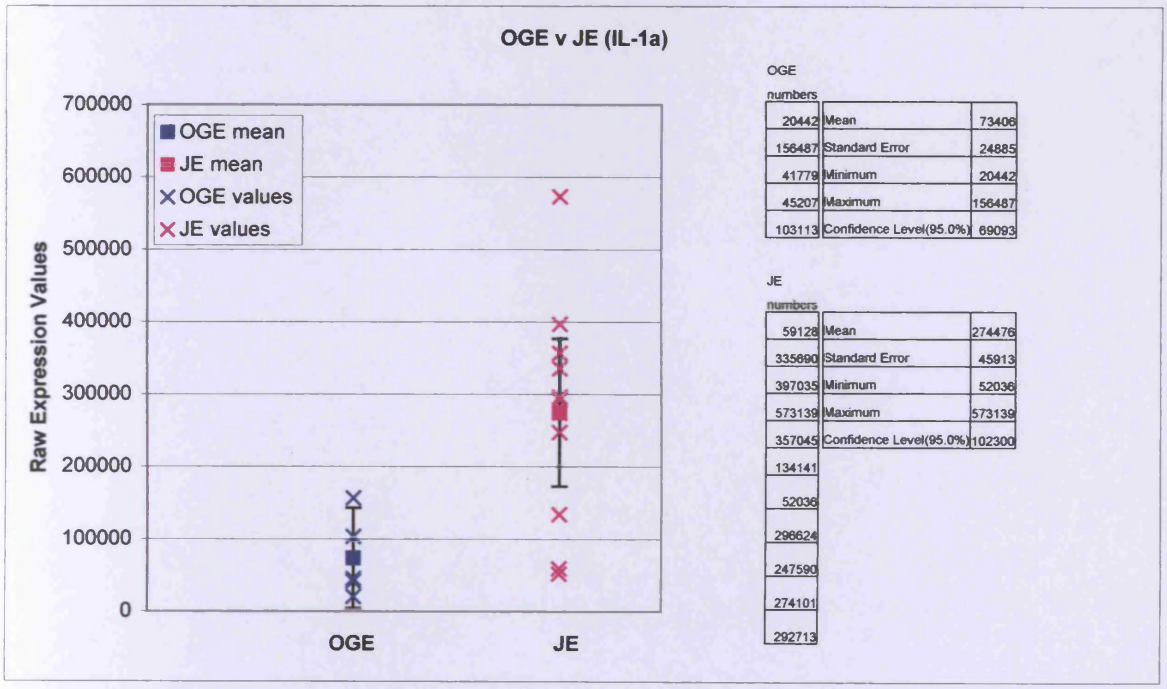

OGE numbers

20442	Mean	73406
156487	Standard Error	24885
41779	Minimum	20442
45207	Maximum	156487
103113	Confidence Level(95.0%)	69093

JE numbers

59128	Mean	274476
335690	Standard Error	45913
397035	Minimum	52036
573139	Maximum	573139
357045	Confidence Level(95.0%)	102300
134141		
52036		
296624		
247590		
274101		
292713		

Table 5.19: Raw data plot – epithelia:TGFα

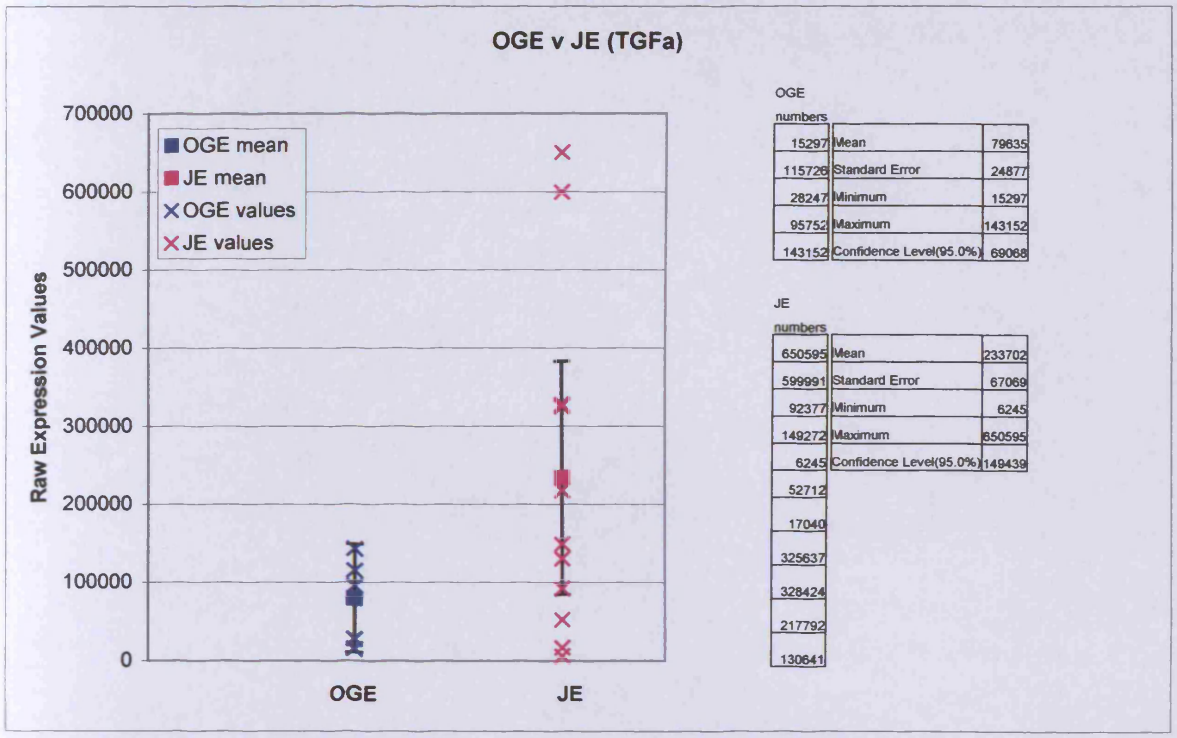

OGE

numbers		
15297	Mean	79635
115726	Standard Error	24877
28247	Minimum	15297
95752	Maximum	143152
143152	Confidence Level(95.0%)	69068

JE

numbers		
650595	Mean	233702
599991	Standard Error	67069
92377	Minimum	6245
149272	Maximum	650595
6245	Confidence Level(95.0%)	149439
52712		
17040		
325637		
328424		
217792		
130641		

5.9 Enzyme-linked immunosorbent assay data

KGF, GM-CSF and TGFα protein levels were measured using both conditioned medium and a cell lysate solution. Five PDL and five OGF fibroblast lines were used. For raw data-tables, see appendix XI.

5.9.1 Keratinocyte growth factor

KGF protein was detected in all PDL and OGF samples. Initial results were obtained from cell culture media samples only (Figure 5.61a). When applying the student's t-test assuming unequal variances, non-lysed samples demonstrated that OGF expressed statistically significant increased protein levels when compared with PDL ($p=0.050$). This finding is apparent when examining means data, PDL being 182pg and OGF being 591pg of KGF protein on average. This represents a 224% increase in KGF protein expressed by OGF compared with PDL.

Figure 5.61a: KGF protein levels in 5 PDL and 5 OGF lines (non-lysed)

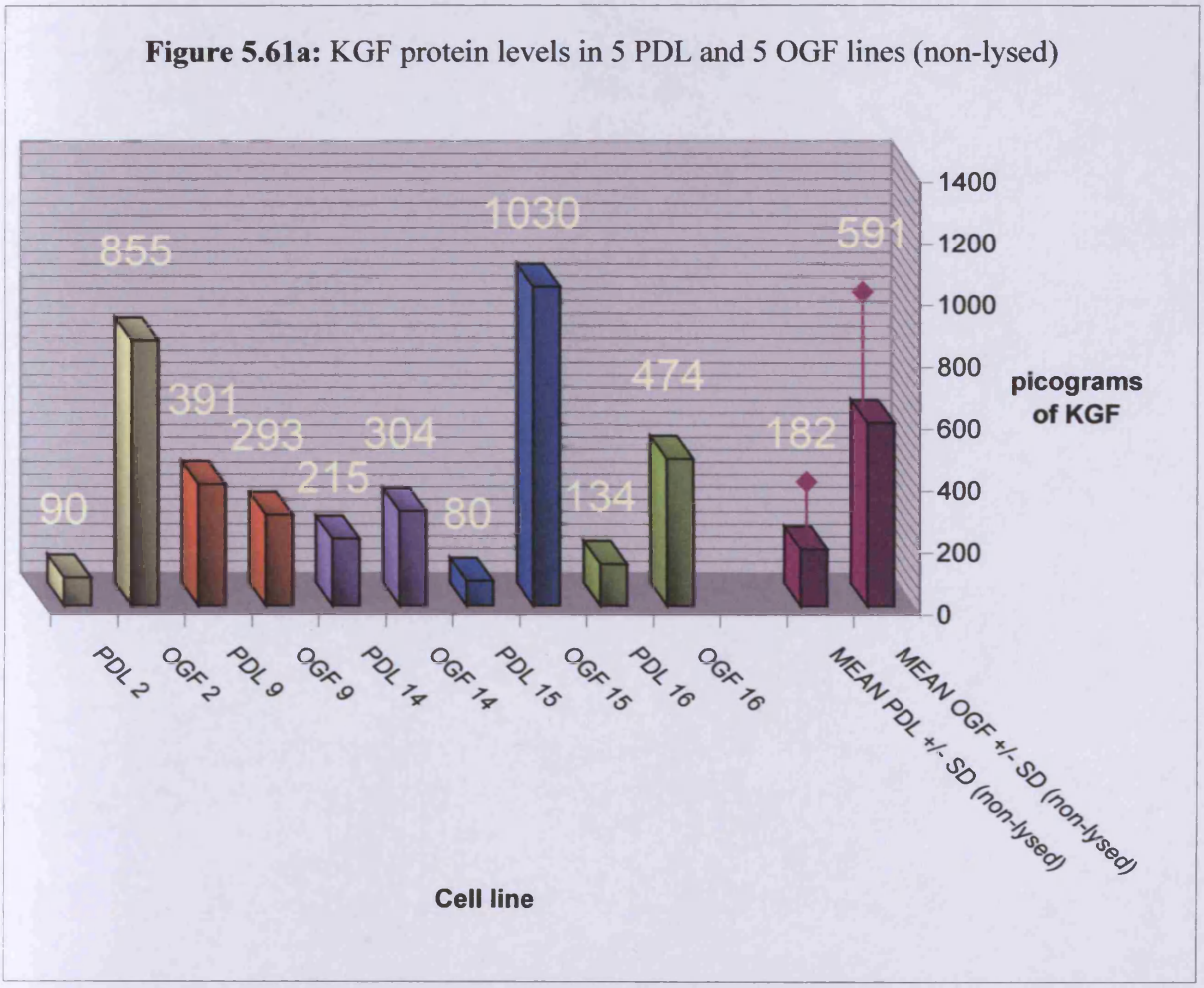

Figure 5.61b demonstrates similar results to those of figure 5.60a except lysed-cell samples produced considerably higher expression levels. Without exception, OGF fibroblasts produced more KGF protein than PDL fibroblasts, which is in agreement with Q-PCR data. When applying the student's t-test to the lysed-sample data differences were again statistically significant (p=0.036). This difference between populations is more clearly demonstrated by the mean value data; PDL being 588pg and OGF samples 1845pg of KGF protein. This represents a 277% increase in KGF protein expressed by OGF compared with PDL.

Figure 5.61b: KGF protein levels in 5 PDL and 5 OGF lines (lysed)

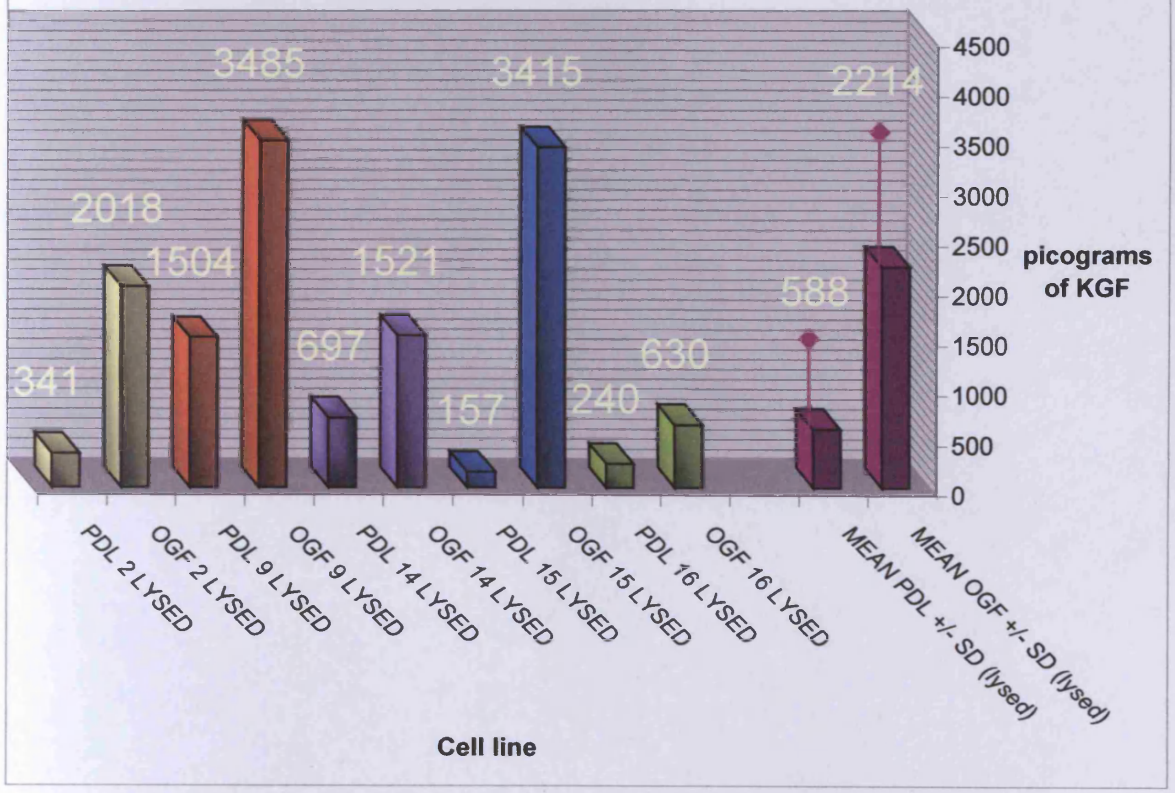

5.9.2 Granulocyte macrophage-colony stimulating factor

ELISA analysis of five paired samples of OGF and PDL fibroblasts for GM-CSF produced variable data; some showed high levels not related to a particular cell type (OGF9 and PDL14). Table 5.62a shows results for cell culture media only. The protein levels are considerably less than those for KGF, in excess of 10-fold lower between matching populations. This is different to the Q-PCR mRNA data that suggest only a 2-fold difference, although variability between mRNA levels and protein transcription levels may account for some disparity. Statistically there was no significant difference between the cell types by students t-test (p=0.92). Means values would confirm this lack of difference with average PDL expression levels being 45pg and OGF 42pg of protein.

Figure 5.62a: GM-CSF protein levels in 5 PDL and 5 OGF lines (non-lysed)

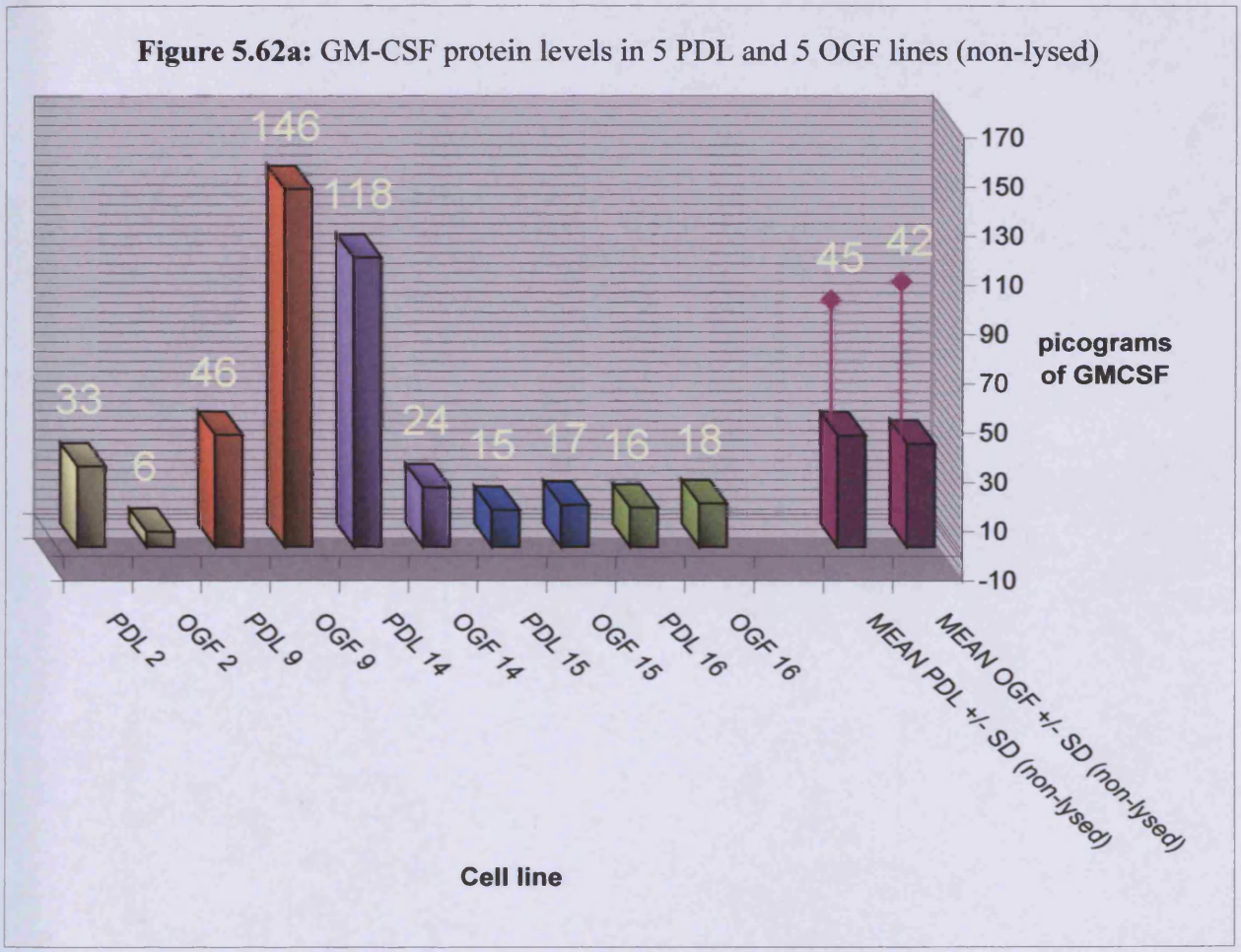

Figure 5.62b shows GM-CSF ELISA protein levels for lysed cell samples. Results were inconsistent, some values being greater and some less than those compared with non-lysed samples. Of four of the five samples the differences between PDL and OGF pairs remained, however, PDL2 was the exception where non-lysed results were the reverse of lysed. Statistically there was no difference between OGF and PDL cell types (p=0.53). The mean data columns demonstrate this more clearly; PDL expression level being 30pg and OGF 37pg of GM-CSF protein.

Figure 5.62b: GM-CSF protein levels in 5 OGF and 5 PDL lines (lysed)

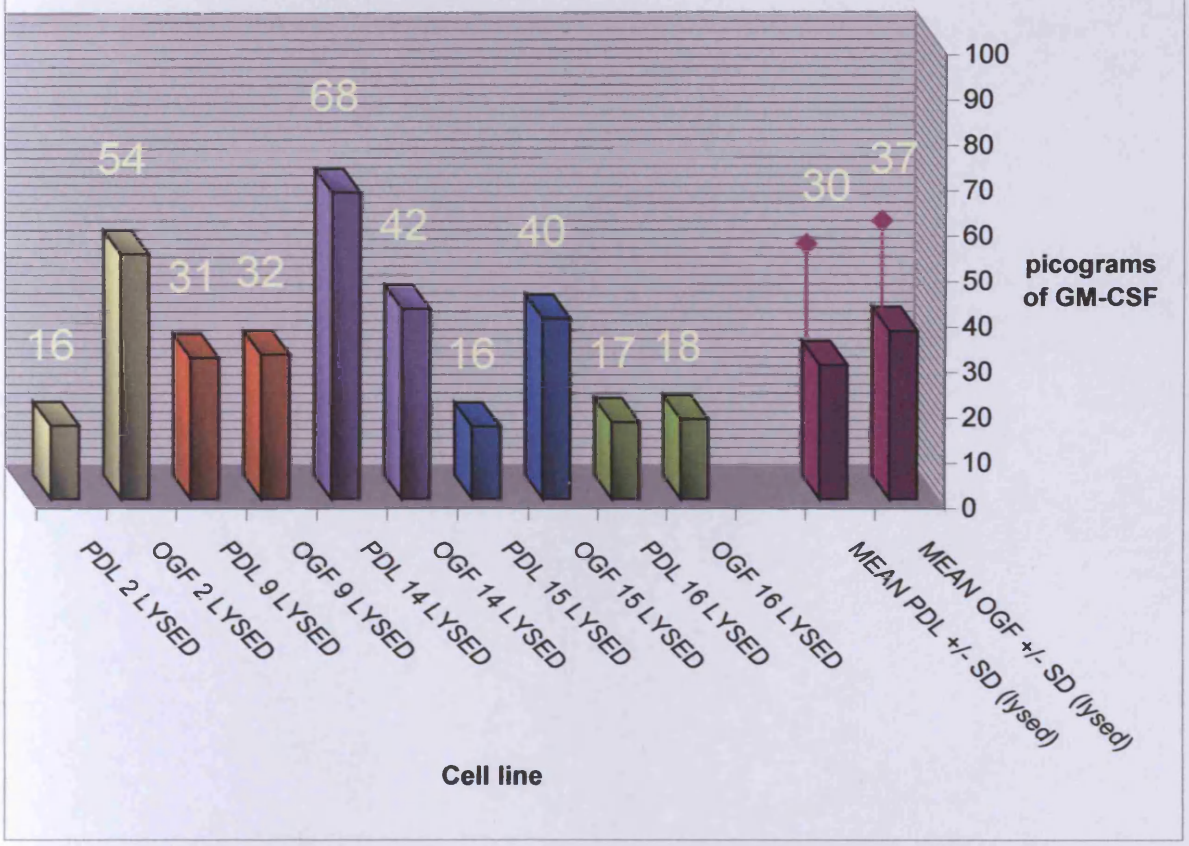

5.9.3 Transforming growth factor alpha

Table 5.63a shows results for cell culture media only, assessed in five OGF and five PDL populations. The results demonstrate widely varying levels of TGFα between cell samples; as a result, the data did not prove to be statistically significant (p=0.12). More generally, there were higher expression levels within OGF populations, in particular the samples OGF9 and OGF15 showed a considerably higher expression level when compared with the other samples. OGF9 proved to be 114% higher and OGF15 99% higher than the mean protein levels. This general trend was confirmed within the mean protein data levels for which PDL was found to be 30pg and OGF 213pg, OGF protein levels being increased on average 610% compared with PDL.

Figure 5.63a: TGF alpha protein levels in 5 PDL and 5 OGF lines (non-lysed)

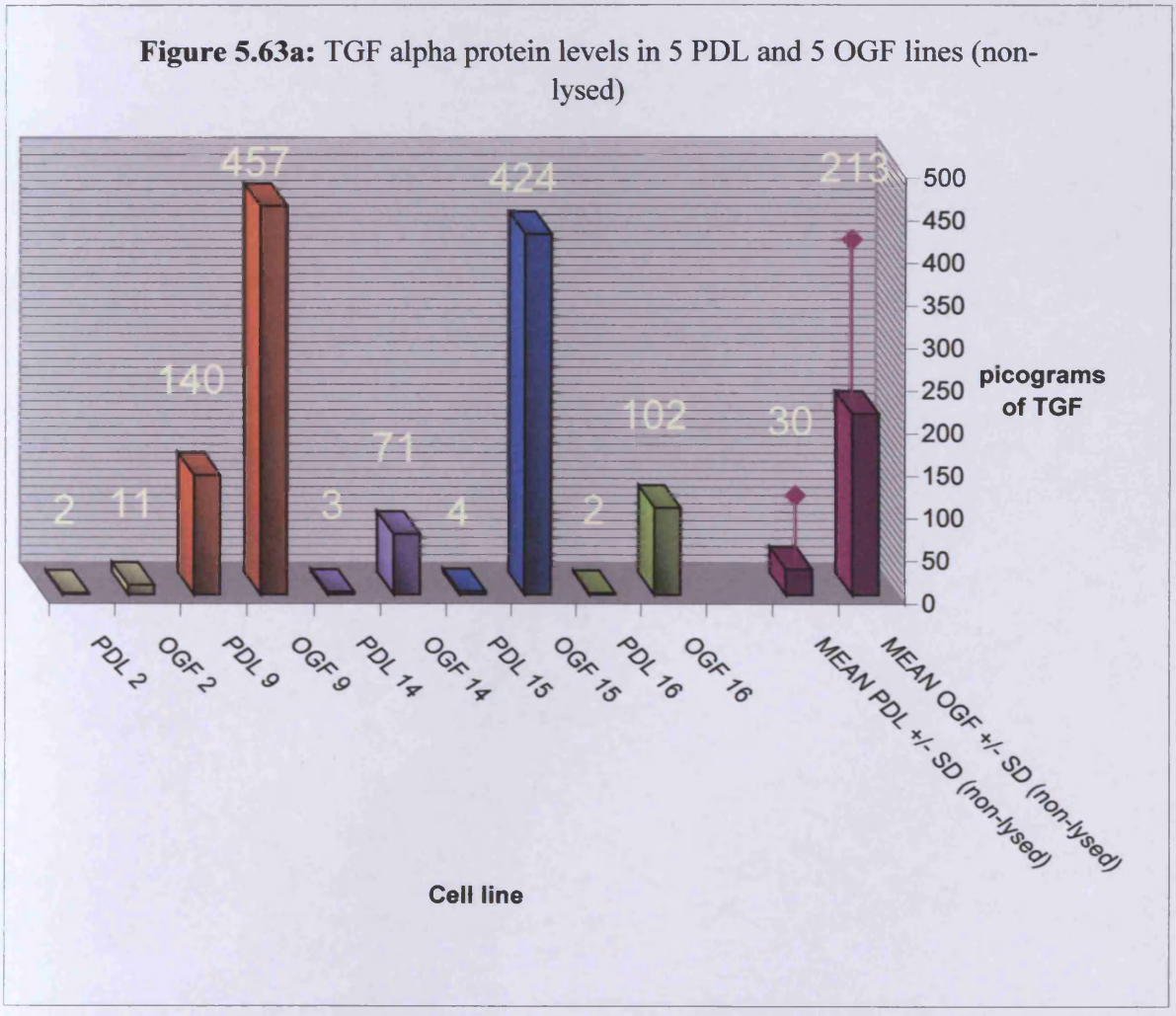

Figure 5.63b shows TGFα protein levels for lysed samples. Lysis of cells did not produce consistently higher results when compared to non-lysed samples; in fact, 9 of 10 results were higher for non-lysed samples. Again, OGF demonstrated higher protein levels when compared with PDL but not to significance (p=0.08). It is apparent from both charts that OGF9 and OGF15 produced considerably larger amounts of TGFα protein compared with other cell populations, OGF9 being 48% higher and OGF15 143% higher than the mean expression levels. The mean expression levels were found to be 1pg for PDL samples and 21pg for OGF samples.

Figure 5.63b: TGF alpha protein levels in 5 PDL and 5 OGF lines (lysed)

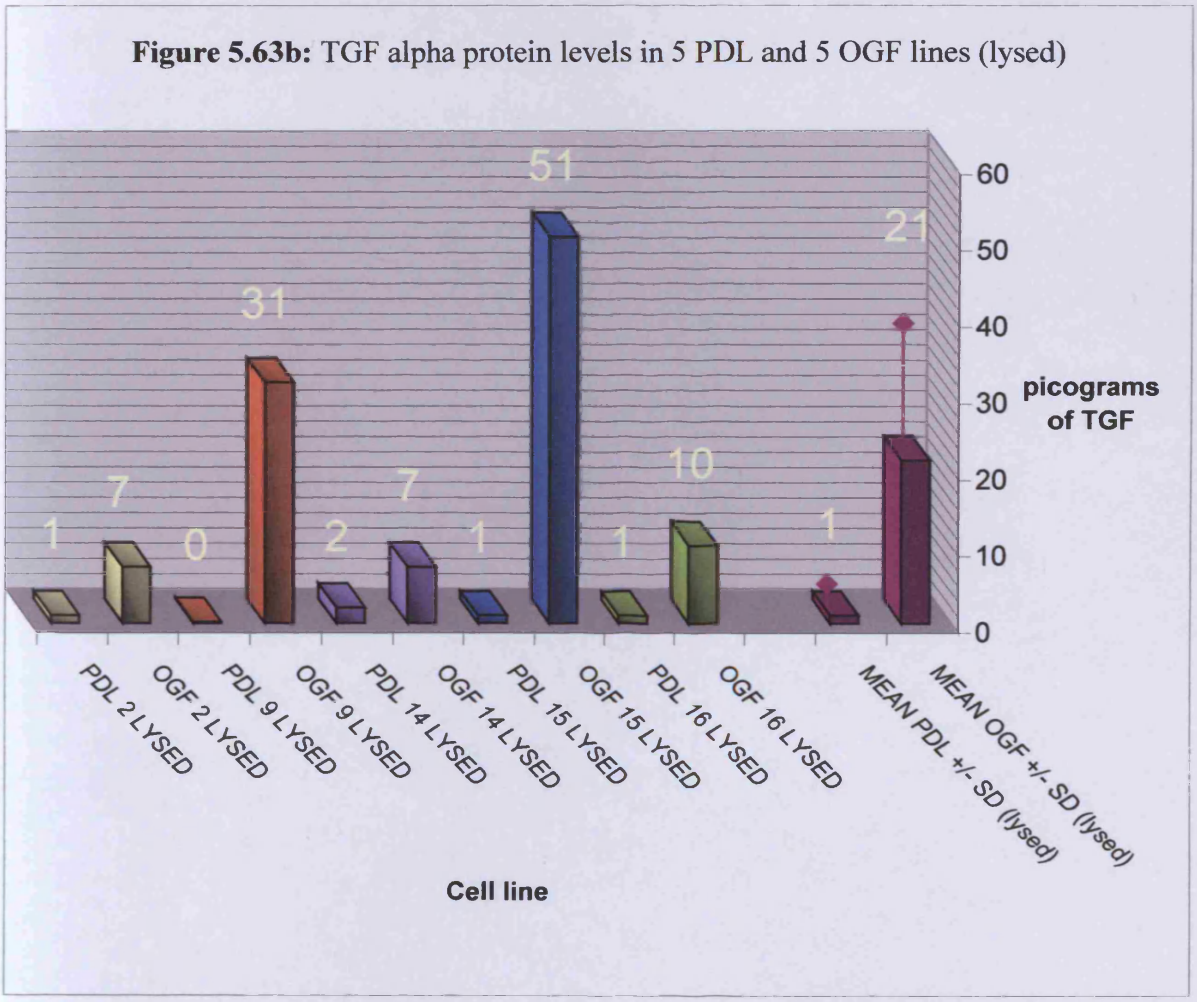

CHAPTER SIX

DISCUSSION

CHAPTER SIX
DISCUSSION

6.1 Introduction

The site of attachment of oral epithelium to the tooth surface consists of a unique epithelium, the junctional epithelium, and only a small anatomical distance separates this JE from the phenotypically different oral-sulcular and oral-gingival epithelia. An alteration in the junctional phenotype, together with epithelial proliferation and down-growth along the root surface are characteristic features of periodontal disease. To date, fully adequate explanations are lacking as to what occurs to maintain the steady state of JE during health, or its transition to a migratory phenotype with the onset of periodontitis.

6.2 Pathogenesis of periodontal disease

Microbiological influences on the initiation and progression of periodontal disease have been much investigated (Page and Schroeder, 1976; Socransky *et al.*, 1984 and Listgarten, 1986). Studies have shown that bacteria, and their metabolites, are capable of destroying the CT interface between tooth and gingivae, essentially instigating a wound healing response; it is theorised that JE then migrates into the created space (Grant *et al.*, 1979). Goldman and Cohen (1980) were the first to suggest that during health, the density of periodontal ligament fibres inserted into the tooth prevent epithelial down-growth of JE. It may be true that the presence of periodontal ligament fibres plays an inhibitory role, but apical down-growth does not automatically occur around osseointegrated dental implants despite the lack of insertion of a ligament (Listgarten *et al.*, 1991), suggesting the action of additional factors.

As periodontal disease undergoes periods of active migration, quiescence and even repair (Goodson *et al.*, 1982 and Albandar *et al.*, 1986) it seems unlikely that a simple epithelial wound healing response provides a complete explanation for periodontal disease processes. Certainly, it does not explain what events occur at the cellular and molecular level that prompts JE to (or not to) migrate into the resultant wound space (Mackenzie and Hill, 1984). It would appear that the role of bacteria and their metabolites on JE detachment and viability may be primarily indirect and act through changes in the "living conditions" of the periodontal cells, rather than having direct effects on the cells of the epithelial attachment apparatus (Overman *et al.*, 1994). It appears that some signalling mechanism beyond that of simple physical barriers are required to maintain the JE during health and permit its migration during disease.

Fibroblasts are capable of reacting to and synthesising an array of biological mediators that influence epithelial behaviour; differential expression of these factors could promote differences in the overlying epithelium. Mackenzie (1984) described a model in the mouse that demonstrated the effect of CT on the JE phenotype. In that model, epithelia from different areas of the mouse oral cavity were transplanted, in an *in vivo* system, to areas of deep CT and seemed to re-differentiate producing many of the characteristics of JE. In that environment the epithelium was both non-migrating and adopted a new phenotype, showing the same pattern of reactivity for both lectins and keratins as the JE *in-situ*. In contrast to sub-epithelial CT, deep CT appeared to lack the permissive, and possibly directive, influences necessary for the differentiation of epithelial cells into a keratinised phenotype. It became apparent that an epithelial phenotype characteristic of JE could arise when oral epithelium is brought into contact with the "deep" CT (Mackenzie and Hill, 1984). This gave rise to the idea that the underlying PDL may directly control and maintain the passive nature of JE in health and possibly therefore the uniquely passive behavioural properties of JE can be explained by its interactions with a periodontal CT that has a reduced ability to produce cytokines and which differs from that of OGF.

If non-permissiveness of PDL tissues is accepted as a working hypothesis for JE stability during health, the question arises as to why apical migration of the JE occurs at all during periodontal disease. As long as JE cells are in contact, or are adjacent to the PDL CT, they should remain in a non-migratory state. This is of course not the case in periodontal disease and it is conceivable that outgrowth or activation of different subpopulations of fibroblasts may cause perturbations in epithelial-mesenchymal interactions that, in turn, could modify the course of maturation of overlying epithelia. Schroeder and Listgarten (1977) theorised that such changes could be initiated by an inflammatory response and that inflammation and its sequelae play an important role in the circulating cytokines at the ADJ. Inflammatory cytokines have the potential to interact with homeostatic cytokines and modify the basic patterns of differentiation (Mackenzie, 1994). Reduced levels of gingival inflammation are associated with loss of epithelium with the typical appearance of OSE (Schroeder and Listgarten, 1977), and the observations of Bosch *et al.* (1989) indicate that inflammation induces expression of CK4, CK13, and CK19 (markers of non-keratinised epithelium) in keratinised OGE. Inflammation thus appears to produce a shift from the OGE towards the OSE phenotype. This shift of phenotype by OSE provides further evidence that JE is different and that it too may be altered by inflammatory products. In the context of periodontitis, the

gingival CTs become infiltrated with inflammatory cells that may promote CT destruction and loss of original spatial orientation between specialised epithelia and gingival and periodontal ligament CT (Mackenzie and Gao, 1993). The more superficial JE cells grow close to the bacterial plaque and the apical and lateral parts of the JE are likely to be influenced by the CT and inflammatory reaction.

6.3 Aims of the study

It is possible that a complex interplay between JE and its underlying CT exists, and that cytokine networks simultaneously influence both epithelial migration and repair. Therefore, the interaction with CT in the stabilisation and modification of epithelium is of particular importance in understanding the development of periodontal pockets in this unique tissue.

The hypotheses tested in this study were that differences between junctional and oral-gingival epithelia are associated with differing influences produced by their sub-epithelial fibroblasts. Further, it was hypothesised that periodontal and gingival fibroblasts differ in their constitutive levels of cytokine expression, and that they are integral in the maintenance of epithelial growth and activation to migration during disease. The aims of this study therefore were to elucidate, using an *in vitro* model of the oral-gingival and junctional epithelia, the extent to which these tissues are stabilised by underlying mesenchymal tissues and specifically the role of fibroblast-cytokine networks in providing the stimuli necessary for epithelial growth and differentiation. Inferences could then be made as to what molecular signalling events may occur to alter oral phenotypes into those recognised during periodontal disease.

6.4 The fibroblast phenotype *in vivo*

Much work identifying and separating the component tissues of the periodontium has been conducted (Bampton *et al.*, 1991; Matsuyama and Izumi, 1997 and McKeown *et al.*, 2003). The periodontal tissues are composed of a number of discrete heterogeneous fibroblast populations, the two principle groups being those derived from the PDL and those derived from the lamina propria (Hassell and Stanek, 1983; Mackenzie *et al.*, 1993; Irwin *et al.*, 1994 and Schor, 1995).

Alkaline phosphatase expression is regarded as being a marker that can differentiate between these fibroblast populations of the periodontium (Kawase *et al.*, 1986; Somerman *et al.*, 1988; Piche *et al.*, 1989; Groeneveld *et al.*, 1993 and Gao *et al.*, 1999). Our work staining for the enzyme in *ex vivo* sections provided clear localisation of a high density of ALP toward the tooth surface (encompassing PDL and JZF zones), with rapidly diminishing intensity toward the oral surface (OGF zone). This sudden transition from ALP-rich to ALP-poor fibroblasts suggests differing phenotypes restricted to their own domain. The well-defined localisation of expressing and non-expressing cells defined zones that could be separated by micro-dissection for subsequent tissue culture manipulations.

6.5 The epithelial phenotype *in vivo*

Oral mucosae display marked regional variations, in particular within the periodontium, which exhibits three structurally different epithelia within a small anatomical zone, the JE, OSE and OGE (Schroeder and Listgarten, 1971). The JE and OGE have been extensively investigated, characterised both histochemically (Morgan *et al.*, 1986; Shabana *et al.*, 1991; Mackenzie *et al.*, 1991 and Bampton *et al.*, 1991) and in terms of cell turnover rate (Loe and Karring, 1969 and Sabag *et al.*, 1984) and JE is now regarded as a unique tissue type. Several studies have shown that JE has a highly unusual pattern of differentiation in which markers typical of stratifying and simple epithelia are co-expressed (Morgan *et al.*, 1986 and Steffensen *et al.*, 1987). JE has been found to be unique with respect to expression of the keratins 8, 18 and 19 (Mackenzie *et al.*, 1991) and in its binding of the lectin, *dolichos biflorus agglutinin* (Bampton *et al.*, 1991).

We found that staining of *ex vivo* gingival cryosections using an extensive panel of monoclonal antibodies demonstrated several markers that allowed identification of the JE zone. Firstly, markers lacking from JE but expressed by the OGE/OSE phenotypes included the cytokeratin pairs 1/10 and 4/13. Positive markers of the JE phenotype included CK8, 18, 19, DBA and MMP-7.

There were however, some patterns that did not conform to previously published data:

Crawford and Hopp (1990) and Gao and Mackenzie (1992) described ICAM-1 as providing differential staining for JE when applied to *ex vivo* sections of gingiva. In

our study, there was at best extremely weak staining of the JE zone of gingival cryosections. Staining throughout the *in vitro* IHC continued to be extremely weak, and may represent a poor monoclonal antibody.

Desmoplakin, described by Matsuyama *et al.* (1997) as demonstrating "differences in staining patterns" of JE and OGE keratinocytes cultured *in vitro*, provided staining of cell membranes for both JE and OGE cells *in vivo* at equal intensity and so did not offer any measure of differentiation.

6.6 The fibroblast phenotype *in vitro*

To enable testing of the first hypothesis the differing fibroblast and epithelial types identified within the periodontium were isolated from human subjects. Histo- and immunohistochemical techniques determined their *in vitro* staining patterns and demonstrated the degree to which the *in vivo* phenotype was retained in culture.

Histochemical characterisation: Studies have shown that when fibroblasts from closely approximated periodontal ligament and gingival connective tissues are grown *in vitro*, there exist large variations between them (Hassell and Stanek, 1983; Irwin *et al.*, 1994 and Schor, 1995), the predominant differentiating histochemical marker for periodontal fibroblast populations being alkaline phosphatase. Several studies have shown that gingival fibroblasts contain relatively low levels of ALP activity compared to cells derived from PDL or bone (Kawase *et al.*, 1986; Somerman *et al.*, 1988; Piche *et al.*, 1989; Beertsen and Van den Bos, 1991 and Goseki *et al.*, 1995). Further work by Gao *et al.* (1999) found that ALP activity was highest in osteoblasts, moderate in PDL and lowest in OGF cells.

In vitro ALP staining of cells grown on a plastic substrate demonstrated distinct differences between examples of the two populations. PDL samples had between 50% and 88% of cells expressing ALP whilst OGF samples rarely exceeded 10% of positive cells. These figures suggest that two phenotypically distinct cell populations exist and that there is a degree of overlap. This overlap may either represent true anatomical variation of the cell types throughout the gingivae or, less likely, contamination during the micro-dissection procedure.

The third population of fibroblasts, JZF, provides further evidence that intrinsic histochemical differences are maintained in culture. Their ALP expression levels were intermediate between PDL and OGF. It may of course be that these fibroblasts represent a "third" individual phenotype within the attachment tissues, or more likely, that there exists a spatial transition between PDL and OGF zones where two differing phenotypes intermingle at varying ratios. These consistent regional differences provide further evidence that our laboratory separation procedures were appropriate for separating the fibroblast populations.

Growth-rate studies: *in vitro* studies have shown that PDL and OGF populations differ in their proliferative abilities. Mariotti and Cochran (1990) and Ogata and Niisato (1995) found PDL fibroblasts to proliferate at a slightly higher rate than OGF. Although not directly studied such a strict growth-rate difference between cultures were not identified in our culture conditions, but PDL fibroblasts did have a more limited replicative life span than OGF. All fibroblasts showed a reduced ability to proliferate with high passage, but whereas PDL fibroblasts rarely passaged beyond P7, OGF samples usually ceased to replicate at P9 or P10. These findings suggest that the *in vitro* life span of PDL fibroblasts may be shorter than OGF and this correlates with data published by Sawa *et al.* (2000) who found high expression levels of ALP in cells deemed to have long telomeres (regarded as being "biologically" young) whilst those having short telomeres (old) showed weaker ALP activity. It is prudent to point out here that it was not known how many cells were plated at the initial isolation stage. There is the possibility that differences in passage number attained may merely relate to significant fold-changes in the number of cells at P0.

6.7 The epithelial phenotype *in vitro*

Antibody characterisation: Differences in keratin expression have been used to demarcate the epithelia of the attachment zone by staining *ex vivo* tissue sections with a panel of mABs. Several studies then focussed on finding markers that differentiate between OGE and JE *in vivo* when grown *in vitro*. Altman *et al.* (1988) isolated rat JE cells as well as gingival and palatal samples and found that the epithelia differed and remained distinct in tissue culture. Specifically they found differential expression of keratin specific antibodies AE1, AE3 and desmoplakin I+II between JE and gingival epithelial cells. Bampton *et al.* (1991) using the lectin *dolichos biflorus agglutinin* in a panning technique successfully isolated and cultured keratinocytes from human JE and compared their *in vitro* phenotype with that of cells grown

from the oral-sulcular and attached OGE. All cells expressed CK4, 7, 14, 18 and 19 indicating, at least with respect to their keratin expression, that cells from the three areas of the gingiva appear to revert to one phenotype in culture. Other studies have hound phenotypic differences to persist including Gao and Mackenzie (1992) who demonstrated that during standardized *in vitro* culture conditions OGE lost expression of the differentiation markers CK1 and 10 and acquired some expression of CK19, but less so than that of JE. Matsuyama and Izumi (1997) established a culture of human JE cells derived from epithelial tissue attached to the tooth surface. Again, the expression pattern of CK19 was observed not only for the junctional-type cells but also for cells from gingival tissue, however, as in Bampton's work, DBA did prove to be specific in reacting only with JE cells. Clearly, these studies show that the JE phenotype is not entirely stable within their tissue culture environments although it would appear that some phenotypic markers do remain.

Within this study the panel of mAB staining was repeated on both epithelial colonies cultured both on plastic substrate and cell smears prepared from them. When viewed in their entirety the results provided clear evidence for the maintenance of phenotypic differences *in vitro*, principally by those markers previously identified in the literature CK8, 18, 19 and DBA antibodies all demonstrated staining localised to JE cells either uniquely or with a higher intensity of fluorescence (Bampton *et al.*, 1991 and Mackenzie and Gao, 1992).

The majority of staining patterns corresponded to the *in vivo* work but there were some patterns that did not:

Cytokeratins 1 and 10, which are markers of differentiated keratinocytes were evident in small amounts within JE samples, this may possibly imply some differentiation within the culture system not normally noted within the JE phenotype or some aberrant cross-reactivity of antibody.

There was weak staining of some flattened, apparently suprabasal OGE cells for CK4 and 13 *in vivo.* These cytokeratins normally being localised to the crestal portions of the gingivae only. It is feasible that cells from the gingival crest were incorporated into cultures during the micro-dissection procedure.

Weak *in vitro* staining of some OGE keratinocytes for CK19 was evident. CK19 is described as a marker of the basal cells of oral epithelia, however the positively stained cells were too few in number to represent the entire basal section. A number of culture conditions have been implicated in CK19 induction and will be discussed below.

Growth-rate studies: BrdU experimentation presented two observations. Firstly, that the OGE keratinocytes demonstrated a higher growth-rate (confined to the holoclone fraction) when compared with JE keratinocytes typically producing colonies of, on average, double the number of cells over six days. However, the BrdU uptake by the two populations was almost identical, the percentage of actively dividing cells being 33% for JE and 30% for OGE. As equal numbers of cells were plated and their BrdU uptake at a point in time were equal this implies either that JE cells in culture have an intrinsically slower cell-cycling (inter-mitotic) time with respect to OGE, a finding that corroborates data achieved by Gao and Mackenzie (1992), or that they suffer an increased rate of apoptosis. This provides more evidence perhaps to suggest that the JE phenotype is modulated by its spatial arrangement within tissues.

Secondly, JE samples showed a sharp decrease with passage in the ability to divide and colonise the dishes and so all samples failed to populate culture flasks beyond P3. OGE began a similar decline in proliferative ability at passages beyond P5. In both it was macroscopically evident that growth retardation coincided with an increase in numbers of the abortive, paraclone–like colonies and a reduction in the holoclone-like colonies. These differences in ability to proliferate under identical conditions suggest that this may represent a true *in vitro* difference between the two populations. JE may be a less robust phenotype that undergoes exhaustion of the proliferative fraction of its cells when asked to undergo significant increases in population expansion. Again, as with fibroblast isolation procedures there may have been a significant difference in the numbers of cells plated at P0 that may have an effect on the subsequent number of passages and divisions the cells would undergo.

6.8 Phenotypic transition in culture

The four cell populations investigated could be accurately identified *in vivo* and subsequently separated and cultured within the *in vitro* environment. However, it is apparent that the phenotypic markers were susceptible to time-dependant changes whilst in culture.

Fibroblasts: ALP expression by all fibroblast populations was lost within a relatively short number of passages; OGF cultures did not contain any ALP positive cells by P4, JZF by P6 and PDL by P9. This implies existence of functional differences between the two populations that exist *in vivo* and initially *in vitro*, and that are lost on increasing passage (Irwin *et al.*, 1994b). The results support findings by Goseki *et al.* (1996) and more recently, Sawa *et al.* (2003) who found lowered ALP expression within aged cultures. Changes in phenotype have been found within *in vitro* PDL populations for other potential differentiation markers including; osteonectin (secreted protein, acidic and rich in cysteine/SPARC by Shiba *et al.* (2000) and osteopontin and osteonectin by Sawa *et al.* (2003).

These finding have implications as to the functional attributes of fibroblasts in culture at increasing passage numbers. In particular, it would seem to indicate that lower passage fibroblasts are likely to be more successful in regenerating and mimicking the *in vivo* situation. This striking example of shifting phenotype in culture may be due to limitations in the media and or growth conditions, or may represent reversion to a base phenotype (whilst in culture) that does not require the full spectrum of three-dimensional signalling that would exist in the *in vivo* tissues.

Keratinocytes: Differences between the *ex vivo* and *in vitro* staining indicate a shift in cellular phenotype. The principle changes between *ex vivo* sections and *in vitro* colonies were in the cytokeratins CK1 and 10, which are usually markers of keratinised, differentiated epithelia. The cytokeratins were evident in small amounts within JE samples implying some differentiation within the culture system that is not normally noted within JE *in vivo*.

In addition, there was weak staining of some flattened, suprabasal OGE cells for CK4 and 13 when grown in culture, possibly representing a de-differentiation of the keratinised OGE phenotype toward a non-keratinising phenotype.

Weak staining of some OGE keratinocytes for CK19 was evident *in vitro*, possibly indicating a shift toward the JE phenotype as described by Bampton *et al.* (1991). Studies have been conducted into possible modulators, particularly retinoic acid, of cytokeratin expression by keratinocytes in culture and retinoic acid is known to modulate stratified squamous epithelial differentiation to induce the expression of basal cell CK19 and the suprabasal keratins CK1/10 and CK4/13 (Eckert and Green, 1984 and Crowe *et al.*, 1991). Retinoic acid has

minor effects on the marker expression of JE but markedly enhanced expression of cytokeratins 8, 18, 19, vimentin and ICAM-1 within OGE (Gao and Mackenzie, 1996). These observations indicate that the response to retinoic acid can affect the phenotypes expressed by epithelia *in vitro* and suggest that such mechanisms may be related to the altered phenotypic patterns expressed by gingival epithelia *in vivo* (Gao and Mackenzie, 1996).

Interestingly, Breitkreutz *et al.* (1984) took keratinocytes that showed only a reduced programme of differentiation in primary culture, as indicated by ultrastructure and keratin composition, and found almost complete restoration of epidermal function was achieved after transplantation onto adult mice. In this *in vivo* environment, well-structured epithelia developed with restoration of both typical ultrastructure and *in vivo*-type keratin expression within 2 weeks. Thus, although keratinocytes in primary culture differ somewhat from those *in vivo*, they have not irreversibly lost the capacity for complete differentiation.

Summary: Examination of cytokeratin expression patterns within JE and OGE both *in vivo* and *in vitro* have provided evidence that their phenotypes are intrinsically different (Gao and Mackenzie, 1993). Mackenzie and Tonetti (1995) demonstrated, by mAB panel phenotypically indistinguishable JE reconstituted from OGE around dental implants. This suggests that rather than its developmental origin; the unusual JE phenotype is determined by the relationship of the epithelium to the tooth surface (Salonen, 1986) and underlying CT. If it is accepted that this geometry of physical apposition to a tooth be partly responsible for the JE phenotype, OGE must also intrinsically have the ability to re-differentiate into JE despite developing from an entirely different embryological interaction. Therefore, control of these cells phenotypes appears to be partly intrinsic and partly extrinsic. Alternatively, of course we could consider the possibility that the JE formed from OGE, although showing the same mAB staining is not identical but may be a close simulacrum.

This positive identification of two separate fibroblast and epithelial populations *in vivo* and demonstration that these phenotypes were at least partially maintained *in vitro* indicated that the first hypothesis was tenable and allowed work to continue in testing the further hypotheses.

6.9 Organotypic cultures

Co-cultures of keratinocytes on 3T3s do not correspond to the *in vivo* situation due to the lack of geometry and CT signalling. This is why organotypic cultures have been developed with a distinct CT layer and external environment that simulates the *in vivo* situation more closely. Culturing in combination with mesenchymal cells has been found to re-develop some of the histological characteristics observed within normal full thickness skin and gingiva (Odioso *et al.*, 1995; Garlick *et al.*, 1996; Delcourt-Huard *et al.*, 1997 and Chinnathambi *et al.*, 2003). Organotypic cultures provide a valuable tool for the study of keratinocyte cell behaviour and mechanisms that control the spatial variation of epithelial phenotypes in an environment more closely resembling those found *in vivo* (Gao and Mackenzie, 1992).

The production of modulating growth factors is regulated by cytokines such as interleukin-1 that are generated by epithelial cells to form a feedback loop, in which epithelia signal fibroblast production of stimulatory factors which in turn act to maintain the epithelia (Maas-Szabowski *et al.*, 2001). Taken together these findings demonstrate the importance of epithelial-connective tissue interactions, where presence of both fibroblasts and their products are central to development and maintenance of normal patterns of epithelial differentiation.

To test the influence of fibroblasts on epithelial morphology, expression of cytokeratin protein and to compare the differing abilities of periodontal ligament fibroblasts and gingival fibroblasts to support the growth of epithelium, we bio-engineered homotypic and heterotypic oral mucosae using cultured adult human cells. In five series of experiments, matrices were prepared containing either PDL or gingival fibroblasts and then plated with JE or OGE. Homotypic cultures constructed with OGE supported by OGF, and JE supported by PDL simulated the *in vivo* spatial arrangement. Heterotypic combinations, OGE supported by PDL and JE supported by OGF allow fibroblasts ability to direct growth and differentiation to be assessed.

In homotypic combinations, epithelial morphology and protein expression closely mimicked those *in vivo*. Histological sections of OGE and JE keratinocytes incorporated into the organotypic culture system showed consistent differences in epithelial thickness. Firstly, the homotypic recombinations:

1) OGE grown upon OGF resulted in the thickest epithelium with the most developed basal layer.

2) JE grown upon PDL showed little growth beyond 1-2 cell thickness.

Exact localisation of mAB staining was difficult within PDL/JE cultures due to the thin nature of the epithelium however patterns for both set-ups appeared to be consistent with those for epithelia cultured on plastic, with differentiation between JE and OGE indicated by CK8/18, 19 and DBA.

In heterotypic combinations, the morphologies differed considerably from the homotypic set-up:

1) OGE grown upon PDL showed good stratification and maturation but a visible reduction in thickness compared to OGE cultured upon OGF. This would indicate either a reduced ability of PDL fibroblast to support its overlying epithelium or possibly a re-differentiation of the OGE toward a JE phenotype by the PDL fibroblasts. Evidence for this was sought from the mAB staining which showed basal cells of the altered OGE expressing CK19 and DBA, features that were not evident in OGE homotypic culture.

2) Similarly, JE grown upon OGF produced an epithelium of 4-6-cell thickness that represented a considerable growth increase when compared with homotypic cultures of JE/PDL. This suggests an increased ability of OGF to dictate epithelial growth and development, possibly driving the JE toward a more OGE phenotype. The mAB staining provided some evidence for this; basal cells of the JE when cultured with OGF expressed low levels only of CK8/18, somewhat less than JE in homotypic culture. In addition, the suprabasal cells of the JE began expressing CK13, a pattern not seen in previous JE staining.

These results suggest that fibroblasts within organotypic culture have some differing influence on keratinocyte differentiation. If the CTs have complete control of differentiation and growth of their overlying epithelium, an *in vivo* situation could arise where JE becomes juxtaposed to OGF (and its array of mitogens), its response may then result in a shift to a migratory phenotype. It is important to remember at this point that microbial interactions at

the attachment zone have been implicated in phenotypic change of the JE (Mackenzie and Gao, 1993 and Mackenzie and Tonetti, 1995). It is possible that bacterial products (or the host response to them) bring about the initial processes that result in JE being exposed to differing CT influences. It may be expected that heterotypic organotypic combinations produce a more obvious shift in the epithelial phenotypes than was evident experimentally. This suggests that the intrinsic autocrine control of epithelial cells, in organotypic culture at least, is stronger than extrinsic regulation by mesenchymal fibroblasts.

In summary, it would appear that both the epithelial and CT components are integral in the growth, development and maintenance of a mature epithelium. At the morphological level these findings support our hypothesis that different CTs have differing abilities to support growth of overlying epithelia, probably because of intrinsically decreased or altered expression of epithelial mitogens (cytokines).

6.10 Cytokines and their maintenance of the epithelium

Cytokine networks involved in epithelial-mesenchymal interactions are slowly being unravelled within skin models and reports exist describing the spatial distribution of cytokines and their receptors that may provide a basis for understanding JE behaviour. Epidermal keratinocytes have been shown to produce a series of soluble proteins, both *in vivo* and *in vitro*, that modulate their own growth and that of other dermal and epidermal cell types (Maas-Szabowski and Shimotoyodome, 1999). The skin, a close approximation of the gingivae, has been the subject of numerous *in vivo* and *in vitro* studies of certain cytokine networks (Schroeder, 1995 and Werner and Grose, 2002). However, evidence for other cytokines and in particular their presence within periodontal tissues, is either conflicting or absent.

The complexity of these interactions makes it difficult to determine which cytokines are of particular importance to epithelial proliferative and migratory responses seen in periodontal disease (Alexander and Damoulis, 1994) or even wound healing (Stephens and Thomas, 2002 and Thomas and Harding, 2002). However, the results of both transgenic and functional studies indicate a central role particularly for KGF in particular, both in developmental interactions and in the normal maintenance and wound healing responses of adult epithelia.

6.10.1 Fibroblast Q-PCR data

Quantitative PCR data identified mRNA for several cytokines, but provided no evidence of the concomitant expression of their receptors on fibroblasts. This agrees with literature describing the expression of cytokines by mesenchymal tissues (Finch *et al.*, 1995b) and localisation of their receptors within the overlying epithelia. Fibroblast populations were found to express KGF, KGF2, HGF, GM-CSF and TGFα they also expressed the IL-1α receptor.

Many studies have investigated the mitogenic effects of KGF (Finch *et al.*, 1989, Wilson *et al.*, 1993 and Sotozono *et al.*, 1995) upon epidermal keratinocyte proliferation; however, data for KGF expression within oral tissues are conflicting. Mackenzie and Gao (2001) found that PDL did not express KGF whilst McKeown *et al.* (2003) found no significant difference between PDL and OGF in their production and secretion of KGF *in vitro*. Gron *et al.* (2001) reported that PDL produced more KGF than OGF. The Q-PCR analyses of our study showed that there was considerable heterogeneity within each of the three sets of fibroblasts, there being differences between OGF and PDL with respect to all of the proteins studied. OGF samples consistently expressed higher levels of cytokines when compared with PDL with mean levels being 2.1-fold greater for KGF, 1.5-fold for KGF2, 3.2-fold for HGF, 1.5-fold for GM-CSF, 1.6-fold for IL-1αR and 2.6-fold greater for TGFα.

These data indicate that PDL has the ability to produce KGF (and HGF) but at levels somewhat lower than the adjacent gingival CT. Evidence for production of KGF at the protein level was provided by ELISA techniques and they too demonstrated that PDL populations consistently produce lower levels when compared with OGF. Whether the varying levels of these growth factors released from fibroblasts are sufficient for biological effect remains a question and it may be that that these differences in cytokine expression levels have effects *in vivo*, principally and that lower production of KGF/HGF by PDL effectively limits or maintains JE in its stable, non-migrating state during health. Further, these variations in cytokine levels may represent differences to be found throughout the cell population, possibly imparting upon individuals a greater or lesser risk of developing periodontitis.

An additional unexpected finding was the identification of TGFα expression by the majority of fibroblast samples. It is well documented within the literature that TGFα plays a role as an autocrine acting epithelial mitogen (Maas-Szabowski *et al.*, 2002 and Momose *et al.*, 2002) but few studies describe production of TGFα by fibroblasts. ELISA protein production gave variable results with two of five OGF populations producing considerable levels. Again, this heterogeneity could be interpreted as a function of particular members of the population that may be more or less prone to periodontitis. Lowered levels of TGFα have been found in patients suffering chronic periodontal disease (Mogi *et al.*, 1999) therefore the two samples expressing high levels may represent "protected" patients in a "low risk category" for stimulation to epithelial growth and hence development of periodontal disease.

JZF results were more difficult to interpret. As previously discussed (chapter 5.1), the anatomical origin of JZF is thought to be from the CT beneath the JE. This represents a zone that both anatomically, and by virtue of its ALP expression, that occupies a central position between the PDL and OGF (table 5.1). It might be expected therefore that Q-PCR data would place cytokine expression levels at an intermediate value. For KGF, KGF2 and TGF this was the case but HGF, GM-CSF, and IL-1αR did not conform to one fibroblast type or the other, results actually being higher than both PDL and OGF by a minimum of 1.4-fold, 2-fold, and 2.4-fold respectively. These results would tend to contradict the premise that there exists a gradual transition from PDL to OGF cell-type through the gingiva and instead may signify a "third" fibroblast cell type. However, a possible explanation for the increased cytokine expression levels may rest with the anatomical positioning of these cells. Located adjacent to the JE attachment and close to the gingival sulcus there is likely to be bacteria with their metabolites perfusing the CT. These metabolites have the ability to modulate cytokine expression independently of the surrounding tissues (Uitto *et al.*, 1988; Birkedal-Hanson, 1993 and Zambon *et al.*, 1994, Chapter 1) so may have extrinsically altered the JZF cytokine expression profile so that it no longer resembles its tissue of origin.

6.10.2 Fibroblast ELISA data

ELISA provided further confirmatory evidence that cytokines detected by Q-PCR were present at the protein level within cell samples:

Keratinocyte growth factor: Protein was detected in all PDL and OGF samples and with the exception of non-lysed PDL/OGF9 sample; all OGF samples demonstrated a higher protein level compared with PDL. This agrees with Q-PCR data.

Granulocyte macrophage-colony stimulating factor: These data were variable and subsequently significant differences between PDL and OGF samples were not found. More evident were individual samples that produced considerably higher readings; OGF9 and PDL14 in particular showed upward of 10-fold higher expression levels compared with their counterparts.

Transforming growth factor alpha: These results demonstrate widely varying levels of TGFα between cell samples; generally, there were higher expression levels within OGF populations, within the samples OGF9 and OGF15 showing a considerably higher expression level compared to the other samples. This may represent a particular phenotype present within individuals and it is interesting to note that the OGF9 and OGF15 samples also provided the highest levels of KGF recorded.

6.10.3 Keratinocyte Q-PCR data

There were also large differences between the data for OGE and JE. The epithelial data in contrast to that for fibroblasts, demonstrated the presence of receptors to KGF, HGF and GM-CSF within both JE and OGE. Interestingly, OGF populations exhibited higher levels of known epithelial mitogens whereas JE keratinocytes demonstrated increased levels of their receptors. JE samples expressed 2.5-fold higher levels of HGFR and 6.5-fold higher GM-CSFR; this increased expression level of receptors was unexpected and more difficult to interpret. JE would be expected to express lower levels of receptors in its non-migratory (healthy) state in response to the lower levels of stimulatory cytokines provided by the adjacent PDL fibroblasts. However, the converse may well be true, with higher receptor levels being a physiological response to the normally low levels of circulating cytokines expressed by the underlying PDL. Further, these receptors may become operational and in part explain the JE subsequent ability to migrate with the onset of periodontal disease. It should be noted here that keratinocytes are cultured in an artificial *in vitro* environment and as such are stimulated by media constituents EGF and cholera toxin so cannot be regarded as entirely normal.

A significantly increased 4.0-fold level of IL-1α was noted for JE samples. IL-1 regulates the production of other stimulatory cytokines by fibroblasts within CTs such that feedback loops are generated (Braulch *et al.*, 1994) and these feedback loops signal fibroblast production of stimulatory factors that in turn act to maintain the epithelia (Maas-Szabowski *et al*, 2001). It was found that epidermis (and presumably OGE) stimulates CT production of KGF/HGF (and other cytokines) via an IL-1α dependant pathway. Therefore, with the increased IL-1α mRNA level found within JE, it reasonable to expect that JE could readily upregulate KGF/HGF expression by PDL and react by migrating. Clearly, this is not the case during health where epithelial homeostasis is maintained. This presents two possibilities:

1) Firstly, that PDL fibroblasts intrinsically lack the ability to respond to the IL-1α message. Q-PCR data showing reduced KGF/HGF expression by PDL fibroblasts would corroborate this.
2) Secondly, that IL-1α protein production is not complete and/or there exist inhibitors of the IL-1 pathway that if lost may result in the progression to destructive periodontitis. Of course, these results took place *in vitro* as stated by the above caveat.

It is known that the recombination of keratinocytes and fibroblasts *in vitro* can result in epithelial acquisition of a new phenotype (Cunha *et al.*, 1985) and it is possible to presume that the junctional phenotype is controlled *in vivo* by circulating epithelial-mesenchymal interactions. More specifically that the ALP-positive phenotype of PDL CT is inextricably linked to the overlying JE phenotype. Further, factors associated with bacterial inflammation can substitute for permissive factors produced by dermal cells or could perhaps act to favour selective outgrowth of fibroblasts of a permissive phenotype. These epithelial-mesenchymal interactions would then be implicated in the progression from health to disease during the onset of periodontitis.

6.11 General discussion

Previous studies (Dabelsteen and Wandal, 1997 and McKeown *et al.*, 2003) have inferred that there is distinct heterogeneity between periodontal fibroblast populations; our study confirmed that at least two distinct periodontal fibroblast populations could be cultured and differentiated histochemically. A similar finding was elucidated for the oral epithelia involved

in periodontal disease, namely the JE and its anatomically adjacent OGE. JE was found to express, at the RNA level, greater levels of receptors to a variety of epithelial mitogens.

The intimate anatomical nature of the gingival attachment zone has made investigations of intrinsic levels of cytokines expressed by fibroblasts and epithelial cells in this region difficult, making any conclusions as to the nature of the epithelial regulation during health and disease difficult to draw. The ability to successfully separate, culture, expand and characterise these cells *in vitro* has helped elucidate certain detailed characteristics. This study provides data to show differences of several key epithelial mitogens between two very closely opposed tissue types of the periodontium at the mRNA and protein level.

Further, the study assessed a number of approaches for preparing organotypic cultures and has successfully developed a method that can produce patterns of stratification comparable to that of the oral mucosa. The differences observed in epithelial mAB staining patterns *in vitro* indicate that the phenotype of JE is intrinsically different to that OGE. When recombined into homotypic culture the OGE phenotype is maintained, so much so that the epithelium stratifies and matures. Heterotypic culture however shows partial deviation of the phenotype toward that dictated by the CT component of origin. Taken together, these findings highlight the importance of keratinocyte-fibroblast interactions during establishment of epithelial patterns of differentiation, and the roles played by cytokines in this biological process. The results are consistent with the hypothesis that the sub-epithelial CT influences the phenotype of the JE, as well as other epithelia (Hill and Mackenzie, 1984 and Mackenzie, 1987), and that changes in these influences can lead to changes of the epithelial phenotype and the acquisition of new patterns of behaviour.

6.12 Future considerations

It seems unlikely that one factor could attribute to the stability or otherwise of the JE, therefore it is important that future studies be directed toward dissecting the role of cytokine networks in both normal epithelial maintenance and disease. It would be advantageous to repeat the quantitative assays with further populations of cells to enable greater statistical significance. Statistically significant changes would add weight to the argument that differing cytokine networks are responsible for the maintenance of phenotype *in vivo*. It would also be pertinent, if possible, to repeat such studies on populations of cells derived from diseased sites

where it may be expected that cytokine levels would differ, it would be interesting to see if once removed from their inflammatory *in vivo* location whether the phenotype would revert in culture.

Changes in constitutive cytokine expression levels may be altered by the host response to the bacterial micro-flora associated with progression of periodontitis. Our examination of baseline cytokine measurements could be compared with epithelia exposed to a series of such bacterial derived factors. Further, the serum levels within the media may affect the baseline expression levels *in vitro* and future modifications and refinements to epithelia media including omission of FBS may provide cells that are more representative of the *in vivo* state. As specific cytokines become implicated in epithelial-mesenchymal interactions and more becomes known of their role recombinant cytokines could be added to the organotypic system with the view to inducing or abrogating epithelial growth.

Finally, if cytokine changes prove to be linked with epithelial migration, this may have implications for therapeutic techniques. Altering an adverse cytokine balance may favour a more resilient epithelial phenotype.

GIFT OF REAGENTS

With thanks to:

- Dr. Scott McKeown

Royal Victoria Hospital, School of Dentistry, Oral Research Centre, Belfast.

Periodontal and gingival fibroblast populations.

- Professor Irene Leigh

St. Bartholomew's and the Royal London Dental Hospital, London.

Monoclonal antibodies to the keratins 1, 8, 10, 14, 16, 18 and 19

REFERENCES

Abe T, Hara Y, Abe Y, Aida Y, Maeda K (1996). Isolation of alkaline phosphatase positive gingival fibroblasts from patients with chronic inflammatory periodontal disease. *J Periodontal Res* 31: p285-93.

Albandar JM, Rise J, Gjermo P, Johansen JR (1986). Radiographic quantification of alveolar bone level changes. A 2-year longitudinal study in man. *J Clin Periodontol* 13(3): p195-200.

Alexander MB, Damoulis PD (1994). The role of cytokines in the pathogenesis of periodontal disease. *Curr Opin Perio*: p39-53.

Altman LC, Nelson CL, Povolny B, Fleckman P, Dale BA, Maier RV, Soderland C, Baker C (1988). Culture and characterisation of rat junctional epithelium. *J Periodontal Res* 23: p91-99.

Armitage GC (1999). Development of a classification system for periodontal diseases and conditions. *Ann Periodontol* 4(1): p1-6.

Asselineau D, Bernard BA, Bailly C, Darmon M, Prunieras M (1986). Human epidermis reconstructed by culture: is it normal? *J Invest Dermatol* 86: p181-86.

Bampton JL, Shirlaw PJ, Topley S, Weller P, Wilton M (1991). Human junctional epithelium: demonstration of a new marker, its growth *in vitro,* and characterisation by Lectin reactivity and keratin expression. *J Invest Dermatol* 96(5): p708-17.

Barrandon Y, Green H (1985). Cell size as a determinant of the clone-forming ability of human keratinocytes. *Proc Natl Acad Sci U S A* 82(16): p5390-4.

Barrandon Y, Green H (1987). Three clonal types of keratinocyte with different capacities for multiplication. *Proc Natl Acad Sci U S A* 84(8): p2302-6.

Basdra EK, Komposch G (1997). Osteoblast-like properties of human periodontal ligament cells: an *in vitro* analysis. *Eur J Orthod* 19: p615-21.

Becker W (1999). Periodontal regeneration: myth or reality? *Journal of Californian Dental Association* 27(2): p118-24.

Beertsen W, Everts V, Van den hooff A (1974). Fine structure of fibroblasts in the periodontal ligament of the rat incisor and their possible role in tooth eruption. *Arch Oral Biol* 19(12): p1087-98.

Beertsen W, Everts V (1990). Formation of acellular root cementum in relation to dental and non-dental hard tissues in the rat. *J Dent Res* 69(10): p1669-73.

Beertsen W, Van Den Bos T (1991). Alkaline phosphatase induces the deposition of calcified layers in relation to dentin: an *in vitro* study to mimic the formation of afibrillar acellular cementum. *J Dent Res* 70(3): p176-81.

Beertsen W, McCulloch CAG, Sodek J (1997). The periodontal ligament: a unique, multifunctional connective tissue. *Periodontology 2000* 13: p20-40.

Bell E, Ehrlich HP, Buttle DJ, Nakatsuji T (1981). Living tissue formed *in vitro* and accepted as skin-equivalent tissue of full thickness. *Science* 211: 4486): p1052-4.

Birchmeier C, Birchmeier W, Brand-Saberi B (1996). Epithelial-mesenchymal transitions in cancer progression. *Acta Anat (Basel)* 156(3): p217-26.

Birchmeier C, Gherardi E (1998). Developmental roles of HGF/SF and its receptor, the c-Met tyrosine kinase. Trends Cell Biol 8(10): p404-10.

Birkedal-Hansen H (1993). Role of cytokines and inflammatory mediators in tissue destruction. *J Periodontal Res* 28: p500-10.

Bosch FX, Ouhayoun JP, Bader BL (1989). Extensive changes in cytokeratin expression patterns in pathologically affected human gingiva. *Virchows Arch B Cell Pathol Incl Mol Pathol* 58: p59-77.

Bottaro DP, Rubin JS, Finch PW, Aaronson SA (1990). Characterisation of the receptor for keratinocyte growth factor. *J Biol Chem* 265(22): p12767-70.

Bottaro DP, Rubin JS, Faletto DL, Chan AM, Kmiecik TE, Vande Woude GF, Aaronson SA (1991). Identification of the hepatocyte growth factor receptor as the c-met proto-oncogene product. *Science* 251(4995): p802-4.

Boukamp P, Breitkreutz D, Stark HJ, Fusenig NE (1990). Mesenchyme mediated and endogenous regulation of growth and differentiation of human skin keratinocytes derived from different body sites. *Differentiation* 44(2): p150-61.

Boyko GA, Melcher AH, Brunette DM (1981). Formation of new periodontal ligament by periodontal ligament cells implanted *in vivo* after culture *in vitro*. A preliminary study of transplanted roots in the dog. *J Periodontal Res* 16(1): p73-88.

Braulche M, Angermeyer K, Hubner G, Werner S (1994). Large induction of keratinocyte growth factor expression by serum growth factors and pro-inflammatory cytokines in cultured fibroblasts. *Oncogene* 9: p3199-204.

Breathnach AS (1971). The Herman Beerman lecture: embryology of human skin, a review of ultrastructural studies. *J Invest Dermatol* 57(3): p133-43.

Breitkreutz D, Bohnert A, Herzmann E, Bowden PE, Boukamp P, Fusenig NE (1984). Differentiation specific functions in cultured and transplanted mouse keratinocytes: environmental influences on ultrastructure and keratin expression. Differentiation 26(2): p154-69.

Carmichael RP, McCulloch CAG, Zarb GA (1991). Quantitative immunohistochemical analysis of keratins and desmoplakins in human gingiva and peri-implant mucosa. *J Dent Res* 70(5): p899-905.

Chedid M, Rubin JS, Csaky KG, Aaronsen SA (1994). Regulation of keratinocyte growth factor gene expression by interleukin-1. *J Biol Chem* 269(14): p10753-57.

Cheon HG, LaRochelle WJ, Bottaro DP, Burgess WH, Aaronson SA (1994). High-affinity binding sites for related fibroblast growth factor ligands reside within different receptor immunoglobulin-like domains. *Proc Natl Acad Sci U S A* 91(3): p989-93.

Chinnathambi S, Tomanek-Chalkley A, Ludwig N, King E, DeWaard R, Johnson G, Wertz PW, Bickenbach JR (2003). Recapitulation of oral mucosal tissues in long-term organotypic culture. *Anat Rec* 270A(2): p162-74.

Chomczynski P, Sacchi N (1987). Single-step method of RNA isolation by acid guanidinium thiocyanate-phenol-chloroform extraction. *Ann Bio* 162(1): p156-59.

Chou HH, Takashiba S, Maeda H, Naruishi K, Nishimura F, Arai H, Lu H, Murayama Y (2000). Induction of intracellular interleukin-1 beta signals via type II interleukin-1 receptor in human gingival fibroblasts. *J Dent Res* 79(9): p1683-8.

Christensen M, Poulsen SR (1996). Immunolocalisation of transforming growth factor alpha in normal human tissues. *Histochem Cell Biol* 105: p391-400.

Clark RAF (1991). Cutaneous wound repair. In: *Physiology, Biochemistry, and Molecular Biology of the skin.* LA Goldsmith editor. Oxford: Oxford University Press, pp. 576-601.

Clausen H, Moe D, Buschard K, Dabelsteen E (1986). Keratin proteins in human oral mucosa. *J Oral Pathol* 15(1): p36-42.

Clauser C, Nieri M, Franceschi D, Pagliaro U, Pini-Prato G (2003). Evidence-based mucogingival therapy. Part 2: Ordinary and individual patient data meta-analyses of surgical treatment of recession using complete root coverage as the outcome variable. *J Periodontol* 74(5): p741-56.

Cobb CM (1996). Non-surgical pocket therapy: mechanical. *Ann Periodontol* 1(1): p443-90.

Cork MJ, Crane AM, Duff GW (1996). Genetic control of cytokines. Cytokine gene polymorphisms in alopecia areata. *Dermatol Clin* 14(4): p671-78.

Costea DE, Loro LL, Dimba AEO, Vintermyr OK, Johannessen AC (2003). Crucial effects of fibroblasts and keratinocyte growth factor on morphogenesis of reconstituted human oral epithelium. *J Invest Dermatol* 121(6): p1479-86.

Cotsarelis G, Kaur P, Dhouailly D, Hengge U, Bickenbach J (1999). Epithelial stem cells in the skin: definition, markers, localization, and functions. *Exp Dermatol* 8(1): p80-8.

Crawford JM, Hopp B (1990). Junctional epithelium expresses the intercellular adhesion molecule ICAM-1. *J Periodontal Res* 25: p254-56.

Crawford JM (1992). Distribution of ICAM-1, LFA-3, and HLA-DR in healthy and diseased gingival tissues. *J Periodontal Res* 27: p291-298.

Crowe DL, Hu L, Gudas LJ, Rheinwald JG (1991). Variable expression of retinoic acid receptor (RAR beta) mRNA in human oral and epidermal keratinocytes; relation to keratin 19 expression and keratinization potential. *Differentiation.* 48(3): p199-208.

Cubitt CL, Lausch RN, Oakes JE (1994). Differential regulation of granulocyte-macrophage colony-stimulating factor gene expression in human corneal cells by pro-inflammatory cytokines. *J Immunol* 153(1): p232-40.

Cunha GR, Bigsby RM, Cooke PS, Sugimura Y (1985). Stromal-epithelial interactions in adult organs. *Cell Death Differ* 17(3): p137-48.

Dabelsteen S, Wandall HH (1997). Keratinocyte growth factor mRNA expression in periodontal ligament fibroblasts. *Eur J Oral Sci* 105: p593-98.

Delcourt-Huard A, Corlu A (1997). Reconstituted human gingival epithelium: non-submerged *in vitro* model. *In vitro Cell Developmental Biology* 33: p30-36.

Derynck R (1988). Transforming growth factor alpha. *Cell* 54(5): p593-5.

Derynck R (1992). The physiology of transforming growth factor-alpha. *Acta Otolaryngol* 58: p27-52.

Dinarello CA (1989). Interleukin 1 and its biologically related cytokines. *Adv Immunol* 44: p153-205.

Dinarello CA. (2002). The IL-1 family and inflammatory diseases. *Clin Exp Rheumatol.* 20(5 Suppl 27): S1-13.

Eckert RL, Green H (1984). Cloning of cDNAs specifying vitamin A-responsive human keratins. *Proc Natl Acad Sci U S A* 81(14): p4321-25.

Eley BM, Cox SW (1998). Advances in periodontal diagnosis. 1. Traditional clinical methods of diagnosis. *Br Dent J* 184(1): p12-6.

Emoto H, Tagashira S, Mattei MG, Yamasaki M, Hashimoto G, Katsumata T, Negoro T, Nakatsuka M, Birnbaum D, Coulier F, Itoh N (1997). Structure and expression of human fibroblast growth factor-10. *J Biol Chem* 272(37): p23191-4.

Feghali-Assaly M, Sawaf MH (1994). Cytokeratin profile of the junctional epithelium in partially erupted teeth. *J Periodontal Res* 29: p185-95.

Feghali-Assaly M, Sawaf MH (1997). In-situ hybridisation study of cytokeratins 4, 13, 16, and 19 mRNA's in human developing junctional epithelium. *Eur J Oral Sci* 105: p599-608.

Finch PW, Rubin JS, Miki T, Ron D, Aaronson SA (1989). Human KGF is FGF-related with properties of a paracrine effector of epithelial cell growth. *Science* 245(4919): p752-5.

Finch PW, Lengel C, Chedid M (1995a). Cloning and characterization of the promoter region of the human keratinocyte growth factor gene. *J Biol Chem* 270(19): p11230-7.

Finch PW, Cunha GR, Rubin JS, Wong J, Ron D (1995b). Pattern of keratinocyte growth factor and keratinocyte growth factor receptor expression during mouse fetal development suggests a role in mediating morphogenetic mesenchymal-epithelial interactions. *Dev Dyn* 203(2): p223-40.

Fitzgerald SM, Chi DS, Hall HK, Reynolds SA, Aramide O, Lee SA, Krishnaswamy G (2003). GM-CSF induction in human lung fibroblasts by IL-1beta, TNF-alpha, and macrophage contact. *J Interferon Cytokine Res* 23(2): p57-65.

Formanek M, Knerer B, Kornfehl J (1999). Cytokine expression of human oral keratinocytes. *ORL J Otorhinolaryngol Relat Spec* 61(2): p103-7.

Fuchs EV, Coppock SM, Green H, Cleveland DW (1981). Two distinct classes of keratin genes and their evolutionary significance. *Cell* 27(1 part 2): p75-84.

Fusenig NE, Breitkreutz D, Boukamp P, Bohnert A, Mackenzie IC (1991). Epithelial-mesenchymal interactions in tissue homeostasis and malignant transformation. In: *Risk markers of oral disease.* NW Johnson editor. Cambridge: Cambridge University Press, pp. 218-56.

Fusenig NE (1994). Epithelial-mesenchymal interactions regulate keratinocyte growth and differentiation *in vitro*. In: *The Keratinocyte Handbook.* IM Leigh, EB Lane and FM Watt editors. Cambridge: Cambridge University Press, pp. 71-94.

Gao Z, Mackenzie IC, Williams DM, Cruchley AT, Leigh I, Lane EB (1988). Patterns of keratin-expression in rests of Malassez and periapical lesions. *J Oral Pathol* 17(4): p178-85.

Gao Z, Mackenzie IC, Cruchley AT, Williams DM, Leigh I, Lane EB (1989). Cytokeratin expression of the odontogenic epithelia in dental follicles and developmental cysts. *J Oral Pathol Med* 18(2): p63-7.

Gao Z, Mackenzie IC (1992). Patterns of phenotypic expression of human junctional, gingival and reduced enamel epithelia *in vivo* and *in vitro*. *Epithelial Cell Biol* 1(4): p156-67.

Gao Z, Mackenzie IC (1996). Influence of retinoic acid on the expression of cytokeratins, vimentin, and ICAM-1 in human gingival epithelia *in vitro*. *J Periodontal Res* 31(2): p81-9.

Garlick JA, Taichman LB (1994). Fate of human keratinocytes during re-epithelialization in an organotypic culture model. *Lab Invest* 70(6): p916-24.

Garlick JA, Parks WC, Welgus HG, Taichman LB (1996). Re-epithelialisation of human oral keratinocytes *in vitro*. *J Dent Res* 75(3): p912-18.

Gherardi E, Stoker M (1990). Hepatocytes and scatter factor. *Nature* 346(6281): p228.

Goldman HM, Cohen DW (1980). *Periodontal therapy*. St. Louis: C.V. Mosby.

Goldstein IJ, Hayes CE (1978). The lectins: carbohydrate-binding proteins of plants and animals. In: *Advances in Carbohydrate Chem Biochem*, pp. 127-340.

Goodson JM, Tanner AC, Haffajee AD, Sornberger GC, Socransky SS (1982). Patterns of progression and regression of advanced destructive periodontal disease. *J Clin Periodontol* 9(6): p472-81.

Goseki T, Shimizu N, Iwasawa T, Takiguchi H, Abiko Y (1996). Effects of *in vitro* cellular aging on alkaline phosphatase, cathepsin activities and collagen secretion of human periodontal ligament derived cells. *Mech Ageing Dev* 91(3): p171-83.

Goseki M, Oida S, Takeda K, Ogata Y, Iimura T, Maruoka Y, Sasaki S (1995). Identification of bone-type alkaline phosphatase mRNA from human periodontal ligament cells. *J Dent Res* 74(1): p319-22.

Gosselin F, Gervaise M, Neveux Y, Portier MM (1989). Reconstitution *in vitro* of human gingiva. *C R Acad Sci III* 309(9): p323-29.

Gosselin F, Magloire H (1990). Cytokeratins as molecular markers in the evaluation of the precise differentiation stage of human gingival epithelium reconstituted *in vitro*. *Arch Oral Biol* 35: p217s-21s.

Gould TR, Brunette DM, Dorey J (1983). Cell turnover in the periodontium in health and periodontal disease. *J Periodontal Res* 18(4): p353-61.

Grant DA, Stern IB, Everett FG (1979). *Periodontics*. St. Louis: C.V. Mosby.

Groeneveld MC, Everts V, Beertsen W (1993). A quantitative enzyme histochemical analysis of the distribution of alkaline phosphatase activity in the periodontal ligament of the rat incisor. *J Dent Res* 72(9): p1344-50.

Groeneveld MC, Van Den Bos T, Everts V, Beertsen W (1996). Cell-bound and extracellular matrix associated alkaline phosphatase activity in rat periodontal ligament. *J Periodontal Res* 31: p73-79.

Gron B, Andersson A (1999). Blood-group-related carbohydrates are expressed in organotypic cultures of human skin and oral mucosa. *APMIS* 107: p779-90.

Gron B, Stoltze K, Andersson A, Dabelsteen E (2001). Oral fibroblasts produce more HGF and KGF than skin fibroblasts in response to co-culture with keratinocytes. *APMIS* 110(12): p892-98.

Guo L, Yu Q, Fuchs E (1993). Targeting expression of keratinocyte growth factor to keratinocytes elicits striking changes in epithelial differentiation in transgenic mice. *EMBO* 12(3): p973-86.

Haffajee AD, Socransky SS, Goodson JM (1983). Clinical parameters as predictors of destructive periodontal disease activity. *J Clin Periodontol* 10(3): p257-65.

Haffajee AD, Socransky SS (1994). Microbial aetiological agents of destructive periodontal disease. *Periodontology 2000* 5: p78-111.

Hanada T, Yoshimura A (2002). Regulation of cytokine signaling and inflammation. *Cytokine Growth Factor Rev* 13(4-5): p413-21.

Hancock G, Kaplan G, Cohn Z (1988). Keratinocyte growth regulation by the products of the immune cells. *J Exp Med* 168: p1395-1402.

Harris H (1990). The human alkaline phosphatases: what we know and what we do not know. *Clin Chim Acta* 186(2): p133-50.

Hassell TM, Stanek III EJ (1983). Evidence that healthy human gingiva contains functionally heterogeneous fibroblast subpopulations. *Arch Oral Biol* 28(7): p617-25.

Heiji L, Wennstrom J, Lindhe J, Socransky SS (1980). Periodontal disease in gnotobiotic rats. *J Periodontal Res* 15(4): p405-19.

Higuchi R, Dollinger G, Walsh PS, Griffith R (1992). Simultaneous amplification and detection of specific DNA sequences. *Biotechnol* 10: p413-17.

Hill MW, Mackenzie IC (1984). The influence of differing connective tissue substrates on the maintenance of adult stratified squamous epithelia. *Cell Tissue Research* 237: p473-78.

Hillman G, Hillman B, Geurtsen W (1995). Immunological determination of IL-1 beta in inflamed human gingival epithelium. *Arch Oral Biol* 40(4): p353-59.

Hormia M, Ylanne J, Virtanen I (1990). Expression of integrins in human gingiva. *J Dent Res* 69(12): p1817-23.

Hormia S, Owaribe K (2001). The dento-epithelial junction: cell adhesion by type-I hemidesmosomes in the absence of a true basal lamina. *J Periodontol* 72: p788-97.

Howells GL (1995). Cytokine networks in destructive periodontal disease. *Oral Diseases* 1: p266-70.

Igarashi M, Irwin CR, Locke M, Mackenzie IC (2003). Construction of large area organotypical cultures of oral mucosa and skin. *J Oral Pathol Med* 32(7): p422-30.

Irwin CR, Picardo M, Ellis I, Sloan P, Grey A, McGurk M, Schor SL (1994). Inter- and intra-site heterogeneity in the expression of fetal-like phenotypic characteristics by gingival fibroblasts: potential significance for wound healing. *J Cell Sci* 107(Pt 5): p1333-46.

Jimenez PA, Rampy MA (1999). Keratinocyte growth factor-2 accelerates wound healing in incisional wounds. *J Surg Res* 81(2): p238-42.

Johnson GD, Nogueira Araujo GM (1981). A simple method for reducing the fading of immunofluorescence during microscopy. *J.Immunol Methods* 43(3): p349-50.

Johnson NW, Hopps RM (1974). Epithelial cell proliferation in gingiva of macaque monkeys studied by local injections of (3H)thymidine. *Arch Oral Biol* 19(3): p265-8.

Ju WD (1991). Tumorigenic transformation of NIH 3T3 cells by the autocrine synthesis of transforming growth factor alpha. *The New Biologist* 3: p380-88.

Kautsky MB, Fleckman P, Dale BA (1995). Retinoic acid regulates oral epithelial differentiation by two mechanisms. *J Invest Dermatol* 104(2): p224-29.

Kawaguchi Y, Hara M, Wright TM (1999). Endogenous IL-1alpha from systemic sclerosis fibroblasts induces IL-6 and PDGF-A. *J Clin Invest* 103(9): p1253-60.

Kawase T, Sato S, Miake K, Saito S (1988). Alkaline phosphatase of human periodontal ligament fibroblast-like cells. *Adv Dent Res* 2(2): p234-39.

Kinane DF (2000). Aetiology and pathogenesis of periodontal disease. *Ann R Australas Coll Dent Surg* 15: p42-50.

Kivela-Rajamaki MJ, Teronen OP, Maisi P, Husa V, Tervahartiala TI, Pirila EM, Salo TA, Mellanen L, Sorsa TA (2003). Laminin-5 gamma2-chain and collagenase-2 (MMP-8) in human peri-implant sulcular fluid. *Clin Oral Implants Res* 14(2): p158-65.

Kollar H, Baird GR (1970). Tissue interactions in embryonic mouse tooth germs. I. Reorganization of the dental epithelium during tooth-germ reconstruction. *J Embryol Exp Morphol* 24(1): p159-71.

Kornman KS, Crane A, Wang HY, di Giovine FS, Newman MG, Pirk FW, Wilson TG, Jr., Higginbottom FL, Duff GW (1997). The interleukin-1 genotype as a severity factor in adult periodontal disease. *J Clin Periodontol* 24(1): p72-7.

Kreuger JG, Krane JF, Carter DM, Gottlieb AB (1990). Role of growth factors, cytokines, and their receptors in the pathogenesis of psoriasis. *J Invest Dermatol* 94: p135s-140s.

Kristoffersen EK, Caffesse RG, Nasjleti CE, Kristoffersen TO (1983). Ultrastructural study of induced keratinisation in sulcular gingival epithelium in rhesus monkeys. *Acta Odontol Scand* 41(4): p227-40.

Laiho M, Keski-Oja J (1989). Growth factors in the regulation of pericellular proteolysis: a review. *Cancer Res* 49(10): p2533-53.

Lakowicz JR, Maliwal BP (1983). Oxygen quenching and fluorescence depolarisation of tyrosine residues in proteins. *J Biochem* 258(8): p4794-801.

Lekic P, Rojas J, Birek C, Tenenbaum H, McCulloch CAG (2001). Phenotypic comparison of periodontal ligament cells *in vivo* and *in vitro*. *J Periodontal Res* 36: p71-79.

Lenoir MC, Bernard BA (1990). Architecture of reconstructed epidermis on collagen lattices varies according to the method used: a comparative study. *Skin Pharmacol Appl Skin Physiol* 3(2): p97-106.

Li T, Browne RM, Matthews JB (1997). Immunocytochemical expression of growth factors by odontogenic jaw cysts. *Mol Pathol* 50: 1): p21-7.

Lindberg K, Rheinwald JG (1990). Three distinct keratinocyte subtypes identified in human oral epithelium by their patterns of keratin expression in culture and in xenographs. *Differentiation* 45: p230-41.

Listgarten MA, Schifter CC, Laster L (1985). 3-year longitudinal study of the periodontal status of an adult population with gingivitis. *J Clin Periodontol* 12(3): p225-38.

Listgarten MA (1986). Pathogenesis of periodontitis. *J Clin Periodontology* 13: p418-25.

Listgarten MA (1987). Nature of periodontal diseases: pathogenic mechanisms. *J Periodontal Res* 22(3): p172-8.

Listgarten MA, Lang NP, Schroeder HE, Schroeder A (1991). Periodontal tissues and their counterparts around endosseous implants [corrected and republished with original paging, article originally printed in *Clin Oral Implants Res* 1991 Jan-Mar; 2(1): p1-19. *Clin Oral Implants Res* 2(3): p1-19.

Locci P, Lilli C, Marinucci L, Baroni T, Pezzetti F, Becchetti E (1993). Embryonic skin fibroblasts release TGF alpha and TGF beta able to influence synthesis and secretion of GAG. *Cell Mol Biol (Noisy-le-grand)* 39(4): p415-26.

Loe H, Theilade E, Jensen SB (1965). Experimental gingivitis in man. *J Periodontol* 36: p177-87.

Loe H, Karring T (1969). Mitotic activity and renewal time of the gingival epithelium of young and old rats. *J Periodontal Res* 4: p18-9.

Loe H, Morrison E (1986). Periodontal health and disease in young people: screening for priority care. *Int Dent J* 36(3): p162-67.

Lossdorfer S, Gotz W, Jager A (2002). Localization of IL-1alpha, IL-1 RI, TNF, TNF-RI and TNF-RII during physiological drift of rat molar teeth--an immunohistochemical and *in-situ* hybridisation study. *Cytokine* 20(1): p7-16.

Lovegrove JM (2004). Dental plaque revisited: bacteria associated with periodontal disease. *J N Z Soc Periodontol* 87: p7-21.

Luger TA, Schwarz T (1994). *Epidermal Growth Factors and Cytokines*. New York: Marcel Dekker Inc.

Maas-Szabowski N, Shimotoyodome A (1999). Keratinocyte growth regulation in fibroblast co-cultures via a double paracrine mechanism. *J Cell Sci* 112: p1843-53.

Maas-Szabowski N, Stark HJ, Fusenig NE (2000). Keratinocyte growth regulation in defined organotypic cultures through IL-1 induced keratinocyte growth factor expression in resting fibroblasts. *J Invest Dermatol* 114: 6): p1075-84.

Maas-Szabowski N, Szabowski A, Stark HJ, Andrecht S, Kolbus A, Schorpp-Kistner M, Angel P, Fusenig NE (2001). Organotypic co-cultures with genetically modified mouse fibroblasts as a tool to dissect molecular mechanisms regulating keratinocyte growth and differentiation. *J Invest Dermatol* 116(5): p816-20.

Mackenzie IC, Hill MW (1981). Maintenance of regionally specific patterns of cell proliferation and differentiation in transplanted skin and oral mucosa. *Cell Tissue Res* 219(3): p597-607.

Mackenzie IC, Fusenig NE (1983). Regeneration of organised epithelial structure. *J Invest Dermatol* 81: p189s-94s.

Mackenzie IC (1984). The role of epithelial-mesenchymal interactions in epithelial migration and differentiation. *J Periodontal Res* 19: p656-60.

Mackenzie IC, Hill MW (1984). Connective tissue influences on patterns of epithelial architecture and keratinisation in skin and oral mucosa of the adult mouse. *Cell Tissue Res* 235(3): p551-9.

Mackenzie IC (1987). Nature and mechanisms of regeneration of the junctional epithelial phenotype. *J Periodontal Res* 22(3): p243-5.

Mackenzie IC, Dabelsteen E, Mandel U (1989). Expression of blood group antigen-related carbohydrates by human gingival epithelia. *J Periodontal Res* 24(5): p289-97.

Mackenzie IC, Rittman G, Gao Z, Leigh I, Lane EB (1991). Patterns of cytokeratin expression in human gingival epithelia. *J Periodontal Res* 26(6): p468-78.

Mackenzie I, Rittman G, Bohnert A, Breitkreutz D, Fusenig NE (1993). Influence of connective tissues on the *in vitro* growth and differentiation of murine epidermis. *Epithelial Cell Biol* 2(3): p107-19.

Mackenzie IC, Gao Z (1993). Patterns of cytokeratin expression in the epithelia of inflamed human gingiva and periodontal pockets. *J Periodontal Res* 28(1): p49-59.

Mackenzie IC, Tonetti MS (1995). Formation of normal gingival epithelial phenotypes around osseo-integrated oral implants in humans. *J Periodontol* 66(11): p933-43.

Mackenzie IC, Gao Z (2001). Keratinocyte growth factor expression in human gingival fibroblasts and stimulation of *in vitro* gene expression by retinoic acid. *J Periodontol* 72(4): p445-53.

Mann A, Breuhahn K, Schirmacher P, Blessing M (2001). Keratinocyte-derived granulocyte-macrophage colony stimulating factor accelerates wound healing: Stimulation of keratinocyte proliferation, granulation tissue formation, and vascularization. *J Invest Dermatol* 117(6): p1382-90.

Mariotti A, Cochran DL (1990). Characterisation of fibroblasts derived from human periodontal ligament and gingiva. *J Periodontol* 61(2): p103-11.

Mason IJ (1994). The ins and outs of fibroblast growth factors. *Cell* 78(4): p457-52.

Massague J (1990). The transforming growth factor-β family. *Annu Rev Cell Biol* 6: p597-641.

Matsuyama T, Izumi Y (1997). Culture and characterisation of human junctional epithelial cells. *J Periodontol* 68(3): p229-39.

McCulloch CAG, Bordin S (1991). Role of fibroblast subpopulations in periodontal physiology and pathology. *J Periodontal Res* 26: p144-54.

McFarlane CG, Reynolds JJ, Meikle MC (1990). The release of interleukin-1 beta, tumour necrosis factor-alpha and interferon-gamma by cultured peripheral blood mononuclear cells from patients with periodontitis. *J Periodontal Res* 25: p156-163.

McKeown ST, Hyland PL, Locke M, Mackenzie IC, Irwin CR (2003). Keratinocyte growth factor and scatter factor expression by regionally defined oral fibroblasts. *Eur J Oral Sci* 111(1): p42-50.

Meager A (1990). *Cytokines*. New Jersey: Prentice Hall Reference Series.

Metcalf D (1992). The granulocyte macrophage-colony stimulating factors. *Science* 229: p16-22.

Miki T, Bottaro DP, Flemming TP, Smith CL, H BW, Aaronson SA (1992). Determination of ligand binding specificity by alternative splicing: two distinct growth factor receptors encoded by a single gene. *Proc Natl Acad Sci U S A* 89: p246-50.

Miyauchi M, Sato S, Kitagawa S, Hiraoka M, Kudo Y, Ogawa I, Zhao M, Takata T (2001). Cytokine expression in rat molar gingival periodontal tissues after topical application of lipopolysaccharide. *Histochem Cell Biol* 116(1): p57-62.

Mlinek A, Buchner A (1975). *In vitro* cultivation of adult human gingiva I. primary epithelial outgrowth from gingival explants. *J Periodontal Res* 10(2): p73-78.

Mogi M, Otogoto J, Ota N, Inagaki H, Minami M, Kojima K (1999). Interleukin 1 beta, interleukin 6, beta 2-microglobulin, and transforming growth factor-alpha in gingival crevicular fluid from human periodontal disease. *Arch Oral Biol* 44(6): p535-39.

Moll R, Franke WW (1982). The catalogue of human cytokeratins pattern of expression in normal epithelia in tumour and cultured cells. *Cell* 31: p11-24.

Momose M, Murata M, Kato Y, Okuda K, Yamazaki K, Shinohara C (2002). Vascular endothelial growth factor and transforming growth factor alpha and beta-1 are released from human cultured gingival epithelial cells. *J Periodontol* 73(7): p748-53.

Montagnani S, Postiglione L, Giordano-Lanza G, Meglio FD, Castaldo C, Sciorio S, Montuori N, Spigna GD, Ladogana P, Oriente A, Rossi G (2001). Granulocyte macrophage colony stimulating factor (GM-CSF) biological actions on human dermal fibroblasts. *Eur J Histochem* 45(3): p219-28.

Morgan PR, Johnson NW, Leigh IM, Lane EB (1986). Structure of gingival epithelium is revealed by monoclonal antibodies to keratins. In: *Borderlands between caries and periodontal disease III.* T Lehner and G Cimasoni editors. Geneva: Geneva medecine et hygiene.

Morgan PR, Leigh IM, Purkis PE, Gardner ID, GNP van Muijen, Lane EB (1987). Site variation in keratin expression in human oral epithelia: an immunocytochemical study of individual keratins. *Epithelia* 1: p31-43.

Moughal NA, Adonogianaki E, Thornhill MH, Kinane DF (1992). Endothelial cell leukocyte adhesion molecule-1 and intercellular adhesion molecule-1 (ICAM-1) expression in gingival tissue during health and experimentally induced gingivitis. *J Periodontal Res* 27: p623-30.

Nair BC, Mayberry WR, Dziak R, Chen PB, Levine MJ, Hausmann E (1983). Biological effects of a purified lipopolysaccharide from Bacteroides gingivalis. *J Periodontal Res* 18(1): p40-49.

Nishikawa K, Sasaki T, Tanaka M, Uchida H, Endo Y, Fukuma H, Chuman H, Beppu Y, Matsumoto K, Nitta K (1987). Experimental model for predicting metastatic ability of tumors using chick embryo. *Jpn J Clin Oncol* 17(4): p319-25.

Nixon CS, Steffen MJ, Ebersole JL (2000). Cytokine responses to treponema pectinovorum and treponema denticola in human gingival fibroblasts. *Infect Immun* 68(9): p5284-92.

Nojima N, Kobayashi M, Shionome M, Takahashi N, Suda T, Hasegawa K (1990). Fibroblastic cells derived from bovine periodontal ligaments have the phenotypes of osteoblasts. *J Periodontal Res* 25: p179-85.

Nyman S, Gottlow J, Karring T, Lindhe J (1982). The regenerative potential of the periodontal ligament. An experimental study in the monkey. *J Clin Periodontol* 9(3): p257-65.

Odioso LL, Doyle MJ (1995). Development and characterisation of an *in vitro* gingival epithelial model. *J Periodontal Res* 30: p210-19.

Ogata Y, Niisato N, Sakurai T, Furuyama S, Sugiya H (1995). Comparison of the characteristics of human gingival fibroblasts and periodontal ligament cells. *J Periodontol* 66(12): p1025-31.

Ohshima M, Sakai A, Sawamoto Y, Seki K, Ito K, Otsuka K (2002a). Hepatocyte growth factor system in gingiva: HGF activator expression by gingival epithelial cells. *J Oral Sci* 44(3-4): p129-34.

Ohshima M, Sakai I, Ito K, Otsuka K (2002b). Hepatocyte growth factor in periodontal disease: detection of HGF in gingival crevicular fluid. *J Periodontal Res* 37: p8-14.

Oksanen J, Hormia M (2002). An organotypic *in vitro* model that mimics the dento-epithelial junction. *J Periodontol* 73(1): p86-93.

Otsuka K, Pitaru S, Overall CM, Aubin JE, Sodek J (1988). Biochemical comparison of fibroblast populations from different periodontal tissues: characterization of matrix protein and collagenolytic enzyme synthesis. *Biochem Cell Biol* 66(3): p167-76.

Ouhayoun JP, Gosselin F (1985). Cytokeratin patterns of human oral epithelia: differences in cytokeratin synthesis in gingival epithelium and the adjacent alveolar mucosa. *Differentiation* 30(2): p123-29.

Overman DO, Salonen JL (1994). Characterisation of the human junctional epithelial cells directly attached to the tooth in periodontal disease. *J Dent Res* 73: p1818-1823.

Page RC, Schroeder HE (1976). Pathogenesis of inflammatory periodontal disease. A summary of current work. *Lab Invest* 34(3): p235-49.

Page RC (2002). The etiology and pathogenesis of periodontitis. *Compend Contin Educ Dent* 23(5 Suppl): p11-4.

Pan YM, Firth JD (1995). Multilayered culture of periodontal ligament epithelial cells a model for junctional epithelium. *J Periodontal Res* 30: p97-107.

Papaioannou W, Cassiman JJ (1999). Multi-layered periodontal pocket epithelium reconstituted *in vitro*: histology and cytokeratin profiles. *J Periodontol* 70(6): p668-77.

Parenteau NL, Bilbo P, Nolte CJ, Mason VS, Rosenberg M (1992). The organotypic culture of human skin keratinocytes and fibroblasts to achieve form and function. *Cytotechnology* 9(1-3): p163-71.

Piche JE, Carnes DL, Graves DT (1989). Initial characterization of cells derived from human periodontia. *J Dent Res* 68(5): p761-67.

Rheinwald JG, Green H (1975). Serial cultivation of strains of human epidermal keratinocytes: the formation of keratinising colonies from single cells. *Cell* 6(3): p331-43.

Rittman BR, Mackenzie IC, Rittman GA (1982). Lectin binding to murine oral mucosa and skin. *Arch Oral Biol* 27(12): p1013-9.

Rotaru H, Choi JY, Hong SP, Lee YC, Yun KI, Kim SG (2003). Transforming growth factor-alpha and oral fibroma: Immunohistochemical and *in-situ* hybridisation study. *J Oral Maxillofac Surg* 61(12): p1449-54.

Rowling PJ, Raxworthy MJ, Wood EJ, Kearney JN, Cunliffe WJ (1990). Fabrication and reorganization of dermal equivalents suitable for skin grafting after major cutaneous injury. *Biomaterials* 11(3): p181-5.

Rubin JS, Osada H, Finch PW, Taylor WG, Rudikoff S, Aaronson SA (1989). Purification and characterization of a newly identified growth factor specific for epithelial cells. *Proc Natl Acad Sci USA* 86(3): p802-06.

Rubin JS, Bottaro DP, Chedid M, Miki T, Ron D, Cunha GR, Finch PW (1995). Keratinocyte growth factor as a cytokine that mediates mesenchymal-epithelial interaction. *Exs* 74: p191-214.

Sabag N, Mery C, Garcia M, Vasquez V, Cueto V (1984). Epithelial reattachment after gingivectomy in the rat. *J Periodontol* 55(3): p135-41.

Salonen J, Santti R (1983). An attempt to simulate junctional epithelium of human gingiva *in vitro*. *J Periodontal Res* 18(3): p311-7.

Salonen JI, Santti R (1985). Ultrastructural and immunohistochemical similarities in the attachment of human oral epithelium to the tooth *in vivo* and to an inert substrate in an explant culture. *J Periodontal Res* 20: p176-84.

Salonen JI, Kautsky MB, Dale BA (1989). Changes in cell phenotype during regeneration of junctional epithelium of human gingiva *in vitro*. *J Periodontal Res* 24(6): p370-7.

Salonen J, Oda D, Funk SE, Sage H (1991a). Synthesis of type VIII collagen by epithelial cells of human gingiva. *J Periodontal Res* 26(4): p355-60.

Salonen J, Uitto VJ, Pan YM, Oda D (1991b). Proliferating oral epithelial cells in culture are capable of both extracellular and intracellular degradation of interstitial collagen. *Matrix* 11(1): p43-55.

Salonen J (1994). Proliferative potential of the attached cells of human junctional epithelium. *J Periodontal Res* 29(1): p41-5.

Sanale A, Firth JD, Uitto V, Putnins EE (2002). Keratinocyte growth factor (KGF)-1 and -2 protein and gene expression in human gingival fibroblasts. *J Periodontol* 37(1): p66-74.

Sawa Y, Phillips A, Hollard J, Yoshida S, Braithwaite MW (2000). The *in vitro* life-span of human periodontal ligament fibroblasts. *Tissue Cell* 32(2): p163-70.

Sawa Y, Yamaoka Y, Kuroshima SI, Yoshida S (2003). Reduction of alkaline phosphatase activity in aged human osteogenic periodontal ligament fibroblasts exhibiting short telomeres. *Cell Tissue Res* Epub ahead of print.

Saxen L (1977). Directive versus permissive induction. In: *Cell and tissue interactions*. JW Lash and MM Burger editors. New York: Raven Press.

Schaumburg-Lever G (1990). Ultrastructural localisation of lectin-binding sites in normal skin. *J Invest Dermatol* 94(4): p465-70.

Schor SL, Schor AM (1987). Clonal heterogeneity in fibroblast phenotype: Implications for the control of epithelial-mesenchymal interactions. *Bioessays* 7(5): p200-04.

Schor SL (1995). Fibroblast subpopulations as accelerators of tumor progression: the role of migration stimulating factor. *Exs* 74: p273-96.

Schroeder HE, Listgarten MA (1971/77). Fine structure of the developing epithelial attachment of human teeth. *Monogr Dev Biol.* 2nd revised ed. S.Karger, Basal, pp1-164.

Schroder JM (1995). Cytokine networks in the skin. *J Invest Dermatol* 105(1 Suppl): 20S-24S.

Schweizer J, Winter H, Hill MW, Mackenzie IC (1984). The keratin polypeptide patterns in heterotypically recombined epithelia of skin and mucosa of adult mouse. *Differentiation* 26(2): p144-53.

Seifter S, Harper E (1970). Collagenases. *Methods Enzymol* 16: p613-35.

Shabana AHM, Ouhayoun JP, Sawaf MH, Forest N (1991). Cytokeratin patterns of human oral mucosae in histotypic culture. *Arch Oral Biol* 36(10): p747-58.

Shiba H, Nakanishi K, Sakata M, Fujita T, Uchida Y, Kurihara H (2000). Effects of ageing on proliferative ability, and the expressions of secreted protein, acidic and rich in cysteine (SPARC) and osteoprotegerin (osteoclastogenesis inhibitory factor) in cultures of human periodontal ligament cells. *Mech Ageing Dev* 117(1-3): p69-77.

Shimada T, Hasegawa H, Yamazaki Y, Muto T, Hino R, Takeuchi Y, Fujita T, Nakahara K, Fukumoto S, Yamashita T (2004). FGF-23 is a potent regulator of vitamin D metabolism and phosphate homeostasis. *J Bone Miner Res* 19(3): p429-35.

Shirodaria S, Smith J, McKay IJ, Kennett CN, Hughes FJ (2000). Polymorphisms in the IL-1A gene are correlated with levels of interleukin-1alpha protein in gingival crevicular fluid of teeth with severe periodontal disease. *J Dent Res* 79(11): p1864-9.

Smith RS, Smith TJ, Blieden TM, Phipps RP (1997). Fibroblasts as sentinel cells. Synthesis of chemokines and regulation of inflammation. *Am J Pathol* 151(2): p317-22.

Smith PC, Munoz VC, Collados L, Oyarzun AD (2004). *In-situ* detection of matrix metalloproteinase-9 (MMP-9) in gingival epithelium in human periodontal disease. *J Periodontal Res.* 39(2): p87-92.

Smola H, Thiekotter G, Fusenig NE (1993). Mutual induction of growth factor gene expression by epidermal-dermal cell interaction. *J Cell Biol* 122: p417-29.

Smola H, Stark HJ, Thiekotter G, Mirancea N, Kreig T, Fusenig NE (1998). Dynamics of basement membrane formation by keratinocyte-fibroblast interactions in organotypic skin culture. *Experimental Cell Research* 239: p399-410.

Socransky SS, Haffajee AD, Goodson JM, Lindhe J (1984). New concepts of destructive periodontal disease. *J Clin Periodontol* 11: p21-32.

Somerman MJ, Archer SY, Imm GR, Foster RA (1988). A comparative study of human periodontal ligament cells and gingival fibroblasts *in vitro*. *J Dent Res* 67(1): p66-70.

Sonnenberg E, Meyer D, Weidner KM, Birchmeier C (1993). Scatter factor/hepatocyte growth factor and its receptor, the c-met tyrosine kinase, can mediate a signal exchange between mesenchyme and epithelia during mouse development. *J Cell Biol* 123(1): p223-35.

Stark HJ, Baur M (1999). Organotypic keratinocyte co-cultures in defined medium with regular epidermal morphogenesis and differentiation. *J Invest Dermatol* 112(5): p685-91.

Steffensen B, Lopatin DE, Hanks CT (1987). Blood group substances as differentiation markers in human dento-gingival epithelium. *J Periodontal Res* 22: p451-55.

Stephens P, Thomas DW (2002). The cellular proliferative phase of the wound repair process. *J Wound Care* 11(7): p253-61.

Suchett-Kaye G, Morrier JJ, Barsotti O (1998). Interactions between non-immune host cells and the immune system during periodontal disease: role of the gingival keratinocyte. *Crit Rev Oral Biol Med* 9(3): p292-305.

Sugiyama A, Uehara A, Iki K, Matsushita K, Nakamura T, Ogawa T, Sugawara S, Takada H (2002). Activation of human gingival epithelial cells by cell-surface components of black pigmented bacteria to augment production of interlukin-8, granulocyte colony stimulating factor and granulocyte macrophage colony stimulating factor and expression of intercellular adhesion molecule ICAM-1. *J Med Microbiol* 51(1): p27-33.

Sun TT, Tseng SC, Huang AJ, Cooper D, A S (1985). Monoclonal antibody studies of mammalian epithelial keratins: a review. *Ann N Y Acad Sci* 455: p307-29.

Ten Cate AR (1994). *Oral Histology, Development, structure, and function.* 4th ed. St Louis: CV Mosby, pp. 276-312.

Thomas DW, Harding KG (2002). Wound healing. *Br J Surg.* 89(10): p1203-5.

Tomakidi P, Fusenig NE, Kohl A, Komposch G (1997). Histomorphological and biochemical differentiation capacity in organotypic co-cultures of primary gingival cells. *J Periodontal Res* 32(4): p388-400.

Tomakidi P, Breitkreutz D, Kohl A, Komposch G (1999). Normalization of keratinocyte-type integrins during the establishment of the oral mucosa phenotype *in vitro*. *Anat Anz* 181(1): p127-32.

Travis J, Banbula A, Potempa J (2000). The role of bacterial and host proteinases in periodontal disease. *Adv Exp Med Biol* 477: p455-65.

Tyler LW, Matossian K, Todd R, Gallagher GT, White RR, Wong DT (1999). Eosinophil-derived transforming growth factors (TGF-alpha and TGF-beta 1) in human periradicular lesions. *J Endod* 25(9): p619-24.

Uitto VJ, Haapasalo M, Laakso T, Salo T (1988). Degradation of basement membrane collagen by proteases from some anaerobic oral microorganisms. *Oral Microbiological Immunology* 3(3): p97-102.

Uitto VJ, Suomalainen K, Sorsa T (1990). Salivary collagenase. Origin, characteristics, and relationship to health. *J Periodontal Res* 25(3): p135-42.

Uitto VJ, Salonen JI, Firth JD, Jousimies-Somer H, Saarialho-Kere U (2002). Matrilysin (Matrix Metalloproteinase-7) expression in human junctional epithelium. *J Dent Res* 81(4): p241-46.

Waseem A, Dogan B, Tidman N, Alam Y, Purkis P, Jackson S, Lalli A, Machesney M, Leigh IM (1998). Keratin 15 expression in stratified epithelia: downregulation in activated keratinocytes. *J Invest Dermatol* 112(3): p362-9.

Wasi S, Otsuka K, Yao KL, Tung PS, Aubin JE, Sodek J, Termine JD (1984). An osteonectin-like protein in porcine periodontal ligament and its synthesis by periodontal ligament fibroblasts. *Can j Biochen Cell Biol* 62(6): p470-78.

Weidner KM, Arakaki N, Hartmann G, Vandekerckhove J, Weingart S, Rieder H, Fonatsch C, Tsubouchi H, Hishida T, *et al.* (1991). Evidence for the identity of human scatter factor and human hepatocyte growth factor. *Proc Natl Acad Sci U S A* 88(16): p7001-5.

Werner S, Duan DR, Peters KG, Johnson DE, Williams LT (1992). Differential splicing in the extracellular region of fibroblast growth factor receptor-1 generates receptor variants with different ligand binding specificities. *Mol Cell Biol* 12(1): p82-88.

Werner S (1998). Keratinocyte growth factor: a unique player in epithelial repair processes. *Cytokine Growth Factor Rev* 9(2): p153-65.

Werner S, Grose R (2003). Regulation of wound healing by growth factors and cytokines. *Physiol Rev* 83(3): p835-70.

Winter GD (1972). Epidermal regeneration studied in the domestic pig. In: Epidermal wound healing. HI Maibach and DT Rovee editors. Chicago: Yearbook publishers.

Wu JY, Parker LM, Binder NE, Beckett MA, Sinard JH, Griffiths CT, Rheinwald JG (1982). The mesothelial keratins: A new family of cytoskeletal proteins identified in cultured mesothelial cells and nonkeratinizing epithelia. *Cell* 31(Part 2): p693-703.

Xu JW, Ma J, Li TF, Waris E, Alberty A, Santavirta S, Konttinen YT (2000). Expression of epidermal growth factor and transforming growth factor alpha in interfacial membranes retrieved at revision total hip arthroplasty. *Ann Rheum Dis* 59(10): p822-7.

Yamaji Y, Kubota T, Sasaguri K, Sato S, Suzuki Y, Kumada H, Umemoto T (1995). Inflammatory cytokine gene expression in human periodontal ligament fibroblasts stimulated with bacterial lipopolysaccharides. *Infect Immun* 63(9): p3576-81.

Zambon JJ, Grossi S, Dunford R (1994). Epidemiology of subgingival bacterial pathogens in periodontal disease. In: Molecular pathogenesis of periodontal disease. R Genco and S Hamada editors.

APPENDICES

APPENDIX I
CONSENT FORM

Consent Form

Research Project to Study Dental Tissues

I am to have a tooth removed from my mouth as part of my dental treatment and I have been asked whether I will allow this tooth and a small piece of the adjacent gum to be used in a research study.

I have been given the sheet headed **"Information about a research project to study dental tissues"** and this explains what the research is about. Any questions I have about this project have been discussed to my satisfaction with my surgeon. I understand that if I participate in this study all information about me will be kept confidential and that my name will not be known to the people doing the research. I also understand that I am entirely free to choose whether or not I give permission to use my tissue and that my choice will not in any way affect my treatment.

I give permission for my tissue to be used in this research study.

Name of patient: .....

Signature of patient: .....

Name of Surgeon: .....

Signature of Surgeon: .....

Name of witness: .....

Signature of witness: .....

Information about a research project to study dental tissues

What is the research project? The gums are attached to the teeth by a small piece of special tissue called "junctional epithelium". In some people, this tissue becomes inflamed and grows down the root of the tooth. This type of gum disease is a common cause of tooth loss and we are trying to find out how inflammation causes the junctional epithelium to grow and the teeth to become loose.

We have developed new ways of growing the cells from the gums to study them in the laboratory. To do this we take the cells from a small piece of gum and put them in a special solution that allows them to continue to grow in a plastic dish. We can then see how certain chemicals and other cells control the way they grow. To do these studies we need samples of healthy cells from the gum next to a tooth.

What are you asking me to do? As part of your dental treatment you are going to have a tooth removed. We would like your permission to remove a small piece of gum next to the tooth when it is taken out. If you say yes, the tooth will be made numb in the usual way and will then be removed together with a small piece of gum (about 2 x 2 x 4mm, about the size of a nail clipping). This is not expected to cause any problems with the way the tooth socket heals.

Do I have to participate? No. You are entirely free to participate or not to participate in this study as you choose. Your decision will not in any way influence the treatment you receive.

Will I benefit from participating in the study? The results of this research will not directly benefit the patients who participate. However, we do hope that the work we are doing will give us information that will be useful in the future prevention and treatment of gum diseases.

If you wish to know more about this research you are invited to discuss it with the surgeon who will take out your tooth or to contact Professor Mackenzie, Department of Adult Dental Health. (Telephone: 029 20746557).

APPENDIX II
STOCK SOLUTIONS

All trans retinoic acid (ATRA)
For use in FAD medium at an end concentration of 10^{-9}M. Calculations allow 100µl of stock ATRA to be added to 10ml of FAD. Serially diluted in isopropanol, aliquotted into 1ml eppendorfs and stored at -20°C.

Ascorbic acid
For use in FAD medium at a concentration of 50µg/ml., Calculations to allow 100µl of stock ascorbic acid to be added to 10ml of FAD. Diluted in DDH_2O, aliquotted and stored at -20°C.

Cholera Toxin 1000x stock
Place 1mg cholera toxin in 119ml of solution A, filter sterilise and store aliquots at -20°C.

Epidermal growth factor 1000x stock (EGF)
Place 100µg EGF in 10ml solution A, filter sterilise and store aliquots at -20°C.

Hydrochloric acid 4M (HCl)
To 34.3ml, concentrated HCl add 65.6ml DDH_2O.

Hydrocortisone 1000x stock
Place 4mg hydrocortisone in 10ml solution A and 1ml ETOH to dissolve producing a 400µg/ml solution, filter sterilise and store aliquots at 4°C.

Insulin
Dilute 100mg in 10ml DDH_2O and 100µl of glacial acetic acid producing a 10mg/ml stock solution. Aliquot and store at 4°C for 3-6 months.

Tris buffered saline 10x stock (TBS)
To 800ml DDH_2O add 60.55g TRIS, 85.2g NaCl, dissolve and make up to 1L at pH to 7.6.

Fixatives
Acetone/methanol
Mixed at a ratio of 1:1 and stored at -20°C.

Paraformaldehyde 4%
To 4g Paraformaldehyde powder add 10ml DDH_2O, 2 drops of 2M NaOH and heat gently to 60°C and stir with stir bar. Once dissolved add 90ml calcium free PBS and make up to 100ml. pH to 7.2 using either dilute HCL or NaOH. Filter before use and store at 4°C.

Anti-fade mountant
To 10ml PBS add 100mg p-phenylenediamine and 90ml glycerol. Store in darkened container at -20°C for up to 6 months.

APPENDIX III
RNA QUANTIFICATION VALUES

Date	Designation	260nm	280nm	Ratio	Amount	1µg
8/5/02	OGF1	0.165	0.089	1.85	330µg/ml	3.0µl
6/8/02	OGF2	0.468	0.254	1.84	936µg/ml	1.1µl
22/7/02	OGF9	0.410	0.234	1.75	820µg/ml	1.2µl
6/8/02	OGF11	0.273	0.146	1.87	546µg/ml	1.8µl
6/8/02	OGF13	0.423	0.223	1.90	846µg/ml	1.2µl
20/6/02	OGF14	0.195	0.107	1.82	390µg/ml	2.6µl
6/8/02	OGF15	0.112	0.059	1.90	224µg/ml	4.5µl
19/12/02	OGF16	0.367	0.211	1.74	734µg/ml	1.3µl
8/5/02	PDL1	0.132	0.084	1.57	264µg/ml	3.8µl
6/8/02	PDL2	0.314	0.178	1.76	628µg/ml	1.6µl
22/7/02	PDL9	0.323	0.192	1.69	696µg/ml	1.6µl
8/5/02	PDL14	0.213	0.120	1.78	426µg/ml	2.4µl
12/8/02	PDL15	0.104	0.072	1.51	218µg/ml	4.6µl
8/8/02	PDL16	0.197	0.105	1.88	395µg/ml	2.5µl
20/6/02	PDL23	0.278	0.158	1.76	555µg/ml	1.8µl
8/5/02	JZF1	0.218	0.122	1.79	436µg/ml	2.3µl
8/8/02	JZF9	0.399	0.215	1.86	798µg/ml	1.3µl
12/8/02	JZF17	0.130	0.071	1.83	260µg/ml	3.8µl
8/8/02	JZF21	0.243	0.142	1.72	486µg/ml	2.1µl
30/4/02	JE1	0.165	0.101	1.63	330µg/ml	3.0µl
5/9/02	JE2	0.320	0.190	1.68	640µg/ml	1.6µl
6/6/02	JE4	0.387	0.229	1.69	774µg/ml	1.3µl
6/6/02	JE6	0.393	0.236	1.67	785µg/ml	1.3µl
10/3/03	JE7	0.337	0.241	1.40	674µg/ml	1.5µl
10/3/03	JE8	0.407	0.272	1.50	814µg/ml	1.3µl
10/3/03	JE9	0.391	0.240	1.63	782µg/ml	1.3µl
18/3/03	JE17	0.333	0.197	1.69	666µg/ml	1.5µl
18/3/03	JE18	0.324	0.200	1.62	648µg/ml	1.5µl
18/3/03	JE21	0.510	0.315	1.62	1020µg/ml	1.0µl
18/3/03	JE22	0.521	0.320	1.63	1042µg/ml	1.0µl
27/3/03	OGE5	0.146	0.089	1.63	292µg/ml	3.4µl
27/3/03	OGE6	0.089	0.050	1.66	178µg/ml	5.6µl
27/3/03	OGE7	0.153	0.092	1.67	306µg/ml	3.3µl
19/12/02	OGE8	0.046	0.029	1.59	92µg/ml	10.8µl
30/04/02	OGE9	0.396	0.278	1.42	793µg/ml	1.3µl
5/9/02	OGE14	0.167	0.090	1.86	334µg/ml	3.0µl

Highlighted results indicate poor mRNA retrieval values. These samples subsequently provided error prone Q-PCR results and were discarded.

APPENDIX IV
EXAMPLE 96 WELL SET-UP FOR Q-PCR

	1	2	3	4	5	6	7	8	9	10	11	12
A	UNKNOWN OGF10 a HGFR	UNKNOWN OGF10 b HGFR	UNKNOWN OGF10 c HGFR	UNKNOWN OGF11 a HGFR	UNKNOWN OGF11 b HGFR	UNKNOWN OGF11 c HGFR	UNKNOWN OGF12 a HGFR	UNKNOWN OGF12 b HGFR	UNKNOWN OGF12 c HGFR	UNKNOWN OGF13 a HGFR	UNKNOWN OGF13 b HGFR	UNKNOWN OGF13 c HGFR
B	UNKNOWN OGF14 a HGFR	UNKNOWN OGF14 b HGFR	UNKNOWN OGF14 c HGFR	UNKNOWN OGF15 a HGFR	UNKNOWN OGF15 b HGFR	UNKNOWN OGF15 c HGFR	UNKNOWN GF7 a HGFR	UNKNOWN GF7 b HGFR	UNKNOWN GF7 c HGFR	UNKNOWN GF9 a HGFR	UNKNOWN GF9 b HGFR	UNKNOWN GF9 c HGFR
C	UNKNOWN PDL1 a HGFR	UNKNOWN PDL1 b HGFR	UNKNOWN PDL1 c HGFR	UNKNOWN PDL2 a HGFR	UNKNOWN PDL2 b HGFR	UNKNOWN PDL2 c HGFR	UNKNOWN PDL9 a HGFR	UNKNOWN PDL9 b HGFR	UNKNOWN PDL9 c HGFR	UNKNOWN PDL15 a HGFR	UNKNOWN PDL15 b HGFR	UNKNOWN PDL15 c HGFR
D	UNKNOWN PDL16 a HGFR	UNKNOWN PDL16 b HGFR	UNKNOWN PDL16 c HGFR	UNKNOWN PDL23 a HGFR	UNKNOWN PDL23 b HGFR	UNKNOWN PDL23 c HGFR	UNKNOWN JZF1 a HGFR	UNKNOWN JZF1 b HGFR	UNKNOWN JZF1 c HGFR	UNKNOWN JZF2 a HGFR	UNKNOWN JZF2 b HGFR	UNKNOWN JZF2 c HGFR
E	UNKNOWN JZF9 a HGFR	UNKNOWN JZF9 b HGFR	UNKNOWN JZF9 c HGFR	UNKNOWN JZF14 a HGFR	UNKNOWN JZF14 b HGFR	UNKNOWN JZF14 c HGFR	UNKNOWN JZF21 a HGFR	UNKNOWN JZF21 b HGFR	UNKNOWN JZF21 c HGFR	GAPDH OGF10	GAPDH OGF11	GAPDH OGF12
F	GAPDH OGF13	GAPDH OGF14	GAPDH OGF15	GAPDH GF7	GAPDH GF9	GAPDH PDL1	GAPDH PDL2	GAPDH PDL9	GAPDH PDL15	GAPDH PDL16	GAPDH PDL23	GAPDH JZF1
G	STD a1 (500pg) 50000000 IL1αR	STD a2 (500pg) 50000000 IL1αR	STD b1 (50pg) 5000000 IL1αR	STD b2 (50pg) 5000000 IL1αR	STD c1 (5pg) 500000 IL1αR	STD c2 (5pg) 500000 IL1αR	STD d1 (500fg) 50000 IL1αR	STD d2 (500fg) 50000 IL1αR	STD e1 (50fg) 5000 IL1αR	STD e2 (50fg) 5000 IL1αR	STD f1 (5fg) 500 IL1αR	STD f2 (5fg) 500 1 IL1αR
H	STD g1 (500ag) 50 IL1αR	STD g2 (500ag) 50 IL1αR	STD h1 (50ag) 5 IL1αR	STD h1 (50ag) 5 IL1αR	NTC a H_2O 300F: 300R 150nM HGFR	NTC b H_2O 300F: 300R 150nM HGFR	NTC c H_2O 300F: 300R 150nM HGFR	NTC d H_2O 300F: 300R 150nM HGFR	GAPDH JZF2	GAPDH JZF9	GAPDH JZF14	GAPDH JZF21

APPENDIX V
GENE EXPRESSION STUDIES

Reverse-transcription amplification buffer master mix

Component	RT Master mix (µl)	Working Concentration
PCR buffer (10X)	2	1x
$MgCl_2$ (25mM)	3	3.75mM
DNTP's (10mM)	5	2mM
Random Hexamer Primers (0.5µg/µL)	2	4
Dithiothreitol (100mM)	2	10mM

PCR amplification master mix

Component	PCR Master mix (µl)	Working Concentration
PCR Buffer (10x)	5	1x
$MgCl_2$ (25mM)	4	2mM
dNTP's (10mM)	4	0.8mM
3' Primers (20µM)	1.25	0.5µM
5' Primers (20µM)	1.25	0.5µM
Taq polymerase (5U/µL)	0.25	0.025U/µl
Nuclease-free H_2O	34.25	
Total volume:	**50µl**	

Q-PCR amplification master mix

Component	Unknown	GAPDH	Standards	NTC's
TaqMan™ buffer A	2.5µl	2.5µl	2.5µl	2.5µl
$MgCl_2$ (25mM)	5.5µl	5.5µl	5.5µl	5.5µl
DNTP's (10mM)	4µl	4µl	4µl	4µl
Probe (150nM)	1µl	1µl	1µl	1µl
3' Primer (300nM)	1µl	1µl	1µl	1µl
5' Primer (300nM)	1µl	1µl	1µl	1µl
Amplitaq Gold	0.25µl	0.25µl	0.25µl	0.25µl
cDNA (0.5µg/µl)	1µl	1µl	2µl Pre-made dilutions	Nil
Nuclease-free H_2O	8.75µl	8.75µl	7.75µl	9.75µl
Total volume:	**25µl**	**25µl**	**25µl**	**25µl**

Tris-borate-EDTA buffer 5x (TBE buffer)
Add contents of packet to 1 litre of DEPC H_2O.

TBE running buffer

1x TBE buffer	200ml
DEPC H_2O	800ml
Ethidium Bromide (10mg/ml)	10µl

2% Agarose gel

Agarose	2.0g
1x TBE buffer	100ml
Ethidium Bromide	4µl

Blue/orange agarose gel loading buffer 6x
Provided in a premixed, ready-to-use form. The dye is used for loading DNA samples into gel electrophoresis wells and tracking migration during electrophoresis. In a 2.0% agarose gel in 0.5x TBE xylene cyanol FF migrates at approximately 4kb, bromophenol blue at approximately 300bp, and orange G at approximately 50bp.

0.4% orange G
0.03% bromophenol blue
0.03% xylene cyanol FF
15% Ficoll® type 400
10mM Tris-HCl (pH 7.5)
50mM EDTA (pH 8.0)

APPENDIX VI
CYTOKINE PRIMER AND PROBE SEQUENCES

Target template	Accession number	PCR Primer sequence		Primer length	Product size (amplicon)
Keratinocyte growth factor (Fibroblast growth factor 7) (KGF)	M60828	FORWARD PRIMER	5'GAAATCAGGACAGTGGCAGTTG3'	22	199bp
		PROBE	5'TCTGGAAAACCATTACAACACATATGCATCAGC3'	33	
		REVERSE PRIMER	5'CAAACATTTCCCCTCCGTTGTG3'	22	
Keratinocyte growth factor receptor (KGFR)	M80634	FORWARD PRIMER	5'TCTGTTCAATGTGACCGAGG3'	20	104bp
		PROBE	5'TTGGCCTGCCCTATATAATTGGAGACCTTACA3'	32	
		REVERSE PRIMER	5'GTTTTGGCAGGACAGTGAGC3'	20	
Keratinocyte growth factor 2 (Fibroblast growth factor 10) (KGF2)	NM004465	FORWARD PRIMER	5'GATACTGACACATTGTGCCTCAGC3'	24	248bp
		PROBE	5'CTGCTTTTTGTTGCTGTTCTTGGTGTCTTCC3'	31	
		REVERSE PRIMER	5'TGGTGAAAGAGAATAGCTTTCTCCA3'	25	
Granulocyte macrophage colony stimulating factor (GMCSF)	M11220	FORWARD PRIMER	5'GAGTGAGACCGGCCAGATGA3'	20	181bp
		PROBE	5'AGGTCCAGGCCACTCCCACCATGGCT3'	26	
		REVERSE PRIMER	5'TTCCCATTCTTCTGCCATGC3'	20	
Granulocyte macrophage colony stimulating factor receptor (GMCSFR)	M73832	FORWARD PRIMER	5'CCCAGGCTCAGTAACAACGAAT 3'	22	181bp
		PROBE	5'CCTCAAATGTGACTCCTTCATGCAGACAAATTT3'	33	
		REVERSE PRIMER	5'CCGCATTGTAGATGAAACAGGAG3'	23	
Interleukin-1-alpha (IL-1α)	M28983	FORWARD PRIMER	5'GAATGAC GCCCTCAATC AAAGTATA3'	25	181bp
		PROBE	5'AATGATCAGTACCTCACGGCTGCTGCA3'	27	
		REVERSE PRIMER	5'TTGGGCAGTCACATACAATTGAGT3'	24	
Interleukin-1-alpha receptor (IL-1αR)	M27492	FORWARD PRIMER	5'TCCAACAGACAGGGCCTAGCT3'	21	181bp
		PROBE	5'AGCAGGGATGTCACGTCTTGAAAAGCCTATT3'	31	
		REVERSE PRIMER	5'AAATTGGCTTGCTTTCTTAGCACTAT3'	26	

Hepatocyte growth factor/Scatter factor (HGF)	XM168542	FORWARD PRIMER	5'CTGTCAATACCATTTGGAATGGAAT3'	25	181bp
		PROBE	5'TTGGGATTCTCAGTATCCTCACGAGC3'	26	
		REVERSE PRIMER	5' TAGCCAACTCGGATGTTTGGAT3'	22	
Hepatocyte growth factor/Scatter factor receptor (HGFR)	XM048918	FORWARD PRIMER	5'CATTTTGGTTGTGTATATCATGGGAC 3'	26	203bp
		PROBE	5'TGCTGTGAAATCCTTGAACAGAATCACTGACA3'	32	
		REVERSE PRIMER	5'ACCAGCGGAGACCCTTCACT3'	20	
Transforming growth factor alpha (TGF-α)	M31172	FORWARD PRIMER	5'AAATGGTCCCCTCGGCTG 3'	18	226bp
		PROBE	5'GCCAACACAATACCCAGAGCGAACAGG3'	27	
		REVERSE PRIMER	5'GCTGGCTTGTCCTCGTGC3'	18	
Glyceraldehyde-3-phosphate dehydrogenase (GAPDH)	M33197	FORWARD PRIMER	5'GCGAGATCCCTCCAAAATCAA 3'	21	176bp
		PROBE	5' TCGTGGAGTCCACTGGCGTCTTCA3'	24	
		REVERSE PRIMER	5'CTTCTCATGGTTCACACCCATG3'	22	

APPENDIX VII
BrdU STAINING: RAW DATA

JE DAY 2		Cell line					
		JE 2	JE 4	JE 6	JE 8	JE1 8	AVE (%)
Colony type number/50	HOLO	32	22	33	37	40	66
	MERO	14	27	20	12	15	35
	PARA	4	1	0	6	1	5
Average colony cell number	HOLO	13	9	13	12	18	13
	MERO	16	12	16	13	13	14
	PARA	23	5	14	14	11	13
Average number of BrdU+ve cells/colony type	HOLO	4	4	3	5	3	4
	MERO	4	2	2	3	4	3
	PARA	4	0	0	0	4	2
Average % of BrdU+ve cells/colony type	HOLO	31	44	23	42	17	31
	MERO	25	17	13	23	31	22
	PARA	17	0	0	0	36	11

JE DAY 4		Cell line					
		JE 2	JE 4	JE 6	JE 8	JE1 8	AVE (%)
Colony type number/50	HOLO	24	17	27	28	25	48
	MERO	15	12	14	16	18	30
	PARA	11	5	14	15	13	23
Average colony cell number	HOLO	30	24	27	29	30	28
	MERO	28	16	18	20	22	21
	PARA	29	7	20	21	17	19
Average number of BrdU+ve cells/colony type	HOLO	13	5	10	7	9	9
	MERO	8	2	5	4	6	5
	PARA	6	0	5	4	2	3
Average % of BrdU+ve cells/colony type	HOLO	43	21	37	24	30	31
	MERO	29	13	28	20	27	23
	PARA	21	0	25	19	12	15

JE DAY 6		Cell line					
		JE 2	JE 4	JE 6	JE 8	JE1 8	AVE (%)
Colony type number/50	HOLO	15	11	17	18	20	32
	MERO	11	17	16	14	22	32
	PARA	24	22	27	28	20	48
Average colony cell number	HOLO	123	70	107	98	80	96
	MERO	78	29	56	67	49	56
	PARA	46	14	22	29	27	28
Average number of BrdU+ve cells/colony type	HOLO	48	11	40	32	30	32
	MERO	10	4	11	10	6	8
	PARA	2	0	2	2	0	1
Average % of BrdU+ve cells/colony type	HOLO	39	16	37	33	38	32
	MERO	13	14	20	15	12	15
	PARA	4	0	9	7	0	4

APPENDIX VII
BrdU STAINING RAW DATA

OGE DAY 2		Cell line					
		OGE 5	OGE 6	OGE 7	OGE 9	OGE14	AVE (%)
Colony type number/50	HOLO	36	32	38	40	31	70
	MERO	7	17	10	16	12	25
	PARA	7	1	7	6	3	10
Average colony cell number	HOLO	14	16	18	15	15	16
	MERO	16	17	17	19	13	16
	PARA	7	21	18	17	8	14
Average number of BrdU+ve cells/colony type	HOLO	5	6	3	4	7	5
	MERO	7	4	4	4	4	5
	PARA	0	2	2	0	0	1
Average % of BrdU+ve cells/colony type	HOLO	36	38	17	27	47	33
	MERO	44	24	24	21	31	29
	PARA	0	10	11	0	0	4

OGE DAY 4		Cell line					
		OGE 5	OGE 6	OGE 7	OGE 9	OGE14	AVE (%)
Colony type number/50	HOLO	26	20	22	29	30	51
	MERO	9	12	13	10	10	22
	PARA	15	18	16	17	18	34
Average colony cell number	HOLO	31	33	38	42	26	34
	MERO	22	25	28	30	26	26
	PARA	7	18	21	16	13	15
Average number of BrdU+ve cells/colony type	HOLO	7	17	12	16	7	12
	MERO	3	7	8	10	2	6
	PARA	0	3	5	4	0	2
Average % of BrdU+ve cells/colony type	HOLO	23	52	32	38	27	34
	MERO	14	28	29	33	8	22
	PARA	0	17	24	25	0	13

OGE DAY 6		Cell line					
		OGE 5	OGE 6	OGE 7	OGE 9	OGE14	AVE (%)
Colony type number/50	HOLO	22	25	22	26	27	49
	MERO	6	7	16	10	10	20
	PARA	22	18	12	14	13	32
Average colony cell number	HOLO	166	187	154	177	203	177
	MERO	32	33	45	29	36	35
	PARA	8	19	20	13	17	15
Average number of BrdU+ve cells/colony type	HOLO	68	54	44	50	46	52
	MERO	4	4	5	1	4	4
	PARA	0	2	3	2	3	2
Average % of BrdU+ve cells/colony type	HOLO	41	29	29	28	23	30
	MERO	13	12	11	3	11	10
	PARA	0	11	15	15	18	12

QUANTITATIVE-POLYMERASE CHAIN REACTION: RAW DATA

Data highlighted in green not included in statistical analysis

PE = Pipetting error

UNDET = Undetected

KGE

OGF	A	B	C	AVE
OGF1	20233	21313	15167	18904
OGF2	7023	24935	2364	11441
OGF9	8409	3914	29405	13909
OGF11	35824	35138	21304	30755
OGF13	29019	49311	41378	39903
OGF14	5587	6840	6284	6170
OGF16	3482	3492	812	2595
AVE	15654	20678	16673	17668

KGFR

A	B	C	AVE
62	183	40	95
464	252	46	254
127	4	117	83
112	237	461	270
UNDET	8	3	4
560	658	866	695
673	834	583	697
285	311	302	300

KGF2

A	B	C	AVE
75886	21984	30541	42804
57756	11102	PE	34429
34634	43665	34523	56411
34534	54555	44544	44544
52175	22155	99484	57938
46567	39876	54666	47036
17025	29151	62376	57938
45511	31784	46591	48729

HGE

A	B	C	AVE
95017	79786	51698	75500
108309	74294	71701	84768
11699	8454	10873	10342
234717	205515	246909	229047
114958	157331	183373	151887
29681	34933	39247	34620
144100	139098	144310	142503
105497	99916	106873	104095

HGFR

A	B	C	AVE	OGF
26	60	107	64	OGF1
205	82	12	100	OGF2
51	16	99	55	OGF9
329	255	220	268	OGF11
60	93	98	84	OGF13
424	819	532	592	OGF14
1691	1875	1686	1751	OGF16
398	457	393	416	AVE

PDL

PDL1	8313	718	2069	3700
PDL2	7823	8396	8461	8227
PDL9	12822	10680	5860	9787
PDL14	5578	5231	5808	5539
PDL16	6485	10970	5205	7547
PDL23	4121	3830	5634	4528
AVE	7520	6638	5506	6555

0	UNDET	UNDET	0
8	23	22	18
166	412	21	200
UNDET	66	UNDET	22
59	UNDET	UNDET	20
50	351	352	251
47	142	68	85

16389	30472	26927	24596
26571	46262	11087	27973
54645	45785	75674	58701
11098	21897	12128	15041
1009	45677	33345	40016
15946	55927	15139	43606
20943	41003	29050	34972

3729	3989	3503	3740
52861	57281	66883	59675
14172	11352	9357	11627
22620	19777	19899	20765
140158	129340	125035	131511
21723	20029	21563	21105
42544	40296	41373	49685

				PDL
7	4	28	13	PDL1
19	77	39	45	PDL2
885	620	UNDET	502	PDL9
44	67	UNDET	37	PDL14
659	97	8	255	PDL16
404	671	876	650	PDL23
336	256	159	250	AVE

JZF

JZF1	4909	9845	2350	5701
JZF9	10444	10464	16766	12558
JZF17	8716	4791	8764	7424
JZF21	4593	5194	3737	4508
AVE	7166	7574	7904	7548

17847(PE)	902	UNDET	0
66	UNDET	3	23
UNDET	0	63	21
147	88	UNDET	78
53	248	17	31

20461	32966	15891	23106
86626	24250	42665	51180
24529	72618	51908	49685
2804	4356	5467	4209
33606	33548	28983	32045

213821	189228	198962	200670
87428	97758	86177	90454
148362	157281	147264	150969
133422	123924	98268	118538
145758	142048	132668	140158

				JZF
390	378	311	360	JZF1
245	228	104	192	JZF9
1	92	274	122	JZF17
267	107	29	134	JZF21
226	201	180	202	AVE

OGE	A	B	C	AVE
OGE5	14	132	6	51
OGE6	14761	15386	8669	12939
OGE7	323	279	111	238
OGE9	678	226	278	394
OGE14	22	27	6	18
AVE	3160	3210	1814	2728

2635	5862	4317	4271
18777	18106	19682	18855
24248	23561	7408	18406
4252	3456	4456	4055
8688	7867	8103	8219
11720	11770	8793	10761

UNDET	UNDET	UNDET	0
UNDET	UNDET	UNDET	0
UNDET	UNDET	UNDET	0
UNDET	UNDET	UNDET	0
UNDET	UNDET	UNDET	0
0	0	0	0

UNDET	UNDET	295000000000	98666666666
UNDET	UNDET	UNDET	0
UNDET	UNDET	UNDET	0
UNDET	UNDET	UNDET	0
UNDET	UNDET	UNDET	0
0	0	67666666666	19000000000

				OGE
19796	21687	37243	26242	OGE5
220053	262798	327241	270031	OGE6
63240	76551	74689	71493	OGE7
66276	61231	59880	62462	OGE9
110567	123427	111990	115328	OGE14
95986	109139	122209	109111	AVE

JE

JE1	1	4	1	2
JE2	3077	2491	2897	2822
JE4	382	274	577	411
JE6	397	278	3	226
JE7	0	1	0	0
JE8	75	84	47	69
JE9	55	131	84	90
JE17	154	419	1389	654
JE18	29	210	173	137
JE21	19	17	19	18
JE22	97	20	15	44
AVE	390	357	473	407

2200	2210	3942	2784
35160	26228	28997	30128
8852	3990	4555	5799
7627	6206	6999	6944
UNDET	UNDET	UNDET	0
2591	4052	4225	3623
7086	7506	3745	6112
1408	6272	7066	4915
6295	9140	7061	7499
25882	46621	39018	37174
28798	31735	27091	29208
11445	13087	12064	12199

UNDET	UNDET	UNDET	0
UNDET	UNDET	UNDET	0
UNDET	UNDET	UNDET	0
UNDET	UNDET	UNDET	0
UNDET	UNDET	UNDET	0
UNDET	UNDET	UNDET	0
UNDET	UNDET	UNDET	0
UNDET	UNDET	UNDET	0
UNDET	UNDET	UNDET	0
UNDET	UNDET	UNDET	0
UNDET	UNDET	UNDET	0
0	0	0	0

UNDET	UNDET	UNDET	0
0	UNDET	UNDET	0
UNDET	UNDET	UNDET	0
0	UNDET	UNDET	0
63900	591000000	UNDET	197021300
UNDET	UNDET	UNDET	0
0	UNDET	UNDET	0
UNDET	1	UNDET	0
5532	UNDET	UNDET	1844
UNDET	UNDET	UNDET	0
UNDET	UNDET	UNDET	0
6312	53737273	0	17911196

				JE
59491	50809	52887	54396	JE1
508097	423620	281518	404412	JE2
116947	147635	171044	145209	JE4
462949	581201	352574	465575	JE5
56316	52618	78552	62495	JE7
185269	120542	170018	158610	JE8
79951	98911	97841	92234	JE9
157000	667316	590959	471758	JE17
233212	267815	268843	256623	JE18
442478	305655	254391	334175	JE21
373654	317951	353859	348488	JE22
243215	275825	242953	253998	AVE

Unreliable results for this RNA

OGF15	9853	3816	26540	13403
PDL15	UNDET	493	53824	18106
OGE8	UNDET	UNDET	UNDET	0

5	16	100	40
UNDET	UNDET	INDET	0
UNDET	UNDET	UNDET	0

235239976	11363	9	235269347
UNDET	UNDET	UNDET	0
UNDET	UNDET	UNDET	0

25100000	24000000	25600000	24900667
UNDET	UNDET	UNDET	0
0	UNDET	895	298

				OGF15
4	8	28	13	OGF15
5	4	90	33	PDL15
UNDET	UNDET	UNDET	0	OGE8

QUANTITATIVE-POLYMERASE CHAIN REACTION – RAW DATA

Data highlighted in green not included in statistical analysis

PE = Pipetting error

UNDET = Undetected

OGF	GM-CSF A	B	C	AVE	GM-CSFR A	B	C	AVE	IL-1A A	B	C	AVE	IL-1AR A	B	C	AVE	TGFA A	B	C	AVE
OGF1	509	1908	868	1095	UNDET	UNDET	UNDET	0	UNDET	UNDET	71	24	6842	7600	9570	8004	712238	86273	721916	506809
OGF2	25096	31520	42952	33189	UNDET	UNDET	UNDET	0	64	6	UNDET	23	13202	7716	6408	9109	697827	438118	20466	385470
OGF9	4284	6925	7604	6271	UNDET	UNDET	UNDET	0	UNDET	UNDET	16	5	9701	7697	8800	8733	172974	UNDET(PE)	6989(PE)	172974
OGF11	6359	3444	3039	4281	UNDET	UNDET	114	38	6	UNDET	25	10	9855	7957	8564	8792	791546	751294	742427	761756
OGF13	1039	1444	2646	1710	UNDET	UNDET	19394	6465	UNDET	UNDET	1215	405	5457	9324	10494	8425	24429	745268	997831	589176
OGF14	5048	16300	19295	13548	UNDET	UNDET	UNDET	0	18	UNDET	UNDET	6	9355	7450	11466	9424	1539	8676	9201	6472
OGF16	3270	1925	599	1931	UNDET	UNDET	UNDET	0	UNDET	UNDET	UNDET	0	20571	15259	11842	15891	180568	198311	164709	181196
AVE	6515	9067	11000	8861	0	0	2787	929	13	1	190	68	10712	9000	9592	9768	368732	318277	379507	371979
PDL																				
PDL1	168	94	458	240	UNDET	UNDET	UNDET	0	UNDET	UNDET	UNDET	0	1559	2479	1063	1700	3429	357339	3555	121441
PDL2	327	1159	662	716	UNDET	UNDET	UNDET	0	UNDET	UNDET	81	27	2080	1635	2134	1950	UNDET(PE)	UNDET(PE)	UNDET(PE)	0
PDL9	10076	6930	8890	8632	UNDET	UNDET	UNDET	0	160	UNDET	UNDET	53	4474	6555	4647	5225	282	184	3372	1279
PDL14	6785	5685	6365	6278	UNDET	UNDET	UNDET	0	UNDET	UNDET	UNDET	0	9246	9572	8879	9232	266870	89	4657	90539
PDL16	10179	8201	1858	6746	UNDET	UNDET	UNDET	0	UNDET	UNDET	UNDET	0	40606	25710	47148	37821	0(PE)	681645	68793	375219
PDL23	9575	11246	15222	12014	UNDET	UNDET	UNDET	0	UNDET	688	929	539	6805	6275	8085	7055	668417	662876	9(PE)	665647
AVE	6188	5553	5576	5771	0	0	0	0	27	0	168	103	10795	8704	11993	10497	156500	283689	13398	250829
JZF																				
JZF1	52516	47466	56748	52243	UNDET	UNDET	UNDET	0	64	UNDET	UNDET	21	16709	9066	11320	12365	1(PE)	645141	UNDET(PE)	645141
JZF9	6292	6091	6696	6360	366474	13300000	UNDET	4555491	UNDET	UNDET	UNDET	0	44567	38043	61211	47940	4(PE)	188066	68665	128366
JZF17	1695	2658	4776	3110	UNDET	UNDET	UNDET	0	UNDET	UNDET	UNDET	0	20764	37546	26578	28296	UNDET(PE)	160365	318927	239646
JZF21	3079	3012	4198	3430	UNDET	UNDET	UNDET	0	UNDET	UNDET	UNDET	0	16304	12260	12653	13739	183892	UNDET(PE)	UNDET(PE)	183892
AVE	15896	14857	18105	16286	91619	3325000	0	1139873	16	0	0	5	24586	24229	27941	25585	45973	248393	96898	299261
OGE																				
OGE5	271	207	80	186	4149	44(PE)	UNDET(PE)	4149	20118	20100	21107	20442	4	UNDET	UNDET	1	25218	6039	14633	15297
OGE6	46	58	166	90	6363	6364	8639	7122	143261	161933	164268	156487	0	7	44	17	123577	100347	123255	115726
OGE7	269	287	243	266	9558	6461	1315	5778	43284	42165	39889	41779	46	25	UNDET	24	24518	37502	22721	28247
OGE9	22	245	105	124	2248	2678	2781	2569	45833	39780	50008	45207	0	20	0	7	99870	89490	97895	95752
OGE14	43	28	11	27	5789	6473	5567	5943	98768	100780	109790	103113	11	44	14	23	120342	132566	176547	143152
AVE	130	165	121	139	5621	4395	3660	5112	70253	72952	77012	73406	12	19	12	14	78706	73189	87010	79635
JE																				
JE1	25	25	9	20	6211	2958	47752	18974	74189	22521	80674	59128	33	2	11	15	693260	630000	628525	650595
JE2	5	8	28	14	8481	7825	39332	18546	651596	127012	228461	336690	67	53	194	105	600000	599751	600222	599991
JE4	25	19	38	27	22656	32017	36826	30500	120195	385430	685479	397038	185	253	158	199	86418	104431	86283	92377
JE6	28	42	3	24	58817	68452	75531	67800	677836	95661	945920	573139	224	168	848	413	123782	174032	150002	149272
JE7	1032	92	UNDET	375	60966	16239	15563	30923	537732	461266	72138	357045	143	20	3	55	6319	5288	7127	6245
JE8	49	27	18	31	9348	32411	67976	36578	51230	151597	199597	134141	17	222	331	190	77716	39985	40434	52712
JE9	18	6	UNDET	8	11412	14180	20440	15344	66074	54130	35904	52036	58	49	20	42	17319	17735	16065	17040
JE17	1429	2236	1129	1598	216261	93594	147730	152528	39350	447793	402730	296624	57	193	884	378	384392	359850	232668	325637
JE18	564	732	1071	789	20538	2346	15378	12754	406779	325223	10767	247590	327	0	1	109	300582	422189	262500	328424
JE21	1	23	12	12	13917	34749	36707	28458	73805	412347	336150	274101	0	316	509	275	189433	230877	233067	217792
JE22	51	32	2	28	37487	66338	9450	37758	396793	181499	299846	292713	599	358	0	319	114111	164605	113207	130641
AVE	293	295	210	266	42372	33737	46610	40906	281416	242225	299768	274476	155	149	269	191	235757	249686	215464	233702
Unreliable results for this RNA																				
OGF15	241	289	1180	570	3	UNDET	UNDET	1	UNDET	UNDET	UNDET	0	3121	3978	3158	3419	209868	7465	10	72448
PDL15	2828	2288	1516	2211	UNDET	UNDET	UNDET	0	UNDET	UNDET	UNDET	0	UNDET	UNDET	746	373	330363	392603	672889	465285
OGE8	UNDET	UNDET	UNDET	0	UNDET	UNDET	UNDET	0	UNDET	UNDET	UNDET	0	UNDET	UNDET	UNDET	0	UNDET	UNDET	UNDET	0

QUANTITATIVE POLYMERASE CHAIN REACTION: EXAMPLE STANDARD CURVE

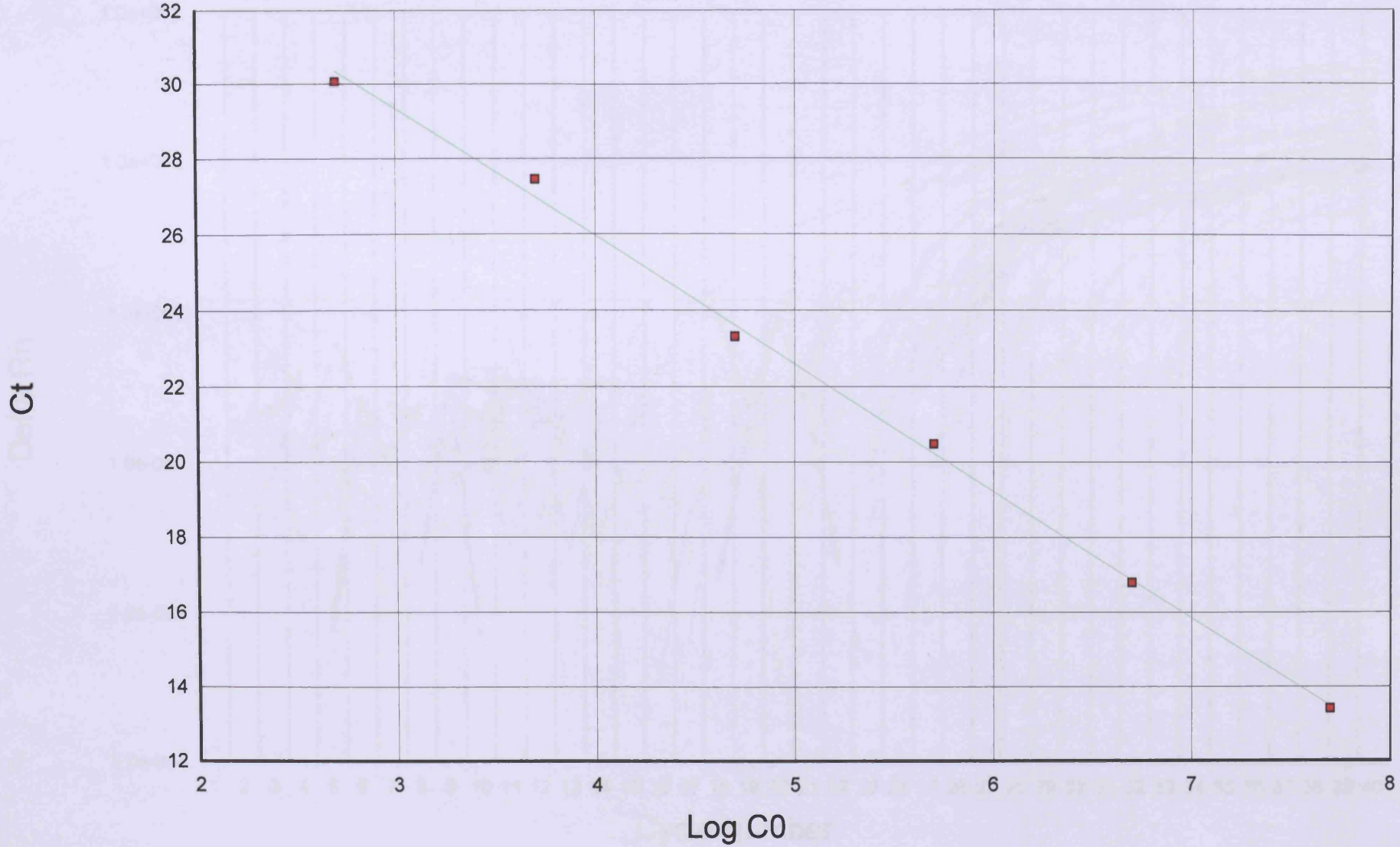

Detector: IL1A receptor, Slope: -3.372578, Intercept: 39.457359, R2: 0.997644
Document: run 6 (Fibs GMCSF) results post analysis 17-1-03

QUANTITATIVE-POLYMERASE CHAIN REACTION: TYPICAL AMPLIFICATION PLOT

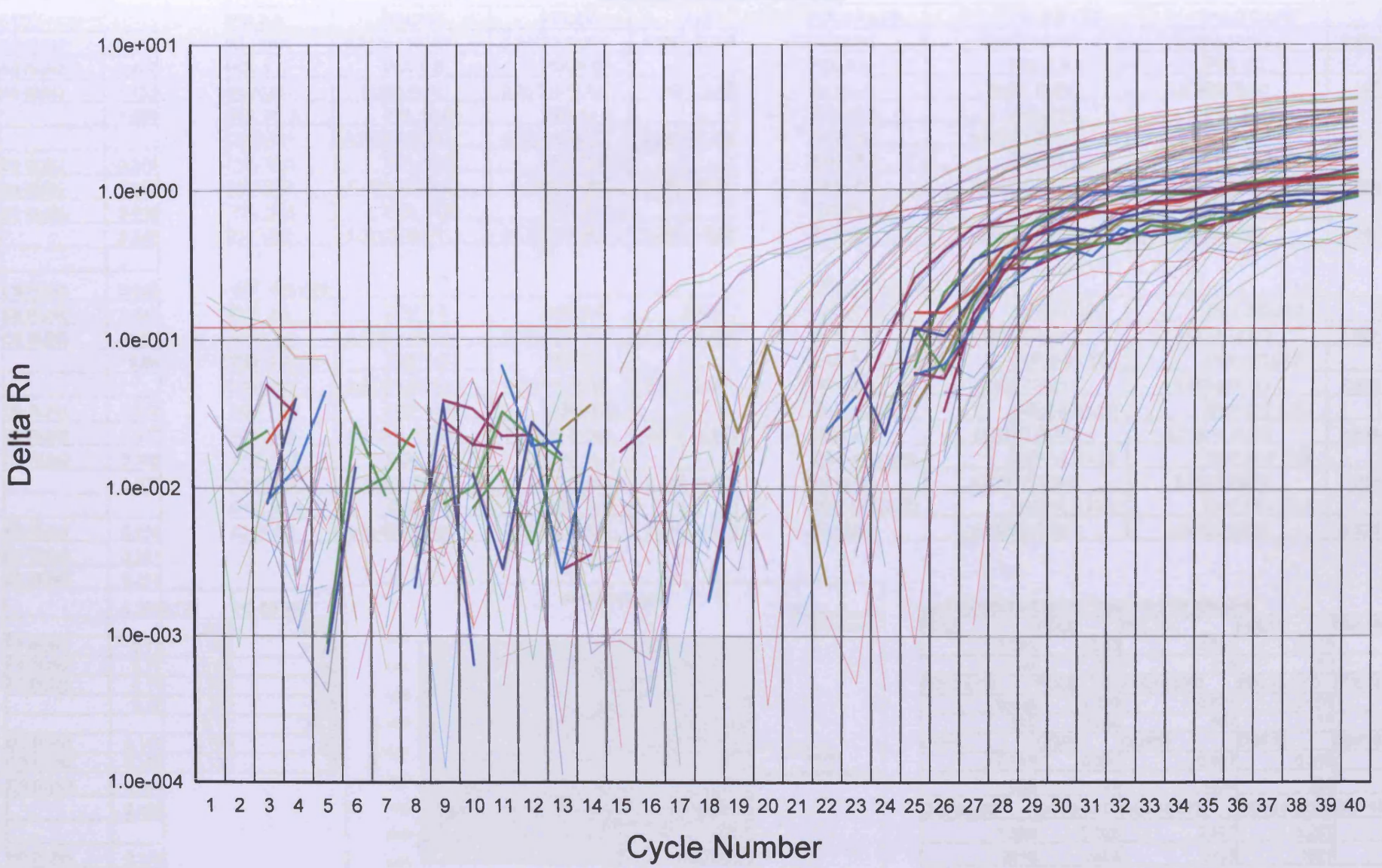

Selected Detector: IL1A receptor; Start: 4; End: 16; Threshold: 0.12107900
Well(s): A1-H12
Document: run 3 (Fibs KGF) results post analysis b 18-12-02

APPENDIX XI - ELISA PROTEIN ASSAY RAW DATA (KGF)

STANDARDS

STD2	
A9 RUN1	1.414
A9 RUN2	1.427
A9 RUN3	1.433
	1.425
B9 RUN1	0.976
B9 RUN2	0.989
B1 RUN3	0.996
	0.987
C9 RUN1	0.627
C9 RUN2	0.641
C9 RUN3	0.651
	0.64
D9 RUN1	0.367
D9 RUN2	0.377
D9 RUN3	0.386
	0.377
E9 RUN1	0.258
E9 RUN2	0.261
E9 RUN3	0.274
	0.264
F9 RUN1	0.17
F9 RUN2	0.17
F9 RUN3	0.17
	0.17
G9 RUN1	0.147
G9 RUN2	0.152
G9 RUN3	0.161
	0.153
H9 RUN1	0.121
H9 RUN2	0.126
H9 RUN3	0.134
	0.127

STD	PG OF KGF
1.425	2000
0.987	1000
0.64	500
0.377	250
0.264	125
0.17	62.5
0.153	37
0.127	0

PDL VALUES

PDL2 A		PDL2 B		PDL2 C		AVE
A3 RUN1	0.247	A4 RUN1	0.245	A5 RUN1	0.256	**0.249**
PDL 9 A		**PDL 9 B**		**PDL 9 C**		
B3 RUN1	0.443	B4 RUN1	0.457	B5 RUN1	0.48	**0.46**
PDL 14 A		**PDL 14 B**		**PDL 14 C**		
C3 RUN1	0.342	C4 RUN1	0.333	C5 RUN1	0.337	**0.337**
PDL 15 A		**PDL 15 B**		**PDL 15 C**		
Y3 RUN1	0.178	Y4 RUN1	0.16	Y5 RUN1	0.186	**0.175**
PDL 16 A		**PDL 16 B**		**PDL 16 C**		
Z3 RUN1	0.313	Z4 RUN1	0.233	Z5 RUN1	0.295	**0.28**

PDL LYSED VALUES

PDL2 A LYD		PDL2 B LYD		PDL2 C LYD		AVE
A6 RUN1	0.44	A7 RUN1	0.42	A8 RUN1	0.414	**0.425**
PDL 9 A		**PDL 9 B**		**PDL 9 C**		
B6 RUN1	1.264	B7 RUN1	1.259	B8 RUN1	1.195	**1.239**
PDL 14 A		**PDL 14 B**		**PDL 14 C**		
C6 RUN1	0.685	C7 RUN1	0.666	C8 RUN1	0.671	**0.674**
PDL 15 A		**PDL 15 B**		**PDL 15 C**		
Y6 RUN1	0.323	Y7 RUN1	0.271	Y8 RUN1	0.295	**0.296**
PDL 16 A		**PDL 16 B**		**PDL 16 C**		
Z3 RUN1	0.363	Z4 RUN1	0.309	Z5 RUN1	0.391	**0.354**

OGF VALUES

OGF 2 A		OGF 2 B		OGF 2 C		AVE
E3 RUN3	0.792	E4 RUN3	0.786	E5 RUN3	0.778	**0.785**
OGF 9 A		**OGF 9 B**		**OGF 9 C**		
F3 RUN3	0.407	F4 RUN3	0.359	F5 RUN3	0.406	**0.391**
OGF 15 A		**OGF 15 B**		**OGF 15 C**		
H3 RUN3	0.895	H4 RUN3	0.997	H5 RUN3	0.828	**0.907**
OGF 14 A		**OGF 14 B**		**OGF 14 C**		
Y3 RUN3	0.394	Y4 RUN3	0.38	Y5 RUN3	0.424	**0.399**
OGF 16 A		**OGF 16 B**		**OGF 16 C**		
Z3 RUN2	0.518	Z4 RUN2	0.513	Z5 RUN2	0.524	**0.518**

OGF LYSED VALUES

OGF 2 A LYD		OGF 2 B LYD		OGF 2 C LYD		AVE
E6 RUN3	1.587	E7 RUN3	1.564	E8 RUN3	1.527	**1.559**
OGF 9 A LYD		**OGF 9 B LYD**		**OGF 9 C LYD**		
F6 RUN3	2.668	F7 RUN3	2.59	F8 RUN3	2.621	**2.626**
OGF 15 A LYD		**OGF 15 B LYD**		**OGF 15 C LYD**		
H6 RUN3	2.622	H7 RUN3	2.505	H8 RUN3	2.604	**2.577**
OGF 14 A LYD		**OGF 14 B LYD**		**OGF 14 C LYD**		
Y6 RUN3	1.235	Y7 RUN3	1.25	Y8 RUN3	1.267	**1.251**
OGF 16 A LYD		**OGF 16 B LYD**		**OGF 16 C LYD**		
Z3 RUN1	0.692	Z4 RUN1	0.584	Z5 RUN1	0.605	**0.627**

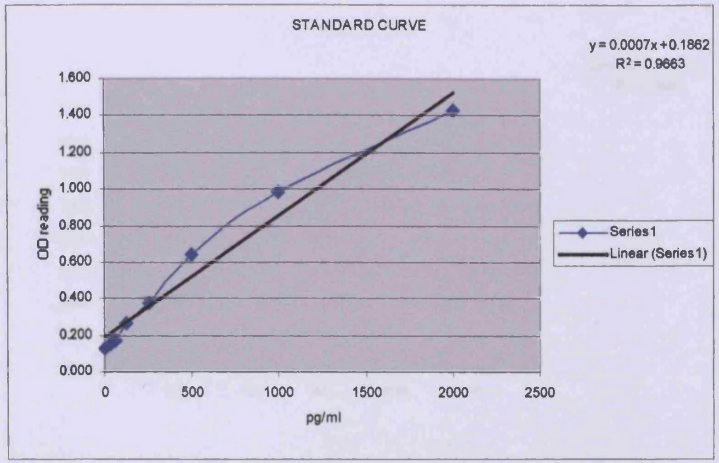

DATA POINTS CONVERTED TO PICOGRAMS

PDL2	PDL9	PDL14	PDL15	PDL16
0.249	0.46	0.337	0.175	0.28
90	391	215	80	134
PDL2 LYD	**PDL9 LYD**	**PDL14 LYD**	**PDL15 LYD**	**PDL16 LYD**
0.425	1.239	0.674	0.296	0.354
341	1504	697	157	240
OGF2	**OGF9**	**OGF15**	**OGF14**	**0GF16**
0.785	0.391	0.907	0.399	0.518
855	293	1030	304	474
OGF2 LYD	**OGF9 LYD**	**OGF15 LYD**	**OGF14 LYD**	**OGF16 LYD**
1.599	2.626	2.577	1.251	0.627
2018	3485	3415	1521	630

APPENDIX XI - ELISA PROTEIN ASSAY RAW DATA (GM-CSF)

STANDARDS

STD	
A1 RUN1	1.514
A1 RUN2	1.531
A1 RUN3	1.546
	1.530
B1 RUN1	0.914
B1 RUN2	0.937
B1 RUN3	0.948
	0.933
C1 RUN1	0.516
C1 RUN2	0.544
C1 RUN3	0.554
	0.538
D1 RUN1	0.284
D1 RUN2	0.304
D1 RUN3	0.312
	0.300
E1 RUN1	0.255
E1 RUN2	0.242
E1 RUN3	0.236
	0.244
F1 RUN1	0.198
F1 RUN2	0.185
F1 RUN3	0.179
	0.187
G1 RUN1	0.136
G1 RUN2	0.146
G1 RUN3	0.151
	0.144
H1 RUN1	0.084
H1 RUN2	0.090
H1 RUN3	0.094
	0.089

PDL VALUES

PDL 2 A		PDL 2 B		PDL 2 C		AVE
A3 RUN3	0.209	A4 RUN3	0.183	A5 RUN3	0.162	**0.185**
PDL 9 A		**PDL 9 B**		**PDL 9 C**		
B3 RUN2	0.231	B4 RUN2	0.195	B5 RUN2	0.182	**0.203**
PDL 14 A		**PDL 14 B**		**PDL 14 C**		
C3 RUN2	0.299	C4 RUN2	0.257	C5 RUN2	0.356	**0.304**
PDL 15 A		**PDL 15 B**		**PDL 15 C**		
Y3 RUN1	0.172	Y4 RUN1	0.128	Y5 RUN1	0.116	**0.139**
PDL 16 A		**PDL 16 B**		**PDL 16 C**		
Z3 RUN3	0.142	Z4 RUN3	0.150	Z5 RUN3	0.139	**0.144**

PDL LYSED VALUES

PDL 2 A LYD		PDL 2 B LYD		PDL 2 C LYD		AVE
A6 RUN2	0.167	A7 RUN2	0.160	A8 RUN2	0.158	**0.162**
PDL 9 A LYD		**PDL 9 B LYD**		**PDL 9 C LYD**		
B6 RUN2	0.155	B7 RUN2	0.183	B8 RUN2	0.210	**0.183**
PDL 14 A LYD		**PDL 14 B LYD**		**PDL 14 C LYD**		
C6 RUN1	0.286	C7 RUN1	0.225	C8 RUN1	0.192	**0.234**
PDL 15 A LYD		**PDL 15 B LYD**		**PDL 15 C LYD**		
Y6 RUN1	0.166	Y7 RUN1	0.148	Y8 RUN1	0.146	**0.153**
PDL 16 A LYD		**PDL 16 B LYD**		**PDL 16 C LYD**		
Z3 RUN1	0.165	Z4 RUN1	0.154	Z5 RUN1	0.154	**0.158**

OGF VALUES

OGF 2 A		OGF 2 B		OGF 2 C		AVE
E3 RUN1	0.119	E4 RUN1	0.092	E5 RUN1	0.107	**0.106**
OGF 16 A		**OGF 16 B**		**OGF 16 C**		
G3 RUN2	0.210	G4 RUN2	0.143	G5 RUN2	0.138	**0.164**
OGF 9 A		**OGF 9 B**		**OGF 9 C**		
F3 RUN2	0.374	F4 RUN2	0.356	F5 RUN2	0.299	**0.343**
OGF 15 A		**OGF 15 B**		**OGF 15 C**		
H3 RUN2	0.182	H4 RUN2	0.152	H5 RUN2	0.130	**0.155**
OGF 14 A		**OGF 14 B**		**OGF 14 C**		
Y3 RUN1	0.172	Y4 RUN1	0.178	Y5 RUN1	0.170	**0.173**

OGF LYSED VALUES

OGF 2 A LYD		OGF 2 B LYD		OGF 2 C LYD		AVE
E6 RUN2	0.241	E7 RUN2	0.209	E8 RUN2	0.194	**0.215**
OGF 16 A LYD		**OGF 16 B LYD**		**OGF 16 C LYD**		
G6 RUN2	0.187	G7 RUN2	0.157	G8 RUN2	0.149	**0.164**
OGF 9 A LYD		**OGF 9 B LYD**		**OGF 9 C LYD**		
F6 RUN2	0.202	F7 RUN2	0.181	F8 RUN2	0.170	**0.184**
OGF 15 A LYD		**OGF 15 B LYD**		**OGF 15 C LYD**		
H6 RUN2	0.239	H7 RUN2	0.202	H8 RUN2	0.143	**0.195**
OGF 14 A LYD		**OGF 14 B LYD**		**OGF 14 C LYD**		
Y6 RUN1	0.199	Y7 RUN1	0.210	Y8 RUN1	0.186	**0.198**

STD	PG GMCSF
1.530	1000
0.933	500
0.538	250
0.300	125
0.244	62.5
0.187	31.2
0.144	15.6
0.089	0

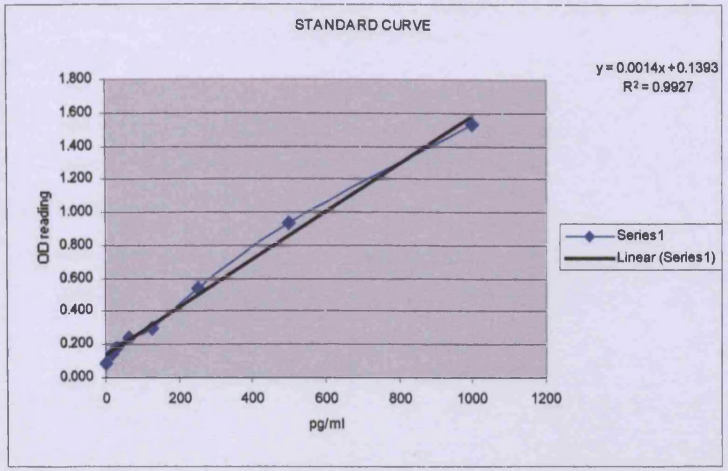

DATA POINTS CONVERTED TO PICOGRAMS

PDL2	PDL9	PDL 14	PDL 15	PDL 16
0.185	0.203	0.304	0.139	0.144
33	46	118	15	16
PDL2 LYD	**PDL9 LYD**	**PDL14 LYD**	**PDL15 LYD**	**PDL 26 LYD**
0.162	0.183	0.234	0.153	0.158
16	31	68	16	17
OGF2	**OGF16**	**OGF9**	**OGF15**	**OGF14**
0.106	0.164	0.343	0.155	0.173
6	18	146	17	24
OGF2 LYD	**OGF16 L**	**OGF9 LYD**	**OGF15 LYD**	**OGF14 LYD**
0.215	0.164	0.184	0.195	0.198
54	18	32	40	42

APPENDIX XI - ELISA PROTEIN ASSAY RAW DATA (TGFα)

STANDARDS

STD	
A1 RUN1	1.223
A1 RUN2	1.232
A1 RUN3	1.229
	1.228
B1 RUN1	0.716
B1 RUN2	0.734
B1 RUN3	0.732
	0.727
C1 RUN1	0.354
C1 RUN2	0.341
C1 RUN3	0.364
	0.353
D1 RUN1	0.223
D1 RUN2	0.225
D1 RUN3	0.228
	0.225
E1 RUN1	0.171
E1 RUN2	0.168
E1 RUN3	0.174
	0.171
F1 RUN1	0.128
F1 RUN2	0.125
F1 RUN3	0.129
	0.127
G1 RUN1	0.074
G1 RUN2	0.073
G1 RUN3	0.074
	0.074

STD	PG OF TGF
1.228	250
0.727	125
0.353	62.5
0.225	31.2
0.171	15.6
0.127	7.8
0.074	0

PDL VALUES

PDL2 A		PDL2 B		PDL2 C		AVE
A3 RUN1	0.113	A4 RUN1	0.116	A5 RUN1	0.119	**0.116**
PDL9 A		**PDL9 B**		**PDL9 C**		
B3 RUN1	0.715	B4 RUN1	0.758	B5 RUN1	0.727	**0.733**
PDL14 A		**PDL14 B**		**PDL14 C**		
C3 RUN1	0.100	C4 RUN1	0.107	C5 RUN1	0.103	**0.103**
PDL15 A		**PDL15 B**		**PDL15 C**		
Y3 RUN1	0.104	Y4 RUN1	0.105	Y5 RUN1	0.106	**0.105**
PDL16 A		**PDL16 B**		**PDL16 C**		
Z3 RUN1	0.097	Z4 RUN1	0.091	Z5 RUN1	0.099	**0.096**

OGF VALUES

OGF2 A		OGF2 B		OGF2 C		AVE
E3 RUN1	0.144	E4 RUN1	0.144	E5 RUN1	0.132	**0.140**
OGF9 A		**OGF9 B**		**OGF9 C**		
F3 RUN1	2.079	F4 RUN1	2.247	F5 RUN1	2.244	**2.190**
OGF11 A		**OGF14 B**		**OGF14 C**		
H3 RUN1	2.091	H4 RUN1	2.010	H5 RUN1	2.017	**2.039**
OGF15 A		**OGF15 B**		**OGF15 C**		
Y3 RUN1	0.428	Y4 RUN1	0.412	Y5 RUN1	0.404	**0.415**
OGF16 A		**OGF16 B**		**OGF16 C**		
Z3 RUN1	0.589	Z4 RUN1	0.525	Z5 RUN1	0.561	**0.558**

PDL LYSED VALUES

PDL2 A LYD		PDL2 B LYD		PDL2 C LYD		AVE
A6 RUN1	0.081	A7 RUN1	0.085	A8 RUN1	0.083	**0.083**
PDL9 A LYD		**PDL9 B LYD**		**PSL16 C LYD**		
B6 RUN1	0.090	B7 RUN 1	0.089	B8 RUN 1	0.087	**0.089**
PDL14 A LYD		**PDL14 B LYD**		**PDL14 C LYD**		
C6 RUN1	0.087	C7 RUN1	0.083	C8 RUN1	0.084	**0.085**
PDL15 A LYD		**PDL15 B LYD**		**PDL15 C LYD**		
Y6 RUN1	0.074	Y7 RUN1	0.071	Y8 RUN1	0.076	**0.074**
PDL16 A LYD		**PDL16 B LYD**		**PDL16 C LYD**		
Z3 RUN1	0.078	Z4 RUN1	0.070	Z5 RUN1	0.076	**0.075**

OGF LYSED VALUES

OGF2 A LYD		OGF2 B LYD		OGF2 C LYD		AVE
E6 RUN3	0.122	E7 RUN3	0.122	E8 RUN3	0.122	**0.122**
OGF9 A LYD		**OGF9 B LYD**		**OGF9 C LYD**		
F6 RUN1	0.229	F7 RUN1	0.238	F8 RUN1	0.231	**0.233**
OGF14 A LYD		**OGF14 B LYD**		**OGF14 C LYD**		
H6 RUN1	0.328	H7 RUN1	0.320	H8 RUN1	0.314	**0.321**
OGF15 A LYD		**OGF15 B LYD**		**OGF15 C LYD**		
Y6 RUN1	0.130	Y7 RUN1	0.118	Y8 RUN1	0.119	**0.122**
OGF16 A LYD		**OGF16 B LYD**		**OGF16 C LYD**		
Z3 RUN1	0.140	Z4 RUN1	0.133	Z5 RUN1	0.132	**0.135**

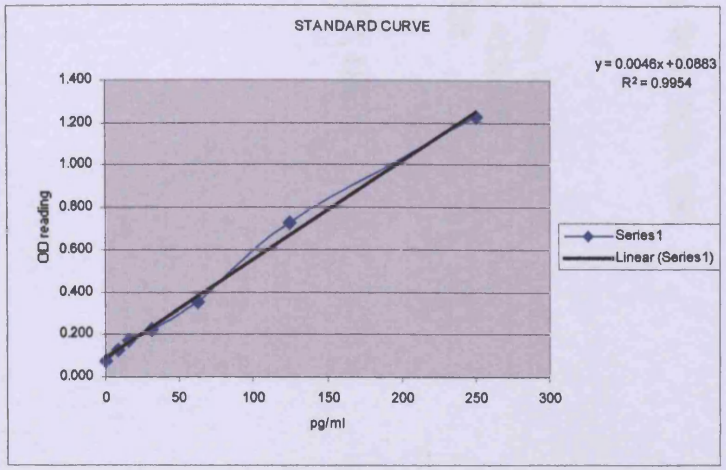

DATA POINTS CONVERTED TO PICOGRAMS

PDL2	PDL9	PDL14	PDL15	PDL9
0.116	0.733	0.103	0.105	0.096
2	140	3	4	2
PDL2 LYD	**PDL9 LYD**	**PDL14 LYD**	**PDL15 LYD**	**PDL9 LYD**
0.083	0.089	0.085	0.074	0.075
1	0	2	1	1
OGF2	**OGF9**	**OGF14**	**OGF15**	**OGF16**
0.140	2.190	2.039	0.415	0.558
11	457	424	71	102
OGF2 LYD	**OGF9 LYD**	**OGF14 LYD**	**OGF15 LYD**	**OGF16 LYD**
0.122	0.233	0.321	0.122	0.135
7	31	51	7	10

APPENDIX XII
SUPPLIERS

ABgene®
ABgene House, Blenheim Road, Epsom, KT19 9AP, UK.
Phone: +44 (0) 1372 723456
Fax: +44 (0) 1372 741414
Web site: http://www.adbio.co.uk

- Eppendorf nuclease free 200µl Cat No. AB0622
- Eppendorf nuclease free 500µl Cat No. AB0489

Ambion® (Europe) Ltd
Spitfire Close, Ermine Business Park, Huntingdon, Cambridgeshire, PE29 6XY, UK
Phone: 01480 373020
Fax: 01480 373010
Web site: www.ambion.com

- Glycogen, nuclease free Cat No. 9510
- RNAwiz™ Cat No. 9736

Applied Biosystems
Lingley House, 120 Birchwood Boulevard, Warrington, WA3 7QH, UK.
Phone: +44 (0) 1925 825650
Fax: +44 (0) 1925 282502
Web site: http://www.appliedbiosystems.com

- ABI PRISM Optical adhesive cover starter kit Cat No. 4313663
- Micro Amp Optical 96-well reaction plate Cat No. 4326659
- TaqMan™ PCR core reagent kit Cat No. N808-0228

Autogen-Bioclear
Holly Ditch Farm, Mile Elm, Calne, Wiltshire, SN11 0PY, UK.
Phone: +44 (0) 1249 819008
Fax: +44 (0) 1249 817266
Web site: http://www.autogen-bioclear.co.uk

- Plasmocin™ (InvivoGen) Cat No. ant-mmp

BDH Ltd (VWR International LTD)
Merck House, Poole, Dorset, BH15 1TD, UK.
Phone: +44 (0) 1202 660444
Fax: +44 (0) 1202 666856
Web site: http://www.bdh.com

- Methanol Cat No. 101586B
- Acetone Cat No. 100034Q

Becton-Dickinson (BD) UK Ltd
Between Towns Road, Cowley, Oxford, OX4 3LY, UK.
Phone: +44 (0) 1865 748844
Fax: +44 (0) 1865 781635
Web site: http://www.bd.com

- Biocoat™ deep 6-well plate Cat no: 355467
- Falcon™ 3µm pore cell culture inserts Cat No. 353092

Bibby Sterilin Ltd
Tilling Drive Stone, Staffordshire, ST15 0SA, UK.
Phone: +44 (0) 1785 812121
Fax: +44 (0) 1785 815066
Web site: http://www.bibby-sterilin.co.uk

- 6 well plates Cat No. 3810-006
- Centrifuge tubes 15ml (Iwaki) Cat No. 2320-015
- Centrifuge tubes 50ml (Iwaki) Cat No. 2347-050
- T25/74 Tissue culture flasks (Iwaki) Cat No. 3103-025/075

Bioline Ltd.
16 The Edge Business Centre, Humber Road, London, NW2 6EW, UK.
Phone: +44 (0) 20 8830 5300+44
Fax: +44 (0) 20 8452 2822
Web site: www.bioline.com

- Agarose multipurpose molecular grade Cat No. Bio-41026

DakoCytomation Ltd
Denmark House, Angel Drove, Ely, Cambridgeshire CB7 4ET, UK.
Phone: +44 (0) 1 353 66 99 11
Fax +44 (0) 1 353 66 89 89
Web site: www.dakocytomation.co.uk

- Anti-BRDU antibodies (Clone Bu20a) Cat No. M0744
- Pap-pen Cat No. S2002
- Rabbit anti-mouse Immunoglobulins FITC Cat No. F0261

Eppendorf UK Limited
Endurance House, Vision Park, Cambridge, CB4 9ZR, UK.
Phone: 01223 200 440
Fax: 01223 200 441
Web site: http://www.eppendorf.com/uk

- Phase lock gel™ heavy 1.5ml Cat No. 0032 007.953

Greiner Bio-One Ltd
Unit 5, Stroudwater Business Park, Brunel Way, Stonehouse, Gloucestershire, GL10 3SX, UK.
Phone: +44 (0) 1453 825 255
Fax: +44 (0) 1453 826 266
Web site: http://www.greinerbioone.com

Invitrogen™ Ltd Life Sciences (incorporating Gibco™)
3 Fountain Drive, Inchinnan Business Park, Paisley, UK.
Phone: 0141 814 6100
FAX: 0141 814 6260
Web site: http://www.invitrogen.com

- Antibiotic/antimycotic 10,000U/ml penicillin G sodium, 10,000µg/ml streptomycin sulphate, 25µg/ml amphoteracin B (AA) Cat No. 15240-062
- Dulbecco's modified Eagle's medium high glucose with phenol red, containing 2mM L-Glutamine (DMEM) Cat No. 41965-039

- Foetal bovine serum (FBS) Cat No. 10106-169
- Newborn calf serum (NBCS) Cat No. 16010-084
- Nutrient mixture F-12 (Ham's F-12) Cat No. 21765-029
- Trypsin 0.25% Cat No. 15050065
- Trypsin/EDTA (0.05% (w/v) trypsin/0.53mM ethylenediaminetetraacetic acid) Cat No. 25300-054

ISL
PO Box 120, Paignton, TQ4 7XD, UK.
Phone: +44 (0) 1803 526556
Fax: +44 (0) 1803 526776
- Fast Read cell counting chambers Cat No. BUS100

Lamb Ltd
Units 4 & 5 Parkview Industrial Estate, Alder close, Loftbridge, Eastbourne, East Sussex, BN23 6QE, UK.
Phone: +44 (0) 1323 737000
Fax: +44 (0) 1323 733000
Web site: http://www.ralamb.co.uk
- Cork disks 20mm Cat No. E7.15/CD
- Harris's haematoxylin Cat No. 033-D

Millipore
Billerica Massachusetts, 290 Concord Road, Billerica, MA 01821, USA.
Phone: (978) 715-4321
Web site: http://www.millipore.com
- Stericup™ Filter Units Vacuum-operated filtration and storage system Cat No. SCGVU10RE
- Millex Filter Units 25 mm Syringe-driven filter units with PVC housing Cat No. SLGPR25LS

Nalgene®
Nalge Europe Ltd, Unit 1a, Thorn Business Park, Hereford, HR2 6JT, UK.
Phone: +44 (0) 1432 263933
Fax: +44 (0) 1432 376567
Web site: www.nalgenelabware.com
- Cryo 1°C Freezing Container, "Mr. Frosty" Cat No. 5100

Promega UK Ltd
Delta House, Chilworth Research Centre, Southampton SO16 7NS, UK.
Web site: http://www.promega.com
- DL-Dithiothreitol, MB grade (DTT) P1171
- DNA ladder (100bp) Cat No. G2101
- Deoxynucleotide triphosphates (dNTP's) Cat No. U1511
- Ethidium bromide Cat No. H5041
- Human genomic DNA Cat No. G3041
- Blue/orange Loading buffer 6x Cat No. G1881
- Moloney murine leukaemia virus reverse transcriptase (MMLV-RT) Cat No. M3681

- Random primers Cat No. C1181
- RNasin® Inhibitor 2500U Cat No. N2111
- *Taq* DNA polymerase Cat No. M1661
- TaqMan buffer A Cat No.M190A

Qbiogene c/o Excell Biotech
Oakland Park Road, Oakland Business Park, Livingstone, Scotland, EH53 OTG, UK.
Website: http://qbiogene.com
Phone: +44 (0) 800 328 8401
Fax: +44 (0) 800 0853090
- MiniCuve 8.10 Electrophoresis Unit

R&D Systems Europe Ltd
19 Barton Lane, Abingdon Science Park, Abingdon, Oxon, OX14 3NB, UK.
Phone: +44 (0) 1235 529449
Fax: +44 (0) 1235 533420
Web site: http://www.rndsystems.com
- Human GM-CSF Quantikine ELISA Kit DGM00
- Human KGF/FGF-7 Quantikine ELISA Kit DKG00
- Human TGF-alpha Quantikine ELISA Kit DTGA00

Roche Diagnostics Ltd (Boehringer Mannheim)
Bell Lane, Lewes, East Sussex BN7 1LG, UK.
Phone: 01273 480444
FAX: 0808 100 99 98
Web site: http://www.roche-applied-science.com
- Collagenase A from *Clostridium histolyticum* Cat No. 49271620
- Amplitaq Gold Cat No. AP 4311806

Sigma-Aldrich Company Ltd
Dorset, England, UK.
Phone: +44 (0) 1202 733114
Fax: +44 (0) 1202 715460
Web site: http://www.sigmaaldrich.com
- 5-Bromo-2'-deoxyuridine (BrdU) Cat No. B9285
- 5-Bromo-4-chloro-3-indolyl phosphate p-toluidine salt (BCIP) B5655
- Albumin bovine serum, lyophilised powder (BSA) A2153
- Chloroform MB grade C2432
- Cholera toxin vibrio cholerae, lyophilised powder C3012
- Diethyl pyrocarbonate (DEPC) D5758
- DMEM x10 D2429
- Epidermal growth factor human (EGF), lyophilised powder E9644
- Ethanol absolute 200 proof, MB grade E7023
- Ethylenediaminetetraacetic acid 0.02% solution Ca^{2+}/Mg^{2+} free (EDTA) E8008
- Hoechst stain solution 33258 Cat No. H6024
- Hydrocortisone, cell culture tested H0888
- Insulin from bovine pancreas, lyophilised powder I1882
- Isopropanol, MB grade I9516
- Mitomycin-C M4287

- Nystatin suspension 10,000U/ml N1638
- Paraformaldehyde P6148
- Pronase Cat No. P6911
- Retinoic acid all trans (ATRA) R2625
- RNase Zap R2020
- Sigmaclean water bath treatment S5525
- Sodium hydroxide standard solution 1N (NaOH) S2770
- Sucrose S7903
- Tris-borate-EDTA buffer 5x (TBE buffer) T3913

Sorvall®
Kendro Laboratory Products Plc, Stortford Hall Park, Bishop's Stortford,
Hertfordshire, CM23 5GZ, UK.
Phone: +44 (1279) 82 77 00
Fax: +44 (1279) 82 77 50
Web site: http://www.sorvall.com

- Biofuge Fresco bench top ultracentrifuge

Swann-Morton Limited
Owlerton Green, Sheffield, S6 2BJ, UK.
Phone: +44 (0) 114 234 4231
Fax: +44 (0) 114 231 4966
Web site: http://www.swann-morton.com

- Disposable No.10 Scalpel blades Cat No. 0501

Thermo Shandon
Runcorn, Cheshire, WA7 1PR, UK.
Phone: +44 (0) 1928 562600
Fax: +44 (0) 1928 562627
Web site: http://www.thermo.com

- Cryomatrix™ Cat No. 6769006

Vector Laboratories Ltd
3, Accent Park, Bakewell Road, Orton Southgate, Peterborough, PE2 6XS, UK.
Phone: (01733) 237999
Fax: (01733) 237119
Web site: http://www.vectorlabs.com

- 3,3'-diaminobenzidine (DAB) Substrate Kit, Cat No. SK-4100
- Vectastain Elite ABC kit Cat No. PK-6200